Methods to move to Zero Energy Commercial Building (ZECB) for the future.

Thesis by:

Wan Iman binti Wan Mohd Nazi

A thesis submitted in partial fulfillment of the requirements

for the Degree of

Doctor of Philosophy

Newcastle University

Newcastle Upon Tyne, United Kingdom

Submitted: October 2016

Abstract

This study aims to develop methods to reduce energy demand in the building sector, which is one of the main energy consumers. An extensive literature review has been carried out to understand the behaviour of buildings' energy consumption and investigate the previous methods proposed in tackling building's energy consumption. This work mainly focused on cooling dominated buildings in a hot and humid region. A typical medium sized commercial office building located in South East Asia was chosen as the case study. The building was audited to analyse its energy performance and mapped out its end-use energy consumption. It was found that the building consumed 7,334,630 kWh energy a year where 87.5% of the energy were spent on supplying a good indoor comfort for the occupant (that involves air conditioning and lighting). A detail data from the building's energy manager was used to build a baseline building model before thermal analysis, and further investigation was carried out to achieve ZECB. It was discovered that 84% of the building's heat gain was emanated from internal sources and 16% from solar. In this study, a whole-building approach encompassing of all the three methods (passive cooling using phase change material, retrofitting procedure based on thermal analysis and combined heat power solar energy generation system) were applied to the target building as a retrofit means that resulted in a zero energy commercial building (ZECB). The methods if implemented is estimated to reduce 52.2% of the total energy consumption with the remaining energy requirement will be fully supplied by on-site solar energy generator. While 573,674.77 kWh excess electricity and 3,531,703 kWh excess cold energy will be supplied to the grid and neighbouring buildings. Parts of the suggested retrofit strategies were fully implemented by the case-study building in February 2016. It is found that the actual energy consumptions after retrofitting were reduced as predicted from the simulation. This proves that the developed methods from this research are applicable to the real world.

Dedication

To the Universe, Mother Nature and time

To all my beloved:

Mom and dad: Zainun and Wan Mohd Nazi

Brothers and sisters: Mahathir, Marini, Taqwa, Adni, Auni, Illiyyin and Ikhlas

My late grandmother may your soul rest in peace, but I wish you were here to see this

My dear soulmate, James T. Linley

Your love, hope, and belief have brought me this far

Alhamdulillah

Acknowledgements

I would like to express my sincere gratitude to:

My supervisors, Dr Yaodong Wang and Professor Tony Roskilly for their guidance and advice that have given a huge contribution to this study.

The staffs and dear colleagues in Sir Joseph SWAN Centre for Energy Research especially Dr Mohammad Royapoor for his help in building's model calibration, Dr Kevin Ma and Dr Huashan Bao for their advice on the thermal energy storage and heat driven chillers.

My project collaborator and also a dear friend, Dato' Azman Yusof (CEO of KCJ Engineering and Pulau Reka companies) and Mr Fuad (the target building's energy manager).

My proofreader, James T. Linley for reading and inspecting my work that has helped me in improving this thesis.

My dear friends Datin Liza Juliana, and Tuan Mohd Shafarid, for your kind help and support.

My sponsor, Majlis Amanah Rakyat (MARA) and the government of Malaysia especially Ministry of Federal Territories, Ministry of Rural and Regional Development and Sustainable Energy Development Authority Malaysia, this work would be not possible without the government support to this humble citizen.

May the universe repay your kindness.

List of Publications

W.I. Wan Mohd Nazi, Y.Wang, and A.P.Roskilly, "Methodologies to Reduce Cooling Load using Heat Balance Analysis: A Case Study in an Office Building in a Tropical Country," Energy Procedia, Vol. 75, pp 1269-1274, 2015

W.I. Wan Mohd Nazi, M.Royapoor, Y.Wang, and A.P.Roskilly, "Office building cooling load reduction using thermal analysis method – A case study," Applied Energy, In Press, Corrected Proof, 2016, doi:10.1016/j.apenergy.2015.12.053

W. I. Wan Mohd Nazi, Y. Wang, and A. P. Roskilly, "A holistic approach to achieving a nearly Zero-Energy Building and a study of the influence of insulation and phase change material on cooling load in a tropical country." Manuscript under revision, *Building and Energy, Feb 2016*.

W.I. Wan Mohd Nazi, Y.Wang, and A.P Roskilly, " A Comprehensive Review of High-Performance Buildings: Definitions, Retrofit Methods to Improve Building's Efficiency and End-use Energy Consumption." Manuscript submitted to *Building and Environment, June 2016.*

Table of Contents

List of Figures

List of Tables

Nomenclature

A

Air conditioning and mechanical ventilation (ACMV)

Annual energy consumption (AEC)

Air handling unit (AHU)

Air changes per hour (ac/h)

American Society of Heating, Refrigerating, and Air-conditioning Engineers (ASHRAE)

Annual cooling consumption (ACC)

Area (A)

Auxiliary (aux)

Total annual energy consumption (ΣAEC)

Total annual electricity consumption (ΣAELC)

B

Building Research Establishment Environmental Assessment Method (ΣBREEAM)

Building's annual energy intensity (ΣBAEI)

Building Energy Index (BEI)

Building consumption input system (BCiS)

C

Ceramic discharge metal lamp (CDM)

Chartered Institute of Architectural Technologists (CIAT)

Chilled water in RTH ($CW_{(RTH)}$)

Chiller's coefficient of performance ($COP_{chiller}$)

Chilled Water Pump (CHWP)

Constant air volume (CAV)

Commercial Building Initiative (CBI)

Coefficient of variation of the root mean square (CV (RMSE))

Cooling (cool)

Combined heat power (CHP)

Concentrating photovoltaic/thermal (CPVT)

Ratio of cooling system's electricity consumption per total building's electricity (Cp)

D

Direct expansion split system (DX split system)

Department of Standards Malaysia (DSM)

Daylight Factor (DF)

Damper opening percentage (DOP)

Distribution Licenses (DL)

Ministry of Human Resources, Department of Health and Safety (DOSH)

E

Cooling system's electric consumption in kWh ($EL_{CS(kWh)}$)

European Union (EU)

Energy Performance of Buildings Directive 2010/31/EU (EPBD)

Energy efficient measures (EEMs)

Estimated energy reduction (E.E.R)

Total building's electricity (Σ El $_{building\ (kWh)}$)

Total cold energy in the form of chilled water in kWh (Σ E $_{CW\ (kWh)}$)

Total cold energy in the form of chilled water in kWh ($E_{CW\ (kWh)}$)

F

Flat plate PV (FPPV)

Feed-in tariff (FiT)

Feed-in Approval Holders (FIAHs)

Floor (F)

Friday (Fri)

Total conditioned floor area (ΣFA)

G

Greenhouse gas (GHG)

Green Energy Office (GEO)

Green Building Index (GBI)

Guidelines for Occupational Safety and Health in the Office (GOSHO)

Gas District Cooling Plant (GDP)

Great British Pound (GBP/ £)

Ground floor (GF)

Solar irradiance (G)

H

Heating Ventilation and Air Conditioning (HVAC)

Heat exchangers (HEXs)

I

International Energy Agency (IEA)

Indoor air quality (IAQ)

Industry Code of Practice on Indoor Air Quality (ICPIAQ)

Indoor environmental quality (IEQ)

Information technology (IT)

K

Kilowatt hour (kWh)

Kilo tonne energy (ktoe)

Kelvin (K)

Kilo Joule (KJ)

Kilogram (kg)

L

Low Energy Office (LEO)

Leadership in Energy and Environmental Design (LEED)

Light emitting diode (LED)

Level (L)

Light output ratio (LOR)

Low emissivity (Low-E)

M

Actual monthly energy consumption (M)

Code of Practice on Energy Efficiency and Use of Renewable Energy for Non-residential Buildings (MS1525)

Member State (MS)

Mean bias error (MBE)

Monday (Mon)

Meter (m)

Maintenance factor (MF)

Miniature CPVT (MCPV)

N

Net-zero energy commercial buildings (nZECB)

National Institute for Occupational Safety and Health (NIOSH)

Net Zero Energy Commercial Building (NZECB)

Number of months (N)

O

Organization of Petroleum Exporting Countries (OPEC)

Organisation for Economic Co-operation and Development (OECD)

P

Predictive mean vote (PMV)

Philips lamp (PL)

Parts per million (ppm)

Power consumption by lighting (P_{sys})

Photovoltaic/thermal (PV/T)

Pressure (P)

Phase change material (PCM)

Q

Instantaneous room's heat gain (Qi)

Cold energy from the absorption chiller ($Q_{cool\ abs}$)

R

Refrigeration tonne hour (RTH)

Relative humidity (R.H)

Ringgit Malaysia (RM)

S

Simulated monthly energy consumption (S)

Coefficient of solar heat gain (SHGC)

T

Temperature (T)

Operative temperature (T_o)

Radiant temperature (T_r)

Temperature of the PV cell (T_{cell})

Thermal energy storage (TES)

Air temperature (T_a)

Outside ambient temperature (T_{out})

Room's temperature (T_{room})

Air conditioning's set point temperature (T_{set})

U

United Natio (UN)

United Nations Environment Programme (UNEP)

U.S Department of Energy (U.S DOE)

Unite State of America (U.S.A)

United Kingdom (U.K)

Thermal conductivity (U-value or U)

Glazing's thermal conductivity (U_g)

Lamp's utilization factor (U_L)

W

West Texas Intermediate (WTI)

Whole Building Design Guide (WBDG)

Watt (W)

Z

Zero Energy Building (ZEB)

Zero Energy Commercial Building (ZECB)

Symbols

Gradient (Δ)

Lighting system's efficiency (η_{LS})

Luminious flux at task area (ϕ)

Lamp's efficiency (η_L)

Lamp's gear efficiency (η_g)

Efficiency (η)

Mass flow rate ($\dot{m}$)

Density (ρ)

Chapter 1. Introduction

There have been a significant change in energy landscape in the past decades due to the uncertainty in energy demand and supplies, volatility in energy prices and changes in energy policies [1][2]. Fossil fuel has been the main energy resource since the ancient time but hugely exploited during the industrial revolution in the 18th to 19th centuries. In the 1970's the first 'oil shock' happened in 1973 due to the oil embargo by the Organization of Petroleum Exporting Countries (OPEC) in retaliation for the Western support of Israel during the Yom Kippur War or Ramadhan War. It is then followed by the second 'oil shock' in 1978 due to Iran Revolution [3][4]. This two political instability in the main oil producer countries resulted in oil shortages in industrial countries, and an increased in the oil price (see Figure 1). Subsequently in the 1970s to the recent years, energy crisis were experienced by one country to another due to volatility in energy prices and an increased in energy demand which resulted in the shortage in energy supply [3][4][5][6]. As the world population increases and many countries are undergoing industrial development, the energy demand keeps on rising [7]. This scenario is further worsened by the global warming. The global warming due to human activities was first acknowledged by a scientist, Svante Arrhenius [8] in 1896. Scientific publications related to environmental pollution and climate change related to human activities escalated in the 1960s to the 1970s [9][10]. In 1979 the first World Climate Conference was organized and in 1988 the global climate was first being acknowledged to be higher than any time since 1880 (see Figure 2) [8][9][10]. Since then, there is a perceived need by the world-leading organisations such as the United Nation (UN), Organisation for Economic Co-operation and Development (OECD) and the European Union (EU) to improve the global energy landscape. Their aim is to attain the energy sustainability and to combat the climate change which resulted from the greenhouse gas (GHG) emission [1][9][11].

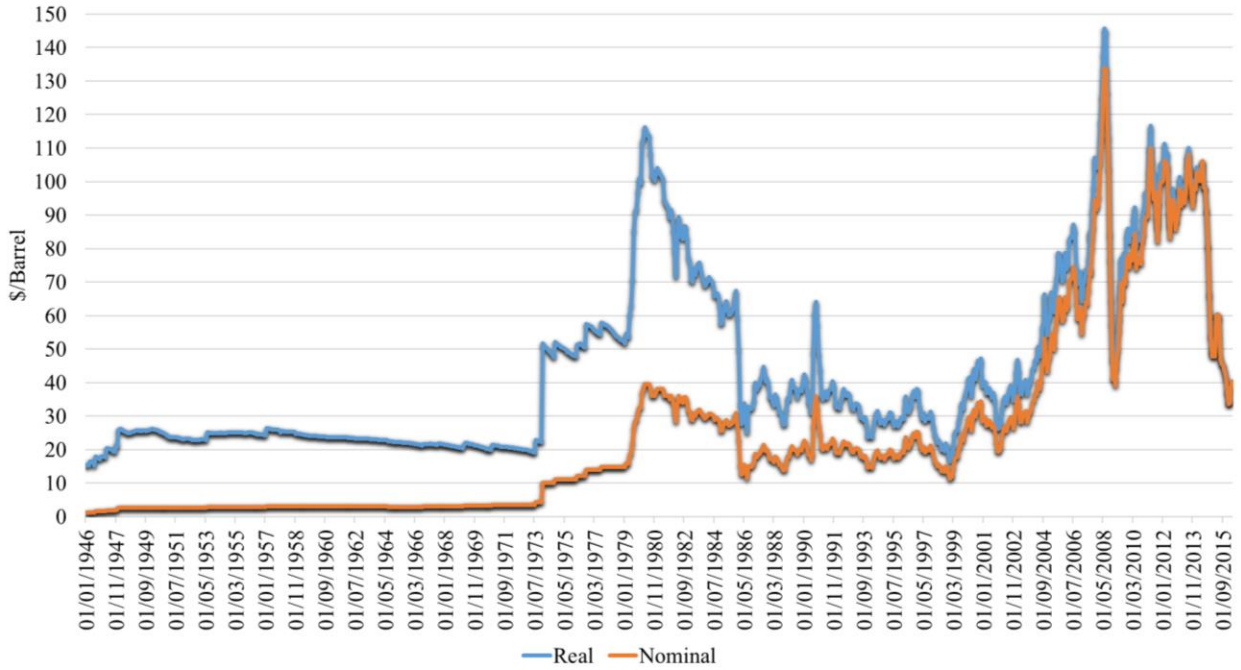

Figure 1. Historical monthly West Texas Intermediate (WTI or NYMEX) crude oil prices per barrel back to 1946. The price of oil shown is adjusted for inflation using the headline CPI and is shown by default on the algorithmic scale [12].

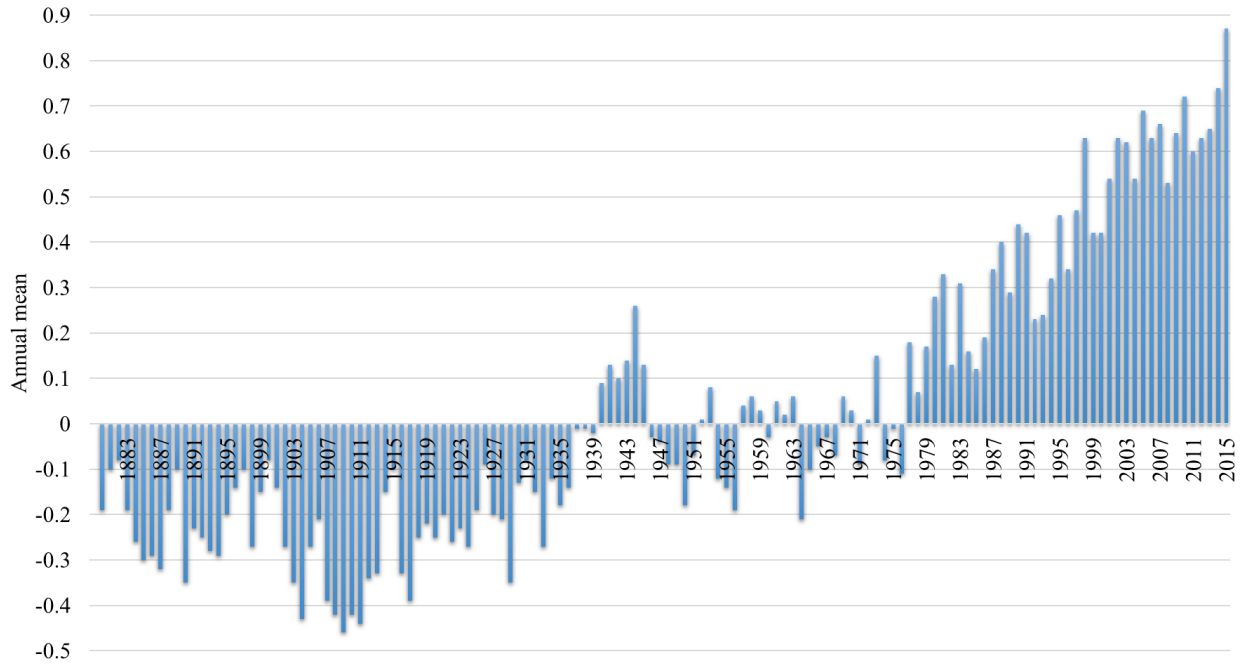

Figure 2:Global Land-Ocean Temperature Index (C) (anomaly with base: 1951-1980) [13].

The GHG were largely contributed by the burning of fossil fuels for energy supply (electricity generation, heating, and transportation) then followed by the land-use changes which include agriculture and deforestation [14][15]. These two factors that contributed to the increase in GHG emission are the main 'fuel' for social and economic development [16][17]. Additionally, the increase in human's population has been the main reason for the growth in the energy demand besides other factors such as industrialisation, development, and consumerism [7]. As can be observed in Figure 3, the total world final energy consumption is proportionate to the increase in the number of world's population. Based on the fact that social and economic development and the growth in human's population are essential for human's sustainability, cutting down energy supply or preventing agriculture are perceived as impractical in solving current energy and environmental problem. Hence, new exploration of clean energy resources, environmentally friendly practices in every aspect of human activities is deemed essential for future sustainability [7][9][18][19][20][21].

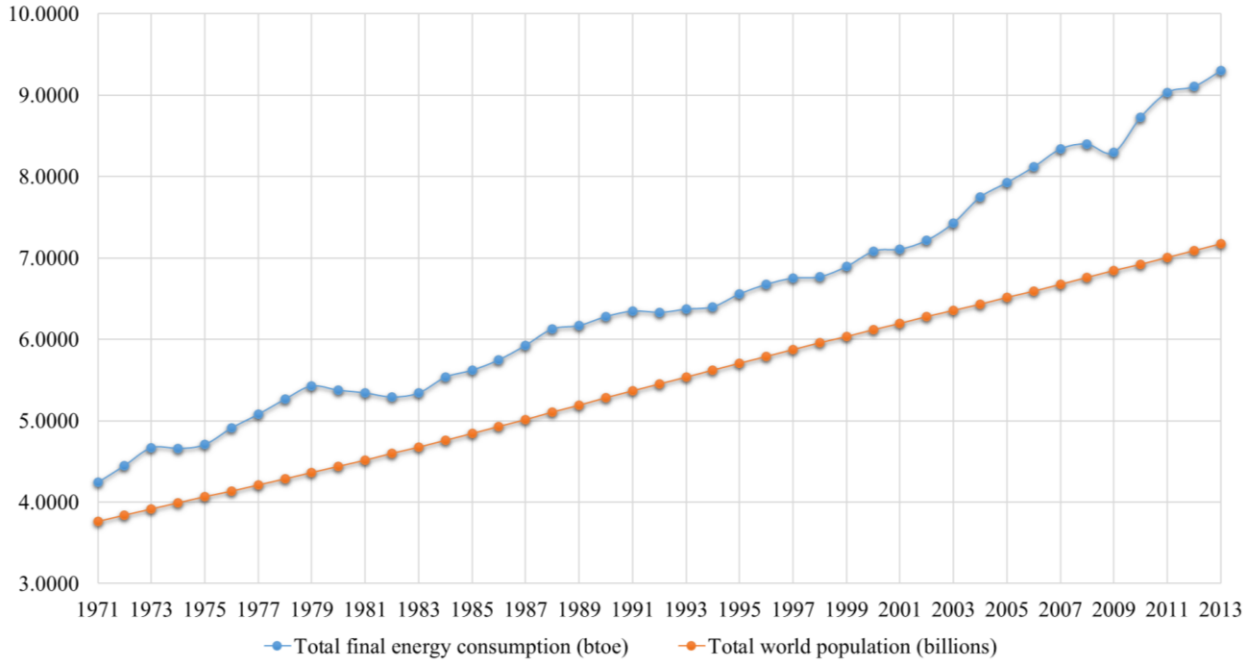

Figure 3: Annual total world population (in billion) and total final energy consumption (in billion tonne of energy) since 1971 to 2013 [18][22][23].

The constraints of the conventional energy resources and the changes in energy policies sparked an interest in alternative energy resources and the development of high-efficiency technology

[7][24]. This recent energy and environment awareness scenario had boosted new consumer behaviour patterns which focus on increasing the energy efficiency ranging from the end-use technology, transportation, household goods, industrial use, and buildings. Even though the excessive cost limits the development of these technologies, it is still estimated to earn a substantial market share in the future [7][25]. These technology breakthroughs accelerate the adoption of renewable energy and help in slowing down the global energy demand [19]. The annual production of the energy from renewables and waste product were increasing even though fossil fuels (natural gas, coal, peat, oil shale, crude, NGL, and feedstock) are still dominating the market share (see Figure 4) [18].

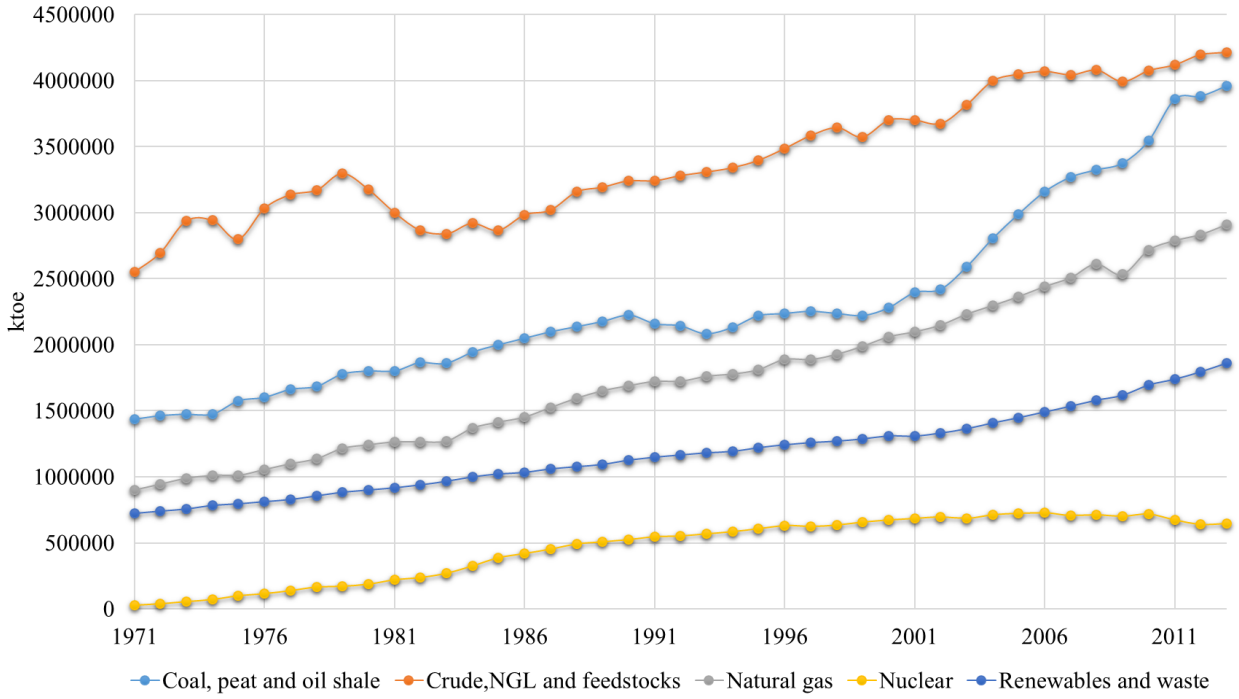

Figure 4: World production of energy resources since 1971 to 2013 [18].

1.1 Contribution to the energy sector

Building Sector account for the largest share of global primary energy demand, that is 45% worldwide [26][27]. This sector is responsible for 41% of the total primary energy consumption in the United States [28], 40% of the total primary energy consumption in the International Energy Agency (IEA) countries [18] and the European region [29], and 30% of total final

consumption in the South East Asian region [30]. Whereas, in term of the global end-use energy demand, buildings is the 3rd largest energy consumer (20%) after industries (54%) and transportation (25%) [31]. The percentage of buildings' global end-use energy demand is expected to increase by an average of 1.5% a year from 2012 to 2040 [31]. The Buildings Sector energy demands annual growth rate in different countries were listed in Table 1. The highest energy demand growth rate by the building sector was in Spain then followed by Malaysia and Thailand. Moreover, this sector is also one of the main contributors for the global GHG emission (30% of the global GHG) [27][32]. In Europe, 36% of the CO_2 was emitted by the Building Sector [29] and 38% in the USA [28]. The CO_2 emission by the Building Sector is estimated to have grown at a rate of 2.5% per year for the commercial buildings and 1.7% per year for the residential buildings [32]. Despite the significant share of the global energy demand and the global GHG emission, Building Sector is claimed to be a sector that possesses the highest potential for reducing the GHG emission based on the available technologies [32]. Hence, making the Building Sector more energy efficient were seen as the main solution for this worldwide crisis [27][32][33][34][35].

Table 1: Buildings sector energy demand annual growth rate by country [30][36].

Country	Energy demand annual growth rate for the buildings sector (%)	Sources
Europe	1.50	Lombard et al., 2008 [32]
USA	1.90	Lombard et al., 2008 [32]
UK	0.50	Lombard et al., 2008 [32]
Malaysia	3.10	SEA Energy Outlook, Sept 2013 [30]
Spain	4.20	Lombard et al., 2008 [32]
Indonesia	1.00	SEA Energy Outlook, Sept 2013 [30]
Thailand	2.40	SEA Energy Outlook, Sept 2013 [30]
Philippines	2.00	SEA Energy Outlook, Sept 2013 [30]

This study address the global energy challenges by developing methods for the Building Sector to move to zero energy commercial buildings (ZECB) which in return, will reduce the energy consumption and increase the adoption of clean energy. It is thus hoped that this work will play a

small part in stimulating global energy security and tackling climate change. Progress is indeed made in small steps.

1.2 Contribution to the existing research

As the regulations on the building's energy and environmental performance are becoming more rigorous, numerical studies were conducted to aid the Building Sector in obtaining the objective and adapting to the changes made to the building's regulations. Previous studies are mainly concentrated on energy efficiency in residential building, small size commercial building and buildings in the cold climate areas. Most of the studies were focused on the improvement of a certain aspect of the building such as the building's envelope, fenestration, material, equipment, local energy generation system, thermal comfort, waste management or the sub-system. Whereas in this study, a holistic approach was taken and promoted throughout the study on a medium size commercial office building located in a hot and humid country. This whole-building approach is in conjunction with the suggested approach by the world leading energy agencies such as the IEA and the United Nations Environment Programme (UNEP) in improving the energy landscape from the Building Sector [27][32]. This thesis presents several contributions to the existing research namely:

- A comprehensive study of the energy distribution and indoor air quality in a typical medium-sized office building in a cooling dominated country (can be found in Chapter 3);
- A finding of the impact of installing a phase change material and an insulation material in a hot and humid country, and the most optimum construction and cooling operational settings to reduce its dependency on cooling system (presented in Section 4.1). Parts of the content in this Section was submitted to the Building and Energy and currently under revision;
- A new retrofit method based on the building's thermal analysis to reduce the building's cooling demand (presented in Section 4.2). The method used a whole-building and holistic approach in tackling the building's energy consumption. The whole-building approach analyses the whole building aspects that contributed to energy consumption and building's heat gain. While the holistic approach cater the problem from both passive and active approaches. Parts of the content in this section was published in Energy Procedia [37] and Applied Energy [38];

- An investigation on powering a typical medium-sized commercial office building in a cooling dominated country with 100% solar energy. This section offers an overview of the solar technologies, the challenges in meeting the demand and the most optimum way to manage the solar power as to increase the whole system's efficiency (presented in Section 4.3);
- An investigation of the whole-building approach to achieve ZECB by combining all the three methods suggested in Section 4.1, 4.2 and 4.3 (presented in Section 4.4);
- An interactive study between a simulations-based analyses with the actual implementation of the suggested methods. This chapter offers a reality check between the research findings and the actual implementation of the target building. The performance gap between the simulation works and the actual implementation, and the stakeholders' preference in decision-making related to retrofit were acknowledged (presented in Chapter 5).

1.3 Organization of the thesis

The findings of this study are presented in the following approach (see Figure 5).

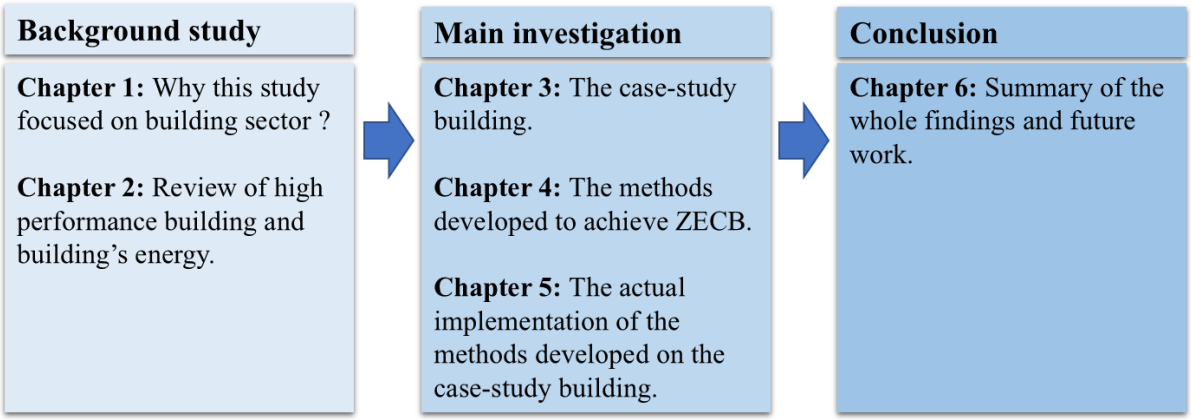

Figure 5: The structure of the thesis.

This chapter (Chapter 1) explained the co-relation between Building Sector and global energy. Chapter 2 presents a comprehensive review of high-performance building and building's end-use energy pattern which directed to the focus of this study. In Chapter 3, a building case-study matching the criteria desired was chosen. The case-study building was analysed, and the audit

results are presented in Section 3.1, and a model of the case-study building was constructed in Design Builder software and presented in Section 3.2. The case-study building model is called baseline model. In Chapter 4, methods to reduce the building's energy consumption were investigated and developed using computer simulation. Three main methods were proposed that are using passive designs (explained in Section 4.1), a holistic retrofit procedures based on the thermal analysis (presented in Section 4.2), and solar-powered cooling system (detail in Section 4.3). All these three methods were combined and applied to the baseline model to achieve ZECB (presented in Section 4.4). In Chapter 5, the outcome of an actual application of the methods suggested in Chapter 4 on the case-study building was analysed and reported. The whole findings are then concluded in Chapter 6 (Section 6.1). The recommendations for future work were presented in Section 6.2.

Chapter 2. Literature Review

This chapter offers a comprehensive review of the factors that have driven the adoption of high-performance buildings and the established terms and their definitions that have been used to describe or quantify the high-performance building before revising the methods applied in the previous studies to increase a building's energy efficiency. The previous studies on the building's end-use energy consumption are then being looked at before shifting to the indoor environment quality topic. The literature review used top-bottom analysis where we analysed the topic from a broader perspective and narrowing it down to the core issue. The sequence of the reviewed topics is as described in Figure 6.

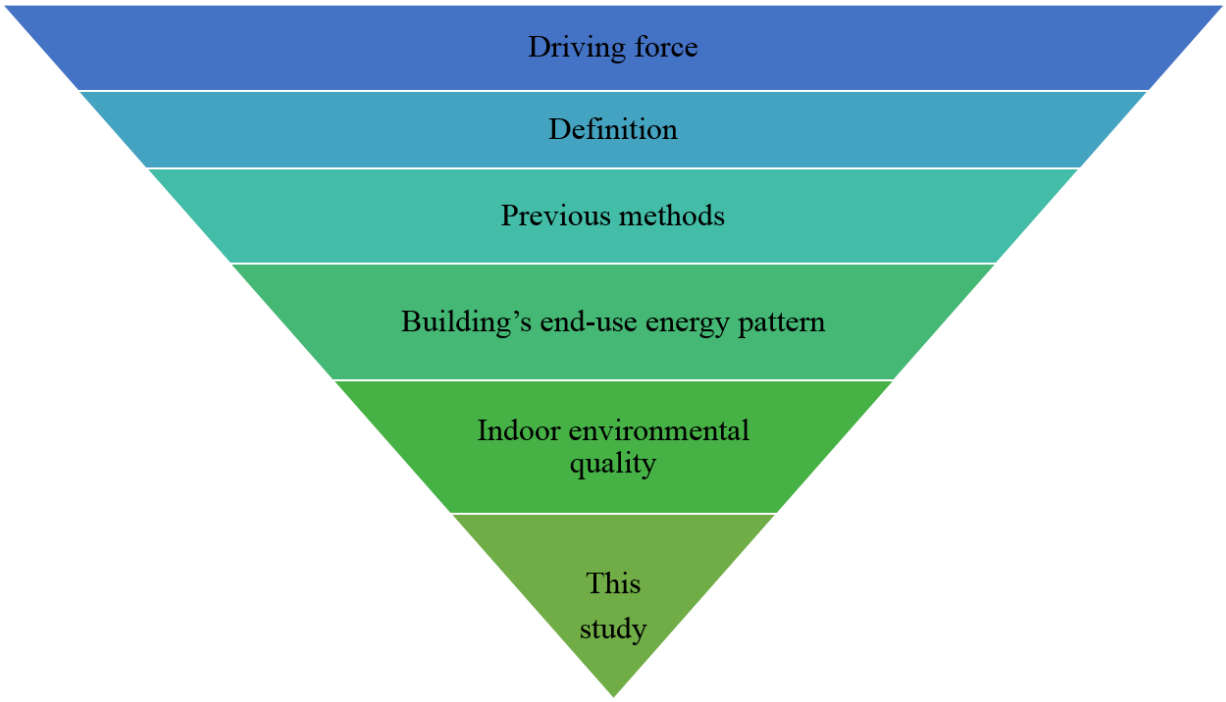

Figure 6: The sequence of the reviewed topics based on the top bottom analysis approach.

2.1 Factors that motivate the adoption of energy efficient buildings

Even though the energy crisis and global warming are the main drive for the shift-change in the Building Sector, the primary motivation for a building developer and building owners to adopt to

the energy efficient buildings are due to the enforcement by the government through legislation, incentive and the benefit that this type of building offers (which includes cost-effective measures) [32][39]. The movement towards high energy efficient buildings started in the 1970s as a result of the post-oil crisis and the rising awareness related to the environmental pollution caused by the massive industrialization in the 18^{th} and the 19^{th} century in the West [40][41]. Although there is an agreement of the advantages that green buildings offer, there is still a lack of green buildings being consructed today [42]. Some of the reasons pointed out by previous studies and publications [26][42][43] are:

- Funding/cost
- The resistance towards a new approach by the construction sector
- A conflict of interest between the different building's stakeholder during its lifetime (from developer, architect, sub-system designers, contractor, and tenants)
- Lack of exposure to the benefits of employing green measures
- Unstructured decision making in the retrofit process

However, with stringent regulations being enforced over GHG emissions [9][11], the developed countries and countries in the European Union have been more proactive in accelerating the progress of reducing the energy and GHG emissions from the Building Sector [26][27][32][33][44]. Whereas, for developing countries, the guidelines were introduced by the government on a voluntary basis to create awareness [26][30].

2.2 High-performance building

Several terms were used across the globe by different organisations to describe a high-performance building. It ranges from Green Building [45][46], Sustainable Building [27][40][46], Low Energy Building, Passive Building, near Zero Energy Building, Zero Energy Building, Net Zero Energy Building, Net Zero Energy Emission Building, Zero Carbon Building, Carbon Neutral Building and PlusEnergy Building. The definition of each term is presented in Table 2. All these terms describe a quality of a Green Building. However, the technical definition may vary between each term.

Table 2: Terms that have been used to describe a high-performance building and its definition.

Term	Definition
Green Building/ Sustainable Building/ High-performance Building	*"Green building is the practice of creating structures and using processes that are environmentally responsible and resource-efficient throughout a building's life-cycle from siting to design, construction, operation, maintenance, renovation, and deconstruction. This practice expands and complements the classical building design concerns of economy, utility, durability, and comfort. Green building is also known as a sustainable or high-performance building*." [40][27][45][46]
Passivhaus (Passive House)	"*A Passive House is a building, for which thermal comfort (ISO 7730) can be achieved solely by post-heating or post-cooling of the fresh air mass, which is required to achieve sufficient indoor air quality conditions – without the need for additional recirculation of air*." [47]
Zero carbon home	"*Requires all new homes from 2016 to mitigate, through various measures, all the carbon emissions produced on-site as a result of the regulated energy use. This includes energy used to provide space heating and cooling, hot water and fixed lighting, as outlined in Part L1A of the Building Regulations. Emissions resulting from cooking and 'plug-in' appliances such as computers and televisions are not being addressed as part of this policy*." [48]
Plusenergiehaus®/ PlusEnergy House	"*The Plusenergiehaus® fulfils a threefold objective: it will be supported exclusively by 100% renewable energy. It will operate CO_2-neutral. Moreover, it reduces the energy consumption so extensively, that it will generate more energy than it will use. Additionally comes the selection of healthy building materials and a feasible market price*" [49]
nearly Zero Energy Building	*"A building that has a very high energy performance, as determined in accordance with Annex I. The nearly zero or very low amount of energy required should be covered to a very significant extent by energy from renewable sources, including energy from renewable sources produced on-site or nearby*." [29]. This term was introduced by the European Union (UE) and the technical definition is determined by the Member States in Table 3.

In the European region, all the EU members have agreed to reduce GHG emissions through the Energy Performance of Buildings Directive 2010/31/EU (EPBD). According to the Directive:

"Member States shall ensure that: (a) by 31 December 2020, all new buildings are nearly zero-energy buildings; and (b) after 31 December 2018, new buildings occupied and owned by public authorities are nearly zero-energy buildings." [29]

The detailed technical definition of an nZEB is determined by every Member State (MS). As of April 2015, nZEB definition by fourteen MS has been approved. The technical definition of nZEB for non-residential buildings by the MS is measured by annual energy intensity, the share of renewables and compliance of a certain building's regulations. The list of maximum annual primary energy intensity for non-residential nZEB as determined by the MS are listed in Table 3 [33].

Table 3: The primary energy intensity for the non-residential near Zero Energy Building (nZEB) as defined by the EU Member States [33].

Country	Maximum primary energy intensity (kWh/m²/year)	
	New building	Existing building
Austria	170	250
Belgium (Brussels)	~ 90	~ 108
Cyprus	125	125
Denmark	25	25
Estonia	90-270	n/a
France	70-110	60% of energy consumed are PE
Latvia	90	90
Romania	50-192	n/a
Slovakia	34-96	n/a

The concept of Zero Energy Building (ZEB) was first demonstrated by Esbensen and Korsgaard in 1977 [50] for a house that was built in a Technical University in Denmark. The attention was only gained in 2008 [51] when the U.S Department of Energy (U.S DOE) launched a Net Zero Energy Commercial Building Initiative (CBI) [52] which aims to achieve marketable Net Zero Energy Commercial Building (NZECB) by 2025. The concept of ZEB was discussed by P. Torcellini et al. in June 2006 [53], D. Crawley et al. in September 2009 [54] and it is then further discussed in A.J. Marszala et al. in 2011 and M. Panagiotidou and R.Fuller in 2013.

The foundation concept of ZEB defined by U.S DOE as:

"An energy-efficient building where, on a source energy basis, the actual annual delivered energy is less than or equal to the on-site renewable exported energy." [52]

However, technically the ZEBs have rather broader definitions which vary from one region to another (parts of the definitions published in previous studies were listed in Table 4). It was also stressed by the U.S DOE that:

"A broadly accepted definition of ZEB metrics and boundaries is foundational to efforts by governments, utilities, or private entities to recognize or incentivize zero energy buildings, and would have a significant impact on the development of design strategies for buildings and help spur greater market uptake of such projects." [52]

Table 4: The definition of ZEB as published in the previous studies.

Term	Definition
Zero Energy Building	"*ZEB concept is the idea that buildings can meet all their energy requirements from low-cost, locally available, nonpolluting, renewable sources. At the strictest level, a ZEB generates enough renewable energy on site to equal or exceed its annual energy use."* [54][55]
net Zero Site Energy	A site NZEB produces at least as much renewable energy as it uses in a year when accounted for at the site [54][55].
net Zero Source Energy	A source NZEB produces (or purchases) at least as much renewable energy as it uses in a year when accounted for at the source. Source energy refers to the primary energy used to extract, process, generate, and deliver the energy to the site. To calculate a building's total source energy, imported and exported energy is multiplied by the appropriate site-to-source conversion multipliers based on the utility's source energy type. [54][55].
net Zero Energy Costs	In a cost NZEB, the amount of money the utility pays the building owner for the renewable energy the building exports to the grid is at least equal to the amount the owner pays the utility for the energy services and energy used over the year. [54][55].
net Zero Emissions	A net zero emissions building produces (or purchases) enough emissions-free renewable energy to offset emissions from all energy used in the building annually. Carbon, nitrogen oxides, and sulfur oxides are common emissions that ZEBs offset. To calculate a building's total emissions, imported and exported energy is multiplied by the appropriate emission multipliers based on the utility's emissions and on-site generation emissions (if there are any) [18][54][55].
net Zero Energy Building	A net zero-energy building (ZEB) is a residential or commercial building with greatly reduced energy needs through efficiency gains such that the balance of energy needs can be supplied with renewable technologies. [51]
Autonomous Zero Energy Building	The building "*…does not require connection to the grid or only as a backup. Stand-alone buildings can supply all their energy needs as they have the capacity to store energy for night-time or winter-time use*." [51][56]

All these terms mainly originated from developed countries. As for developing countries the Green Building, Sustainable Building and ZEB are the terms that are commonly used to describe a high-performance building. Such as in Malaysia, the high-performance commercial office

building is classified into two categories that are Low Energy Office (LEO) building and Green Energy Office (GEO) building. These two type of building were judged based on its primary energy intensity where the maximum annual primary energy intensity for LEO building is 115 kWh/m² and 50 kWh/m² for GEO building [57][58][37]. Each country generally has its Green Building assessment standard such as Leadership in Energy and Environmental Design (LEED) found in the U.S.A, Building Research Establishment Environmental Assessment Method (BREEAM) was discovered in the U.K, Green Building Index (GBI) was found in Malaysia, BCA Green Mark was found in Singapore and Greenship that was found in Indonesia. LEED and BREEAM are widely used worldwide even though it was debated if a building national rating system can be widely adapted to another region.

Ozge Suzer suggested that it is better for the building to opt for the local rating system since the weighting and rating criteria reflect the reality of the country [59]. A simple comparison of the weighting and criteria used by different rating systems for an existing non-domestic buildings are presented in Table 5 (for LEED, GBI, Greenship and BCA Green Mark) and Table 6 (for BREEAM). For BREEAM system, the assessment for an existing non-domestic building is divided into three parts that are: asset, building management and organisational. It can be noticed that a different number of criteria were used to evaluate a building's performance and the weighing point/percentage are also different. However, 'energy performance' is the most important criteria in every building rating systems. This study only focuses on energy performance and indoor environmental performance, whereas the other criteria are essential for sustainable building, but not essential for a Zero Energy Building.

Table 5: The comparison of rating criteria and weighting by LEED, GBI, Greenship and Green Mark.

LEED [60]		GBI [61]		Greenship [62]		Greenmark [63]	
Item	Available Point	Item	Available Point	Item	Available Point	Item	Available Point
Energy and atmosphere	35	Energy	35	Energy	36	Energy	116
Site development	26	IEQ	21	Indoor health and comfort	20	Environmental protection	42
IEQ	15	Site development	16	Water conservation	20	Water conservation	17
Material resources	14	Material resources	11	Site development	16	IEQ	8
Water conservation	10	Water conservation	10	Building environment management	13	Other green features and innovation	7
Innovation	6	Innovation	7	Material resources and cycle	12		
Regional	4						

Table 6: The rating criteria and weighting used by BREEAM for existing non-domestic buildings.

Weightings Percentage (%)			
Item	Part 1: Asset	Part 2: Building Management	Part 3: Organisational
Management	n/a	15	12
Energy	26.5	31.5	19.5
Land use and ecology	9.5	12.5	5
Pollution	14	13	10.5
Materials	8.5	7.5	4.5
Waste	5	n/a	11.5
Water	8	5.5	3.5
Health and wellbeing	17	15	15
Transport	11.5	n/a	18.5

2.3 Previous studies to increase building's efficiency

Previous studies to improve the building's energy performance focused on three main methods that are passive designs [64][65][66][67][68][69][70][71][72][73][74][75][76][77][78][79][46][80][81][82][83][84], active designs [11][20][44][85][86][87][88][89] and whole building approach [37][38][90][91][92][93][94][95][96][97]. Passive designs deal with the construction of a building that can reduce energy consumption such as choices of construction materials, the design of windows and envelope, a building's orientation, and incorporating passive heating, passive cooling and passive lighting in the building design. Active designs, on the other hand, deal with the mechanical system in the building which is added to the building to reduce energy consumption that includes local renewable energy system and the implementation of equipment with improved efficiency. Meanwhile, the whole-building approach examines a building as a whole to reduce its energy dependency, and holistic approach combines both active and passive design to reduce energy consumption.

The whole building approach was recommended by professional bodies (UNEP, U.S DOE, and IEA) to achieve ZEB for both new and existing buildings [27][32][98]. Previous studies show that the energy in buildings is influenced by the interaction of a building's structure and sub-systems [80]. The outcome of the finding indicates that both active and passive designs are equally important in minimising a building's primary energy requirement and with the right designs a building can be made to harness and supply energy.

It is claimed that the whole building approach could yield a larger energy reduction compared to an isolation approach [98][99], and it is important to achieve a cost effective and viable market solution to the Building Sector [27]. Previous studies (on academic buildings [90][92][96], offices [37][38][91][93][100] and residential buildings [94]) that used the whole building approach to improve a building's energy performance for an existing and a new building estimated a reduction of between 36% to 56% on total energy consumption [90][91][92][93][100][94][96] and between 64% and 69% reduction in total cooling and heating load [92]. The key findings of the proposed energy efficient measures (EEMs) from the previous studies that used whole-building approached are listed in Table 7.

A recognized method to achieve low energy buildings known as Passivhaus method was developed through a number of research projects initially made to cater European climate. The method

demonstrates how a massive reduction in the building's HVAC requirement can reduce the buildings' energy consumption to a minimum. The method was aimed at isolating the building from the climate outside and to reduce the building's heat loss [47]. The definition of Passivhaus is:

"A Passivhaus is a building in which thermal comfort can be achieved solely by post-heating or post-cooling the fresh air flow required for a good indoor air quality, without the need for additional recirculation of air." -Passivhaus Institut (PHI) [47]

The main strategies employed by Passivhaus are:

- Good levels of insulation with minimal thermal bridges
- Passive solar gains and internal heat sources
- Excellent level of airtightness
- Good indoor air quality

The methods have been proven successful in cold regions, but will it applicable to tropical and arid regions that experience warm temperatures the whole year round? It was also mentioned by the Passivhaus formal website, that:

"It would be a pitfall just to apply the Central European Passive House design, especially the details used for insulation, windows, and ventilation and just copy these to a completely different situation because there is a specific building tradition in every country and there are specific climatic boundary conditions in every region. Therefore, the specific solution for a Passive House building has to be adapted to the country and the climate under consideration." - www.passipedia.org [47].

As mentioned in the Passivhaus website, the building's code of practice that was implemented in the cold region requires modification if it is to be applied in regions with a different climate. The previous study in the cooling dominated region that implemented insulation material in their studies reported that insulating the building increased the building's energy consumption. A study by Griego et al. on an office building in Mexico reveals that insulating the office's roof and wall resulted in an increased in the building's energy consumption. They explained that this situation happened because of the majority

of the cooling load were originated from internal heat gain. Therefore, adding thermal insulation to the building traps the internal heat gain indoors.

Previous studies to reduce energy consumption in cooling dominated countries focused on reducing cooling load demand in a building as the main method to reduce building' energy consumption. This goal was achieved by implementing passive and active technologies such as changing air conditioning set point temperature, changing constant air volume air conditioner to variable air volume air conditioner, re-sizing air conditioning system, changes in more efficient motors, changes in building envelope and façade, night time ventilation and lighting control. The methods used were summarised in Table 8. Based on the previous studies listed in Table 8, highest energy reduction was achieved by making changes to the air conditioning system. While improving the building envelope by changing the glazing is more effective in energy reducing energy consumption compared to adding insulation to the wall and roof.

Table 7: Summary of the key findings in the previous studies that used whole building approach.

Building type and country	Tool	E.E.R	Approaches	EEMs	Reference
Residential Sweden	Simulink Matlab	55%	Simplified one zone model that represent the whole building. EEMs screening.	Envelope, facades, lighting, equipment, set point temperature.	E. Mata et al., 2013 [94]
Classroom (50m²), Israel	ENERGY	55.5%	Whole building simulation based on the typical classroom in Israel. EEMs screening.	Envelope, night time ventilation, façade.	Y.V.Perez et al., 2009 [95]
Education building (1783.2m²), Arab Saudi	Manual audit work	45%	EEMs were chosen based on the end-use energy consumption.	ACMV resizing, set point temperature, lighting, facades.	H.H Sait, 2013 [96]
Five different type of offices in Europe	Computer modelling	48% to 56%	EEMs were chosen based on the end-use energy consumption and the building's type.	Envelope, HVAC, lighting, passive heating and cooling.	Dascalaki and Santamouris, [101]
Historical university's building (~7000m²), Italy	Energy Plus	69.2% (cooling) 64% (heating)	EEMs were analysed based on its suitability to preserve the building's historical architectures	Passive cool roof, ground source heat plant (GSHP) and storage tank for the GSHP.	A.L.Pisello et al., 2016 [92]
Office (12,500m²), Saudi Arabia	Visual DOE	36%	EEMs were chosen based on the end-use energy pattern.	Set point temperature, operational changes, envelope, glazing, lamps, A/C type.	Iqbal and Al-Homoud, 2007 [91]
Office (1,275m²), Mexico	DOE-2 eQuest	47% (retrofit) 49% (new construction)	EEMs were chosen using the sequential search option.	Lighting, operational, skylight at the lobby, equipment, PV panels.	D.Griego et al., 2015 [102]

Table 8: The previous studies to reduce building's energy consumption in cooling dominated countries.

Location	Climate	Main EEMs (estimated energy reduction)	References
Thailand	Tropical	(a) reduction of the latent load by using desiccant dehumidification system (13.7%) (b) change single glazing to double glazing (13.1%) (c) change CAV to VAV system (9.54%) (d) add a film to the glazing (7.1%) (e) use electronic ballast (5.12%) Other: roof insulation, wall insulation, changes in air conditioning settings, change incandescent to fluorescent lamps: resulted in less than 5% reduction each.	S.Chirarattananon [103]
Malaysia	Tropical	(a) energy saving using high-efficiency motors at load 50%, 75% and 100% calculated based on different engine capacity ranging from 1.5 HP to 25 HP. 76.03 MWh energy reduction was estimated for 25HP motor at 100% load. (b) energy saving by using variable speed drive. 1404 MWh energy saving was estimated by using speed drive at 60% speed reduction for 25HP motor.	R.Saidur [85]
Saudi Arabia	Hot Desert Climate	(a) change to VAV system (17%) (b) efficient glazing (7%) (c) re-schedule of lighting and equipment. (6%) (d) energy efficient lamps (6%) (e) night time ventilation (4%) (f) changes in set point temperature (3%) (g) insulated wall (2%) (h) insulated roof (1%)	I. Iqbal and M.S. Al-Homoud [91]
Saudi Arabia	Hot Desert Climate	(a) an air conditioning control system (25.5%) (b) Improving equipment's power factor (6.1%) (c) glass insulation (2.5%) (d) reduce the number of lamps to achieve 400-500 lux (0.6%)	H.H. Sait [96]
Saudi Arabia	Hot Desert Climate	(a) switching to VAV central system (22.5%) (b) night time ventilation (21.4% to 21.7% depending on schedule) (d) introduce economizer to method (a) - (25.5%)	M. Fasiuddin and I. Budaiwi [88]

2.3.1 Reviews on the previous retrofit approaches

Due to the high numbers of existing unsustainable buildings, great interest was paid on building refurbishment to increase energy efficiency [104]. The importance of improving a building's energy performance was emphasized by the government with the enforcement of sustainable building policies. Article 9 of the Directive 2010/31/EU of the European Parliament and the Council (19th May 2010) [105] on the energy performance of buildings states the importance of stimulating refurbishment of existing buildings into near zero-energy buildings.

In many cases this process is more economical and has a less environmental impact compared to a complete demolition and rebuild [99][104][106]. However, the effectiveness of the process depends on the core building structure and the refurbishment designs [106][107]. Hence, methods to find effective strategies for retrofitting and modelling to predict energy reduction are vital [99][107]. General energy retrofit guides and energy efficient measures (EEMs) were published by various institutions including the US Department of Energy (US DOE) and ASHRAE (in collaboration with other institutes) [98][108][109] as a response to the increasing demand for building refurbishment. Nonetheless, retrofit measures may have different impacts on different buildings due to the variance in design and sub-systems, making the retrofit selection very complex [99].

In previous studies, buildings were audited to determine the area of concerns (which is based on the end-use energy consumption) before applying EEMs. The estimated energy reduction for potential EEMs using this method is normally being made using calculation (see Figure 7) [85][91] or computer simulation (Figure 8) [92][110][111][112]. Several studies selected EEMs based on the multi-objective optimization methods (see Figure 9) [99][107][113][114][115] or cost-benefit analysis (see Figure 10) [93][116]. While, A.L. Pisello et al. used proposed a retrofit approach for historical building (see Figure 11) [92] ,Z. Ma et al. reviewed previous retrofit methods and summarized a systematic approach for sustainable building retrofit (see Figure 12) [99], and J. Park and T. Hong introduced a maintenance management process for a shopping mall to reduce carbon emission [117]. Mainly, the audit process concerns the end-use energy consumption was used to determine the sector that requires a retrofit, but not in depth whole-building approach to defining the building's parameters that contribute towards the large energy share from the sector and heat sources that contribute to cooling demand.

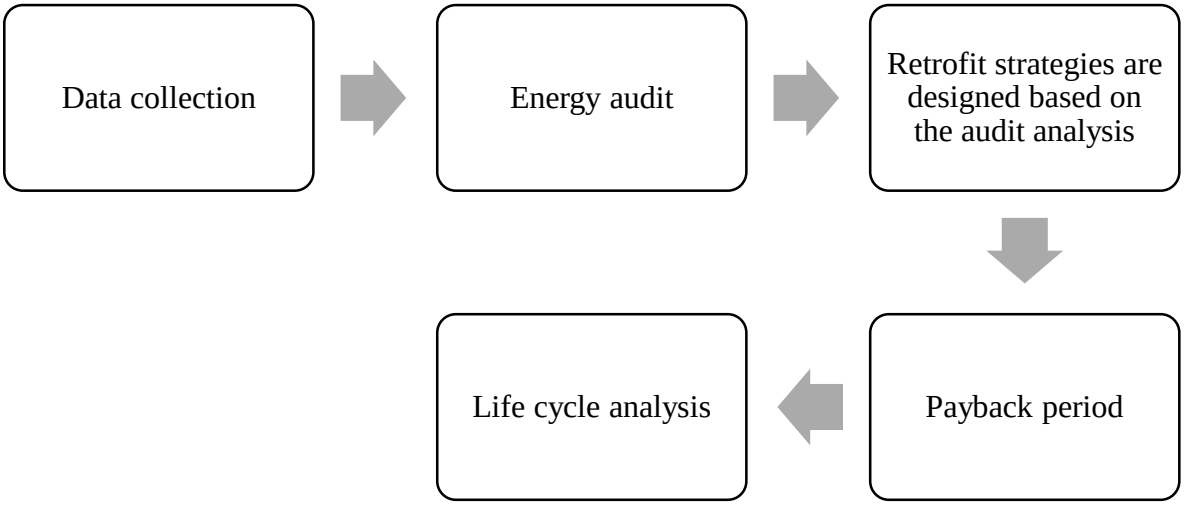

Figure 7: Retrofit method based on audit analysis [85][91].

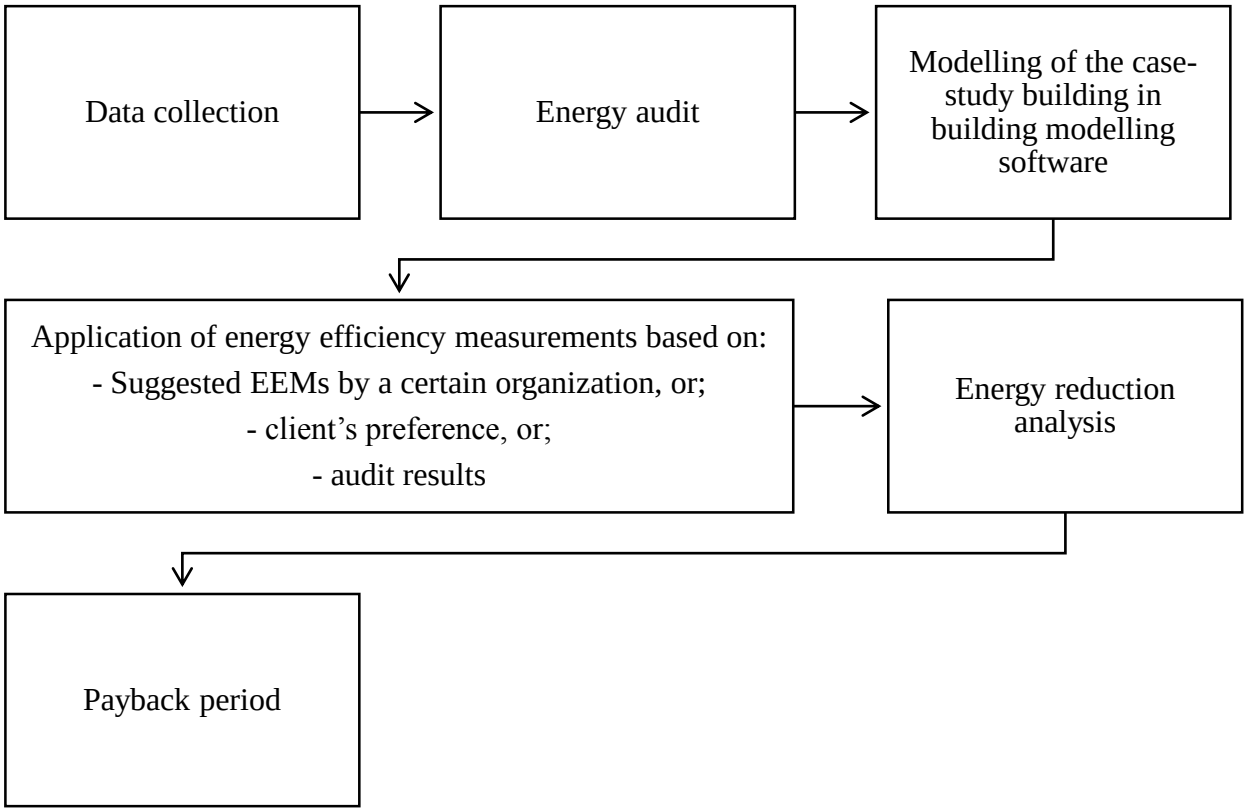

Figure 8: Retrofit procedure based on audit analysis and computer simulation results [92][110][111][112].

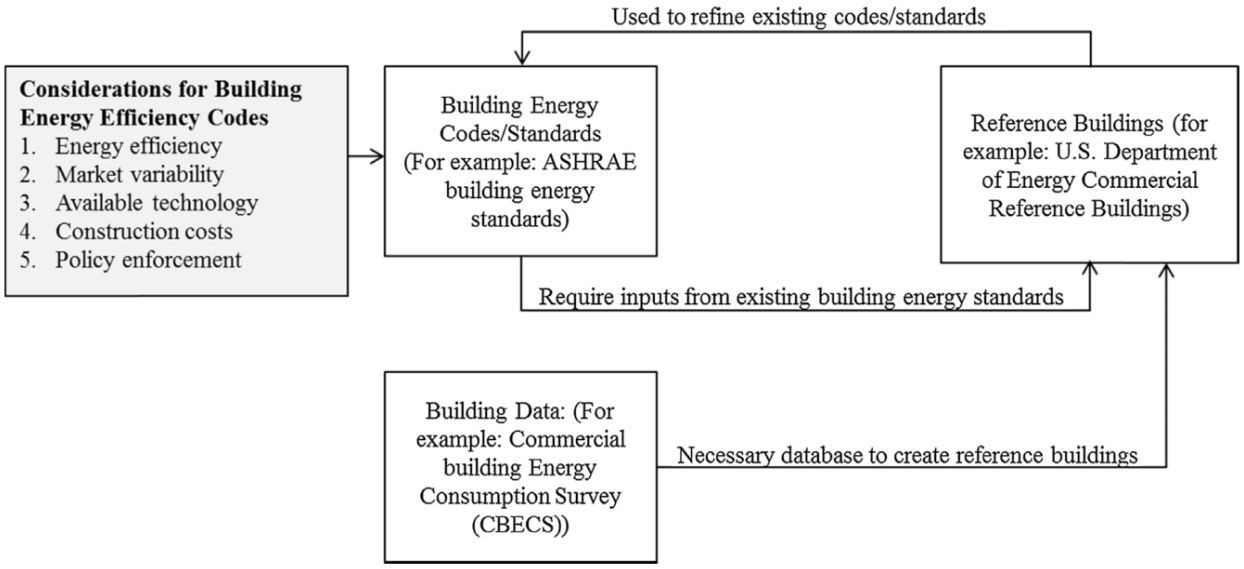

Figure 9: Retrofit procedure based on multi-objective optimisation method published by D. Grieogo e al. [93].

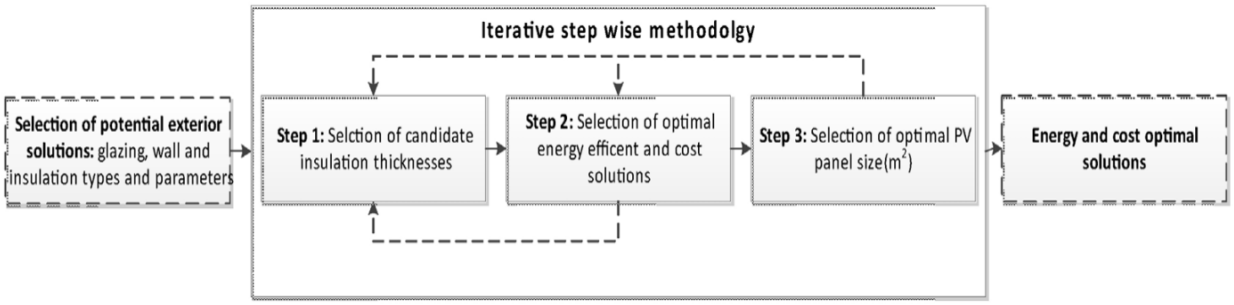

Figure 10: Retrofit based on cost benefit analysis method as published by E. Piksa et al. [223]

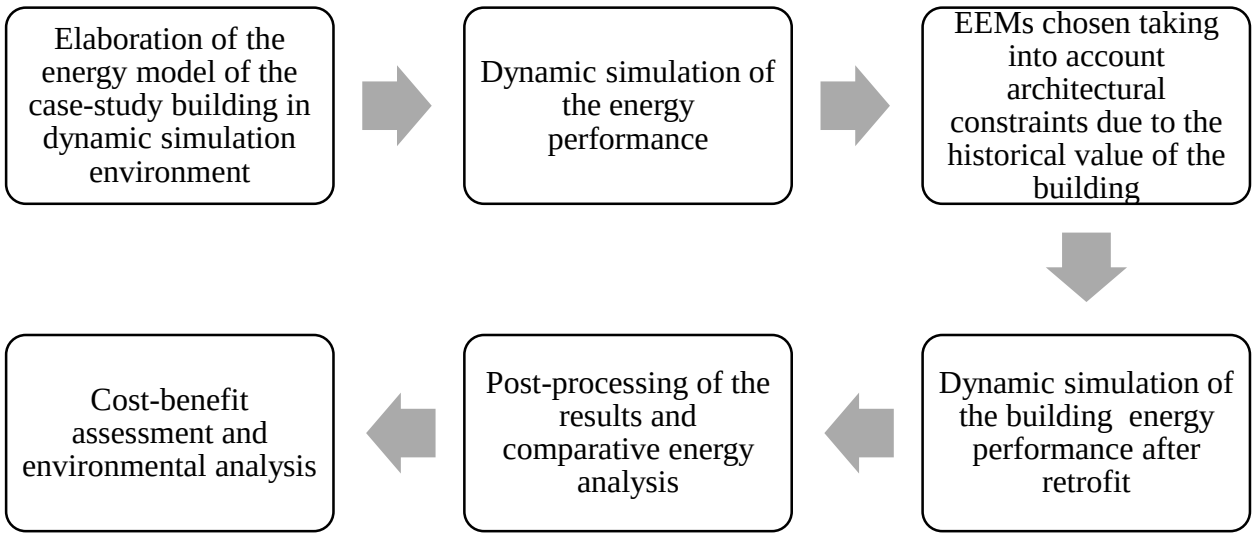

Figure 11: Retrofit method proposed by A. L. Pisello et al. for historical buildings [92].

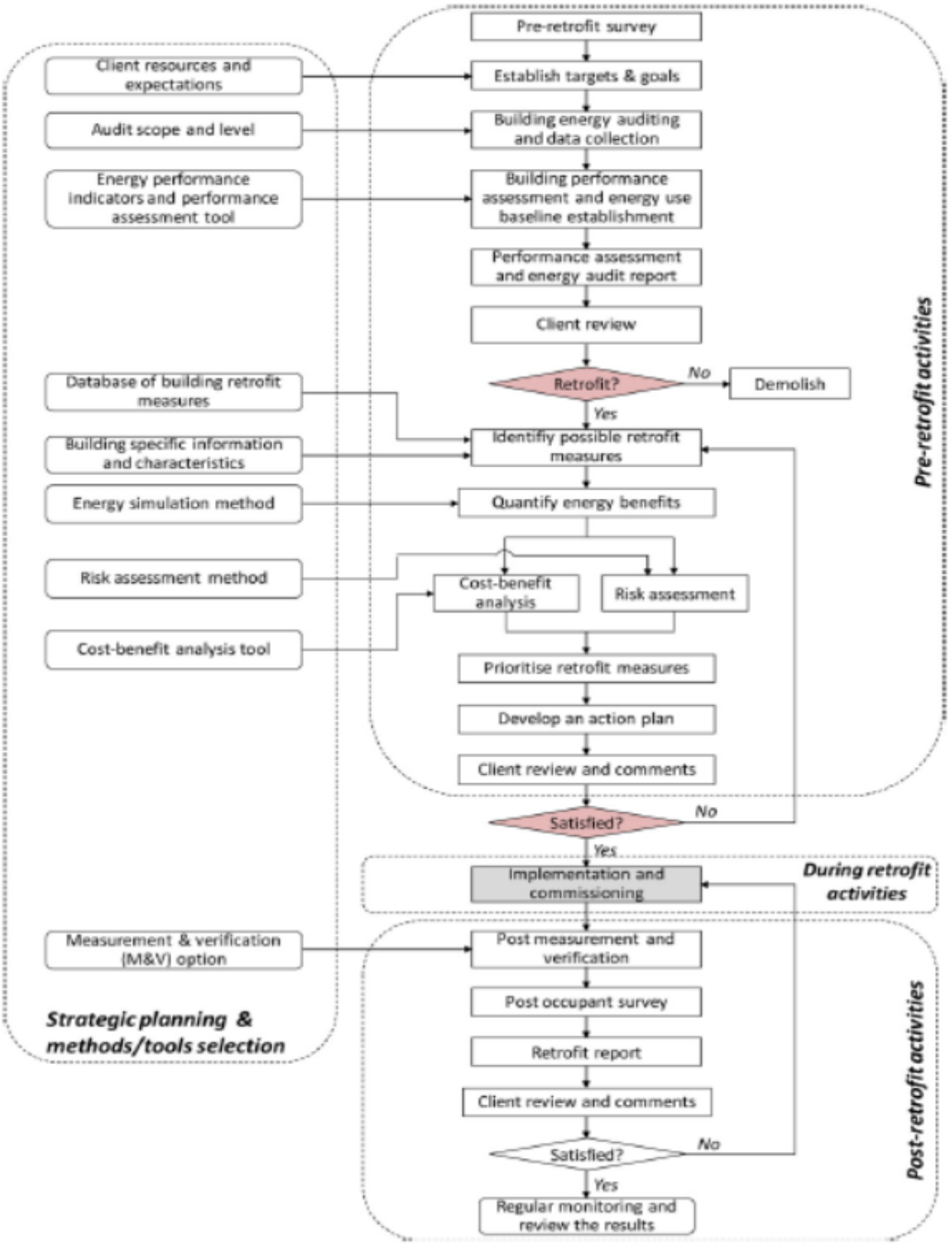

Figure 12: The retrofit method summarised and proposed by Z. Ma et al. [99].

Whereas in the early design phase, sensitivity analysis is widely adopted to determine parameters which significantly contributes towards the performance of the design solution [118]. Sensitivity analysis is a method used during a building's design stage where building's variable such as windows, envelope material, and orientation were modified to discover the impact of different parameters on the building's energy consumption [118][119][120]. Andarini et al. [119] used a sensitivity analysis to obtain parameters that can significantly reduce cooling demand in a shophouse design for the Indonesian climate. A sensitivity analysis was also performed by Yildiz et al. [120] to define parameters in an apartment's design which greatly contributes towards heating and cooling load. While Heiselberg et al. [118] studied a wider range of input parameters to determine their impact on the total energy performance of an office building design. Meanwhile in this study, the retrofit method

Normally, heating and cooling load were assigned as the output variables for the sensitivity analysis as it is a significant energy performance indicator and the major building's energy consumer globally [36][40][118][119][120] [121]. Whereas, in cooling-dominated countries, air conditioning dominated the building's energy share [27][85][86]. A study by S.Aun et al. [122] concluded that Malaysia's office buildings used 64% of the total building's energy for air conditioning. Meanwhile, other tropical countries such as Indonesia, Thailand, and Singapore, spent 51% to 59% of the building's energy budget on air conditioning [85][119]. A summary findings of the buildings' energy intensity and buildings' end-use energy consumption from the previous studies are discussed in Section 2.4.

2.4 Energy use in buildings

The average worldwide building's annual energy intensity (BAEI) based on the information gathered in Table 9 was 233.46 kWh/m²/year. Whereas the typical BAEI for office building range from as low as 69 kWh/m²/year to as high as 355kWh/m²/year [101]. The building's energy consumption depends on various factors primarily the building's design, location, sub-systems and its energy management [80][101][123]. Dascalaki and Santamouris [101] studied five different type of office buildings, and they acknowledged that the building's design (interior and exterior), location (urban, stand-alone), climatic condition and sub-systems play a significant role in determining the building's energy pattern. Huge differences in energy consumption between the same building but located in a different climatic region can be seen. The buildings in the North Coast tend to have almost double of the energy consumption compared to the same type of building which was located in the South Mediterranean.

This observation can also be seen in a study by Peng Xu et al. [124]. The authors analysed 402 buildings in six different cities in China which experience humid subtropical climate. The buildings in the coast (Shanghai and Fuzhou) tend to have higher electricity consumption compared to the buildings in the Midland (Chengdu and Wuhan). Other important findings made by the authors are related to the building's age, construction, floor area and types. It was found that the buildings with low electricity intensity do not necessarily have a good comfort level. In most cases, the office building with low electricity intensity was built since the Soviet Union with corridors in the middle and the offices on the sides with windows. This design allows high daylight penetration into the office which could reduce the building's dependency on artificial lighting. However, these buildings do not employ cooling or heating. Instead, they use ceiling fans. Meanwhile, most of the buildings built in 1990 to 2000 were designed with curtain wall which resulted in high solar heat gain through the window. Authors noted that modern buildings tend to use higher electricity due to the increased of comfort level that they need to meet (such as Heating Ventilation and Air Conditioning (HVAC) system and lighting).

Based on the review made on the previous research about the building's end-use energy consumption (listed in Table 10), it is found that most of the commercial buildings (which include offices, shopping malls, hotels, and museums. [124]) spent most of their energy on HVAC system [86][88][101]. Meanwhile in the cooling dominated countries more than 50% of

the building's energy were used for air conditioning and mechanical ventilation (ACMV) [86][88]. The only exception to this statement is the office in Mexico which used only 8% of its overall energy consumption for cooling (direct expansion (DX) split system with a coefficient of performance 3.10 and set point air temperature 23.9°C) and ventilation fans [93]. The case-study office was located in Salamanca, Mexico which experiences a humid subtropical weather (with maximum temperature 32°C and lowest 12°C during the daytime) [125]. The weather condition is considered as mild which could have contributed to the low cooling consumption.

HVAC system is a necessity in the harsh climate countries to ensure a good indoor environment is being delivered to the occupants. The main purpose of HVAC system as described by the USA Environmental Protection Agency is to *'maintain a good indoor air quality trough adequate ventilation with filtration and provide thermal comfort for the building's occupants'* [126]. This statement is in alignment with a study by BjarneW.Olesen, who described the main purpose of most buildings and HVAC system is to *'provide an environment that is acceptable and does not impair health and performance of the occupants'* [127]. Whereas, for the Chartered Institute of Architectural Technologists (CIAT) comfort air conditioning was described as *'all the conditioning processes applied to the ambient air to obtain an indoor environment that is comfortable regarding temperature and relative humidity'* [128]. So, against all this information, HVAC system is mainly used to ensure a healthy indoor environment for the occupants by regulating the air quality to its desired conditions.

Table 9: The building's energy intensity for a different building type, location, and climate condition.

Building type	Location	Climate	BAEI (kWh/m²/year)	Reference
University	Saudi Arabia	Hot desert climate	266	H.H.Sait [96]
Office	Jeddah, Arab Saudi	Hot desert climate	330	Iqbal and Al-Hamoud [91]
Shopping mall	Dammam, Saudi Arabia	Hot desert climate	275	Fasiuddin and Budaiwi [88]
Office	Mexico	Humid subtropical	106	D.Griego et al. [93]
Office	South Korea	Humid subtropical	189	B.-L.Ahn et al. [129]
Office	Europe	North Coastal	355	Dascalaki and Santamouris [101]
Office	Europe	North Coastal	193	Dascalaki and Santamouris [101]
Office	Europe	North Coastal	328	Dascalaki and Santamouris [101]
Office	Europe	Southern Mediterranean	195	Dascalaki and Santamouris [101]
Office	Europe	Southern Mediterranean	69	Dascalaki and Santamouris [101]
Office	Europe	Southern Mediterranean	196	Dascalaki and Santamouris [101]
Hospital	Malaysia	Tropical rainforest	234	R.Saidur et al. [85]
Office	Typical Malaysia	Tropical rainforest	200-250	S.A Chan [122]
Office	Northern Europe	Humid continental	269-350	Dubois and Blomsterberg [123]
Office	Typical Europe	Unspecified	306	Dubois and Blomsterberg [123]
Office	USA	Unspecified	293	Lombard et al. [36]
Commercial	Thailand	Tropical rainforest	154	Saidur et al. [86]

Table 10: The building's end-use energy consumption for different building types, location, and climate condition.

Building type	Location	Climate	End-use energy consumption (%)			References
			HVAC	Lighting	Equipment and others	
University	Saudi Arabia	Hot desert climate	82.9[C]	4.8	12.2	H.H.Sait [92]
School	Seoul, South Korea	Humid subtropical	12[HC]	37	40	T.Hong et al. [90]
School	Seoul, South Korea	Humid subtropical	5[HC]	37	41	T.Hong et al. [90]
Commercial	Saudi Arabia	Hot desert climate	50[C]	20	30	R.Saidur [82]
Office	Salamanca, Mexico	Humid subtropical	8[C]	41	52	D.Griego et al. [89]
Office	South Korea	Humid subtropical	49.4[HC]	7.2	43.4	B.-L.Ahn et al. [123]
Commercial	Spain	Humid continental	52 [HC]	33	15	Lombard et al [36] , R.Saidur [82]
Office	Europe	North Coastal	90 [HC]	10	0	Dascalaki and Santamouris [115]
Office	Europe	North Coastal	98 [HC]	2	0	Dascalaki and Santamouris [115]
Office	Europe	North Coastal	94 [HC]	6	0	Dascalaki and Santamouris [115]
Commercial	USA	Oceanic	48 [HC]	22	30	Lombard et al [36] , R.Saidur [82]
Commercial	UK	Oceanic	55 [HC]	17	28	Lombard et al [36] , R.Saidur [82]
Office	Europe	Southern Mediterranean	90 [HC]	10	0	Dascalaki and Santamouris [115]
Office	Europe	Southern Mediterranean	98 [HC]	2	0	Dascalaki and Santamouris [115]
Office	Europe	Southern Mediterranean	94 [HC]	6	0	Dascalaki and Santamouris [115]
Hospital	Malaysia	Tropical rainforest	3.45[V]	36.3	60.3	R.Saidur et al. [82]
Commercial	Malaysia	Tropical rainforest	57 [C]	19	24	R.Saidur et al. [82]
Commercial	Thailand	Tropical rainforest	59 [C]	21	20	R.Saidur et al. [82]
Commercial	Singapore	Tropical rainforest	59 [C]	7	34	R.Saidur et al. [82]
Commercial	Indonesia	Tropical rainforest	51 [C]	14	26	R.Saidur et al. [82]

[C] means the building only used HVAC for cooling, meanwhile [H] for heating, [HC] for both cooling and heating, and [V] for the ventilation.

2.5 Indoor environmental quality

An energy efficient building does not necessarily have a good indoor comfort [124]. It is not one of the criteria listed in the ZEB definition as discussed in Section 2.2. However, it is one of the criteria of a high-performance building [27][40][45][46]. A satisfying indoor environment influences occupants' behaviour, health and productivity [40][130][131] which is a very crucial aspect especially for a commercial building and can increase the resale value of the building [130]. The indoor environmental quality is one of the elements being assessed in green building rating systems (GBI, LEED, BCA Green Mark, Greenship) [132][133][134][135]. While W.Turner and S. Doty wrote one of the criteria of the green building, as defined by Energy Management Handbook, is the ability of the building to deliver a good indoor environmental quality to the occupants [40]. The National Institute for Occupational Safety and Health (NIOSH) [136], defined indoor environmental quality (IEQ) as:

'The quality of buildings environment about the health and well-being of those who occupy the space within it. Indoor environmental quality is determined by many factors, including lighting, clean air, and damp contents' [136].

The aspect that determined IEQ could have variation in expressions such as the US GBC defines IEQ as the indoor environment and their impact on the occupants which relies on the IAQ, lighting, thermal condition and ergonomic [137]. Whereas, the Whole Building Design Guide (WBDG) added to more factors that influence the level of IEQ, that are acoustic and equipment but does not acknowledge ergonomic as part of the qualities that define IEQ [130].

Nonetheless, IAQ is widely recognised by professional bodies to contribute to the IEQ [130] [136][137] and it is also part of the quality that contributed to the thermal comfort [40]. Thermal comfort is determined by the indoor temperature (air, radiant, surface), air velocity and personal parameters (depending on occupants' attire and activity types) [40][138]. ASHRAE Standard 62.1 and 62.2 [139], and have been widely adopted globally as a standard for IAQ and ventilation in buildings [127]. Meanwhile, CR 1752 has been developed since 1998 for European Standard [140]. However, it is argued by B.W Olesen that the international standards of IAQ work for every geographical location is often hard to determine [127]. This opinion is in parallel with the statement made by W. Turner and S. Doty that indoor air quality (IAQ) is qualitative and

quantitative, measurable and perceive, and objective and subjective [40] since the personal parameters could vary between individual and geographical location. W.Turner and S. Doty defined a good indoor air quality as the one with tolerable pollutants concentration without causing physical discomfort, allergies, reactions or illness to the occupants [40].

Due to the importance of IAQ for the occupants and residences, a guideline that suits the local condition was developed by local authorities. In Malaysia, standard IAQ for buildings (not included residential) was aligned in 'Industry Code of Practice on Indoor Air Quality (ICPIAQ)' published in 2010 by the Ministry of Human Resources, Department of Health and Safety (DOSH) [141]. Specific indoor environmental guidelines for offices was aligned by the DOSH in the 'Guidelines for Occupational Safety and Health in the Office (GOSHO)' published in 1996 [131] and also in the 'Code of Practice on Energy Efficiency and Use of Renewable Energy for Non-residential Buildings (MS1525:2014)' by the Department of Standards Malaysia (DSM) for a high performance buildings . The guidelines derived from these code of practices are listed in three different sub-sections that are indoor air quality (Section 2.5.1), indoor visual quality (Section 2.5.2) and indoor thermal comfort (section 2.5.3).

2.5.1 Indoor air quality

The indoor air quality is quantified by DOSH and DSM based on three main criteria that are the dry bulb temperature, the relative humidity, ventilation and the amount of contamination in the air. The contamination is caused by several factors depending on the type of contamination. The acceptable standards derived from ICPIAQ, GOSHO, and MS1525:2014 are listed in Table 11. The acceptable limit of a contaminant in the indoor air as defined in ICPIAQ [141] and the causes for every contaminant are listed in Table 12.

Table 11: The minimum acceptable standards for the indoor air quality [131][141][142][143].

Type	Standard limit	Reference
Dry bulb temperature (°C)	23 - 26	MS1525:2007 and ICPIAQ
	20 - 26	GOSHO
Relative humidity (%)	55 - 70	MS1525:2007
	40 - 60	GOSHO
	40 - 70	ICPIAQ
Ventilation	10 ls^{-1}/person or ls^{-1}/m^2	GOSHO
	0.15 - 0.50 m/s	MS1525:2007 and ICPIAQ

Table 12: The acceptable limit of a contaminant in the indoor air as defined in ICPIAQ [141] and the causes for every contaminant [144][145][145].

Type	Acceptable limits	Causes
Carbon dioxide level	≤1000 ppm	Occupant
Ozone	≤0.05 ppm	Photocopier and electrostatic air cleaners.
Carbon monoxide	≤10 ppm	Automobile exhaust, tobacco smoke, generators and gas space heaters.
Formaldehyde	≤0.1 ppm	Building materials, automobile exhaust and tobacco smoke.
Volatile organic compounds (VOC)	≤3 ppm	Solvents, workplace cleansers, pesticides, disinfectants, and glues.

2.5.2 Indoor visual quality

Regarding the indoor visual quality, this study only considers the visual quality related to light. The basic metrics to measure light consist of three main components that are:

- Luminous flux is the amount of light emitted from the source
- Illuminance is the amount of light incident to the surface
- Luminance is the amount of light reflected from a surface

The mainly used method to measure the quality of light in a space is illuminance level which is quantified by lux or lumen per meter squared. Guidelines for suitable illuminance level at different areas are normally given by the local government bodies such as in Malaysia, the

guidelines were given by GOSHO and MS1525:2014 (as listed in Table 13). The suggested illumination level at office by MS1525:2014 is 300 - 400 lux. The value is higher than the recommended lighting illumination level at offices suggested by Lighting at Workplace published by Health and Safety Executive of United Kingdom (HSE), that is 200 lux [146] and lower that the Guidelines of Office Ergonomics (GOE) published by the government of Singapore [147][that suggested 500 lux.

Table 13: The standard luminance level for different zones in the building as suggested by MS1525:2014 [142][143].

Zone	MS1525:2014
Car park	50
Corridors, passageway, stairs	100
Lifts	100
Entrance and exit	100
Hotel bedroom	100
Escalator	150
Lounge	150
Restroom	150
Restaurant, canteen, café	200
Kitchen	150 - 300
General office	300 - 400

Another important measurement in quantifying visual quality is daylight. Daylight is another source of light apart from artificial lighting. Optimising daylight receives onto a space can reduce a building's dependency on artificial lighting. However, a high amount of daylight can also cause glares which resulted in discomfort to human eyes. There are several methods to measure day light performance for visual quality such as daylight factor (D.F), daylight autonomy (DA) and useful daylight illuminance (UDI) [148]. D.F is the percentage of daylight incident on a surface compared to the daylight receives directly from an overcast sky. It is calculated based on the standard overcast sky and the calculated D.F using computer simulation is visualise on a grid in a given space. The daylight distribution across the room or space can be seen based on the D.F visualisation. DA is the percentage of working hours where the required luminance level can be met by daylight alone. Meanwhile, UDI measures the percentage of working hours that space receives adequate daylight level and classify the daylight receives into three categories that are

insufficient (daylight less than 100 lux), useful (daylight in between 100 lux and 2000 lux) and discomfort (daylight more than 2000 lux) [148].

In Malaysia, for an existing building, the quality of daylight is quantified based on the D.F and the guideline is given by MS1525:2014 (see Table 14). Since Malaysia receives high sun radiation all year round, the main problem for a building design related to daylight concerns glares. To avoid glare problem and to optimise daylight usage, the most suitable D.F as suggested by MS1525:2014 is in the range of 1 to 6.

Table 14: The classification of the average daylight factor for windows without glazing by MS1525:2014 [142][143].

Daylight factor (%)	Distribution
> 6	Very bright with thermal and glare problem
3 to 6	Good
1 to 3	Fair
0 to 1	Poor

2.5.3 Thermal comfort

Thermal comfort was defined by American Society of Heating, Refrigerating, and Air-conditioning Engineers (ASHRAE) in ASHRAE 55 as *'that condition of mind which expresses satisfaction with the thermal environment'* [149]. ASHARE 55 and ISO 7730 are widely used standards to determine thermal comfort and Predictive Mean Value established by P.O Fanger was used in the standard mentioned above as a mean to predict human's comfort [138][150] [151][152][153]. PMV method was developed based on the physiological comfort condition where the human's body need to maintain inner body temperature at 37°C by maintaining a heat balance between the body and the surrounding [152][153]. The human's heat balance is expressed by the equation (2.1) and (2.2) where equation (2.1) is used for a person without clothing and equation (2.2) for a person with clothing. The sensation scale based on the calculated PMV is shown in Table 15.

$$S = M \pm W \pm R \pm C \pm K - E - RES \quad (2.1)$$

$$M \pm W - E - RES = Kcl = \pm R \pm C \quad (2.2)$$

Where:

S = Heat storage

W = External work

M = Metabolism

R = Heat exchange by radiation

C = Heat exchange by convection

K = Heat exchange by conduction

K = Heat conduction through the clothing

E = Heat loss by evaporation

RES = Heat exchange by respiration.

Table 15: PMV sensation scale [150].

PMV values	Sensation
-3	Cold
-2	Cool
-1	Slightly cool
0	Neutral
1	Slightly warm
2	Warm
3	Hot

As explained by P.O Fanger in his book, Thermal Comfort the PMV calculation is rather complicated and hardly suitable for calculation by hands. Hence, it is suggested to simulate the value using a computational method or a table established by P.O Fanger [153]. The simplified equation for the PMV is shown in the equation (2.3) [154]. PMV value is a function of the room air temperature, relative air humidity, mean radiant air temperature, air velocity, human's metabolic rate and clothing [153][155].

$$PMV = [0.303\, e^{-0.036M} + 0.028] \times L \qquad (2.3)$$

Where:

M = metabolic rate

L = thermal load

Based on the ISO 7730 and ASHRAE 55 comfort range is achieved if the PMV values are in the range of -1 and +1 [156][157]. P.O Fanger explained that this method might not be able to satisfy 100% occupants, but it is developed to find the best environmental condition to suit a large group of people sitting together in the same room climate [138]. Some studies argued that the sensation indicator may vary to people in a different climate. Some field studies were carried out in different climatic region using PMV method, and the results were compared to the sensation scale preferred by the occupants. The studies reported that there is a significant difference between the calculated thermal state and the preferred thermal state by the occupants [150][155][156][157][158][159].

However, despite the highly debated topic of methods of measuring indoor thermal comfort, mean predictive vote (PMV) established by P.O Fanger [150][138][151] was used as the indicators to measure the offices' thermal comfort. This method was selected for its global reputation in measuring thermal comfort for buildings with HVAC system under steady state condition [150][155][156][160][161]. Plus, this quality is not covered in Malaysia's code of practice. However, the actual preferred thermal condition by the occupants will be prioritized.

2.6 Summary

"Buildings have a relatively long lifespan, and therefore, actions taken now will continue to affect their greenhouse gas emissions over the medium-term." United Nations Environmental Programme, Sustainable Buildings and Climate Initiative, 2009 [32].

The literature review using top-bottom analysis (where we analysed the topic from a broader perspective and narrowing it down to the core issue) reveals that we spent most of the energy for our comfort in the building (see Table 10). Combining the energy used by HVAC system and lighting, the total energy consumption exceeds the energy used for other sectors in the building. Peng Xu et al. and Lombard et al. also stated that the building's energy consumption keeps on increasing as the human's demand for comfort level increases [36][124]. This fact was also acknowledged by the well-known method to achieve low energy buildings that are, Passivhaus

method where the buildings demonstrate how a massive reduction in the building's HVAC requirement can reduce the buildings' energy consumption to a minimum. The Passivhaus concept was developed in Germany to cope with the European cold climate by opting for an airtight and highly insulated construction. The methods have been proven successful in cold regions, but will it applicable to tropical and arid regions that experience warm temperatures the whole year round? It was also mentioned by the Passivhaus formal website, that:

"It would be a pitfall just to apply the Central European Passive House design, especially the details used for insulation, windows, and ventilation and just copy these to a completely different situation because there is a specific building tradition in every country and there are specific climatic boundary conditions in every region. Therefore, the specific solution for a Passive House building has to be adapted to the country and the climate under consideration." - www.passipedia.org [47].

As mentioned in the Passivhaus website, the building's code of practice that was implemented in the cold region requires modification if it is to be applied in regions with a different climate. The previous study in the cooling dominated region that implemented insulation material in their studies reported that insulating the building increased the building's energy consumption. A study by Griego et al. on an office building in Mexico reveals that insulating the office's roof and wall resulted in an increased in the building's energy consumption. They explained that this situation happened because of the majority of the cooling load were originated from internal heat gain. Therefore, adding thermal insulation to the building traps the internal heat gain indoors [102]. Based on the previous studies in cooling dominated countries (listed in Table 8), highest energy reduction was achieved by making changes to the air conditioning system. While improving the building envelope by changing the glazing is more effective in energy reducing energy consumption compared to adding insulation to the wall and roof.

Previous studies also demonstrated how the same type of building but located at different climate could have a significant difference in their energy consumptions [101][124]. So what is the thermal pattern of commercial buildings in hot climates? Moreover, what are the suitable criteria for buildings in the hot region to reduce the building's HVAC demand? Will it apply to an existing medium-size commercial building in hot climate regions (previous studies are mainly concentrated in cold regions, residential and small size buildings)? What is the best retrofit approach to achieve ZEB for this type of building?

In summary, it is, therefore, necessary to carry out further research to find the answers/solutions to these questions. With the existing technologies and knowledge, reducing energy consumption and carbon emission from the building sector is possible for both the developed and developing countries alike [32][105]. In this study, it is believed that by reducing a building's HVAC requirement (the successful approach demonstrated by Passivhaus to achieve nZEB) and increasing the renewable use, ZEB is achievable for an existing medium-size commercial office building. This study gives an insight in answering the most important questions and will give a contribution in accelerating the adoption of ZEB.

Chapter 3. The Target Building

A medium size office building with a typical modern office structure located in a hot climate region was taken as the target building. The building was audited (presented in Section 3.2) to get a clear understanding of the building's performance and sub-systems. The detail audit work is then used to build a baseline building model in Design-Builder software (presented in Section 3.3). Parts of this section was published in journals by W.I.Wan Mohd Nazi et al. [38] and W.I.W Nazi et al. [37].

3.1 Building audit

A medium size office building in Putrajaya, Malaysia, was taken as the building case study (shown in Figure 13 and Figure 14) as it represents cooling-dominated nature of modern offices in Malaysia. It is located at Lat 3.12°, longitude 101.55° in South East Asia region, experiencing hot and humid weather trough out the year. The site plan of the target building referred from Google map [162] are shown in Figure 15, Figure 16, Figure 17 and Figure 18. The audit work was aimed to get a clear understanding of the building's performance, sub-systems and construction.

Figure 13: A picture of the target building taken during a field visit.

Figure 14: A picture of the target building taken during a field visit.

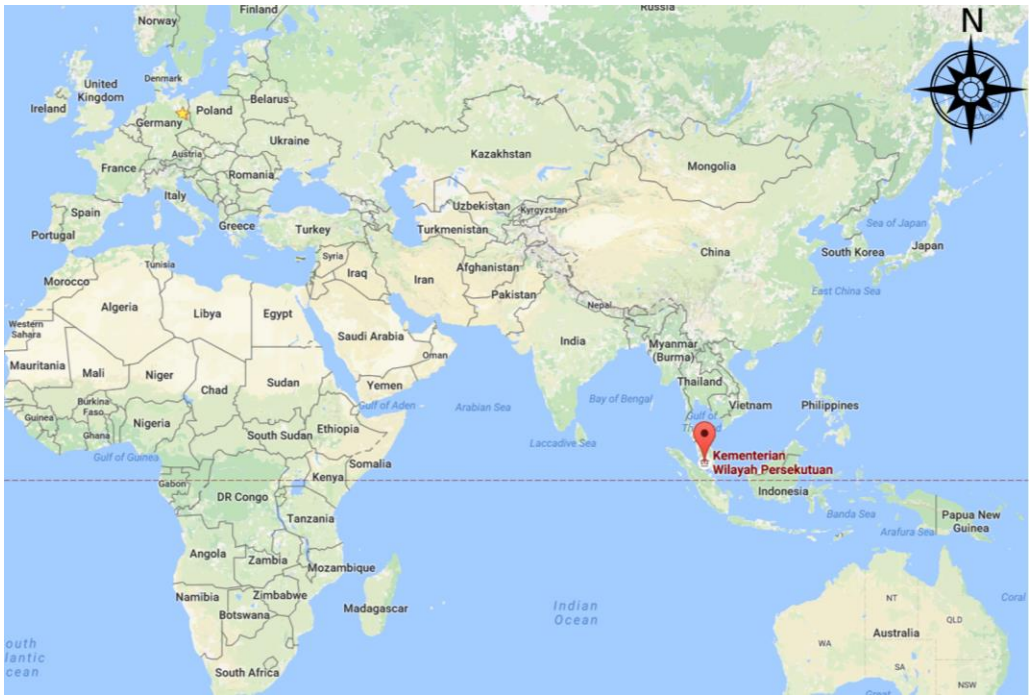

Figure 15: The case-study building (red symbol) on world map [162].

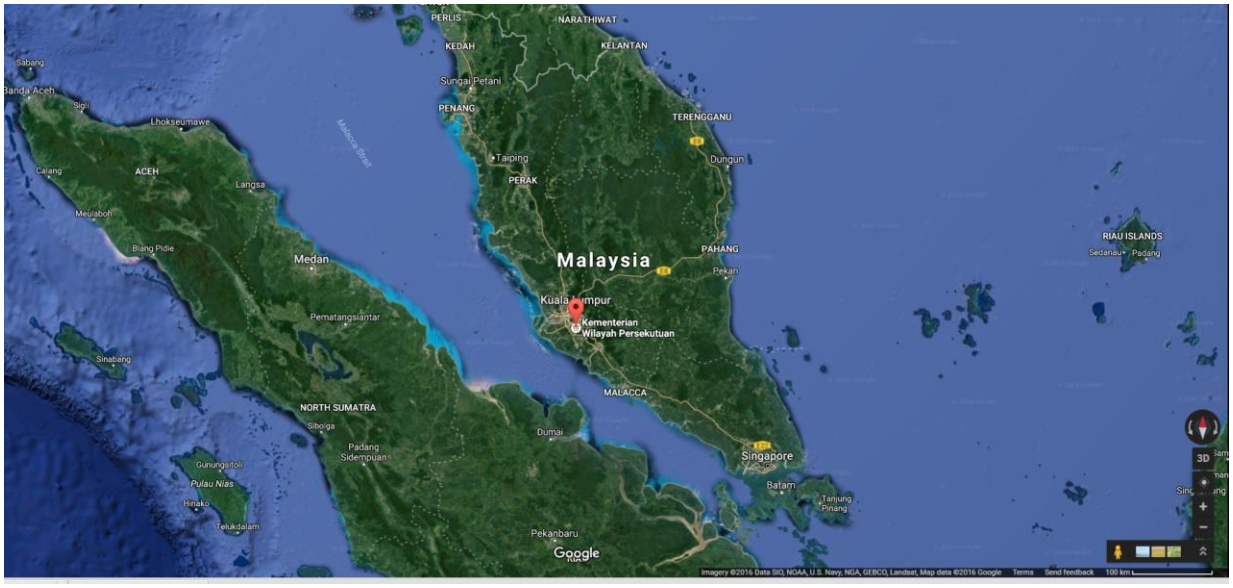

Figure 16: The case-study building (red symbol) on Malaysia map [162].

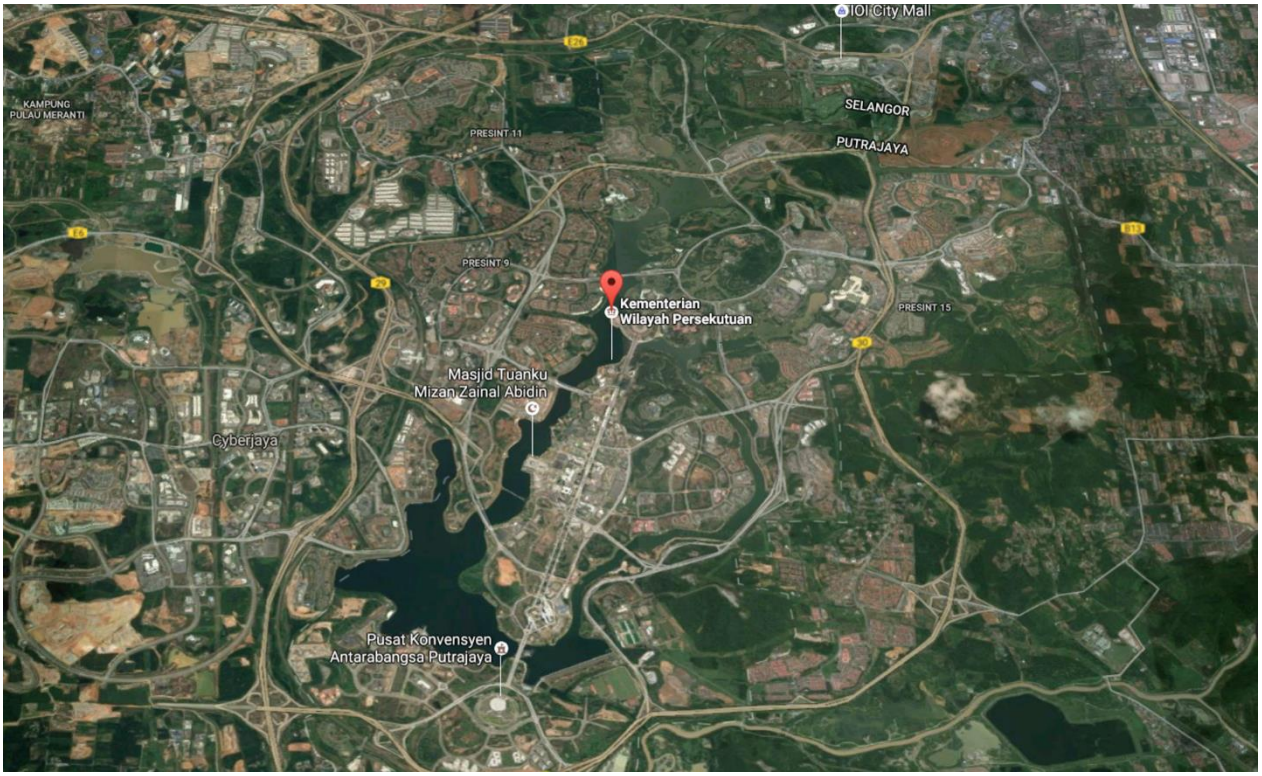

Figure 17: The case-study building (red symbol) on Putrajaya map [162].

Figure 18: The site map of the case-study building (red symbol) [162].

3.1.1 Methods

To better understand the nature of the target building and to aid the modelling process, the building's data was gathered through personal interviews with the building's energy manager, site visits, online building consumption input system (BCiS) and the annual audit reports. The audit report was performed and written by the qualified energy consultants and the facility management company [163][164]. The Building Energy Index (BEI) was used as a benchmark to compare the current building energy performance with the low energy office (LEO) suggested by the Malaysian government [57][122]. BEI is calculated using equation (3.1) [85][86] while the annual energy consumption for the building is expressed by the equation (3.2). It is a sum of the building's annual electricity consumption and the estimated energy used for chilled water supplied to the building. The estimated energy utilized by the external Gas District Cooling Plant (GDP) chiller is shown in equation (3.3) [163][164]. The chilled water usage is recorded in refrigeration tonne hour (RTH). Therefore, the values are converted to kWh (1 RTH is equivalent to 3.5 kWh). It is assumed that there are no energy losses while the chilled water travels from the GDP to the building.

$$BEI = \Sigma AEC / \Sigma FA_{(conditioned)} \quad (3.1)$$

$$AEC = \Sigma El_{building(kWh)} + \Sigma E_{CW(kWh)} \quad (3.2)$$

$$E_{CW\,(kWh)} = (CW_{(RTH)} \times 3.5) / COP_{chiller} \quad (3.3)$$

Where:

Building energy index (BEI)

Total annual energy consumption (ΣAEC)

Total conditioned floor area ($\Sigma FA_{(conditioned)}$)

Total chilled water in kWh ($ECW_{(kWh)}$)

Chilled water in RTH ($CW_{(RTH)}$)

Chiller's coefficient of performance ($COP_{chiller}$)

The building's energy usage and the indoor environmental measurement (air temperature, humidity, carbon dioxide level and lux) were referred to the building audit report ([164]) and BMS. The equipment used for the measurement is listed in Table 16.

Table 16: List of equipment used for indoor environmental measurement.

Equipment model	Usage	Accuracy
Testo 540	Illuminance	All measurement: +/- 3%
pSENSE RH	CO_2	For 0 to 2000 ppm measurement: +/- 5%
HT305	Air temperature and humidity	RH measurement : +/- 3% Air temperature measurement: -0.8°C

3.1.2 Results and Discussion

3.1.2.1 The background of the target building

The target building consists of two underground floors and a ground floor that connects the North and South building. Only the building's communal areas and offices in the North block were studied. It is a hub for Malaysia's Ministry of Federal Territories administration allocating 351 government servants (in North building alone), while the South building was rented to private

sectors. The 10 years old (as in 2016) office complex is equipped with two levels of underground parking spaces, a cafeteria, an auditorium and a communal hall. The findings concerning the building's specification are summarized in sub-sections 4.1 to 4.5. The building's fabric and floor plan were derived from the architect's drawings. The building information is summarized in Table 17 and further elaborated in the subsections. Meanwhile, the weather data was referred to Malaysia Meteorological Department and Design Builder's weather data (presented in Figure 19 and Figure 20).

Table 17: Summary of the case study building specification gathered from [33] and architect's drawings.

Component	Description
Weather	Hot and humid (tropical weather)
Floor area	40,477 m² (total floor area)/ 35,659 m² (conditioned area)
Occupants	351 (peak time). The ratio of person per floor area is 39.4m² per person.
Major zones	Lobby, corridors, toilets, AHU rooms, custodian rooms, offices, IT rooms, pantries, parking areas, kitchen, cafeteria, cold room, auditorium, data center and communal hall.
External wall	Brick and cement construction with granite tiles with a total area of 5343 m² including 1442m² of the underground floor. U-value : 2.898 W/m²K
Glazing	Green float glass (8mm). 85% glazed with local shades. Glazing area 4180 m².
Lighting	Provided by 3119 lamps (84.4% of PL-L 36W recessed and surface mounted. Average lighting density in office zones is 4.85 W/m²).
Roof	Total roof area 7263 m²

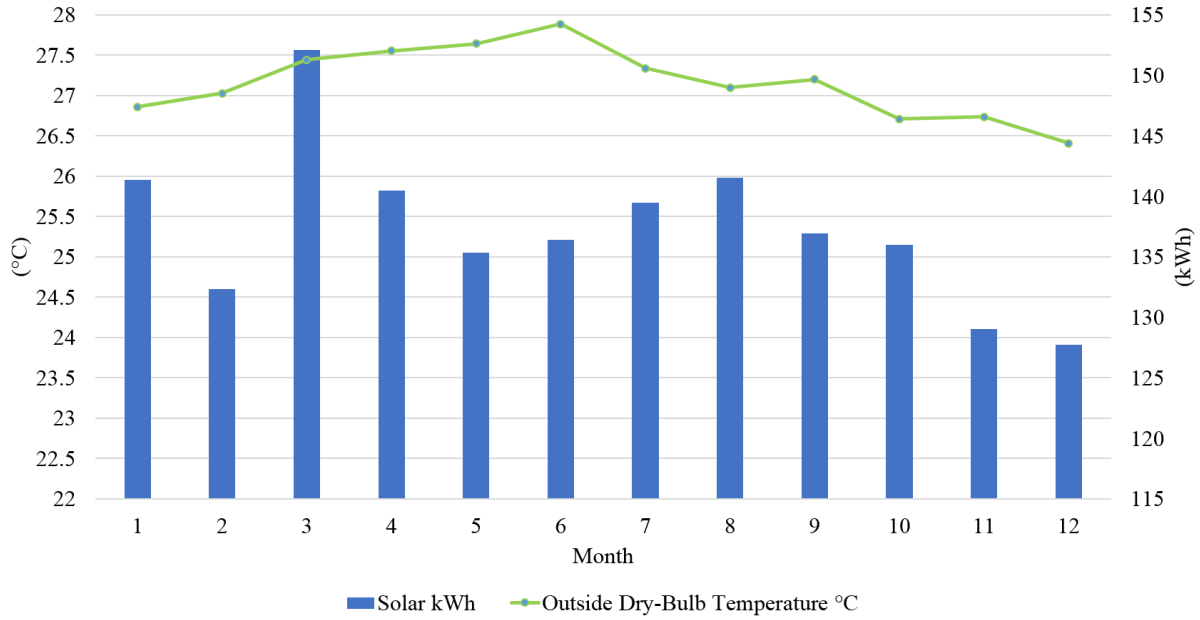

Figure 19: The monthly solar radiation and average outside dry bulb temperature in Putrajaya [149].

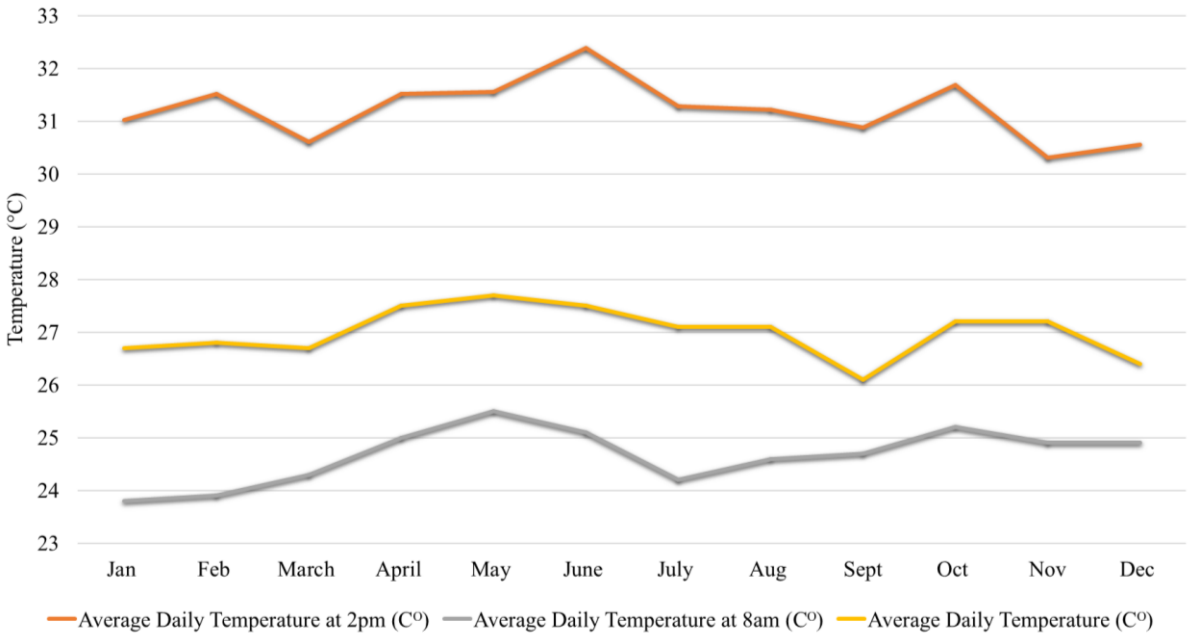

Figure 20: The average monthly dry bulb temperature at 8.00 am, 2.00 pm and the monthly average in Putrajaya in 2012 [165].

3.1.2.1.1 Building monitoring system (BMS)

The building is equipped with a monitoring system (Circutor Power Studio Scada by Monitor Power Energy) that monitors ACMV system (chilled water supply and AHU system) and indoor environment [163][164][166]. Figure 21, Figure 22 and Figure 23 are the pictures of the BMS's monitor for AHU system, CHWP system, and indoor environment's control system.

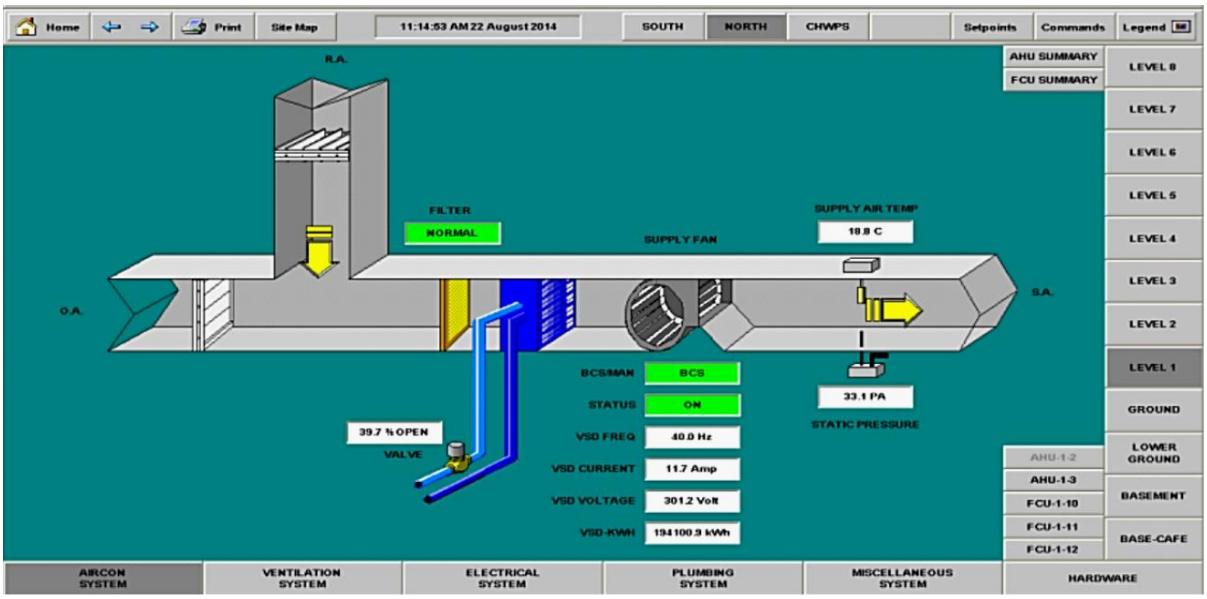

Figure 21: A print screen of the BMS's monitor for AHU control system [154].

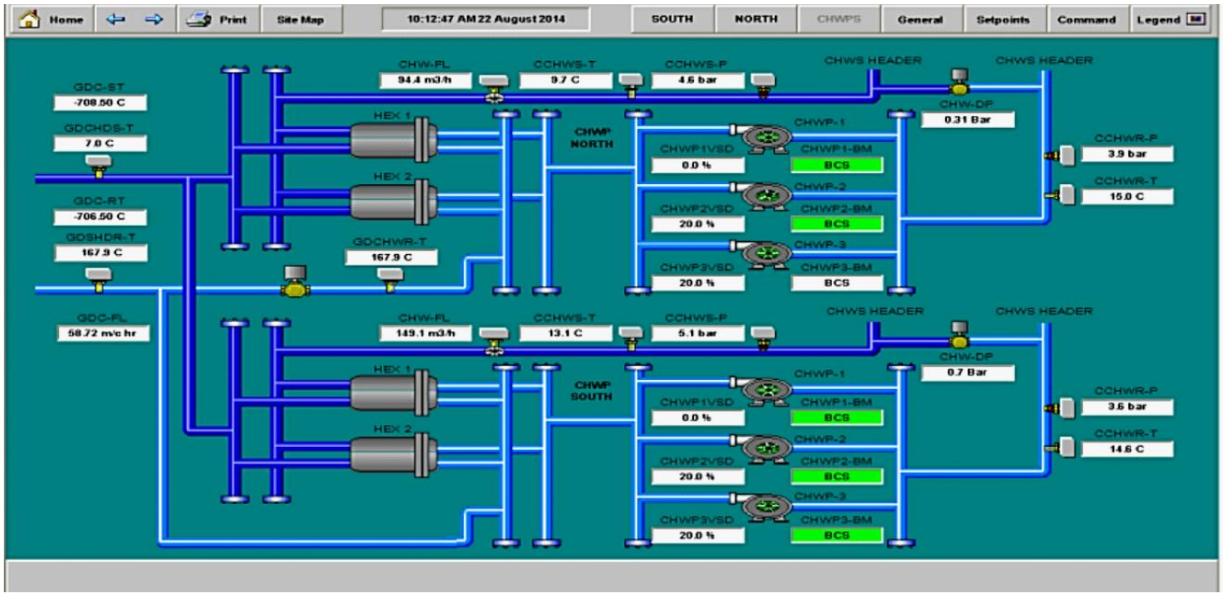

Figure 22: A print screen of the BMS's monitor for CHWP system [154].

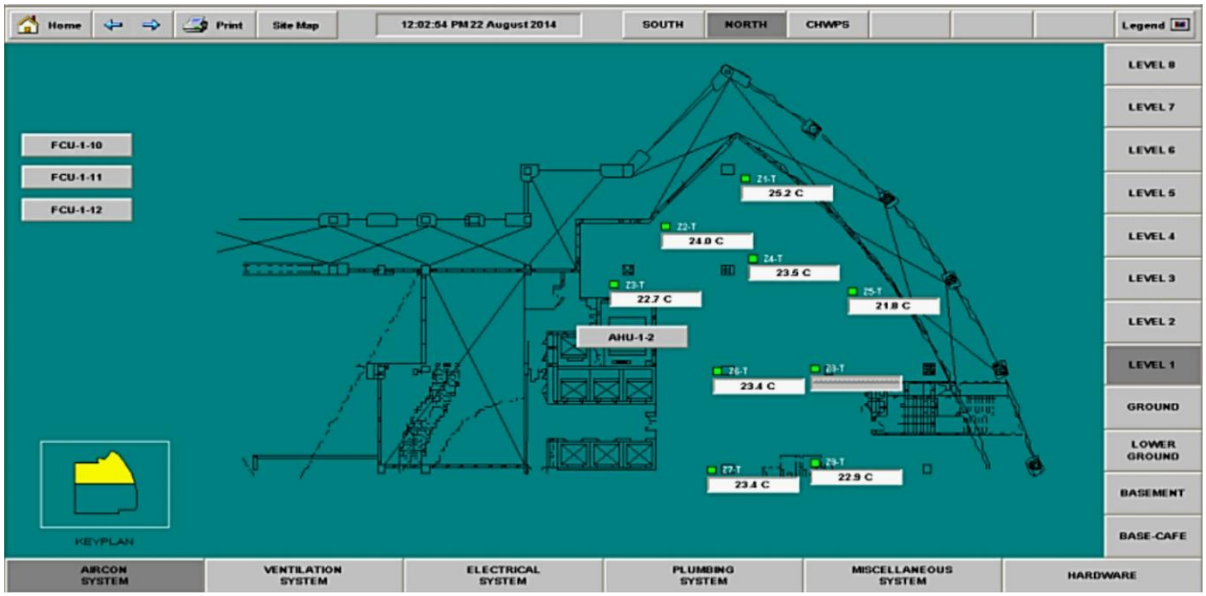

Figure 23: A print screen of the BMS's monitor for indoor environment [154].

3.1.2.1.2 Electricity supply

The building's electricity demand was supplied by the main electricity provider in Peninsular Malaysia (TNB Sdn Bhd) via six 1MVA transformers connected using six 11KV/400V transformers. Four of the transformers were connected to the North building, and another two were connected to the South building. Two electricity generators with 1500 kVA and 750 kVA capacity were also used as a standby in case of a shortage [163][164][166]. Maximum electric demand in 2012 was 1,121 kW, and the minimum was 782.4 kW. The building is classified as Commercial C1 user, and the electricity tariff is listed in Table 18.

Table 18: The building's electricity tariff for the building [43][44][45]

Type	Before Jan 2011	After Jan 2011	After Jan 2014
Charge rate per kWh	RM 0.288/kWh	RM 0.312/kWh	RM 0.365/kWh
Charge rate for each kilowatt of maximum demands per month	RM 23.930/kW	RM 25.90/kW	RM 30.3/kW
Voltage level	415V	415V	415V
Power factor	> 0.85 to 1	> 0.85 to 1	> 0.85 to 1

The electricity for the main grid was mainly generated by natural gas and coal and coke. Table 19 shows the fuel input to power stations in Malaysia in 2011 to 2013 [167].

Table 19: Types of fuel input to power stations in Malaysia in 2011 to 2013 [155].

Year	Natural gas (ktoe)	Diesel (ktoe)	Fuel oil (ktoe)	Coal & coke (ktoe)	Hydropower (ktoe)	Solar (ktoe)	Biomass (ktoe)	Biogas (ktoe)
2011	10,977	981	1,103	13,013	1,850	0	0	0
2012	11,533	811	550	14,138	2,150	11	65	4
2013	13,520	623	392	13,527	2,688	38	164	6

3.1.2.1.3 Air conditioning and mechanical ventilation (ACMV)

The ACMV system is provided by a combination of unitary constant air volume system, AHU systems on every floor, fan coil air conditioning units for the lifts lounge and mechanical ventilation units for the washrooms. The chilled water for cooling system was supplied by an external GDP [163][164]. Also, the cooling energy consumption is logged separately by the district provider since the chilled water is supplied by a GDP. A co-generation system powered by natural gas and absorption chiller was used by the GDP [168]. The chiller's coefficient of performance (COP) is 4.0 [163][164]. A 500kW electric chiller was also used in the building as a backup. The flow of the chilled water from the GDP to the building's equipment and back to the GDP is illustrated in Figure 24, and the chilled water tariff as stated in the supplier-buyer contract is shown in Table 20.

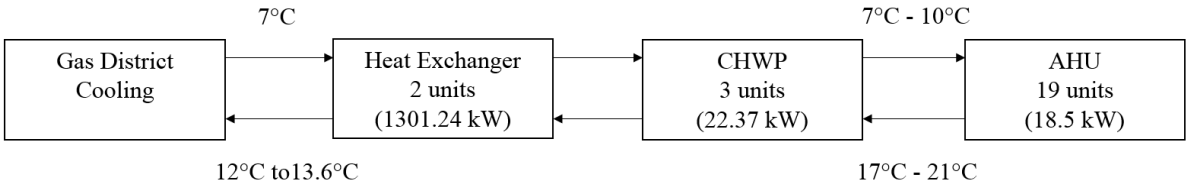

Figure 24: The chilled water flow process from the GDP to the building and return to the GDP [163][164].

Table 20: The chilled water tariff as stated in the supplier-buyer contract.

Type	2011	2013	2014
Charge rate per kWh	RM 0.248/kWh	RM 0.250/kWh	RM 0.271/kWh
Charge rate for each kilowatt of maximum demands per month	RM 114.33/kW	RM 114.33/kW	RM 124.61/kW
Demand in Refrigeration Tonne (RT)	1450	1450	1450

The air conditioner used was a constant air volume (CAV) type air handling unit (AHU) located in the air-conditioned areas in the building. The chilled water supplied by GDC plant was set to reach the heat exchanger at 7°C. The chilled water is then pumped by CHWP to all AHU system in different floors for cooling purposes. Each AHU system will reuse the return air, mixing it with the outside air before conditioning it (filter, cooling and humidify/dehumidify if necessary) before supplying it into the air conditioned rooms. The return chilled water is then pumped back to the heat exchangers (HEXs) before returning to the GDC for re-cooling.

A set of measurements from AHU systems were taken by IEN Sdn Bhd [164] for audit purposes. The measurement was taken in the morning at a specific time and does not represent AHU system performance for the whole time. However, it still can be a good indicator to monitor the chilled water performance and air temperatures in a broad-spectrum. The measurements are presented in Table 21.

Table 21: The air and chilled water measurement at every AHUs in the building.

Area Served	Outside Air		Mix Air		Return Air		Supply Air		Chilled Water	
	T ^{O}C	RH %	DOP %	T ^{O}C	RH %	T ^{O}C	RH %	T ^{O}C	T(in) ^{O}C	T(out) ^{O}C
Office (L1)	0	0	0	24.1	71.1	23.3	73.2	17.6	10	17
Office (L1)	23	78.5	100	23.6	76.8	23.9	74.8	20	-	20
Office (L2)	24	79.6	80	24.5	71.2	23.6	72.1	19.1	10	-
Office (L2)	0	0	0	25	64.7	23	69	17.8	11.5	20
Office (L3)	23	68	50	23.4	67.8	23.2	67.4	17.3	10	-
Office (L3)	23	87.8	50	23.9	77.4	24.4	73.7	20.8	10	-
Office (L4)	0	0	0	23.5	68.5	23	67.7	17	10	18
Office (L4)	24	85.6	50	24	74.6	24	73	20	-	21
Office (L5)	23	77	100	23.4	69.6	23.9	64.8	17	10	18
Office (L5)	24	79.5	50	23.7	67.8	23.7	66.8	16.5	10	19
Office (L6)	0	0	0	25.3	67.7	25	68.1	19.6	10	21
Office (L6)	25	79.1	100	23.9	69.7	23.6	67.5	17.2	9.5	18
Office (L7)	0	0	0	24.4	68.5	24	68.8	18.5	9.5	20
Office (L7)	28	75.2	75	24.6	69.3	24.2	67.1	17.8	9	-

Note: DOP is the damper opening percentage.

The measurement data shows that average chilled water temperature reached AHU at 9°C and the mean temperature it leaves the AHU system was 19.4°C. This data shows that, the chilled water experience an average increment of 10.4°C after cooling the mixture air (fresh air and return air) before supplying it into the air conditioned rooms. The average supplied air was 18.6°C. It can be observed that the chilled water experienced an average increment of 3.4°C while travelling from the CHWP to the AHUs. A better pipe insulation might reduce the heat loss which then will reduce chilled water demand. Based on the measurement taken from the air conditioning system, the ratio of fresh and return air was in the range of 20%-30% fresh air and 80% - 70% return air. A specific ratio of fresh air and return air was not stated in Malaysia building regulation, but China's Building Regulation suggested a ratio of 30% fresh air and 70% return air [70]. Carbon dioxide measurements were also taken in all office zones and the measurements complied with the indoor air quality requirement for an office building. The waste heat recovery practised by

the building could promote energy saving. A detail specification of the cooling system's components is presented in Table 22 and Table 23.

Table 22: The main parts of the cooling system and their power ratings.

Type	Units	Specification	Note
Heat Exchanger (HEX)	2	370 RT each	-
Chilled Water Pump (CHWP)	3	30 HP each	Equipped with variable speed drive but operated on fixed frequencies.
Air Handling Unit (AHU)	19	Rated at 11kW to 18.5kW each	-
Fan Coil Unit	8	Rated at 0.47kW to 2.33kW each	Only 5 were used.
Electric backup chiller	1	500kW	Only used when the supplied chilled water is higher than 8°C

Table 23: The type of cooling system used in every air-conditioned areas and their operation schedule.

Location	Type	Unit	Power Rate (kW)	Schedule
Lower Ground	CHWP	3	67.11	0645-1800 (Mon-Sat)
	ACSU	1	1.34	Not Running
	FCU	1	2.33	0800-1800 (Mon-Sat)
	ACSU	1	1	Not Running
	ACSU	1	1	Not Running
	FCU	1	1	0800-1700 (Mon-Fri)
	ACSU	1	1	Not Running
Café	AHU	1	26	0600-2000 (Mon-Sat)
Basement 1	ACSU	1	1.34	Not Running
	FCU	1	2.33	Not Running
	FCU	1	1	Not Running
	FCU	1	1	Not Running
Ground Floor	AHU	1	11	0655-1900 (Mon-Fri)
	AHU	1	11	0655-1900 (Mon-Fri)
	DB MGN	1	12.24	N/A
Level 1	AHU	1	11	0650-1900 (Mon-Fri)
	FCU	1	0.57	0720-1900 (Mon-Sat)
	FCU	1	0.47	0720-1900 (Mon-Sat)
Level 2	AHU	1	11.25	0640-1900 (Mon-Fri)
	AHU	1	11.25	0640-1900 (Mon-Fri)
	FCU	1	0.9	Not Running
Level 3	AHU	1	11	0630-1900 (Mon-Fri)
	AHU	1	11	0630-1900 (Mon-Fri)
Level 4	AHU	1	11	0630-1900 (Mon-Fri)
	AHU	1	11	0630-1900 (Mon-Fri)
Level 5	AHU	1	11	0635-1900 (Mon-Fri)
	AHU	1	11	0635-1900 (Mon-Fri)
Level 6	FCU	1	11	0650-1900 (Mon-Fri)
	AHU	1	11	0650-1900 (Mon-Fri)
Level 7	AHU	1	18.5	0655-1800 (Mon-Fri)
	AHU	1	18.5	0655-1800 (Mon-Fri)
Level 8	ACSU	1	2.23	Not Running

3.1.2.1.4 Lighting

Lighting was provided by 3,119 lamps ranging from PL-L types and PL-C types, ceramic discharge metal lamp (CDM), fluorescent tubes, light emitting diode (LED), emergency light and metal halide lamp. However, at most areas, a recessed mounted and manually controlled PL-L types and PL-C types were utilized. The power rating and schedule of lamps in every area were attained from *Energy Management & Conservation Program Report* [163]. However, the lamps were listed based on the floors and the main areas such as office spaces, café, and parking lot. The type of light used in small rooms such as AHU rooms, IT rooms, and toilets were not specified but listed altogether with the lamps used in the general areas of each floor. Even though the lighting schedule in main areas was set in BMS but the lighting control system was not functioning, and it was controlled manually by the users. The LED lamps were implemented in 2012 to cater outside areas where lighting was used after office hour from 7.00pm until 7.00 am the next morning. While at the Atrium (ground floor) lighting was supplied by daylight during the day (0730 hours to 1930 hours) and the artificial lighting was switched on at night time only.

3.1.2.1.5 General Office Equipment

There is a total of 529 office equipment in the building which can be categorized into 5 different categories that are computers, general office equipment, pantry equipment, meeting room equipment and other items. The percentage of equipment distribution is shown in Figure 25, and the type of equipment in different categories are listed in Table 24.

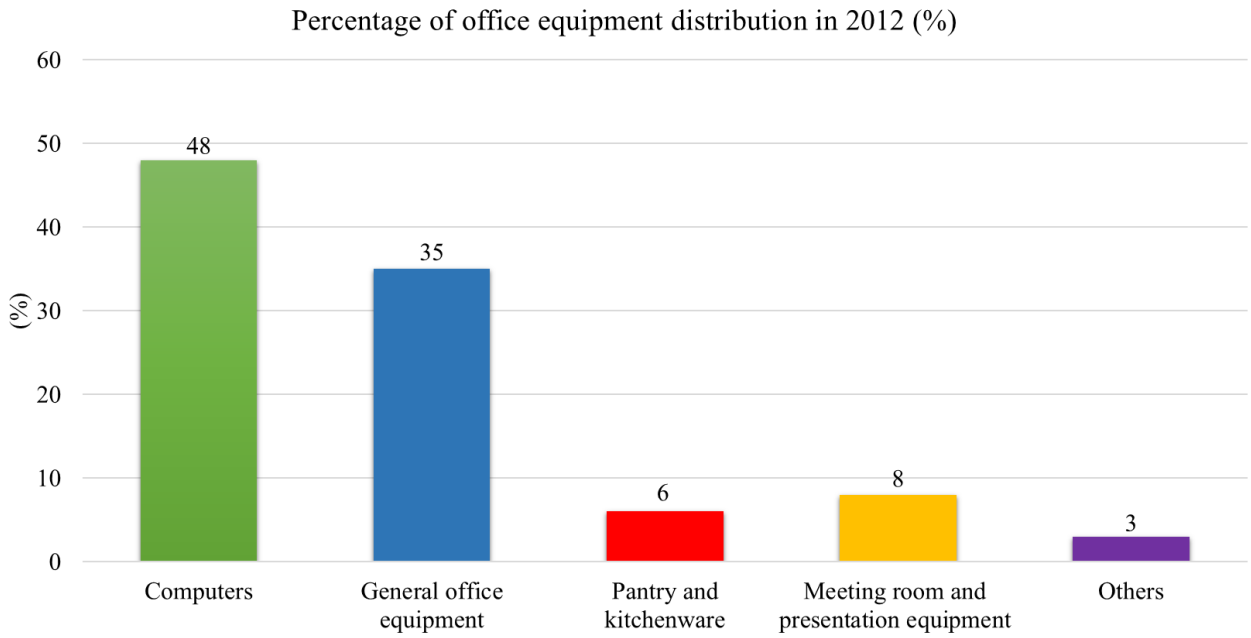

Figure 25: Percentage of office equipment distribution in 2012 [151][164].

Table 24: List of equipment based on its categories [151][152].

Category	Equipment Type
Computers	Desktop and laptops
General office equipment	Small printers, multifunction printers, scanners, paper shredding and photocopies
Pantry and kitchenware	Refrigerator, hot and cold water cooler, toaster, rice cooker, kettle and microwave.
Meeting room and presentation equipment	Meeting room's monitor, PA system, DVD player, television, radio cassette recorder.
Others	Stand fan

Computers (252 units) were the biggest unit of equipment used in the building, followed by general office equipment, meeting room, pantry and others. The equipment in the pantry such as the refrigerators and hot and cold water coolers were switched on 24 hours. The equipment used was a mixture of Energy Star equipment and non-Energy Start equipment biasing more towards non-energy star rated.

3.1.2.2 Space optimisation analysis

In the baseline building, 13,840m² office zones were occupied by 351 employees which means, 39.4m² of the office floor was dedicated to a person. Based on the guidelines from the 'Guidelines and Plan for Building' published by The Department of Prime Minister, Malaysia in 2005 [169] it is stated that the suggested space for an employee is 16 m² while the suggested space for the Minister's office is 616 m² [169]. The space allocation includes workspace, meeting rooms, pantry, toilets, file rooms, kitchen, AHU room, janitor rooms, corridors and other essential areas in an office building. This guideline when followed results in a total area of 8,004 m² for the North building instead of 13,840m². Optimising the space occupancy will reduce energy usage, land usage, and cost.

3.1.2.3 Energy Analysis

In 2012, the building used 7,334,630 kWh of energy to support its operation. That was 5,330,997 kWh of electricity and 2,003,633 kWh energy for chilled water [163]. This figure is the lowest in four years (2009 to 2012). The building's owner is committed to improving the building's energy performance. Hence, the audit was carried out every year to analyse its enactment and planning out possible ways for improvement. The building's monthly energy consumption and carbon emission are shown in Figure 26 [163][164][170].

The average BEI over four years from 2009 to 2012 was 238.53 kWh/m²/year [163][164]. The building's BEI varied from 216.9 kWh/m²/year in 2012 to as high as 254.3 kWh/m²/year in 2011 (see Figure 27). The variation in the building's energy consumption might originate from occupants' behaviour such as how they control lighting and equipment usage. Another reason that could contribute to the variation is equipment replacement to new equipment that is more energy efficient once they have reached their lifetime. Meanwhile in 2012, a significant dropped in the building's BEI was mainly originated from the building undergoes a renovation in the South building from July to December. During this period, every office floors were emptied including the communal areas on the ground floor and first floor. The BEI is slightly lower than the typical BEI for Malaysian office buildings (250 kWh/m²/year) [58][86] and in range with the BEI of Malaysian public hospitals (234 kWh/m²/year) as studied by Saidur et al. [85]. Interestingly, the BEI value is comparatively lower when compared to the average office's BAEI

in Europe (306 kWh/m²/year) [123] and an office's BAEI in Saudi Arabia (330 kWh/m²/year) [91]. The annual BEI values in 2009 to 2012 are listed in Figure 27. The building needed to reduce its total energy consumption by 46.9% to become an LEO building and 76.9% to become a GEO building. This energy reduction is possible primarily through cooling load reduction.

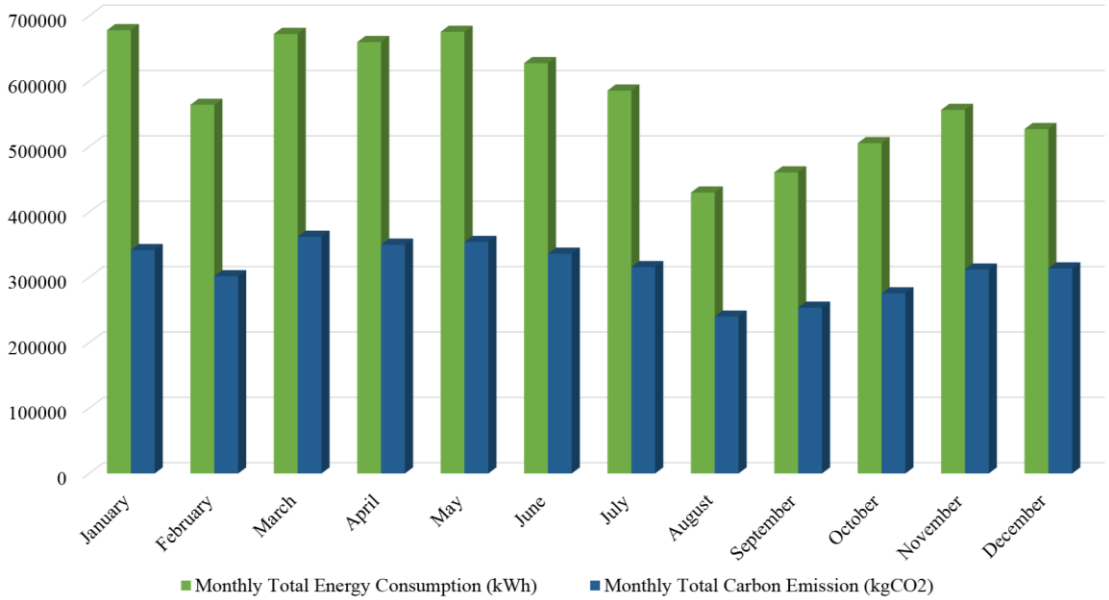

Figure 26: The building's monthly energy consumption and monthly total carbon emission.

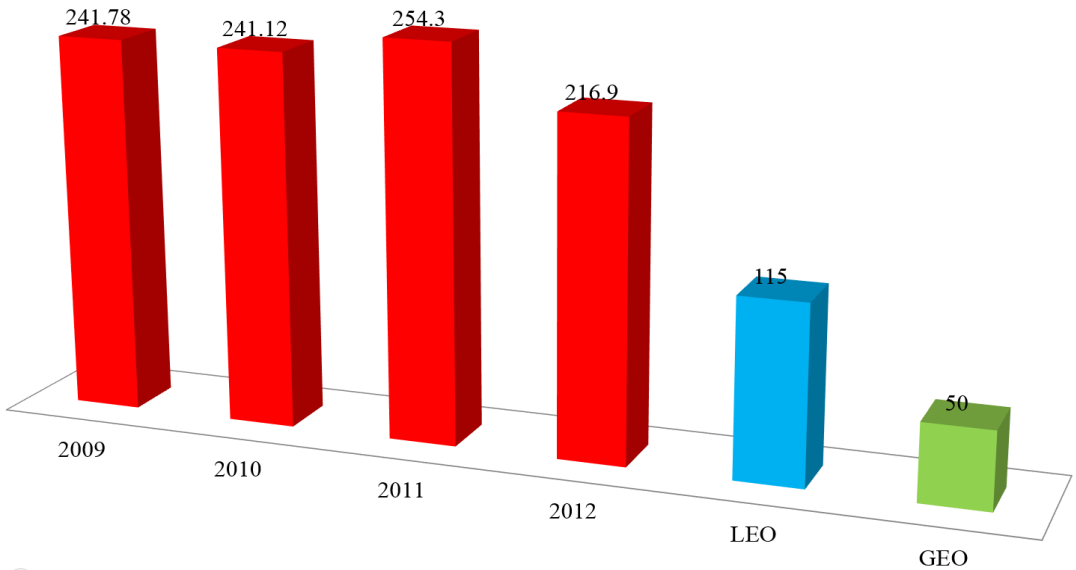

Figure 27: The building annual energy index (BEI) over four years [43][44] compared to BEI for LEO and GEO.

Cooling was responsible for 58.9% of the building total energy consumption [164]. The energy intensity of the cooling system was 127.89 kWh/m²/year that is higher than the BEI benchmark for LEO buildings (114 kWh/m²/year) [57] and passive buildings (120 kWh/m²/year) [171]. The building end-use energy intensity by sectors are shown Table 25. A breakdown of cooling load in every air-conditioned zones (based on a simulation made in Design Builder software) in the building shows that offices consumed majority (78%) of the total building's cooling load then followed by data centre (10%), corridors (6%), cafeteria (3%), IT rooms (2%) and hall and auditorium (1%). The percentage of the annual cooling load in every air-conditioned zones to the building's total cooling load is shown in Figure 28.while the detail value of cooling load in every air-conditioned zones in the building is presented in Table 26.

Table 25: End-use energy intensity by sectors in 2012 [163][164].

	End-use Energy Consumption	
Sectors	Energy intensity (kWh/m²/year)	Percentage of total energy (%)
Cooling system	128	58.9
Lighting	62	28.6
General sockets	15	6.9
Data centre	12	5.5

Table 26: Annual cooling load in different cooling zones based on simulation made in Design Builder software.

Cooling zones	Annual cooling load (kWh)
Offices	3,199,514
Data centre	402,493
Corridors	238,284
Cafeteria	147,128
IT rooms	67,799
Hall and Auditorium	25,963
Total	4,081,181

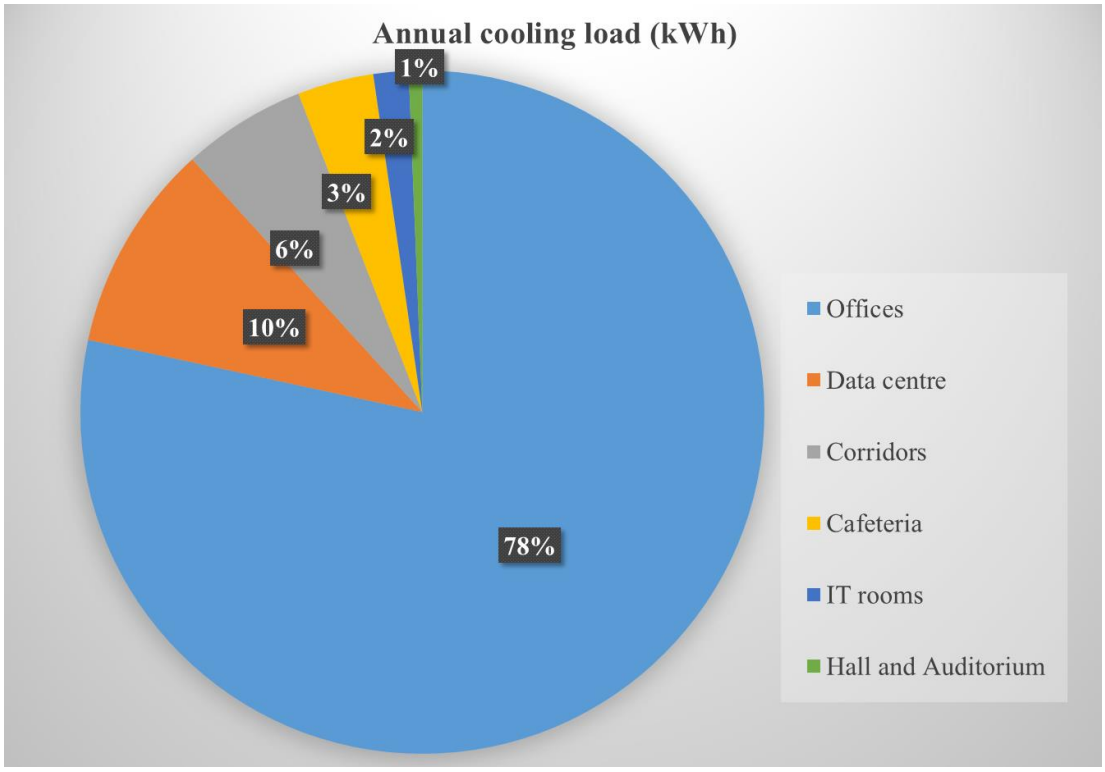

Figure 28: The percentage of the annual cooling load in different air conditioned zones in the building to the total building's cooling load. The data were based on a simulation made in Desgin Builder.

3.1.2.4 Indoor environmental measurements

A set of indoor lux, air temperature, relative air humidity and carbon dioxide measurements were taken at seven different zones on each floor during the building energy audit conducted by IEN Sdn Bhd. The readings were compared to the indoor environmental quality requirement set in MS1525:2014 and DOSH. The suggested indoor environmental values were listed in Table 27 while the recorded measurement at the offices is presented in Table 28 and Table 29.

Table 27: Indoor environmental guidelines by MS1525:2007 and DOSH for office space.

Type	Suggested Value	Guidelines
Lux	300 – 400 lux	MS1525:2014
Air Temperature	23°C – 26°C	MS1525:2014
Air Humidity	55% – 70%	MS1525:2007
Carbon Dioxide	< 1000	DOSH

Table 28: The indoor illumination level, air temperature, RH and carbon dioxide measurement in offices on the ground floor, Level 1, 2, 3 and 4.

Area	Location point	Luminance (lux)	Temperature (°C)	Relative humidity (%)	CO_2 (ppm)
Office GF	B	316	22.1	56.7	725
	C	256	21.7	58.8	711
	D	354	23.9	61.2	645
	E	152	23.3	50.1	643
	F	498	25.3	60.5	632
	Average	315.2	23.3	57.5	671
Office L1	B	231	24.3	61.3	662
	C	205	22.2	65.2	599
	D	230	23.5	59.1	677
	E	170	23.6	69.2	690
	Average	209	23.4	63.7	657
Office L2	B	372	23	65	710
	C	314	22	66	645
	D	334	22	65	634
	E	299	23	64	716
	F	327	22	64	680
	Average	329.2	22.4	64.8	677
Office L3	B	235	23	62.3	752
	C	356	23	60.7	787
	D	352	22	60.4	762
	E	350	23	59.8	752
	F	202	21	60.6	795
	Average	299	22.4	60.7	770
Office L4	C (daylight)	390	23.1	66.7	539
	D	202	21.5	60.2	569
	E	186	21.1	65.9	589
	F	200	21.4	62.8	638
	Average	244.5	21.8	63.9	583

Table 29: The indoor illumination level, air temperature, RH and carbon dioxide measurement in offices at level 5, 6 and 7.

Area	Location point	Luminance (lux)	Temperature (°C)	Relative humidity (%)	CO_2 (ppm)
Office L5	C	276	22.2	64.7	564
	D	256	21.8	67.3	595
	E	292	21.9	67.8	732
	F	124	22.5	67.3	665
	Average	237	22.1	66.8	639
Office L6	B	199	21.2	71.6	591
	C (daylight)	216	22.8	68.4	597
	D (daylight)	377	23.7	65.4	646
	E	295	22.1	65.4	622
	F	193	23.3	66.4	593
	Average	256	22.6	67.4	609.8
Office L7	B (daylight)	204	22.1	68.8	601
	C	335	22.2	66.3	588
	D	350	21.8	68.1	556
	E	210	23.8	61	649
	F	196	21	70.2	574
	Average	259	22.2	66.9	593.6

From the data collected, room temperatures in 23 out of 40 zones in the whole building were lower than the room temperature suggested by MS1525:2014 [143] even though no negative feedback were made to the energy manager related to the room temperature. Meanwhile, the luminance measurements in 24 zones were lower than minimum requirement and 2 zones exceeded the maximum requirement. Only 14 out of 40 zones fell in the right lux requirement. The air humidity level at two zones exceeded the maximum requirement by less than 1.6%. Meanwhile, the carbon dioxide level in the whole building was below the maximum limit stated by DOSH. Table 30 shows the comparison of measured luminance level in the building's common areas and the suggested luminance by MS1525:2014 [142].

Table 30: A comparison of measured luminance level at the building's common areas and the suggested levels by MS1525:2014.

Area	Average luminance	
	Recorded (lux)	Guidelines (lux)
Cafeteria	279.5	200
Parking area B	99.3	50
Parking area LG	89.5	50
Lift lobby B	90	100
Lift lobby cafeteria	78	100
Lift lobby LG	372	100
Lift lobby GF	446	100
Lift lobby L1	430	100
Lift lobby L2	502	100
Lift lobby L3	503	100
Lift lobby L4	396	100
Main lobby GF	357	150
Corridor (windows area) L2	21000	100
Corridor (windows area) L3	25001	100
Corridor (windows area) L4	14840	100

Based on the recorded measurements, all of the areas have higher luminance exposure compared to the suggested luminance levels. These areas are exposed to sunlight during the daytime which resulted in high luminance level. Incorporating automatic daylight dimmer at these areas will contribute to energy reduction for the building in the lighting sector.

3.1.3 Summary

The building's owner and energy manager show a continuous commitment to reducing the building's energy consumption. Based on the data analysed, 87.5% of the total building's energy consumption were spent on air conditioning and lighting system. These two sectors are responsible for delivering a good indoor environment to the occupants. However, the indoor air temperature in the offices and luminance level in the building's areas can be improved to adhere to the local indoor environment guidelines as discussed in Section 2.5. Since the building used 7,334,630 kWh energy a year to support its operation, a deep retrofit is required to enable the

building to achieve net ZECB. This objective is achievable by reducing the building's energy dependent then powering it with renewable energy generated on-site. Further study on methods to achieve net ZECB for the target building were carried out through virtual building simulation. Hence, a model of the target building is built in Design Builder software (using the data gathered from building's energy audit) for further analysis to achieve the objective. The development of the model is presented in Section 3.3 and the methods used to achieve net ZECB are shown in Chapter 4.

3.2 Development of the baseline building model

3.2.1 Introduction

A model of the case study building was constructed using the Design Builder software version 4.2.0.034. It is a complete Graphical User Interface to the Energy Plus simulation engine (from US DOE) which has been intensively used for building modelling in previous research [90][129][154][172][173][174]. It provides an intuitive interface and high-resolution data output on energy consumption, carbon emissions, occupant comfort, and daylight availability [160].

3.2.2 Methods

In this study, the input data listed below was collected by the help from building's facility management and onsite visits to ensure the model reflects the actual building in:

- Geometry: The building's floor plan, geometry and fabric (derived from architect's drawings (see Figure 29, Figure 31 and Figure 30). DXF files created from the architect's drawings (AutoCAD) to import into Design Builder [173].
- Equipment data: Power rating, operation's schedule, equipment quantity in every office floor.
- Lighting: lux measurement, operation's schedule, lamp and luminaire types.
- Occupancy in every floor: number of occupants, type of activities and schedule. It was assumed that all occupants used the equipment and occupied the building at all time during working hours (0830 to 1730) and 50% of the occupants occupied the building at 0700 to 0830 and during recess hour (1300 to 1400). Variation in occupants' behaviour such as opening windows or doors was not taken into account since there isn't any actual data for it.
- Local weather data was collected from Malaysia Meteorological Department [165] and ASHRAE global weather repository provided in Design Builder software [160].
- HVAC system: the building HVAC system schematic drawing, HVAC system and chiller's COP, the average zone's temperature measurement for every office floor and average chilled water temperature for every AHU's was extracted from the building audit reports prepared by facility management [163][164].

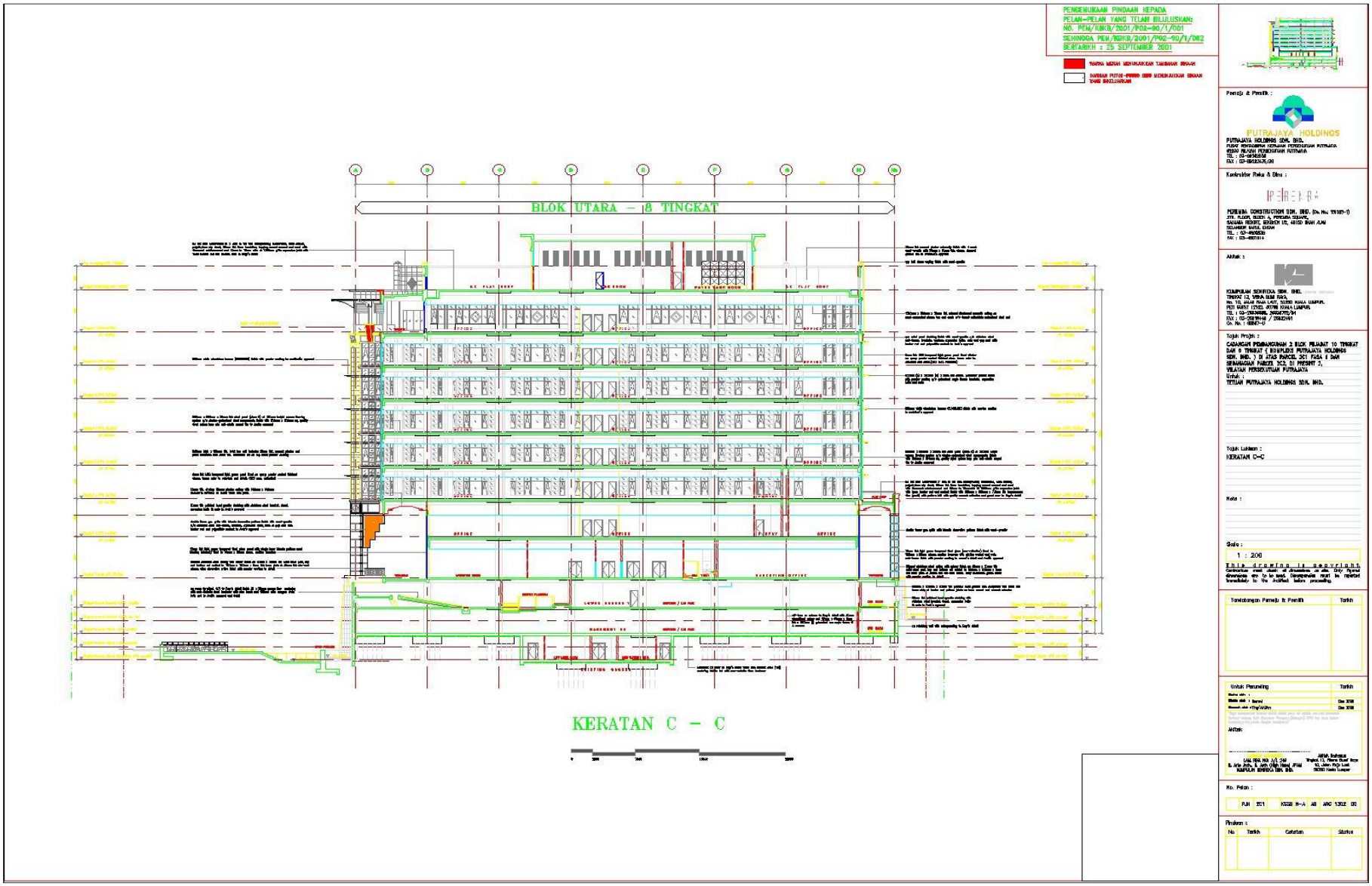

Figure 29: The building's C-C cross section drawings obtained from the energy manager.

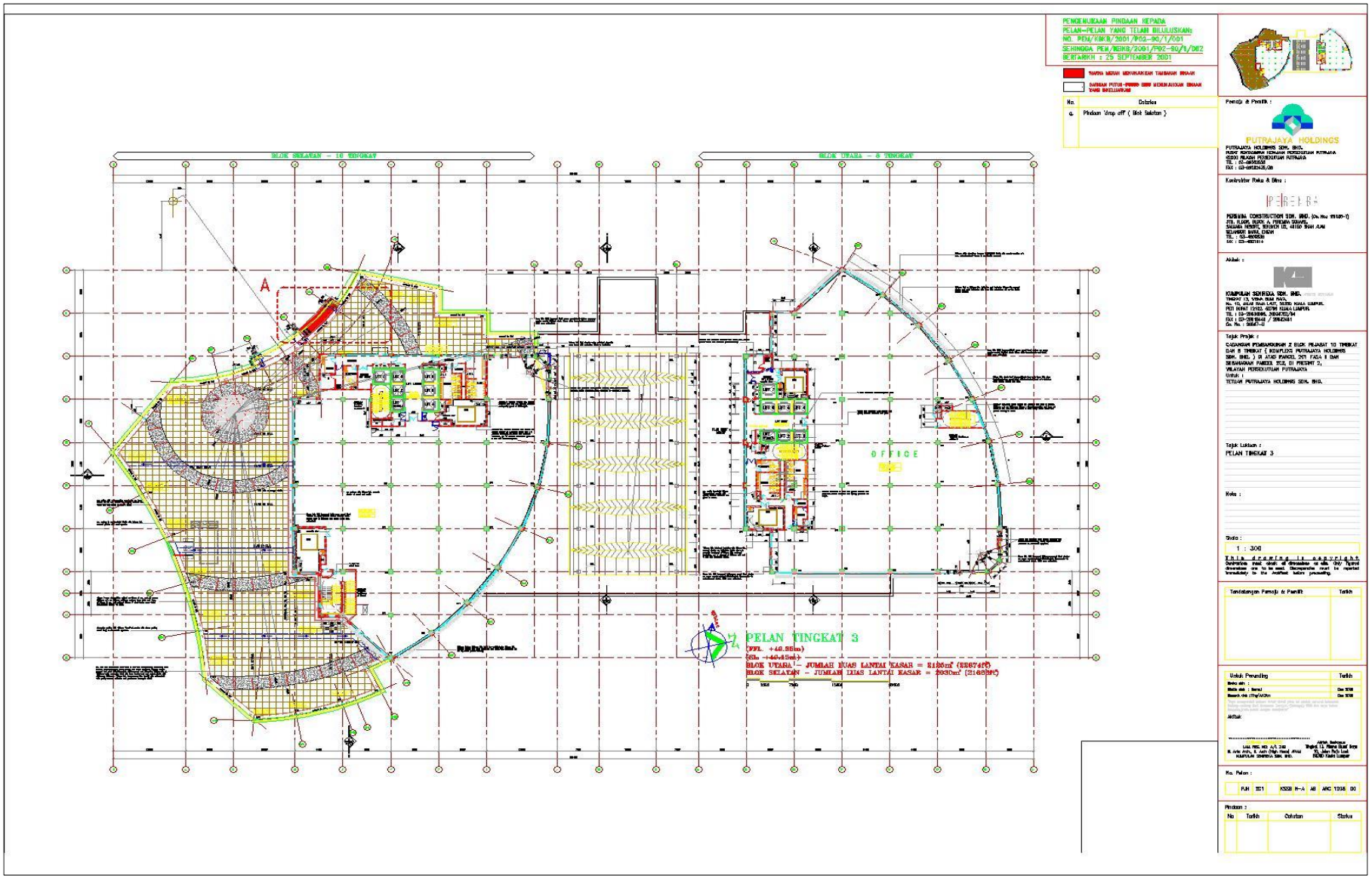

Figure 30: The floor plan of target building's level 3 obtained from the energy manager.

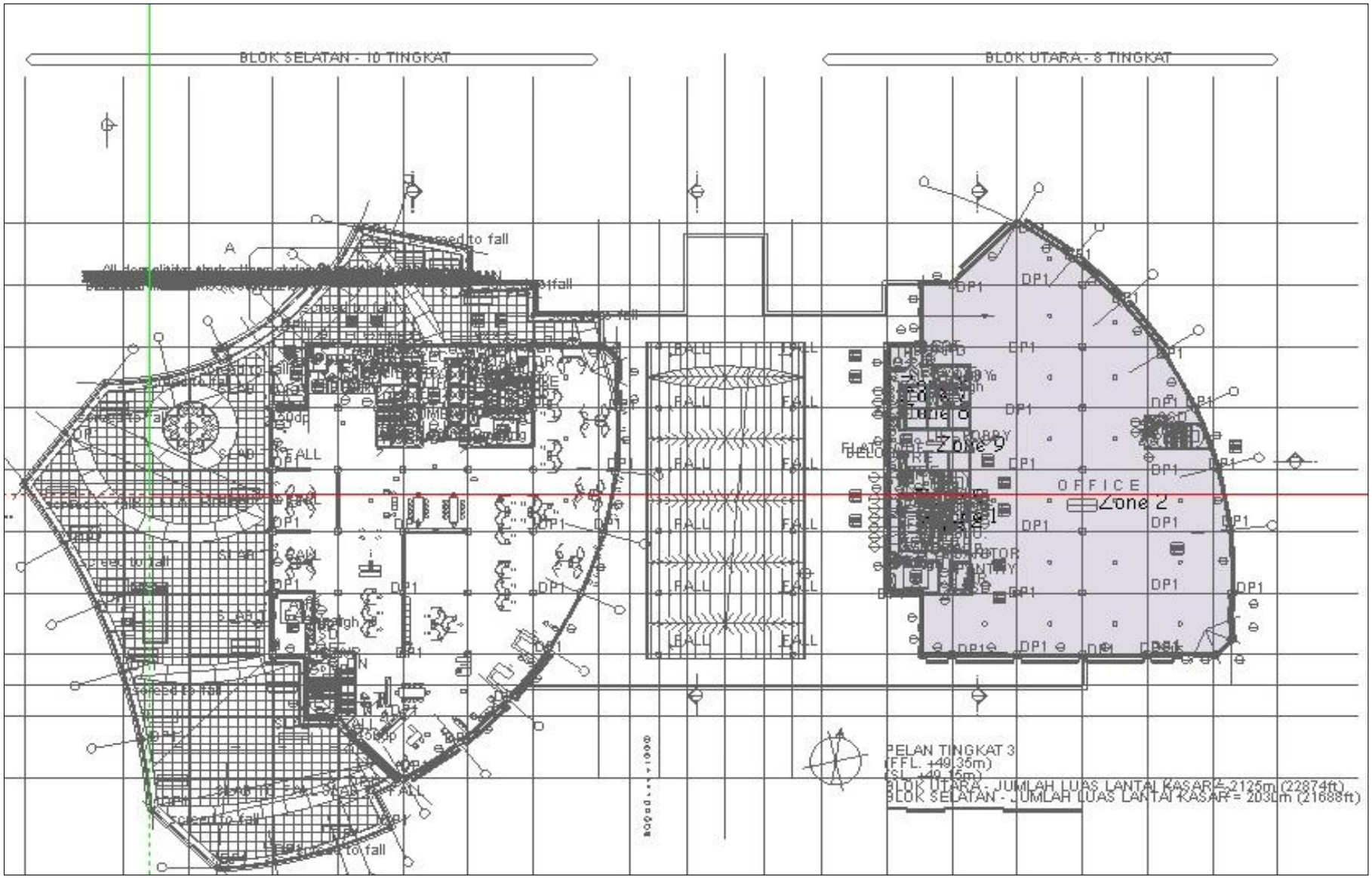

Figure 31: The floor plan of target building's ground floor imported to DXF file in design builder software.

Modelling complex buildings involves inaccuracies and errors due to various input requirements and limitations [172][173]. Studies on building modelling presented ways of increasing the model's prediction accuracy [172][173] and ASHRAE Guide 14 [175] is an established method for measuring a model's accuracy [90][110][172][173]. It is suggested that with instances of monthly data, a building is considered accurate if the CV(RMSE) for monthly values is below ≤+15% and MBE of monthly values is within ±5% [175]. If these tolerances are met, EnergyPlus was demonstrated to be capable of predicting space air temperatures within zones of interest with an accuracy of ± 1.5°C for 99.5% of the time [172].

This software simulates the total energy for the cooling system as 'district cooling' while the building's chilled water was supplied by a district cooling plant. Hence, the actual energy consumption by the cooling system was calculated using equation (3.4) where the monthly electric consumption by the cooling system ($EL_{CS(kWh)}$) is calculated using Equation (3.5). Equation (3.6) calculates CV(RMSE) and equation (3.7) calculates MBE between the simulated and actual results [172]. Model parameter inputs were refined until the tolerance range was met.

$$ACC = EL_{CS(kWh)} + E_{CW\,(kWh)} \quad (3.4)$$

$$EL_{CS(kWh)} = Cp \times \Sigma AELC \quad (3.5)$$

$$CV(RMSE) = \frac{\sqrt{\sum_{i=1}^{N_i} [(M_i - S_i)^2 / N_i]}}{\frac{1}{N_i} \sum_{i=1}^{N_i} M_i} \quad (3.6)$$

$$MBE = \frac{\sum_{i=1}^{N_i} (M_i - S_i)}{\sum_{i=1}^{N_i} M_i} \quad (3.7)$$

Where:

Annual cooling consumption (ACC)

Cooling system's electric consumption in kWh ($EL_{CS(kWh)}$)

Total annual electricity consumption (ΣAELC)

Ratio of cooling system's electricity consumption per total building's electricity (Cp)

Coefficient of variation of the root mean square (CV (RMSE))

Mean bias error (MBE)

Actual monthly energy consumption (M)

Simulated monthly energy consumption (S)

Number of months (N)

3.2.2.1 Building simulation software

This section discussed the building simulation software that is used in this study. Section 3.2.2.1.1 discussed the primary reason for choosing the software, Section 3.2.2.1.2 discussed the EnergyPlus simulation tool and Section 3.2.2.1.3 discussed Design Builder software (a graphical user interface that was used as an interface to EnergyPlus simulation engine).

3.2.2.1.1 Review of building simulation software.

A highly cited review article of existing building simulation software published by D. B. Crawley et al. [176] was used as the main reference in determining the choice of software to be used in this study. D. B. Crawley et al. compares 20 main building energy simulation software regarding their features and capabilities. The comparison was made based on the vendor-supplied information. Table 31 shows the comparison of the number of features available in every software compared to the total features being analysed in Crawley et al. Meanwhile, Table 32 compares a number of renewable energy (RE) systems, pre-configured systems and discrete HVAC components available in the each software. Based on the information published by Crawley et al. it was found that Energy Plus offered the highest number of features in terms of:

- Zone loads;
- Building envelope, daylighting and solar (BDS);
- Infiltration, ventilation and multi-zones airflow (IVAAF);
- HVAC systems (HVAC) and;
- Economic evaluation.

Meanwhile, regarding renewable energy systems and Discrete HVAC components, TRNSYS offered the highest number of systems and components compared to other software then followed by EnergyPlus. In this study, 5 main features mentioned above are the main priority. Hence Energy Plus was chosen as the simulation tool and Design Builder software was used as the user interface software for EnergyPlus.

Table 31: The comparison of the number of features available in every software [176].

Software	Zone loads	BDS	IVAAF	HVAC	Economic Evaluation	Total features available
BLAST	4	2	1	1	0	8
BSim	4	3	6	1	3	17
DeST	6	3	7	2	3	21
DOE-2.1	5	1	1	0	4	11
ECOTECT	3	1	1	1	1	7
Ener-Win	4	1	3	1	1	10
Energy Express	6	0	1	1	2	10
Energy-10	2	1	1	0	1	5
EnergyPlus	8	8	6	2	4	28
eQUEST	4	2	2	0	4	12
ESP-r	5	6	8	2	1	22
IDA-ICE	7	4	4	2	2	19
IES<VE>	9	0	7	2	3	21
HAP	4	5	1	1	3	14
HEED	6	1	1	1	4	13
PowerDomus	4	2	5	1	4	16
SUNREL	3	2	5	1	0	11
Tas	8	4	6	1	2	21
TRACE	5	6	1	1	4	17
TRNSYS	5	3	6	2	4	20
Overall features being compared	9	9	9	2	4	33

Table 32: Comparison of the number of renewable energy systems, pre-configured systems and discrete HVAC components available in the each software [176].

Software	RE systems	Pre-configured systems	Discrete HVAC components	Total available
BLAST	1	14	51	66
BSim	2	14	24	40
DeST	2	20	34	56
DOE-2.1	1	16	39	56
ECOTECT	4	0	0	4
Ener-Win	0	16	24	40
Energy Express	0	5	8	13
Energy-10	2	7	15	24
EnergyPlus	4	28	66	98
eQUEST	2	24	61	87
ESP-r	7	23	40	70
IDA-ICE	1	32	52	85
IES<VE>	3	28	38	69
HAP	0	28	43	71
HEED	0	10	7	17
PowerDomus	1	8	15	24
SUNREL	2	1	3	6
Tas	2	23	26	51
TRACE	0	26	63	89
TRNSYS	12	20	82	114
Total systems identified	12	34	98	144

3.2.2.1.2 Energy Plus

EnergyPlus combined the best feature from Blast and DOE-2 and were built based on recommendations from users and developers about their needs in energy simulation. The software was developed by the developer of DOE-2 program Lawrence Berkeley National Laboratory, and

the developers of DOD's BLAST program (U.S Army Construction Engineering Laboratory and University of Illinois) [177].

The underlying concept used in EnergyPlus is Integrated Simulation where it simulates two main simulation types (heat and mass balance simulation (HMBS) modules and building systems simulation manager (BSSM)) simultaneously. The HMBS module calculates thermal and mass loads based on the time step. Once the HMBS was completed the system will call for the BSSM. BSSM will handle the communication between the heat balance engine and the HVAC system. BSSM also manages data communication between building systems modules (such as HVAC system and electrical system), the building description and the calculation results. The whole EnergyPlus workflow structure is shown in Figure 32. The workflow figure was taken from a journal published by ASHRAE that discussed EnergyPlus software. In HMBS, the room surfaces such as walls, windows, ceiling, and floors have uniform surface temperatures, uniform long and short wave irradiation, diffuse radiating and reflecting surfaces and internal heat conduction [177].

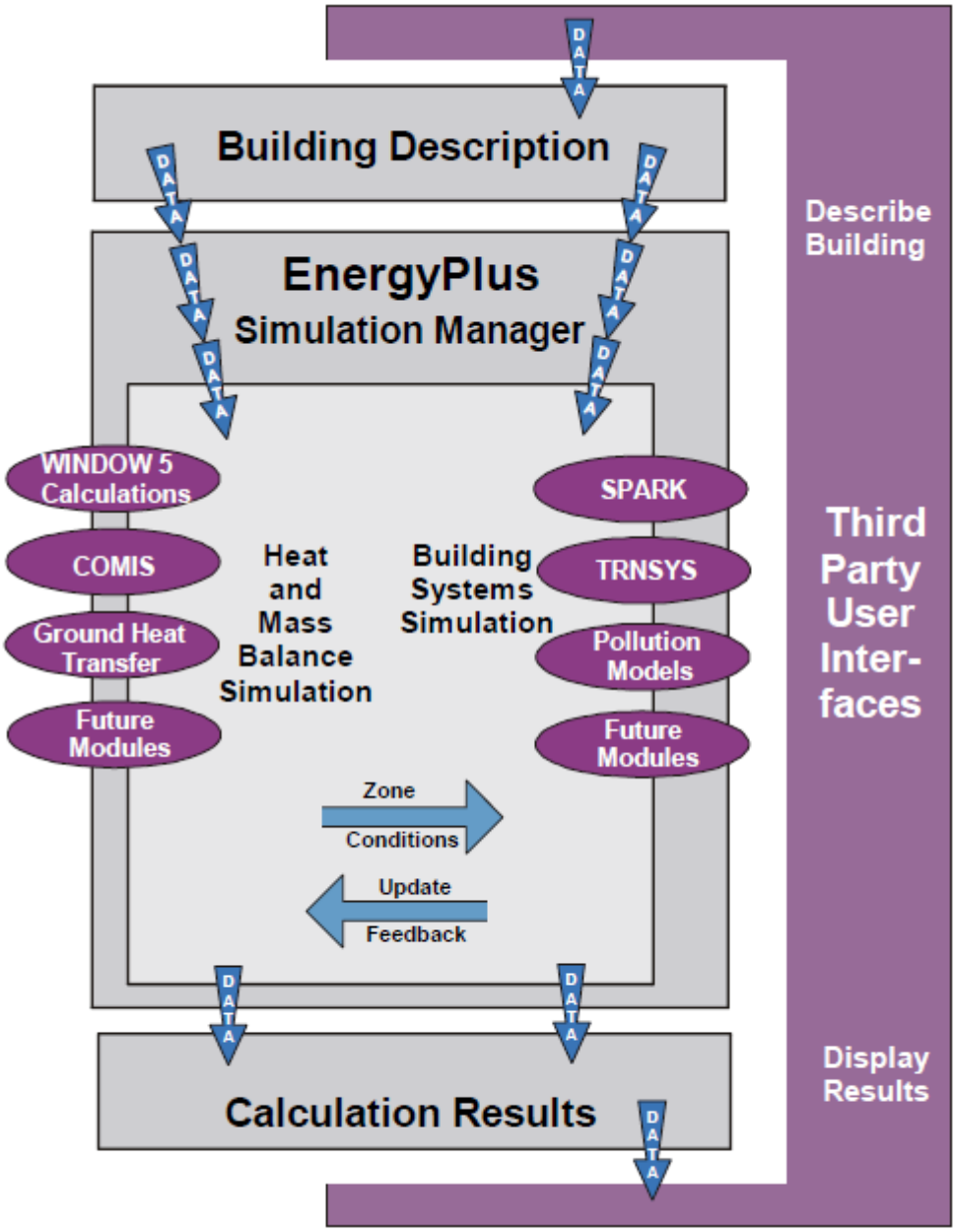

Figure 32: Overall EnergyPlus structure as published in ASHRAE Journal 42 [177].

3.2.2.1.3 Design builder software

Design Builder software is a complete Graphical User Interface to the Energy Plus simulation engine (from US DOE). The first version was launched in 2005 and had been under continuous development. It is intensively used for building modelling in previous research [90][129]

[154][172][173][174]. It provides an intuitive interface and high-resolution data output on energy consumption, carbon emissions, occupant comfort, and daylight availability [160].

It provides easy to use software and high-quality data for building assessors and building designers on energy consumption, carbon emissions, occupant comfort, daylight availability and status of the construction based on national building regulations and certification standards. The software is also a leading provider of Energy Performance Certificates and Building Regulations Compliance checking software in the UK, France, Ireland, and Portugal [71]. It enables the users to construct a building's model adjacent to the original building's specification. Various types of templates, construction materials, equipment and suggested schedule based on ASHRAE standard are included in the library. The user can also itemize the building's model based on the actual practice by adding a new template. There are eight main sectors to control the specification of the building model and simulation (see Table 33).

Table 33: Control Section in Design Builder

Control Section	Description
Activity	Enable the user to specify the occupancy in different zones, occupants' metabolic rate and clothing, holidays, environmental control (such as the heating and cooling set point, humidity, minimum fresh air and luminance level), power density and operational schedule for computers, office equipment, and catering.
Construction	The construction section allows the user to identify the building's materials. A selection of different type of materials is available in the library, or the user can create a new material's file based on the actual material's specification. The user can determine the building's air tightness. The readymade template was also available based on established building's regulations. The estimated cost of the building's construction was calculated based on the material's cost.
Openings	This section enables the user to state different types of opening such as the window, sky-roof, doors, and ventilation. The user can add shading to the windows with choices of window shading or local shading.
Lighting	The software enables the user to choose different lighting templates available in the library or add a new lighting template, and specify the power density, luminaire type, radiant fraction, visible fraction and lighting control.
HVAC	The type of HVAC system can be selected from the HVAC templates' library, or the user can customize the HVAC system based on the actual model. Another specification such as mechanical ventilation, auxiliary energy, heating, cooling, humidity control, district hot water, earth tube, natural ventilation, air temperature distribution, and cost can be itemized too.
Generation	This section allows the user to include on-site electricity generation ranging from the photovoltaic solar panel and wind turbine.
Output	The output options allow the user to select simulation output for heating design, cooling design, energy performance, thermal comfort and daylight. The air contaminant simulation is not provided by the software.
CFD	The software also allows the user to run computational fluid dynamic in the building by specifying the boundary condition.

3.2.2.2 Parameter Input

The case-study building consists of 123 conditioned zones listed in Table 34 spread across 40,477m² building's area. The complexity of the building requires a detailed data acquired from the building's audit reports, interviews and constant contact with the building's energy manager to reduce the level of uncertainties. Some changes in the building's geometry were also made to simplify the model. That is, only the communal areas in the South building were included in the building's model. Hence, the South building in the building model appears to have three-floor levels (lower ground, underground and ground floor) whereas, in reality, it has 12 floors (including two underground floors and a ground floor).

Table 34: The conditioned zones in the case-study building.

Floor	Total area (m²)	Zone
Lower Ground	9310	Parking space
Underground	9310	Parking space, cafeteria, kitchen
Ground floor (South)	4330	AHU room, auditorium, cold room, kitchen, lifts, corridors, multipurpose hall, toilets (female, male and disabled)
Ground floor (Atrium)	858	Lobby and reception area.
North building (every floor from the ground floor to floor 7)	2078	2 AHU rooms, corridor, IT room, custodian's room, lifts, office, pantry, stairs, toilets (female, executive and male).
Floor 8	205	Machines' room

The building inputs are divided into five main categories, which are occupancy, lighting, HVAC, construction, and openings. Input for very categories is listed in Table 35 to Table 41.

Table 35: List of occupancy density and activity types in every zone.

Floor	Zone	Occupancy density (People/m²)	Activity type
Lower Ground	Parking space	0.0059	Standing/walking
Underground	Parking space	0.0059	Standing/walking
	Cafeteria	0.29	Eating/drinking
	Kitchen	0.11	Food preparation
Ground floor (South)	Auditorium	0.34	Seating
	Multi-purpose hall	0.34	Seating
	Corridors	0.1	Standing/walking
	Kitchen	0.1	Food preparation
	Cold room	0.1	Storage
	Toilets	0.1	Standing/walking
	Data centre	0.1	Light office work/standing/ walking
	AHU room	0.1	Light manual work
Ground floor (Atrium)	Lobby	0.1	Standing/walking
	Reception area	0.1	Standing/walking
North building (ground floor to floor 7)	AHU rooms and Custodian's room	0.1	Light manual work
	Lifts	0.1	Standing/walking
	Office ground the floor	0.02	Light office work/standing/ walking
	Office floor 1	0.04	
	Office floor 2	0.02	
	Office floor 3	0.05	
	Office floor 4	0.02	
	Office floor 5	0.04	
	Office floor 6	0.03	
	Office floor 7	0.02	
	Pantry	0.3	Eating/drinking
	Stairs	0.1	Standing/walking
	Toilets	0.24	Standing/walking
	Corridors	0.1	Standing/walking
	IT rooms	0.1	Standing/walking
Floor 8	Light plant room	0.01	Light manual work
Whole building		0.10606	

Table 36: Lighting consumption and luminaire type in every zone.

Floor	Zone	Lighting consumption (W/m^2)	Luminaire type
Lower Ground	Car park	1	Surface mount
Underground	Car park	1	Surface mount
	Cafeteria	15	Recessed
	Kitchen	8	Surface mount
Ground floor (South)	Auditorium	8	Surface mount
	Multi-purpose hall	8	Surface mount
	Corridors	4.6	Suspended
	Kitchen	8	Surface mount
	Cold room	none	None
	Toilets	5	Recessed
	Data center	5	Recessed
	AHU room	5	Surface mount
Ground floor (Atrium)	Lobby	7	Surface mount
	Reception area	4.6	Surface mount
North building (ground floor to floor 7)	AHU rooms and custodian's Room	7	Surface mount
	Lifts	9	Recessed
	Office	7	Recessed
	Pantry	7	Surface mount
	Stairs	7	Surface mount
	Toilets	7	Surface mount
	Corridors	7	Surface mount
	IT rooms	7	Surface mount
Floor 8	Light plant room	7	Surface mount
Whole building		6	

Table 37: Equipment consumption in every zone.

Floor	Zone	Equipment consumption (W/m^2)
Lower Ground	Parking space	0
Underground	Parking space	0
	Cafeteria	3
	Kitchen	59
Ground floor (South)	Auditorium	1.78
	Multi-purpose hall	1.78
	Corridors	0
	Kitchen	43
	Cold room	120
	Toilets	5.48
	Data center	500
	AHU room	0
Ground floor (Atrium)	Lobby	6.19
	Reception area	6.19
North building (ground floor to floor 7)	AHU rooms and custodian's room	0
	Lifts	60
	Office ground floor	14
	Office floor 1	10
	Office floor 2	37
	Office floor 3	41
	Office floor 4	5
	Office floor 5	10
	Office floor 6	10
	Office floor 7	6
	Pantry	60
	Stairs	0
	Toilets	0
	Corridors	0
	IT rooms	50
Floor 8	Light plant room	30
Whole building		36

Table 38: Data input for air conditioning and mechanical ventilation system in every zone.

Floor	Zone	Type	Settings
Lower Ground	Parking space	Mechanical ventilation	2 (ac/h)
Underground	Parking space	Mechanical ventilation	3 (ac/h)
	Cafeteria	KWP Cooling system	26.5 C
	Kitchen	Mechanical ventilation	Min fresh air (sum per person and area)
Ground floor (South)	Auditorium	KWP Cooling system	23
	Multi-purpose hall	KWP Cooling system	23
	Corridors	KWP Cooling system	27
	Kitchen	Mechanical ventilation	min fresh air (sum per person and area)
	Cold room	-	-
	Toilets	KWP Cooling system	-
	Data center	KWP Cooling system	21
	AHU room	-	-
Ground floor (Atrium)	Lobby	Natural ventilation	
	Reception area	KWP Cooling system	24
North building (ground floor to floor 7)	AHU rooms and custodian's room	-	-
	Lifts	-	-
	Office ground floor	KWP Cooling system	23
	Office floor 1	KWP Cooling system	23.5
	Office floor 2	KWP Cooling system	23.5
	Office floor 3	KWP Cooling system	24
	Office floor 4	KWP Cooling system	22.5
	Office floor 5	KWP Cooling system	22
	Office floor 6	KWP Cooling system	22.5
	Office floor 7	KWP Cooling system	21
	Pantry	-	-
	Stairs	-	-
	Toilets	-	-
	Corridors	KWP Cooling system and FCU (for ground floor and 1st floor)	26.7
	IT rooms	KWP Cooling system	21
Floor 8	Light plant room	-	-

Table 39: Input for KWP Cooling system

KWP cooling system	Input
Cooling system type	Constant air volume (CAV)
Auxiliary energy (kWh/m²)	64.18
Cooling system COP	4
Supply air condition (min temperature)	17°C
Min supply air humidity ratio (g/g)	0.009
Chiller	District cooling
Unitary cooling COP	4
Unitary distribution loss	5
Central cooling coil type	Chilled water
Cooling coil set point	13°C
Corresponding outdoor (high temperature)	37°C
Corresponding outdoor (low temperature)	23°C
Air temperature distribution	Mixed
Humidity control	Humidistat min: 55% max: 70%

Table 40: Schedule for the building's main areas.

Zones	Cooling system	Lighting system	Equipment	Occupancy
Offices	Monday to Friday: 0600hours to 1900hours Sunday: Off	Monday to Friday: 0600hours to 1900hours Sunday: Off	0800 - 1730	0800 - 1730
Corridors	Monday to Friday: 0600hours to 1900hours Sunday: Off	24hours	none	0800 - 1730
Data center	24hours	24hours	24hours	24hours
Cafeteria	Monday to Saturday: 0600hours to 1900hours Sunday: Off/Close			

Table 41: Construction design for the building.

Construction	U-value (W/m^2K)	Layers from outer to inner skins and its thickness
Outer wall (atrium and south building)	1.804	[1] Granite 30mm [2] Plaster cement 30mm [3] Brick outer leaf 100mm [4] Brick inner lead 100mm [5] Plaster cement 30mm [6] Granite 30mm
Outer wall (north building)	1.838	[1] Granite 30mm [2] Plaster cement 30mm [3] Brick outer leaf 100mm [4] Brick inner lead 100mm [5] Plaster cement 30mm
Outer wall (north building level 8)	2.221	[1] Plaster cement 30mm [2] Brick outer leaf 100mm [3] Brick inner lead 100mm [4] Plaster cement 30mm
Ground floor	1.7	[1] Granite 30mm [2] Cement plaster 30mm [3] Cast concrete 300mm
Internal floor	2.929	Concrete slab 100mm
Glazing	5.74	[1] Green float glass 8mm [2] Curtain wall, 85% glazed [3] Local shading 1m overhang

3.2.3 Results

The comparison of actual energy usage and simulated energy usage using the ASHRAE Guide 14 shows the building model prediction to be within the acceptance range. The built model is presented in Figure 33, Figure 34, Figure 35 and Figure 36.

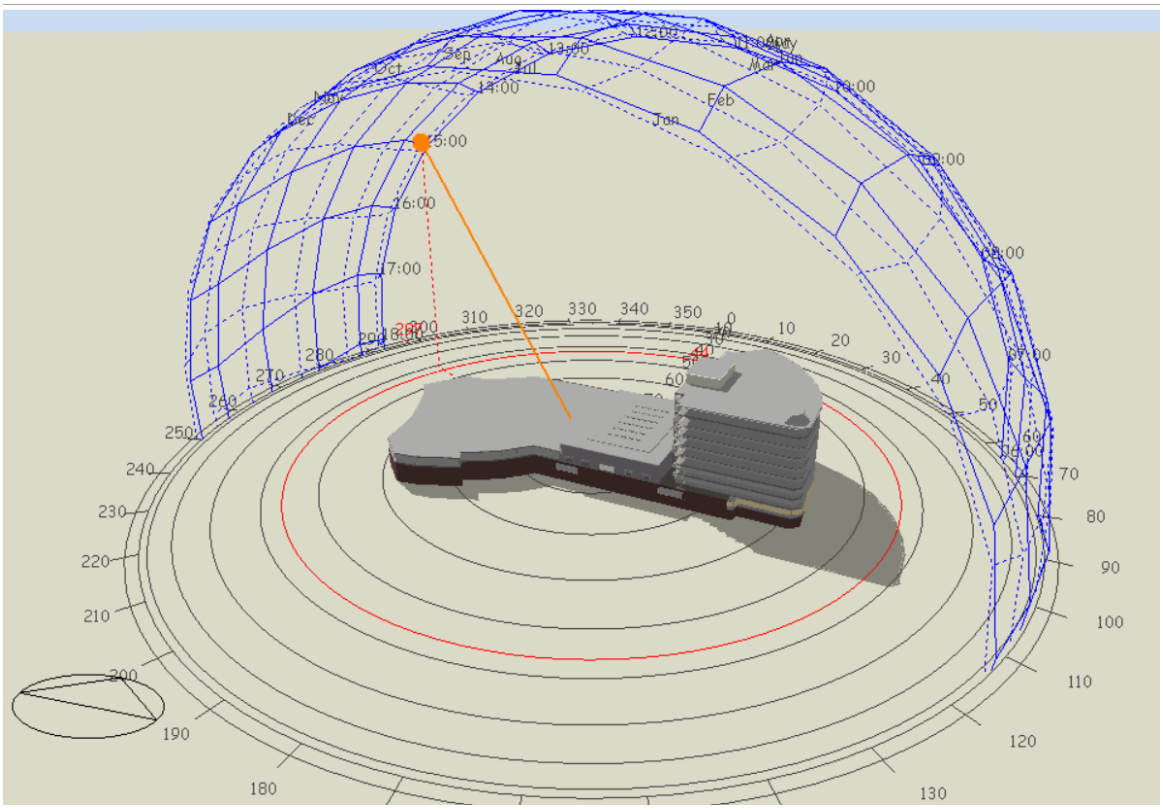

Figure 33: The target building modelled in Design Builder software with detail sun path and shadow.

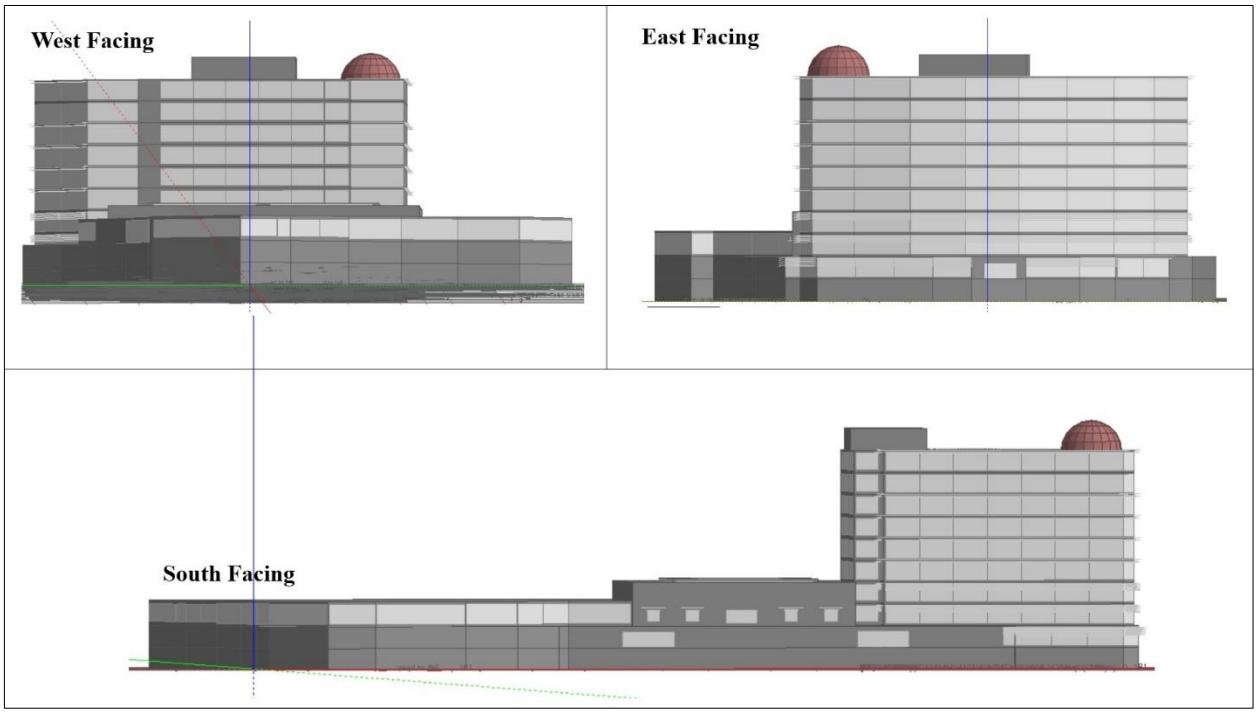

Figure 34: The building model built in Design Builder software.

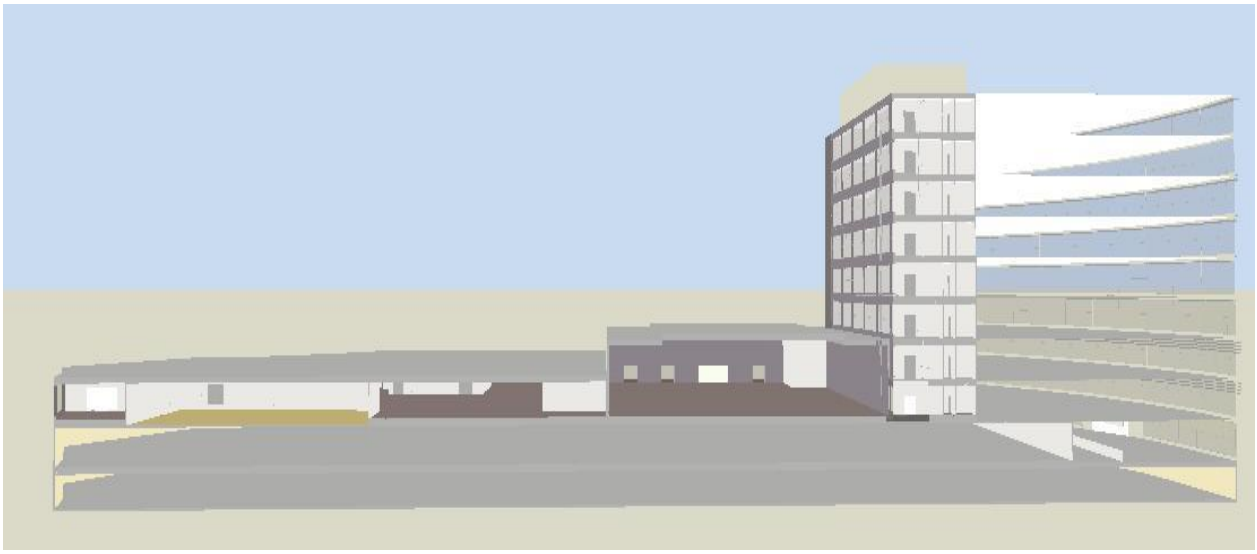

Figure 35: The cross-section of the building model.

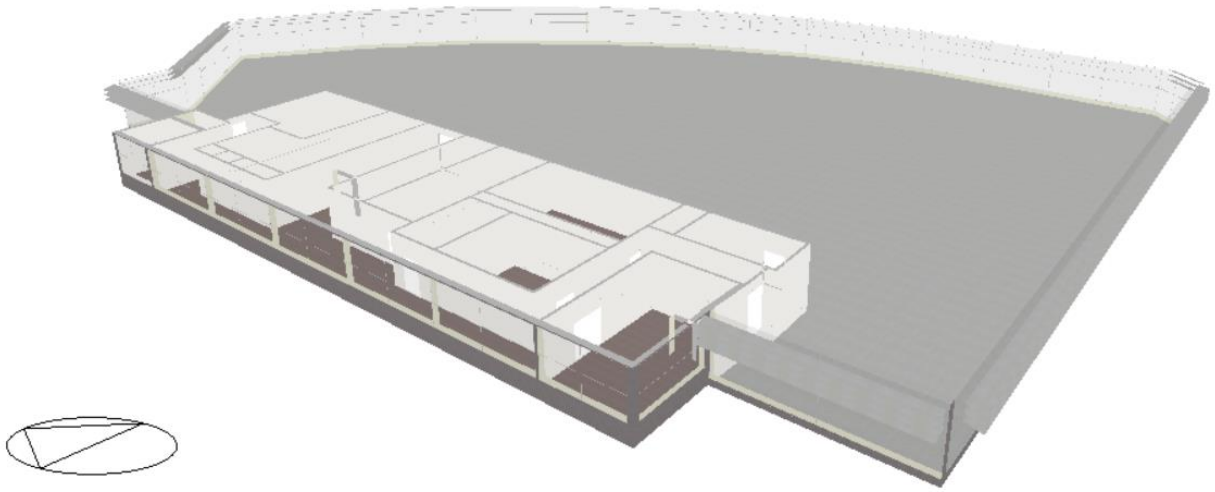

Figure 36: The floor plan of the North Building floors.

The simulated MBE was +1.89% (acceptance criteria is ±5%), and the CV (RMSE) value was 11.09% (less than the 15% requirement). Total energy consumption in 2012 was 7,334,631 kWh while the simulation results predicted it to be 7,195,646 kWh. The comparison of monthly actual and simulated total energy, electricity and energy for cooling usage and its percentage deviation

is shown in Figure 37, Figure 38 and Figure 39. The average energy deviation was +1.29% with the highest deviation on August (over predicted by 20.8%). A summary of the MBE and CV(RMSE) values for the total energy, electricity and energy for cooling is listed in Table 42. The end-use energy consumption by sectors was also compared and presented in Table 43.

Table 42: Summary of the MBE and CV(RMSE) of the total energy, electricity usage and energy for cooling.

	MBE	CV(RMSE)
Total energy usage	1.89%	11.09%
Electricity usage	1.29%	9.65%
Energy for cooling	2.32%	8.03%

Table 43: End-use energy consumption and their deviation.

Type	Actual energy consumption (kWh)	Simulated energy consumption (kWh)	Deviation (%)
Lighting	2,095,081.82	1,791,731.51	14
Equipment	916,931.48	1,166,463.88	-27
Cooling	4,322,616.69	4,221,275.97	2
Total	7,334,629.99	7,179,471.36	2

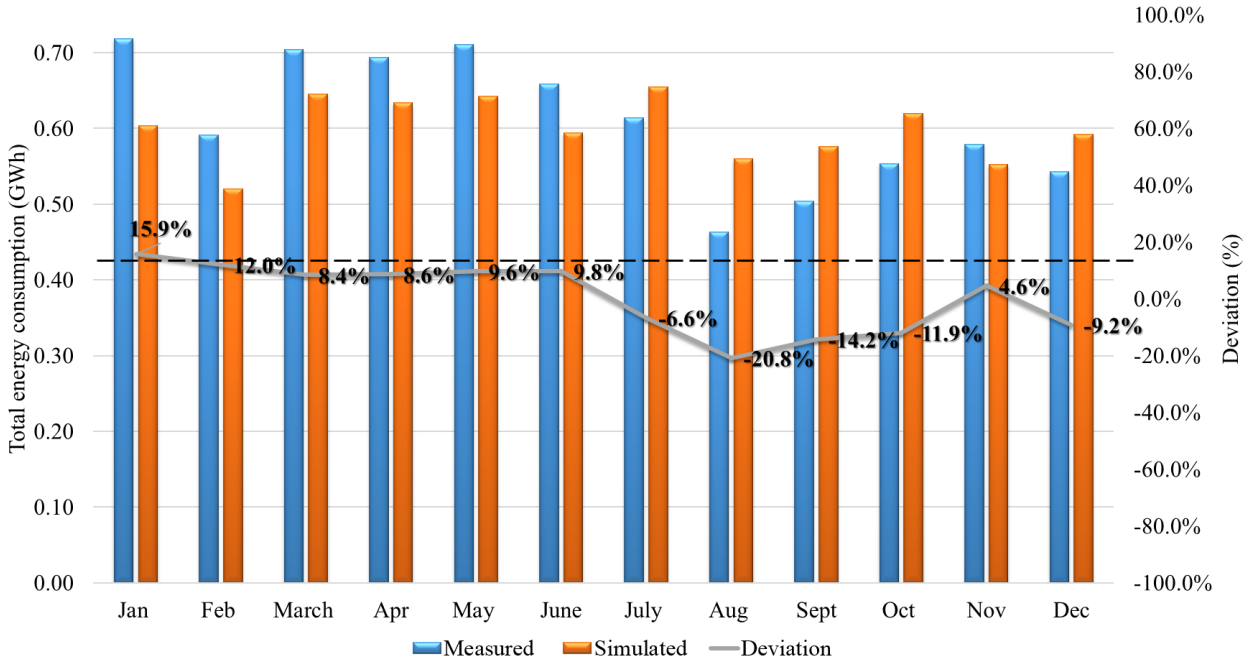

Figure 37: Comparison of the actual and simulated monthly energy consumption.

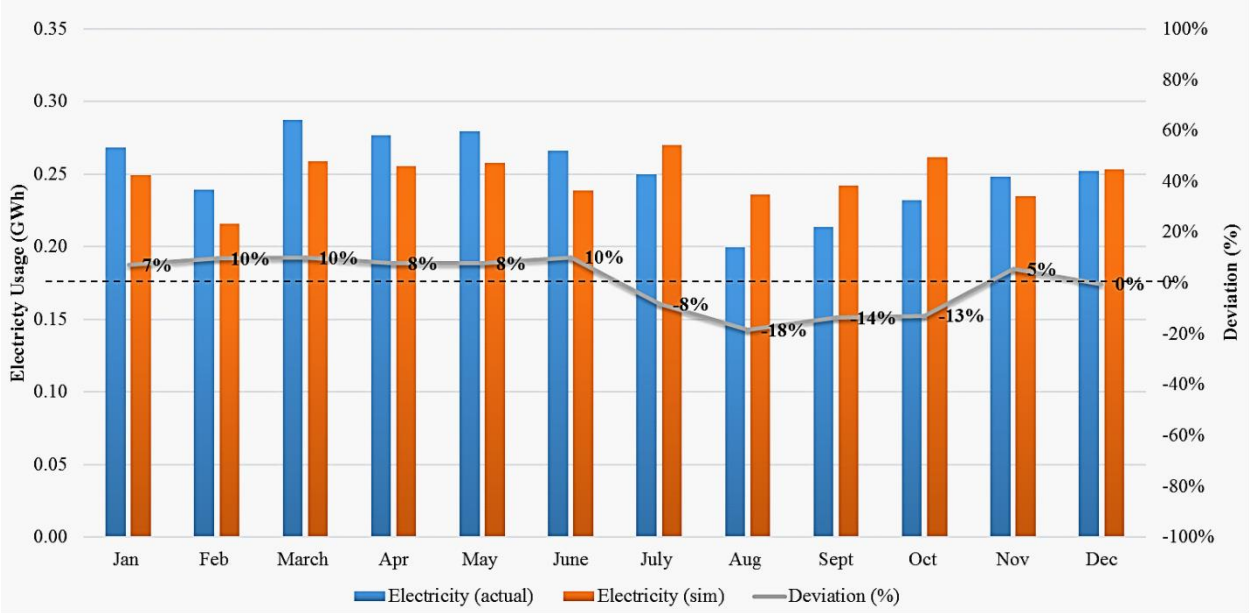

Figure 38: Comparison of the actual and simulated electricity usage.

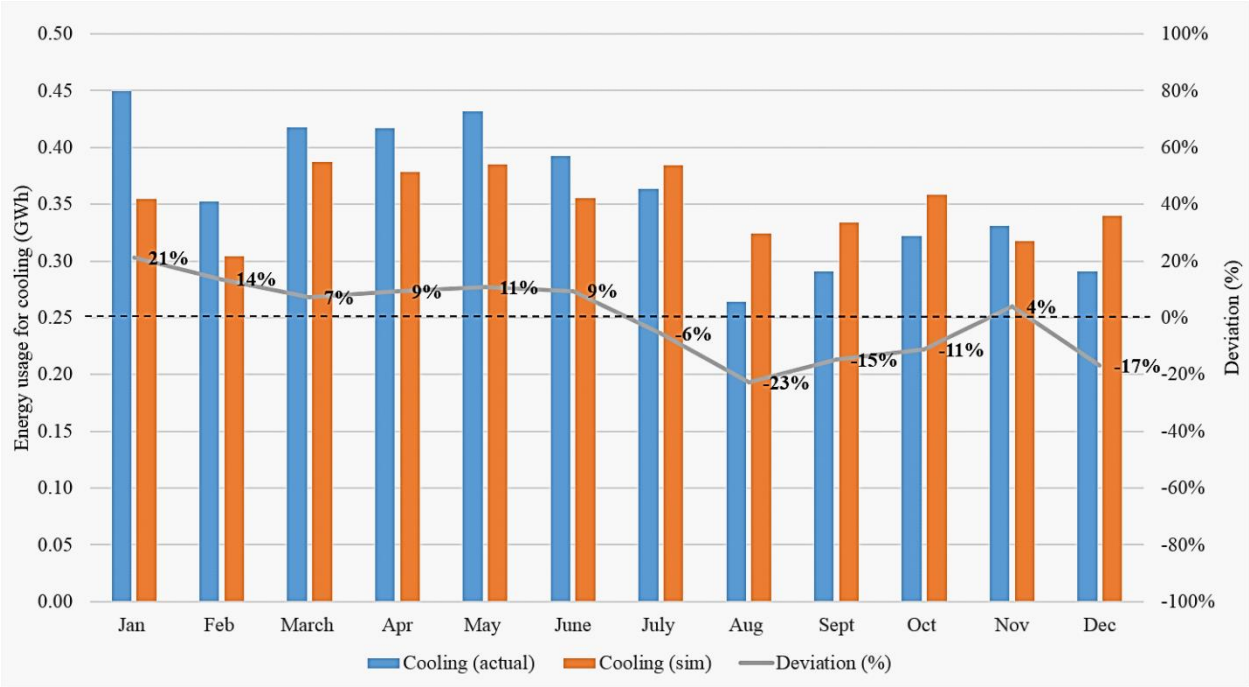

Figure 39: Comparison of the actual and simulated energy usage for cooling.

Further analysis was carried out to figure out the cooling load consumption in different zones. Results are presented in Table 44 and Figure 40. The majority of the cooling demand was originated from the offices (78% of the total building's cooling load) then followed by data centre (10%), corridors (6%), cafeteria (3%), IT rooms (2%) and Hall and Auditorium (1%).

Table 44: Annual cooling load in different cooling zones.

Cooling zones	Annual cooling load (kWh)
Offices	3,199,514
Data centre	402,493
Corridors	238,284
Cafeteria	147,128
IT rooms	67,799
Hall and Auditorium	25,963
Total	4,081,181

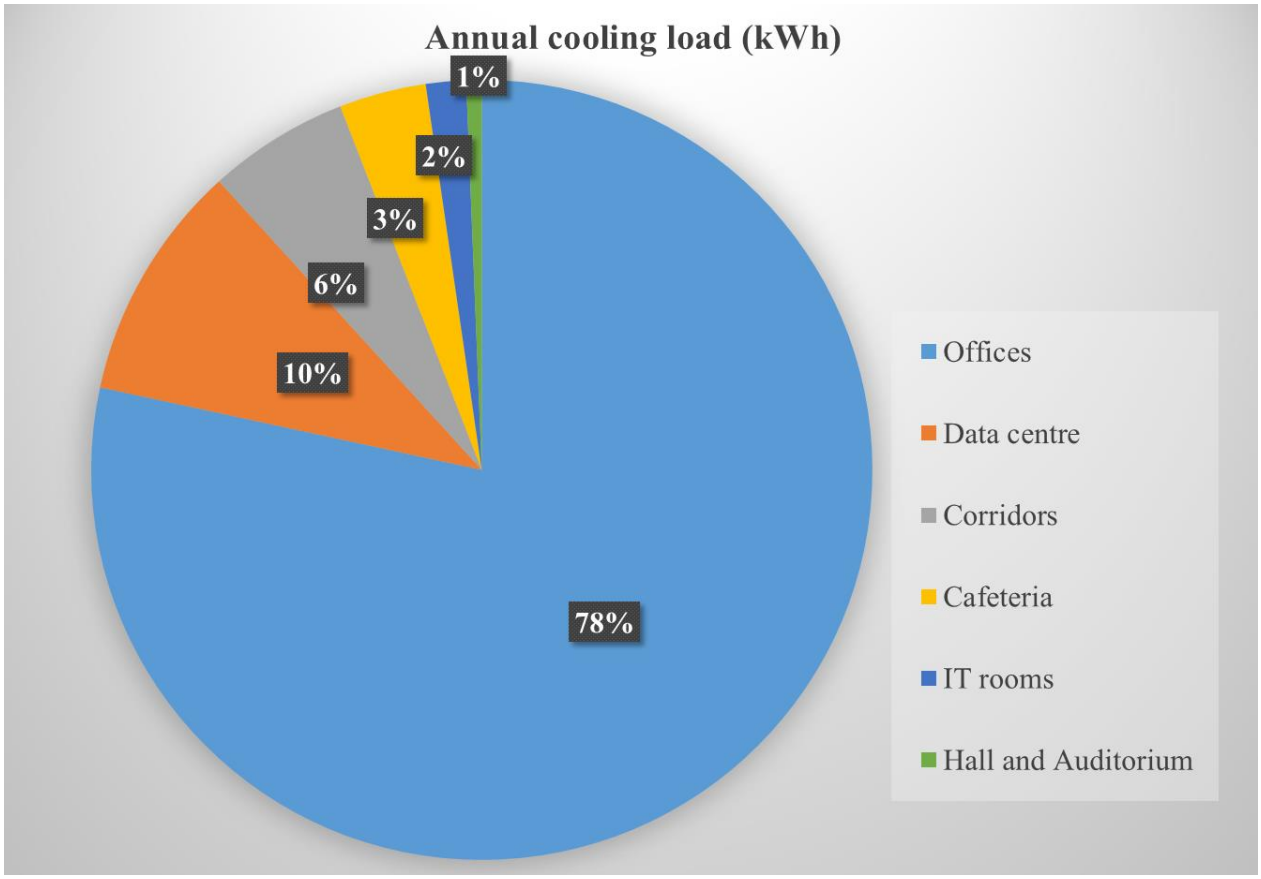

Figure 40: The breakdown of cooling load in different zones.

3.2.4 Discussion and summary

Modelling a complex building involves a greater uncertainty as it involves a large number of zones each with its unique criteria (lighting, envelope, cooling, equipment and occupancy). This building has 123 conditioned zones spread across 40,477 m² building area. Modelling this complex building requires a significant number of details and involves larger uncertainties too.

Minimising uncertainties can increase the model's accuracy. However, uncertainties related to occupants' behaviour (manually controlled equipment and occupancy in the office building) are tough to predict. This statement is supported by the end-use energy deviation analysis, where it shows that sectors that suffer the highest deviation are office equipment (over predicted by 27%) then followed by lighting (under predicted by 14%). For this building, lighting in maintenance rooms such as AHU rooms, IT rooms, machines' rooms, office's pantry and office zones were all manually controlled. The occupancy, equipment and lighting schedule for these zones were set

based on the normal practices as advised by the energy manager while operation and settings for cooling system (under predicted by 2%) are centrally controlled by the facility management.

Other contributors towards the deviation are operational changes throughout the year that gave an impact on the energy usage. In this case study, the building undergoes a renovation in the South building from July to December. During this period, every office floors were emptied, and the energy consumption in the South building' communal area is highly uncertain. Plus, due to a celebration in August, a large number of employees applied for a holiday. These contributed to a greater deviation during that period. While, a detail information from the building's facility management regarding the building's equipment, schedule, floor plan, fabric and average indoor environment settings essentially contributes towards achieving a standardized building model.

In a nutshell, most of the deviation are rooted from the operational control of the sub-systems in the building that were manually controlled, rather than errors in the building (envelope and sub-systems) settings.

Chapter 4. Holistic Approach to Achieve ZECB for an Existing Building

Air conditioning and lighting make up 87.5% of the total building's energy consumption (as shown in Chapter 3) whereas another 12.5% goes to the general socket and data centre. These findings acknowledge the fact that most of the building's energy were spent on ensuring a good indoor environment for the occupants. Previous studies explore the potential of reducing the energy usage in mainly domestic and small size office buildings by the mean of active designs, passive designs or the combination of both that is a holistic design. In this chapter, a holistic approach to achieving a zero energy commercial office building is proposed.

In Section 4.1, 4.2 and 4.3, an isolation approach were presented before combining the three methods together in Section 4.4. The methods are split into four main sections that are:

- Section 4.1 detailing about a passive approach to reduce cooling load (part of this work was submitted to Building and Energy, it is under revision);
- Section 4.2 present a novel retrofit methods to reduce cooling load based on the thermal analysis (part of this work was published in [37] and [38]);
- Section 4.3 presented a solar powered cooling system and;
- Section 4.4 all the three methods were applied to the target building as a whole-building approach.

4.1 Passive designs to reduce cooling load.

4.1.1 Introduction

A building's energy consumption increases as the human's demand for comfort level increases [36][124]. A properly designed building is proven to use less energy compared to typical buildings types [80]. A high-performance building envelope normally has one or more of these attributes: a low thermal conductivity (U-value), higher airtightness and high thermal mass capacity [72][73][80]. These specifications, if employed, can reduce the external heat gain, reduce energy loss from the air conditioned zones to the outer surroundings and provide a good indoor thermal comfort with less energy requirement [72][73][80]. This fact was also acknowledged in the Passivhaus method where the buildings demonstrate how a massive reduction in the building's HVAC requirement can reduce the buildings' energy consumption to a minimum. The Passivhaus concept was developed in Germany to cope with the European cold climate by opting for an airtight and highly insulated construction. The method was aimed at isolating the building from the climate outside and to reduce the building's heat loss [47]. The main strategies employed by Passivhaus are:

- Good levels of insulation with minimal thermal bridges
- Passive solar gains and internal heat sources
- Excellent level of airtightness
- Good indoor air quality

The methods have been proven successful in cold regions, but will it applicable to tropical and arid regions that experience warm temperatures the whole year round? It was also mentioned by the Passivhaus formal website, that:

"*It would be a pitfall just to apply the Central European Passive House design, especially the details used for insulation, windows, and ventilation and just copy these to a completely different situation because there is a specific building tradition in every country and there are specific climatic boundary conditions in every region. Therefore, the specific solution for a Passive House building has to be adapted to the country and the climate under consideration.*" - *www.passipedia.org [47].*

As mentioned in the Passivhaus website, the building's code of practice that were implemented in the cold region requires modification if it is to be applied in regions with a different climate. Previous studies in cooling dominated countries that implemented insulation material in their studies reported that insulating the building increased the building's energy consumption. A study by Griego et al. reported that the use of insulation materials in their case-study buildings (an office in Mexico) yielded the opposite results. They explained, the heat gain in the building is far greater than the external solar heat gain penetrated into the building. Therefore, insulating the building traps this heat which resulted in an increase in the HVAC load [93]. Meanwhile, a study of a classroom in Israel (hot summer Mediterranean weather) reported, insulating the external of the roof and high thermal mass on the inside is more energy efficient. This study also reported that the internal heat gain is higher than the external heat gain. The insulation prevents solar heat gain from coming into the room, and the thermal mass absorbs internal heat gain and releases it at night time [95]. These two studies demonstrated the impact of adding insulation to the building's envelope on the building's energy consumption for a building in two different climates. The outcomes demonstrates how the same building's envelope give a different impact on building in different climates. This statement were supported by the previous studies by Dascalaki and Santamouris [101] and Peng Xu et al.

Ruolang Zeng et al. and Yinping Zhang et al. developed a mathematical equation manipulating a building's predicted heat gain to find the most optimum criteria for the building's envelope material and natural ventilation to minimise cooling load [97][178]. Meanwhile, Hatice Sozer studied the effect of passive solar design techniques for the hotel buildings in a cooling dominated climate [80]. These findings are useful for the buildings in the design phase. As for an existing building, adding insulation material [64][79][81][82][84], PCM [73][179][180][181][182][183] or using a low energy cooling system [154][184] were studied to reduce the load demand for HVAC system. Most of the studies on insulation compared different types of insulation material, different configuration (either on the inside or outside of the wall) and different climatic conditions mainly to find the most optimum thickness to reduce HVAC load. These studies reported that there are differences in performance at different climates [64][79][81][82][84]. Whereas for the PCM, most of the studies incorporated PCM panels/board into the building's wall [73][179][180][181][182], ceilings and floor [183]. It was reported that the performance of PCM depends on its melting/freezing point, latent heat, building's construction design and climates [179][181][183]. Based on the previous studies, it can be seen

that the performance of the insulation material and PCM depends on the climate, and the installation of this material predominantly managed to reduce HVAC's load.

In this section (Section 4.1), the main aim is to study the most optimum configuration for the building's envelope that is suitable to cater retrofitting process for a medium size office building located in the tropical region. [124]. Previous work on the passive designs implemented on the building envelope to reduce a building's HVAC demand focused on:

- using insulation material to the building's wall
- incorporating phase change material into the building's construction (mainly phase change material (PCM) panels/board in the building's wall structure)
- manipulating the building's thermal mass

To achieve the goal of this section, a series of simulations of the building' ground floor office and IT room were conducted to determine the best retrofit arrangement to improve the building's envelope (wall, ceiling, and floor but does not include windows) to reduce the target building's cooling load. Insulation material and PCM will be used in this study due to their proven performance in reducing building's HVAC load. PCM type such as the PCM blanket or PCM paint were chosen since it is easier to install in an existing building and studies on this type of PCM on building's performance is still scarce. In fact, studies on the installation of PCM and insulation material on building envelope for retrofitting in the tropical region for a medium-size commercial office building is still limited. Hence, the aim of this study is to:

(a) Determine the best retrofit arrangement to improve the building's envelope (wall, ceiling, and floor but does not include windows) to reduce the target building's cooling load
(b) Investigate the impact of using insulation and PCM on the air conditioned zones.
(c) Discover the most optimum settings for PCM and insulation materials in air conditioned zones in tropical settings.
(d) To give guidelines for architects, building developers and building designers on potential passive retrofitting approaches to achieving nZEB in tropical countries.

4.1.2 Methods

Two different types of air-conditioned rooms in the building were tested; rooms with air conditioning operating 24 hours and rooms with scheduled air conditioning operations (office hour). The office and IT room on the ground floor of the building model were used for the

experiment. The ground floor office room representing rooms with scheduled air conditioning and ground floor IT room represent the rooms with 24 hours air conditioning. It is assumed that the energy interaction will be the same for every office and server room due to the similarities in their physical outlet, internal content, and air conditioning system.

To simplify the initial analysis on the most optimum construction types for the office and IT room, only the ground floor structure was taken into consideration. An adjustment on the ground floor's ceiling was made so that it reflects the actual building structure by employing the roof structure instead of the initial concrete slab as the roof. This is to ensure enough insulation was given to the office and IT room from the solar heat gain so the result will not be far deviated once the new construction was applied to the whole building model. However, it is assumed that the heat gains from the neighbouring floors are negligible. The ground floor building model used for simulation is shown in Figure 41.

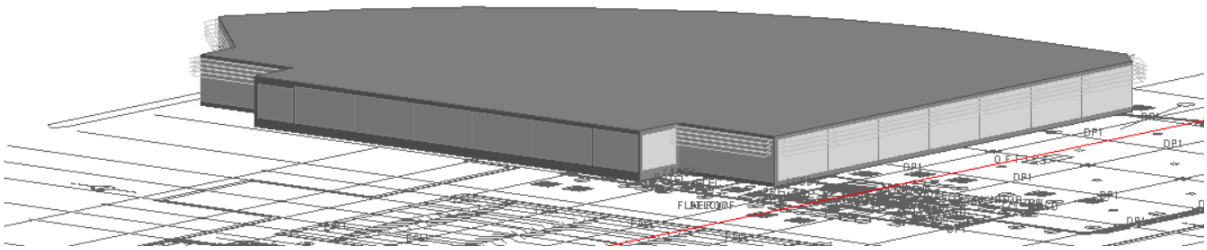

Figure 41: The simplified building's model that was used to investigate different PCM and insulation arrangement in different types of air-conditioned rooms.

4.1.2.1 Most optimum room constructions and ACMV schedules

Different types of insulations were compared and selected based on its resistivity value, embodied carbon and lifetime before being used in the simulation. While PCM materials were selected based on the latent heat storage capacity, melting temperature and feasibility of application for a building construction. In this study, two PCM products that are ENERCIEL manufactured by Winco Technologies [185] and ENRG Blanket manufactured by Phase Change

Energy Solution [186]) were selected for a simulation based performance comparison. Different scenarios that consist of a different room's constructions were listed in Table 45, and each construction's specification was detailed in Table 46 and illustrated in Figure 42 to Figure 45.

Table 45: List of scenarios to find the most optimum arrangement for PCM and insulation materials in an air conditioned zones.

Scenarios	Arrangements			
	Floor	Roof	Wall	Partition
Base and Base*	Floor 1	Roof 1	Wall 1	Partition 1
1 and 1*	Floor 2	Roof 2	Wall 2	Partition 2
2 and 2*	Floor 2	Roof 3	Wall 2	Partition 2
3 and 3*	Floor 2	Roof 4	Wall 2	Partition 2
4 and 4*	Floor 1	Roof 5	Wall 1	Partition 1
5 and 5*	Floor 1	Roof 5	Wall 2	Partition 2
6 and 6*	Floor 1	Roof 6	Wall 1	Partition 1

Table 46: The U-values, cost and thermal quality of the construction type.

Construction type	U-Values (with and without bridging) W/m².K	Internal heat capacity KJ/m².K	Cost GBP/m²	Thermal quality
Roof 1	0.373	0	100	Good thermal quality with unlikely mould growth.
Roof 2	0.164	0	175	
Roof 3	0.174	32.15	175	
Roof 4	0.175	0	150	
Roof 5	0.328	0	125	
Wall 1	1.838	139.55	250	
Wall 2	0.188	78.694	300	
Floor 1	1.702	195.90	150	
Floor 2	0.185	52.85	200	
Partition 1	1.69	126.12	150	
Partition 2	0.187	30.43	200	

Figure 42: The roofs/ceilings construction for the simulation work.

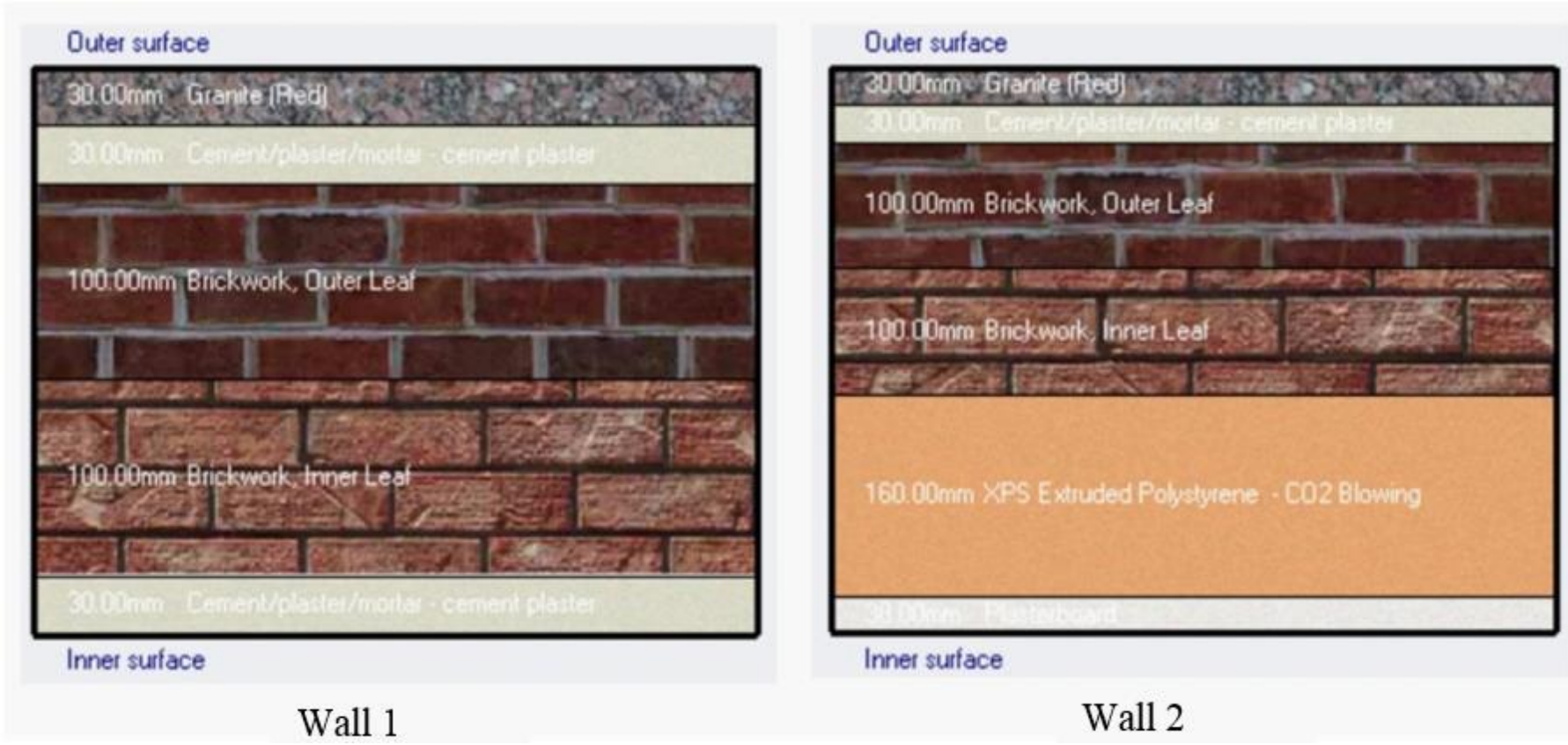

Figure 43: The wall construction for the simulation work.

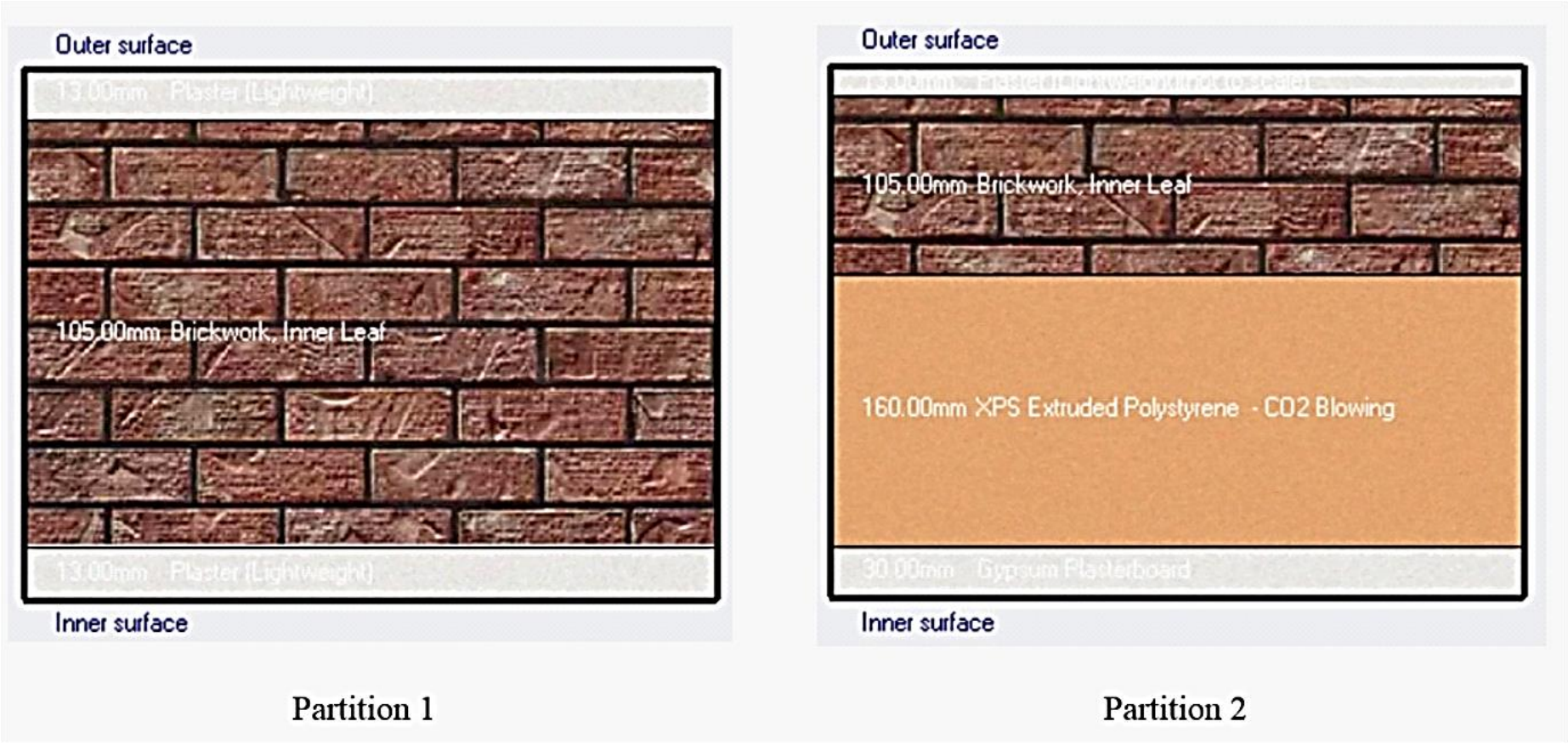

Figure 44: The partition construction used in the simulations.

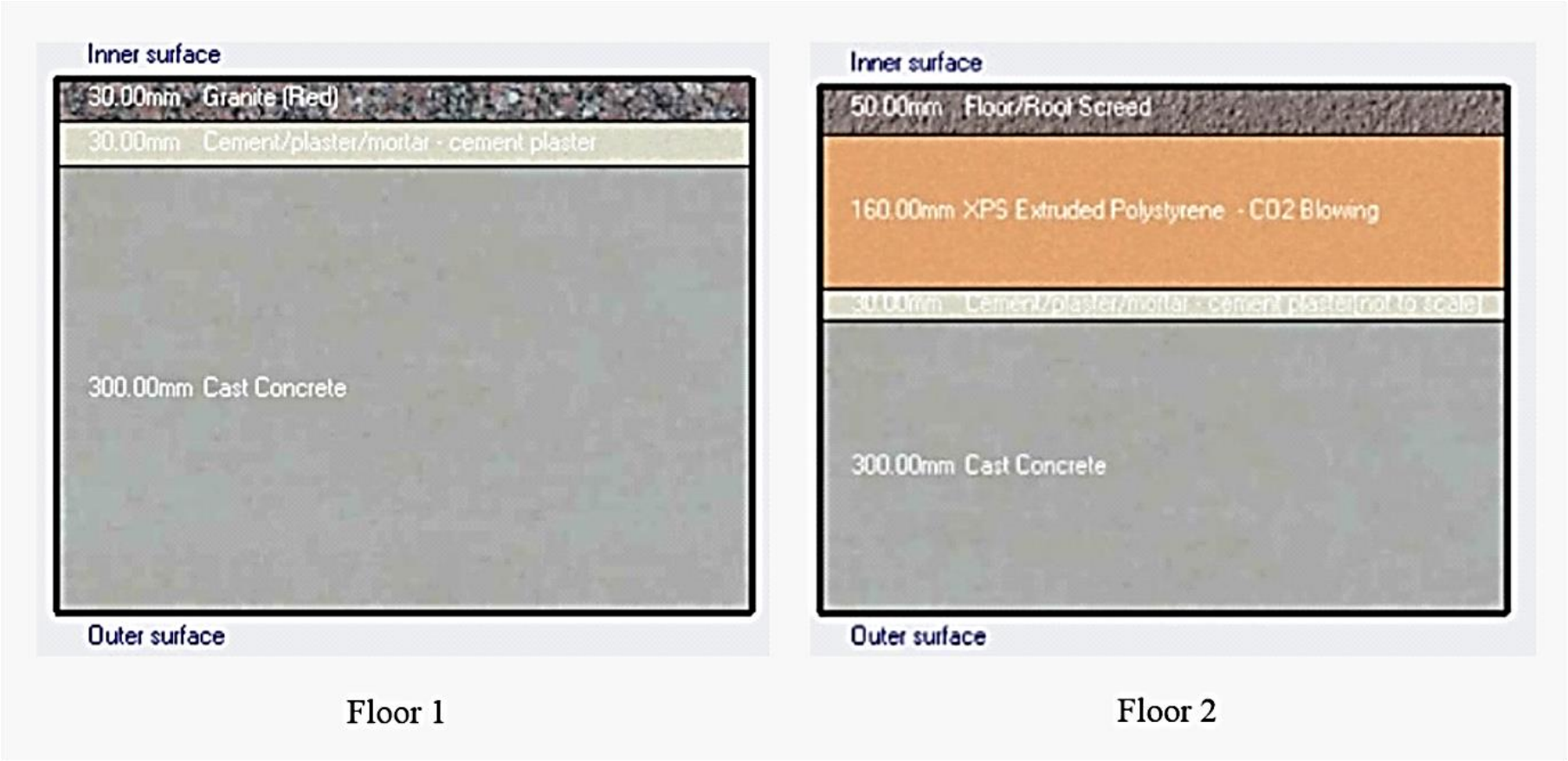

Figure 45: The floors construction for the simulation work

The ENRG Blanket encapsulated the pure PCM into thin sheet rolls which vary in length and are easily installed on the ceilings, while the ENERCIEL product is available as a coating that can be sprayed or painted on the walls, ceilings, and floorings. Sample pictures of these products are shown in Figure 46, and the specifications of both products are listed in Table 47. The melting point temperatures were chosen based on several experiments that were carried out to determine the suitable PCM's melting point for both types of PCM. Choices of PCM types (storage capacity and melting point) play a significant role in determining the amount of energy saving. The same PCM brand (BioPCM and ENERCIEL) with different melting point (25°C, 26°C, 27°C, 28°C and 29°C) were tested. The highest energy reduction was achieved by BioPCM with melting point 29°C. The enthalpy values for each PCM types at different temperature are shown in Figure 47 and Figure 48 [158].

Figure 46: (Left) The ENERCIEL product and (Right) the ENRG Blanket product. Pictures were courtesy of Winco Technologies and Phase Change Energy Solution websites [185][186].

Table 47: PCM material specifications [160][185][186].

Specification	ENRG Blanket	ENERCIEL
Product's name in Design Builder	BioPCM M182/Q29	Winco28
Thermal energy storage capacity per square meter (kWh/m²)	0.574	0.633
Melting temperature (°C)	29	28
Conductivity (W/m.K)	0.2	0.148
Specific heat (J/kg.K)	1970	8750
Density (kg/m³)	235	863
Temperature coefficient (W/m.K²)	1.108	1.108
Embodied carbon	0.08	0.08
Cost per surface area (GBP/m²)	25	25

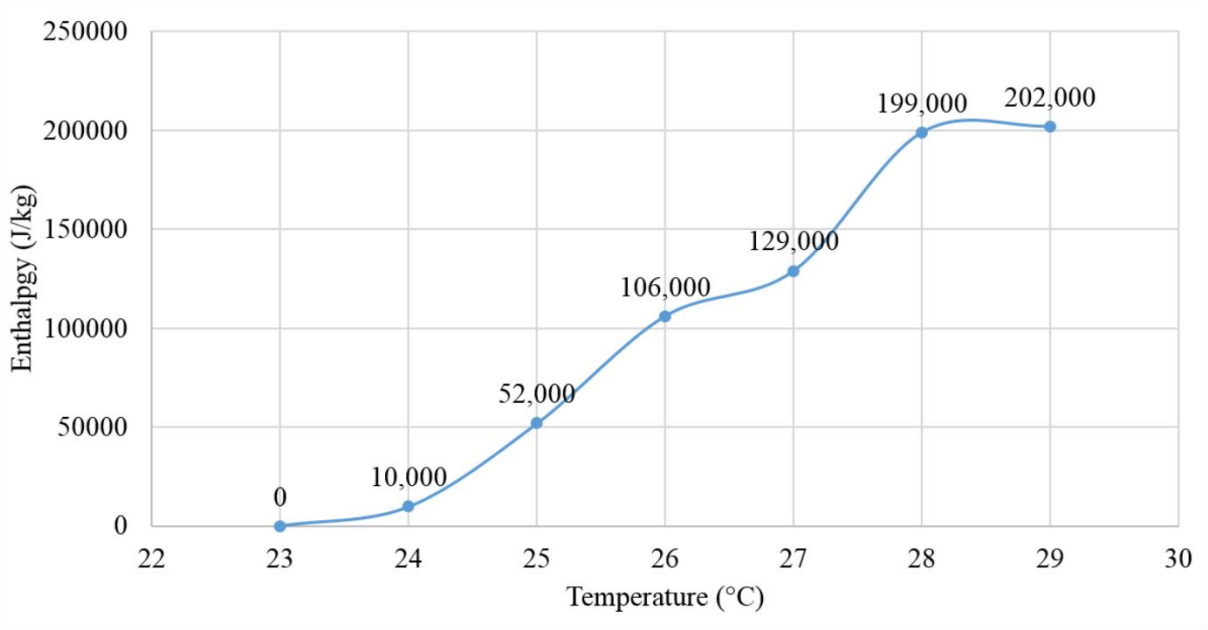

Figure 47: The ENERCIEL (Winco28) enthalpy values at different temperature.

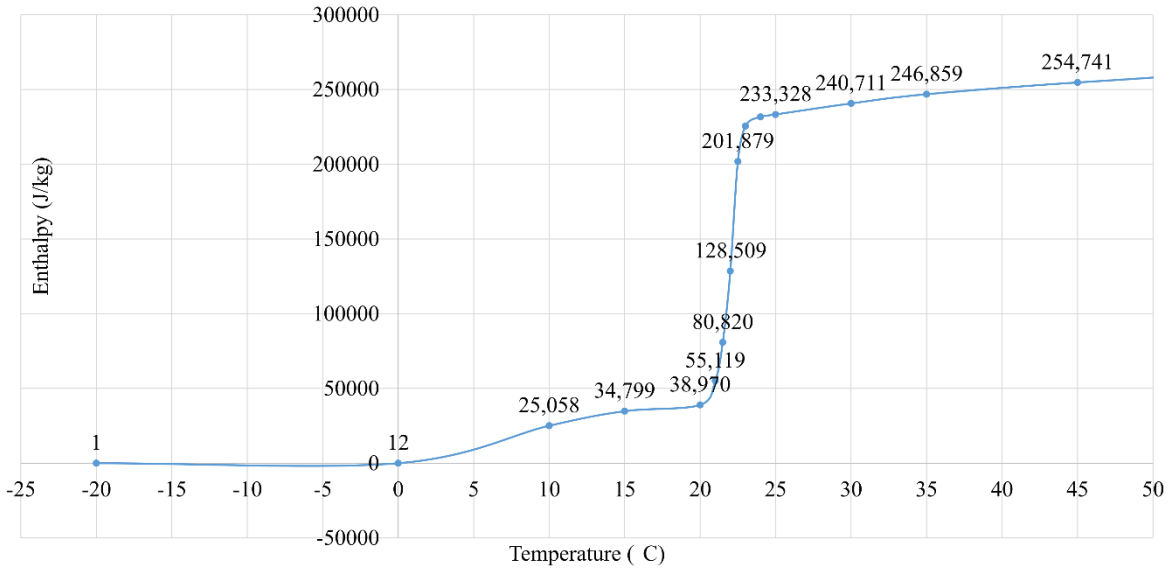

Figure 48: The ENRG Blanket (BioPCM M182/Q29) enthalpy values at various temperatures

In Scenario Base and Scenario 1 to 6 for the office zone, the set point temperature setting for the air conditioning was set at 24°C and scheduled to operate at 0700 to 1730 every work day. Meanwhile for Scenario Base* and Scenario 1* to 6* in the office, night time ventilation was added, and the air conditioning schedule was modified to optimise the energy reduction while maintaining a good thermal comfort. While for the IT room, Scenario 1, 2 and 3 were tested and the air conditioning was scheduled to operate 24hours with the set point temperature fixed at 21°C. The ACMV settings for all scenarios are listed in Table 48.

Table 48: The ACMV settings for every simulation scenarios for the office.

Scenario	T_{set}	AC schedule	MV schedule
Base, Base*, 1, 2, 3, 4, 5 and 6	24°C	0700 to 1730	off
2* and 3*	24°C	0700 to 1700	1700 to 2400 and 0000 to 0600
4*	26°C	0700 to 1700 (with varying load percentage. Refer Figure 49)	1700 to 2400 and 0000 to 0700
5* and 6*	25°C	0700 to 1700 (with varying load percentage. Refer Figure 49)	170 to 2400 and 0000 to 0630

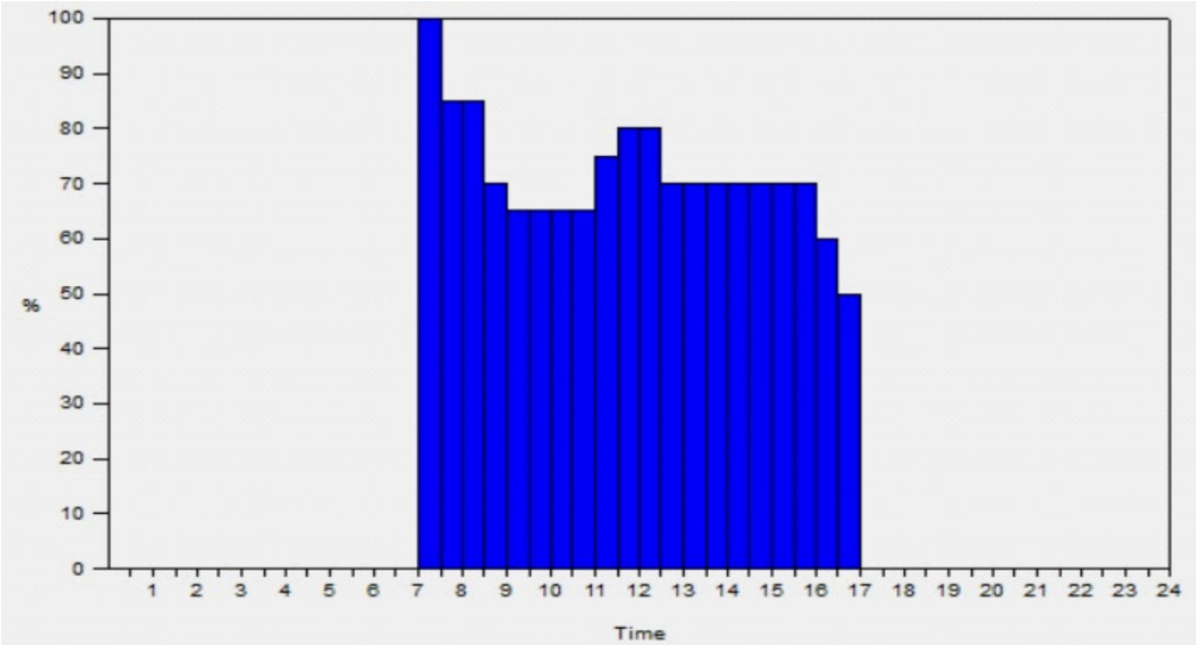

Figure 49: The cooling load schedule for the office room (hourly load percentage).

4.1.2.2 Simulation settings

There are two main solution algorithms used for simulation in EnergyPlus: CTF and Finite Difference. The default algorithm is CTF that is known as the state space method. While 1-D Finite Difference solution is used in the construction element for PCM simulation. Two types of schemes were used to conduct finite difference model that are Fully Implicit 1st Order and Crank Nicolson 2nd order. In this study, the fully implicit first order is used since it is more stable over time compared to Crank Nicolson 2nd order. However, the only disadvantage of this option is, it can be slower. The parameters used to simulate building model with PCM is shown in Figure 50. This simulation setting can be found at Simulation Options tab. The suggested values for time step is 12. Higher time step will increase the accuracy but will increase the simulation times. Space discretisation constant suggested by Design Builder was 3, relaxation factor 1, and inside surface temperature convergence criteria 0.01. A lower value for inside surface convergence criteria will increase the accuracy, but it will also increase the simulation time [160]. In this study, the inside surface convergence criteria were set at 0.002. Space discretion constant determines the number of nodes used to represent each material in the construction material. The nominal distance associated with a node, ΔX is calculated using equation (4.1.1) [160]:

$$\Delta X = (C \times \alpha \times \Delta t)^{0.5} \qquad \text{Equation (4.1.1)}$$

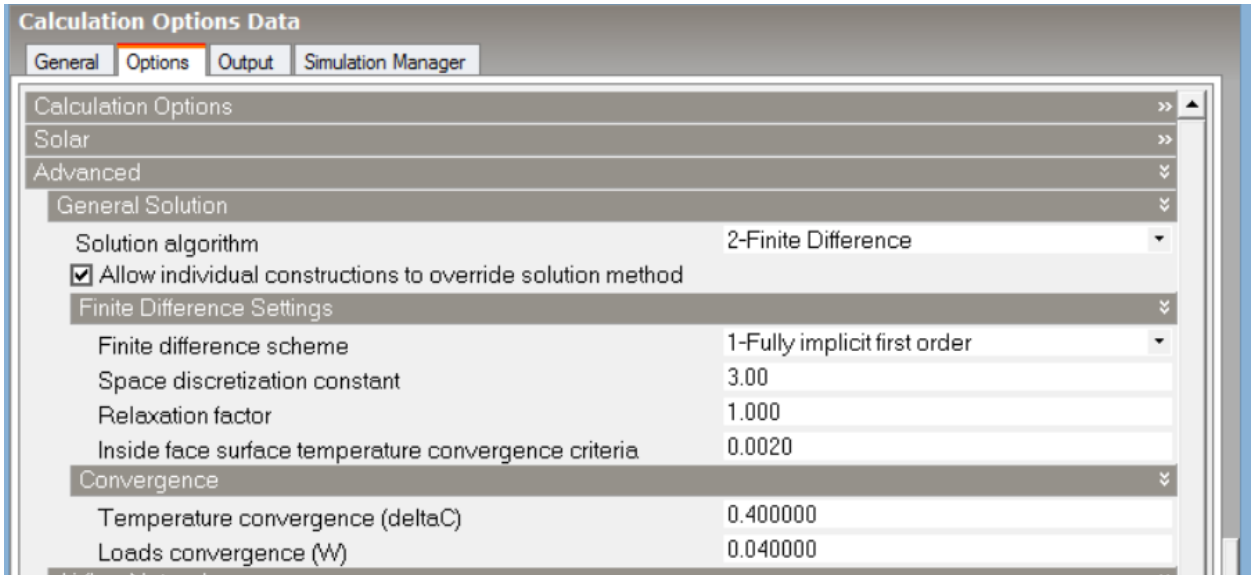

Figure 50: Simulation settings for the building model with PCM.

4.1.2.2 Whole building and performance evaluation

The outcomes from Section 4.1.2.1 are then applied in the air-conditioned areas in the building. The thermal comfort in the offices and the energy performance were evaluated. Further modification of the ACMV's settings was made until the indoor comfort is within the suggested range for the office zones. Meanwhile, for the IT rooms, the requirement was to ensure that the air temperature is below 21.5°C to avoid equipment overheating. The energy and economic performance were evaluated based on the equation (4.1.1) to (4.1.7).

Annual cooling load reduction	= Cooling load$_i$ - Cooling load$_n$	(4.1.2)
Energy reduction	= Energy$_i$ - Energy$_n$	(4.1.3)
Energy reduction cost (RM/kWh)	= Initial cost / ΣEnergy reduction	(4.1.4)
ΣEnergy reduction (kWh)	= Annual energy reduction × lifetime	(4.1.5)
Payback period (year)	= ΣRetrofit cost / ΣSaving on energy bills	(4.1.6)
ΣSaving on energy bills (RM)	= ΣEnergy reduction × Energy price per kWh	(4.1.7)
ΣRetrofit cost	= [(Material cost/m^2) × installation area] + installation cost	(4.1.8)

Where:

Initial/baseline (i)

After retrofit (n)

Total (Σ)

4.1.3 Results and Discussion

The annual cooling load and external infiltration for every scenario were compared to examine the room's construction that resulted in the least additional energy requirement to maintain the requisite thermal comfort. The results (listed in Table 49) suggested that a different construction type best suits a different cooling requirement. For an office room where the cooling system was only used during the office period, Scenario 4* deemed to offer the highest cooling load reduction (49.21%) while maintaining the desired thermal comfort. It is then followed by Scenario 6* (48.16%) and Scenario 5* (40.35%). Meanwhile for a room with 24 hours cooling requirement, a fully insulated construction (Scenario 3) yield to use the least energy to maintain the required room temperature. Other notable findings were observed from the simulation results and will be further discussed in Section 4.1.3.1 while the application on a whole building and performance evaluation is discussed in Section 4.1.3.2. Whereas Section 4.1.3.3 presents the economic analysis of the suggested method.

4.1.3.1 Most optimum construction and ACMV schedules.

One of the most important findings of the use of PCM in a building's construction with a scheduled air conditioning in a hot and humid region is its requirement for breathability. In this study, breathability refers to the building's ability to transfer heat and ventilation. It is observed that the installation of PCM (Scenario 1, 2, 4, 5, 6, 4*, 5* and 6*) could overcome the benefit of using a fully insulated room (Scenario 1, 2, 3 and 3*) when being paired up with a night time ventilation system and walls with higher U-values (Scenario 4* and 6*). Besides acting as a pre-cooling, the night time ventilation is necessary to allow a good charging and discharging period for the PCM for it to be effective in providing free cooling during the day [187].

An additional latent load can be seen in the base case, Scenario 4 and Scenario 6 at midnight (Figure 51). At night time, the outside air relative humidity could reach 100%. Rooms with breathable walls (high U-values) tend to transfer the moisture from outside into the room. This high moisture content could cause condensation when the room's atmosphere comes in contact

with a cold surface which then leads to mould. The mould problem can be avoided by using insulation, dehumidification, and ventilation [188]. In the base case, Scenario 4 and Scenario 6, the rooms were not insulated or ventilated. In order to avoid mould problem the humidistat was automatically turned on when the R.H rises above 70%. This resulted in an additional latent cooling load at night. The energy usage for night time ventilation was far less than the energy use to dehumidify the room's R.H and in fact, the mechanism also pre-cool the room which resulted in the elimination of peak cooling load in the morning when the cooling system was switched on. The use of nighttime ventilation and re-setting the air conditioning set point temperature and operation schedule for the base case resulted in a 13.69% cooling load reduction.

Table 49: Total external infiltration and cooling load in January and its percentage reduction in different scenarios.

Zone	Scenarios	External Infiltration kWh	Total Cooling Load kWh	Cooling Reduction %
Office	Base	2130.10	23093.00	0.00
	1	1408.76	15619.67	32.36
	2	1408.75	15619.74	32.36
	3	1408.76	15619.70	32.36
	4	1567.06	17971.85	22.18
	5	1424.80	16193.80	29.88
	6	1498.80	17182.20	25.60
Office	Base*	1522.03	19932.60	13.69
	2*	49.03	24670.33	-6.83
	3*	103.18	23911.49	-3.54
	4*	949.20	11728.47	49.21
	5*	1086.00	13775.87	40.35
	6*	1036.05	11971.25	48.16
IT room	Base	21.55	826.31	0.00
	S1	16.29	674.82	18.33
	S3	16.29	674.72	18.34
	S4	20.91	821.92	0.53

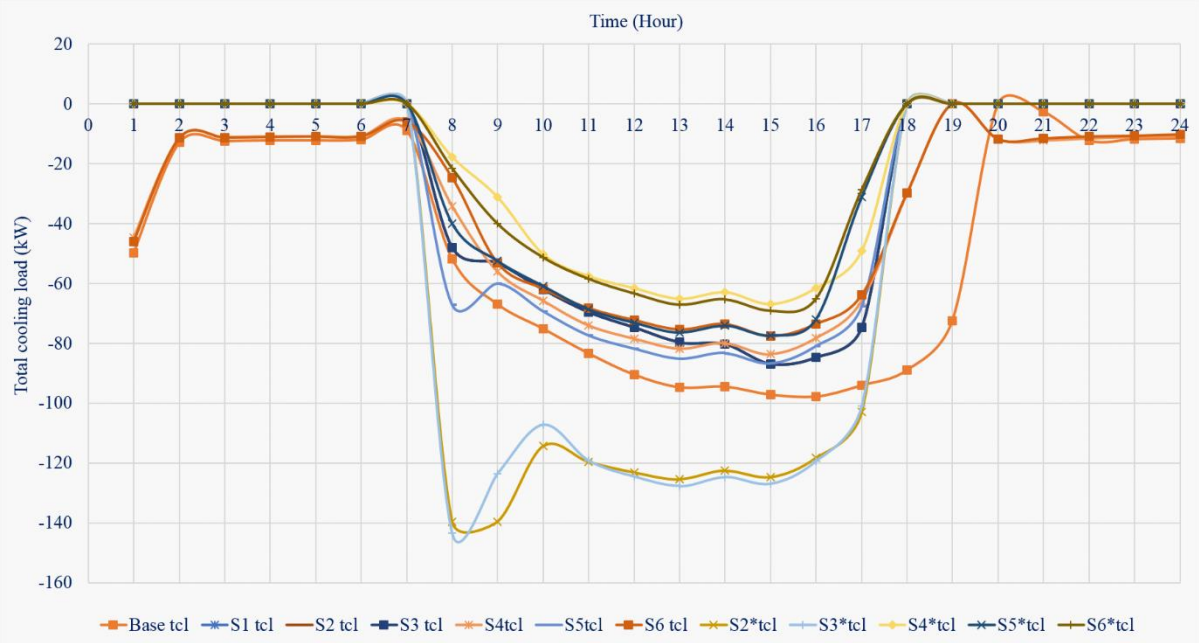

Figure 51: Total hourly cooling load for the ground floor office in every scenario on 2nd January for 24 hours.

Four scenarios with PCM application were compared in Figure 52 to show the PCM performance in a different room's construction and ACMV settings. Scenario 1 represents a fully insulated room with PCM, Scenario 4 represents a typical construction with PCM, Scenario 4* represents a typical room construction with PCM and night time ventilation and Scenario 5* represents a partially insulated room with PCM and night time ventilation. It can be seen that night time ventilation is very crucial in making sure that the PCM is effective in supplying free cooling during office hours. This free cooling resulted in the reduction of total cooling load. However, the higher reduction is shown in Scenario 4* compared to Scenario 5*.

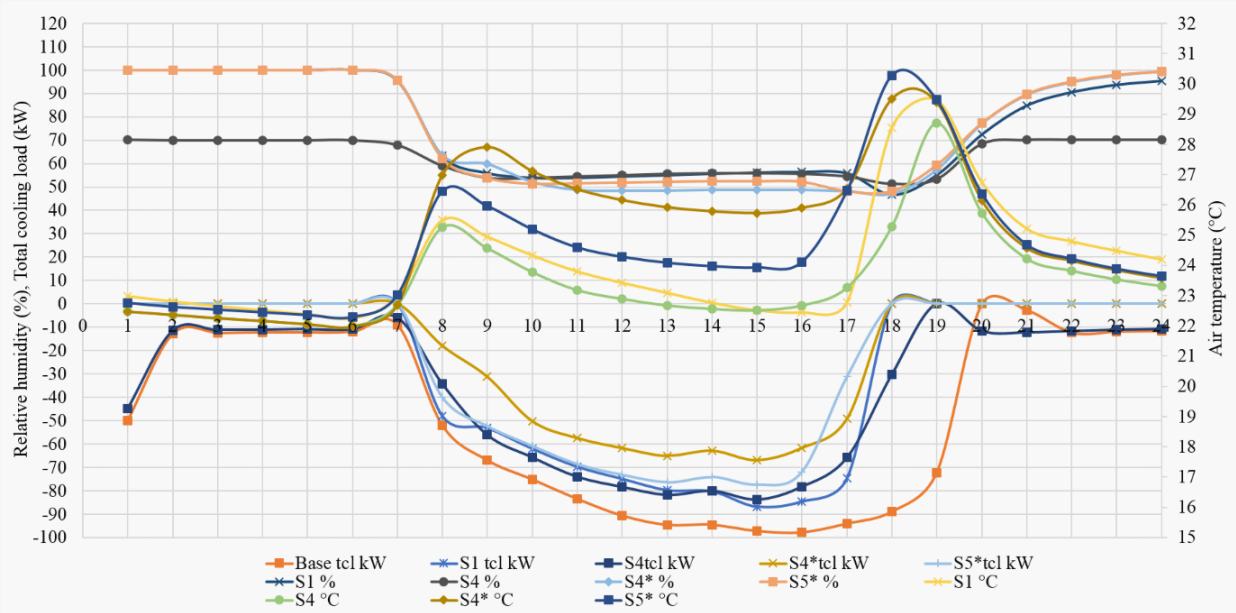

Figure 52: The hourly indoor relative humidity, air temperature, sensible cooling load and latent cooling load for the ground floor office room from the 0700 (2nd January) to 0700 (3rd January).

The maximum cooling system set point temperature to ensure a good thermal comfort in Scenario 5* is 25°C while as for Scenario 4* it could reach 26°C (refer to Figure 53 and Figure 54). The differences in both scenarios were the walls and partitions in Scenario 4* which have a higher thermal conductivity compared to Scenario 5*. During office hours, internal heat gain (heat from respiration, equipment and lighting) was higher than the external heat gain (heat from solar). The theory of thermal conduction, Fourier's Law (Equation (4.8)) states that 'the time rate of heat transfer through a material is proportional to the negative gradient in the temperature and to the area, at right angles to that gradient, through which the heat flows.'

$$\Delta Q/\Delta t = U \times A \times (-\Delta T) \qquad (4.1.8)$$

Where:

Gradient of thermal energy (ΔQ)

Gradient of time (Δt)

Material's thermal conductivity (U)

Gradient in the temperature (ΔT)

Area (A)

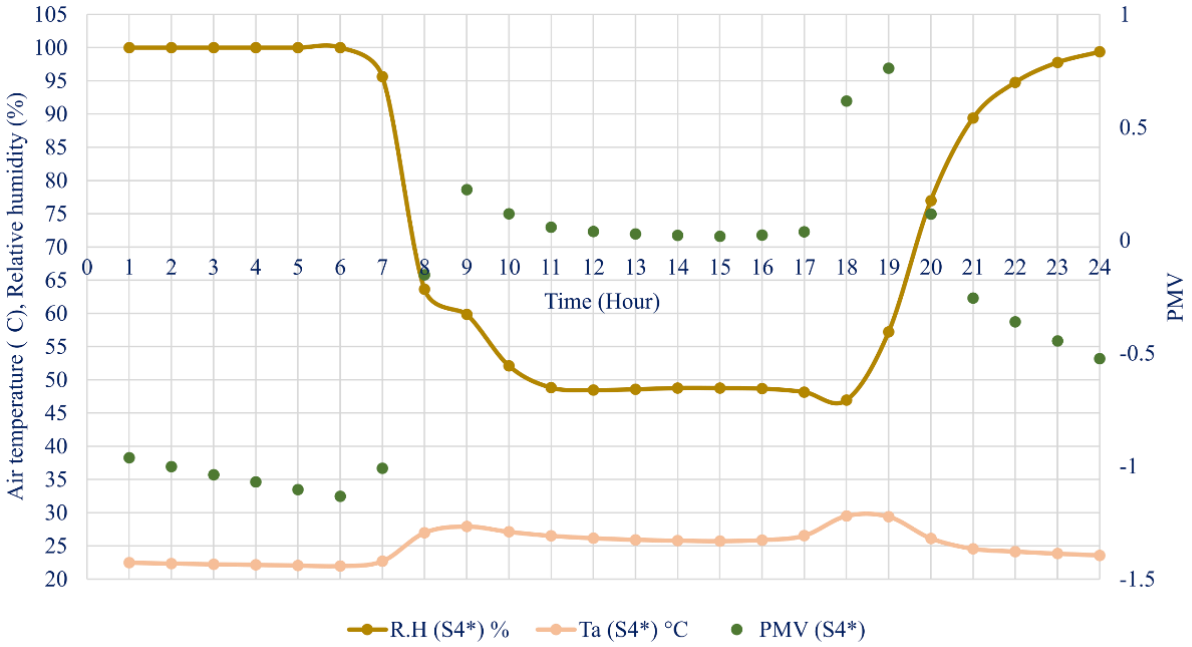

Figure 53: The office's hourly indoor air temperature, relative humidity, and PMV for the ground floor office in Scenario 4* on the 2nd January.

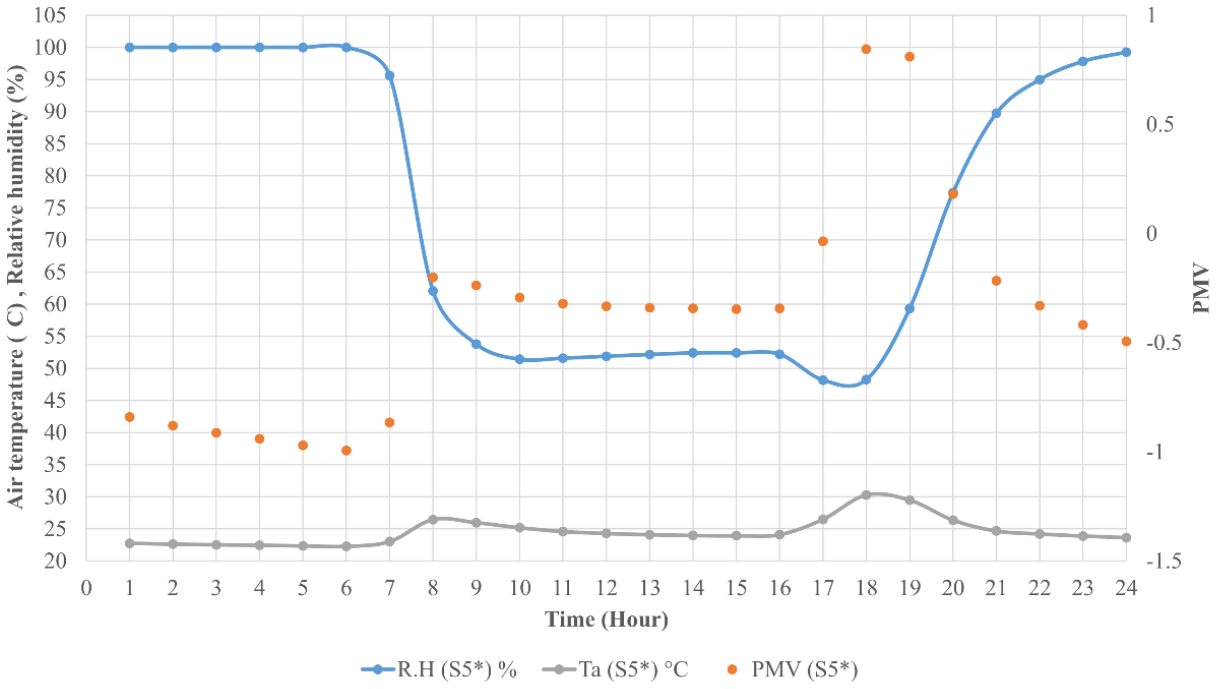

Figure 54: The office's hourly indoor air temperature, relative humidity, and PMV for the ground floor office in Scenario 5* on the 2nd January.

In natural conditions when the air conditioning was not switched on, the room's air temperature was higher than the outside air temperature (see Figure 55). Hence, in a natural state, the cooling process happens when the heat flows from the room to the outside surroundings. The rate of heat transfer depends on the room's U-values and surface area. The cooling process was further enhanced by the use of air conditioning and PCM. This explains why Scenario 4* (high U-values construction) requires less energy in providing a good thermal comfort for the occupants compared to Scenario 5* (low U-values construction).

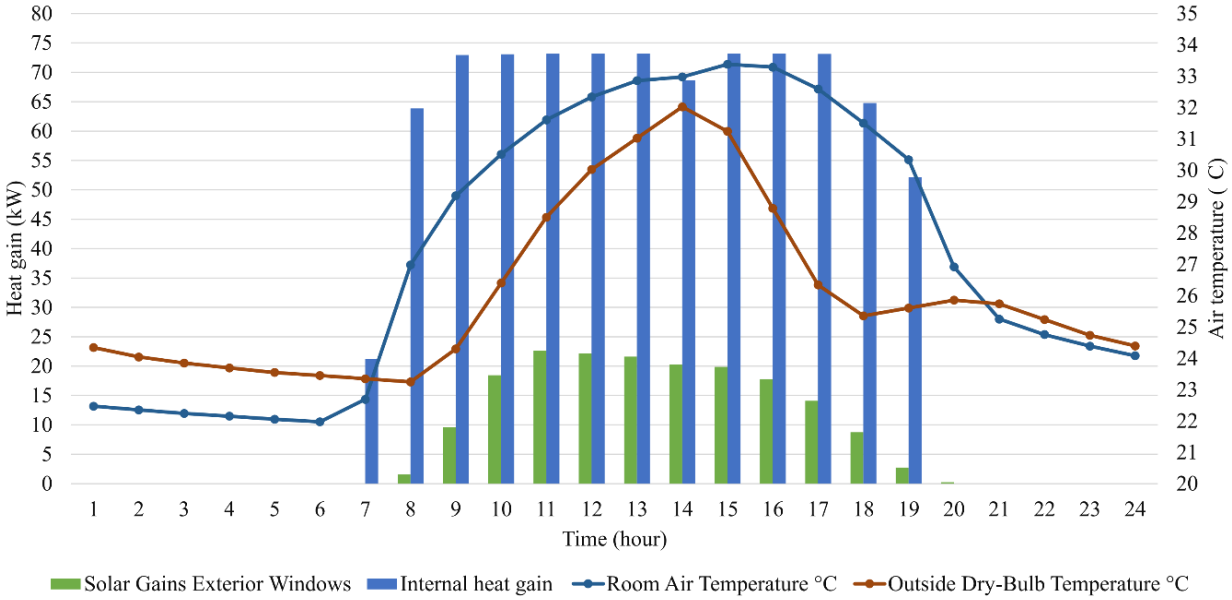

Figure 55: The ground floor's hourly internal and external heat gain, the room's temperature without cooling and the outside air temperature on the 2nd of January.

Conversely, for a fully insulated room, the night time ventilation resulted in an increment in the total cooling load (Scenario 2* and 3*). Figure 56 shows a comparison of the hourly sensible cooling load, hourly latent cooling load, relative humidity and air temperature for the Scenario Base, Scenario 3 and Scenario 3* at the office room. It can be observed that the fully insulated room (Scenario 3 and Scenario 3*) experienced a peak latent load in the morning. The peak latent load increased from 35 kWh (in Scenario 3) to 85 kWh (in Scenario 3*) when the night time ventilation was introduced to the fully insulated room. Scenario 3* shows the highest hourly sensible cooling load during office hours and highest room temperature after office hours.

Meanwhile, in Scenario 3 the indoor air temperature is the highest during office hours, the air relative humidity is the highest after office hours and the sensible cooling load is the lowest during office hours.

This observation is explained by the fact that the fully insulated room has a low breathability. After the air conditioning was switched off, the room retains heat and humidity that was produced during office hours. The warm and humid condition is worst when the night time ventilation ditributes the outside air which contains high humidity into the room. The warm and humid condition of the room resulted in condensation when the room's air was in contact with the colder surfaces (such as windows since the outside air was colder at night time). The condensation process released a substantial amount of heat into the room which is then being retained by the fully insulated walls. This phenomenon resulted in a peak latent load in the morning and a high sensible cooling load during the day. Breathable walls allow moisture and heat to be absorbed and released from the upper concentration to the lower concentrated atmosphere [188]. To prove this hypothesis, the indoor air characteristics at 0300 in the Scenario Base, Scenario 3 and Scenario 3* are compared in Table 50. As can be seen, the room's air temperature is close to the dew-point temperature for scenario 3 and 3* and the relative humidity in both scenarios are significantly higher than the Scenario Base. The outside dry bulb temperature at 0300 on the 3rd of January was 23.7°C.

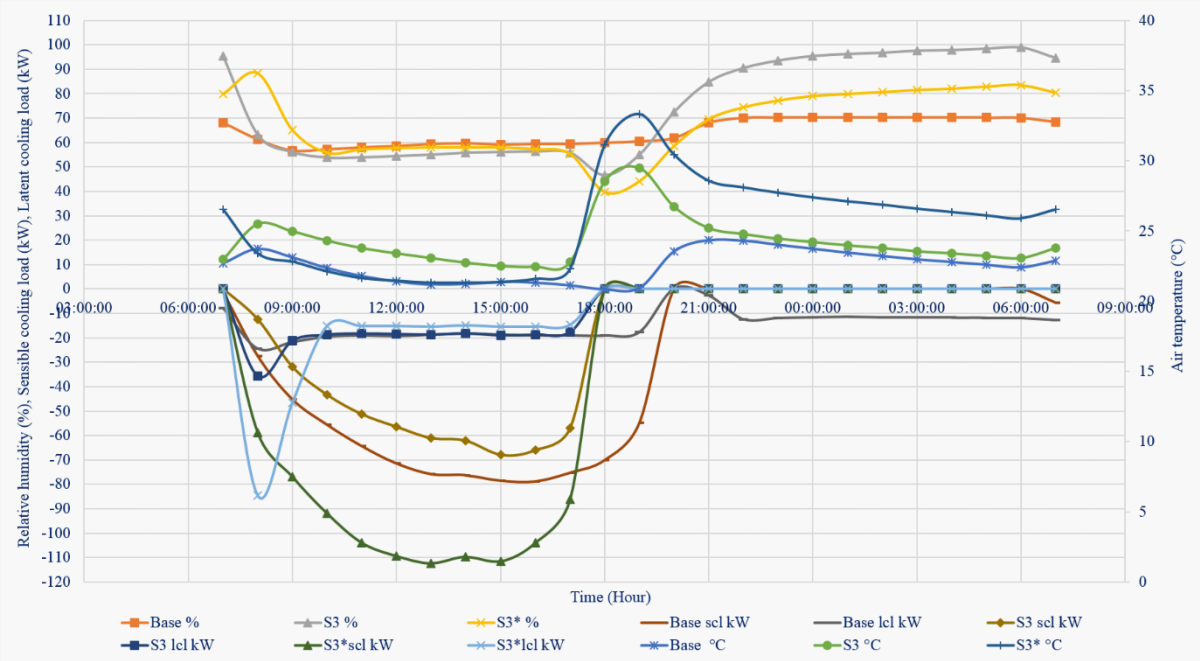

Figure 56: The office's hourly indoor air temperature, relative humidity, latent and sensible cooling load in different scenarios. 24 hours data on 2nd January. Note: scl is the sensible cooling load, lcl is the latent cooling load.

Table 50: The office's indoor air characteristics at 0300 (3rd Jan) in different room's scenarios.

Type	Base	S3	S3*
Relative humidity (%)	70.2	97.5	81.4
Air temperature (°C)	23.0	23.6	26.6
Enthalpy (J/g)	54.7	69.6	72.6
Dew point (°C)	17.3	23.2	23.2
Absolute humidity (g/m³)	14.5	20.8	20.6

However, a fully insulated room without the night time ventilation could reduce up to 32.36% of the cooling load by retaining the cold and reducing heat leakage during office hours (which resulted in the low sensible cooling load during office hours in Scenario 3). The disadvantages of this construction occur when the night time ventilation was introduced and the possibility of condensation to happen at night time which will lead to the mould problem. Meanwhile, the IT room requires 24 hours cooling, hence making it fully insulated (Scenario 1 and 3) enables the room to retain its cold energy for a longer period imitating a cold room. The condensation can be

avoided since the room's air is continuously conditioned to the desired room temperature and humidity. However, as explained earlier, PCM in Scenario 1 was not effective without night time ventilation [182] and when installed in a fully insulated room. Therefore, it is concluded that the most optimum construction type for a room with 24 hours cooling is Scenario 3.

4.1.3.2 Application on the whole building

Applying the findings from Section 4.1.3.1 into all the areas with air conditioning which are, installing scenario 4* at the corridors, offices and cafeteria and scenario 3 at the IT rooms and data centre resulted in 22.36% reduction in total cooling load and 13.24% reduction in the building's total energy consumption. The comparison of the buildings energy consumption and the building's total cooling load before and after retrofit are listed in Table 51.

Table 51: The energy consumption and cooling load before and after the retrofit.

	Baseline (kWh)	Passive cooling (kWh)	Reduction (kWh)	Reduction (%)
Total energy consumption	7179471.36	6229050.40	950420.96	13.24
Total cooling load	4213853.11	3271838.51	942014.60	22.36

The total annual cooling load reduction using the PCM installation varied between every office (see Table 52) with the highest reduction attained by the ground floor office (148,854.80 kWh), and the lowest cooling reduction was achieved by the office at the 3rd floor (76,260.20 kWh). This is mainly because of PCM absorbs heat and only reduce sensible cooling load, not latent cooling load. The amount of heat can be absorbed depend on the total PCM's thermal energy storage capacity. This value is given by the manufacturer which is a product of thermal energy storage capacity multiplied by PCM's area (meter squared of PCM material). The total thermal energy storage capacity of the installed PCM in every floor is theoretically the same since the materials used and the amount of materials used are the same. However, this value is also affected by the effectiveness of charging and discharging of PCM materials through night time forced ventilation. Plus, PCM only absorbs heat during working hour which will only reduce the sensible cooling load. The installation of PCM does not reduce latent cooling load, and the

amount of sensible cooling load and latent cooling load are different on every floor. In office rooms, latent load originated from human occupancy.

An analysis of different heat sources and the amount of cooling load reduction shows that only the heat gain from occupancy has the opposite pattern of the cooling load reduction. The ground floor office has the lowest heat gain from occupancy and the highest cooling load reduction, while the third-floor office has the highest heat gain from occupancy and the lowest cooling load reduction. The annual cooling load reduction and heat gain from occupancy in every office are shown in Figure 57. The overall amount of cooling load reduction might be influenced by the initial total sensible heat gain and latent heat gain in the room, and the effectiveness of PCM's discharging process through night time ventilation. Meanwhile, for the IT rooms, the cooling load reduction ranges between 3,044.00 kWh to 3,555.00 kWh annually (see Table 53). The hourly cooling load for the ground floor office building before and after retrofit (simulated using the actual baseline model) is presented in Figure 58.

Table 52: Total cooling load reduction in every zone installed with PCM.

Zone	Base kWh	Retrofit kWh	Cooling load reduction kWh	Cooling load reduction %
Office GF	374,537.2	225,682.4	148,854.8	39.7
Office 1	331,774.5	248,638.6	83,135.9	25.1
Office 2	483,497.4	384,219.3	99,278.1	20.5
Office 3	476,984.4	400,724.2	76,260.2	16.0
Office 4	366,308.8	262,458.8	103,850.0	28.4
Office 5	398,350.3	285,075.3	113,275.0	28.4
Office 6	390,081.8	290,622.1	99,459.7	25.5
Office 7	377,979.2	241,547.3	136,431.9	36.1
Corridor GF	22,005.27	11,609.19	10,396.1	47.2
Corridor 1	27,250.28	14,646.07	12,604.2	46.3
Corridor 2	35,220.23	20,322.6	14,897.6	42.3
Corridor 3	35,220.23	20,932.21	14,288.0	40.6
Corridor 4	30,070.45	20,900.21	9,170.2	30.5
Corridor 5	27,489.28	20,691.49	6,797.8	24.7
Corridor 6	38,705.21	20,333.09	18,372.1	47.5
Corridor 7	27,191.91	19,535.28	7,656.6	28.2
Corridor South	111,015.1	97,437.86	13,577.2	12.2
Café	147,127.8	12,1533.1	25,594.7	17.4
Total	3,700,809.0	2,706,909.0	993,900.26	26.9

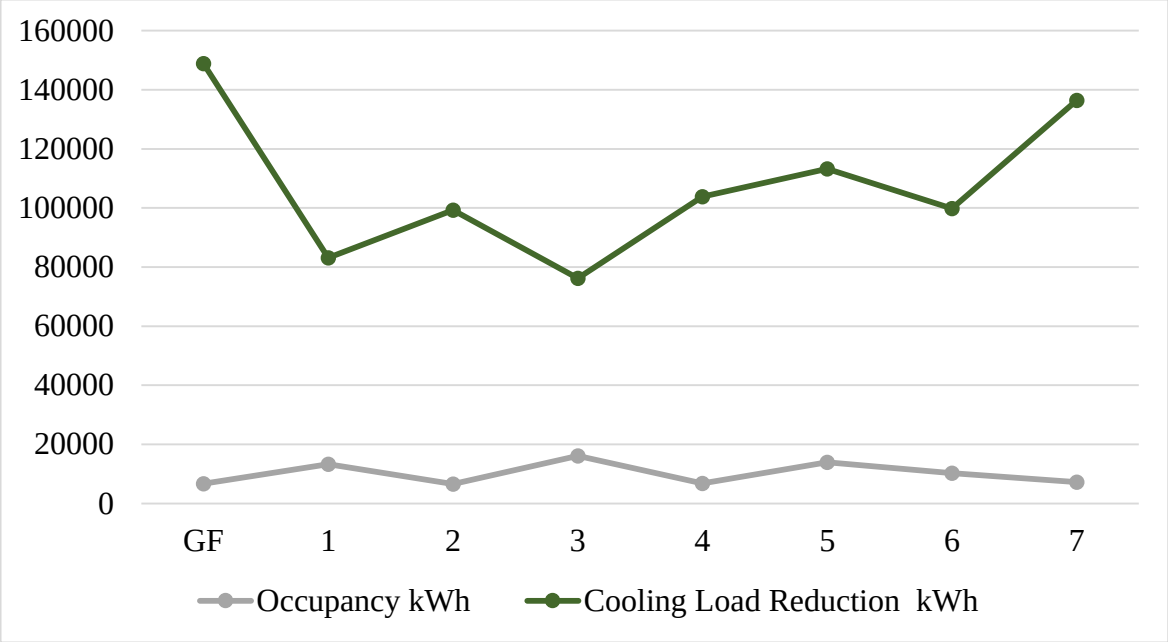

Figure 57: The annual cooling load reduction and heat gain from occupancy in every office.

Table 53: The simulated annual cooling load for the IT room before and after the retrofit.

Floor	Base (kWh)	Retrofit (kWh)	Reduction (kWh)	Reduction (%)
GF	9,292	6,126	3,166	34.1
1	8,142	5,031	3,111	38.2
2	8,336	5,073	3,263	39.1
3	8,334	5,079	3,255	39.1
4	8,323	5,204	3,119	37.5
5	8,329	5,285	3,044	36.5
6	8,333	5,065	3,268	39.2
7	8,709	5,154	3,555	40.8
Total	67,798	42,017	25,781	38.0

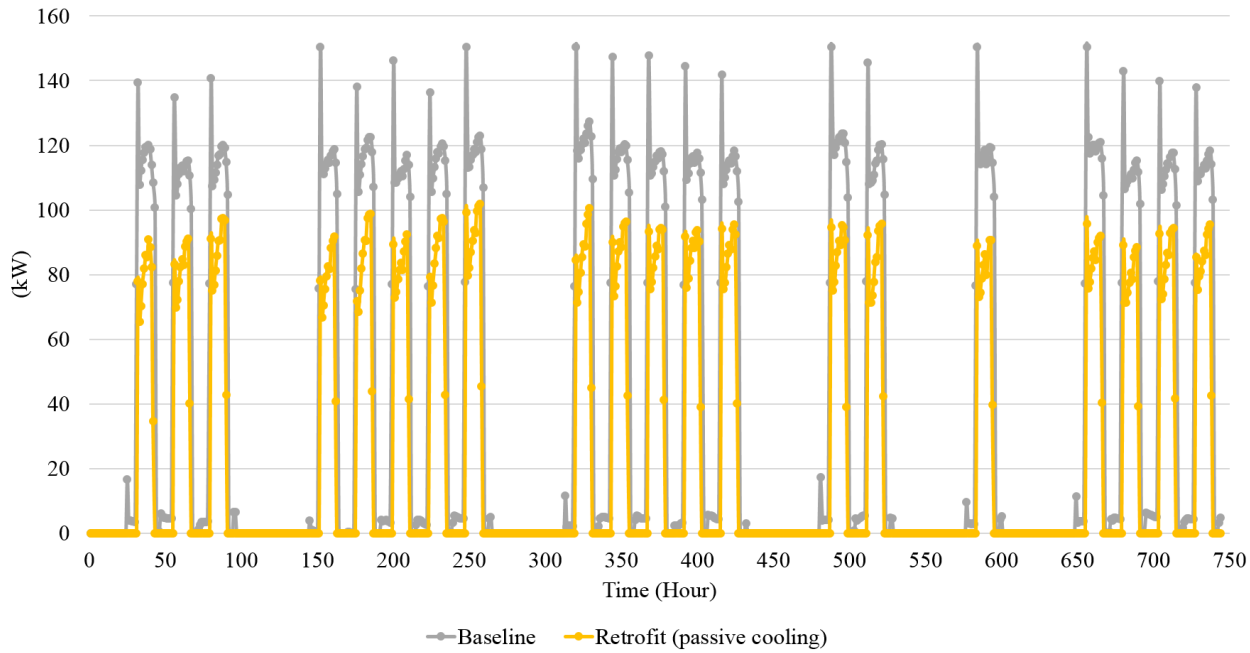

Figure 58: The simulated hourly total cooling load in January for the ground floor office before and after retrofit (installation of passive cooling).

A comparison of the simulated cooling load in January between the office and IT room located in the simplified ground floor model and office in the actual baseline model before and after retrofit are shown in Table 54 and Table 55.

Table 54: A comparison of the simulated cooling load in January between the office in the simplified ground floor model and office in the actual baseline model before and after the retrofit.

Type	Baseline kWh	Retrofit kWh	Reduction kWh	Reduction %
Simplified model	23,093.00	11,728.47	11,364.53	49.20
Actual baseline model	30,235.79	19,361.51	10,874.28	36.00

Table 55: A comparison of the simulated cooling load in January between the IT room in the simplified ground floor model and IT room in the actual baseline model before and after the retrofit.

Type	Baseline kWh	Retrofit kWh	Reduction kWh	Reduction %
Simplified model	644.97	424.36	220.61	34.20
Actual baseline model	772.22	509.34	262.87	34.04

There was 9.5% difference in the simulated cooling load reduction for the ground floor office when it was simulated using the simplified model, and the simulation made using the actual building model (consisting of other floors and areas). Meanwhile, there were only a 0.16% differences between the cooling load reduction for the IT room when it was simulated using the simplified model and the actual baseline model. This is due to the 26.47% standard deviation and +2.2% mean bias error in the total cooling load between the simplified ground floor model and the ground floor in the actual baseline model. The monthly cooling load and solar heat gain through exterior windows at the ground floor in the simplified model and the actual baseline model is shown in Table 56.

The simplified version was modified to leave only the ground floor without the 1st to the 7th floor. The roof was modified to imitate the rooftop construction in the 7th floor to reduce solar gain. However, even though the total cooling load in the simplified model was lower than the total

cooling load of the ground floor in the actual baseline model, the total heat gain in the simplified version is higher than the actual baseline model. The differences can be seen in the solar heat gain through windows, whereas the heat gain in another aspect were 100% the same. The simplified model may not experience additional heat transfer from the neighbouring floors, and the internal heat was lost into the ground which resulted in the lower total energy consumption and total cooling load. Meanwhile, the IT room was fully insulated in both models and does not have windows. Hence, it has higher resistance to the thermal transfer in both situations. However, the simplified model was used to investigate different PCM and insulation settings on different types of air-conditioned rooms before applying it to the actual baseline building model to investigate the energy and cooling load reduction as a whole (as explained in Section 4.1.2).

Table 56: The monthly cooling load and solar heat gain through exterior windows at the ground floor in the simplified model and the actual baseline model.

Month	Total Cooling		Solar Gains Exterior Windows	
	Simplified baseline kWh	Actual baseline's GF kWh	Simplified baseline kWh	Actual baseline's GF kWh
January	23802.15	32702.77	7034.576	5312.272
February	20575.75	28157.69	6591.681	4837.49
March	27142.81	36094.9	7534.467	5481.646
April	26586.64	35928.74	7138.52	5287.33
May	26747.63	36019.95	7058.597	5265.639
June	24380.14	33040.8	7015.647	5239.083
July	28789.65	39075.24	7175.352	5383.648
August	23596.58	32078.88	7208.003	5373.74
September	23077.88	31619.17	6905.276	5099.304
October	26550.26	35955.38	6975.237	5057.847
November	23100.82	31453.83	6594.346	4882.718
December	24328.67	33706.66	6667.279	4982.815

4.1.3.3 Economic analysis

The economic analysis was carried out based on the payback period and the energy reduction cost. The energy reduction cost was analysed based on total energy reduction for the whole

building's remaining lifetime or the product's lifetime (whichever came first). The total retrofit cost for the PCM is based on the price rate provided in Design Builder software and the total retrofit cost for insulation material is based on the quotation given by XPS extruded polysterene manufacturer (Cellecta Company based in UK [189]). The price given is for a general guideline, it may vary depending on the seller's price. The prices were based on bulk purchase and the total retrofit cost is based on the materials' cost. The detail cooling load and economic analysis results for the retrofitting are presented in Table 57 and Table 58.

Table 57: The economic analysis for the IT rooms (installation of insulation materials).

Zone	Installation area	Insulation cost	Payback period	Estimated energy reduction cost
	m^2	RM	Year	RM/kWh
IT rooms GF	66.5	6,916	6.8	0.0546
IT rooms L1	66.5	6,916	6.9	0.0556
IT rooms L2	66.5	6,916	6.6	0.0530
IT rooms L3	66.5	6,916	6.6	0.0531
IT rooms L4	66.5	6,916	6.9	0.0554
IT rooms L5	66.5	6,916	7.1	0.0568
IT rooms L6	66.5	6,916	6.6	0.0529
IT rooms L7	66.5	6,916	6.0	0.0486
Total	532	55,328	6.7	0.0537

Table 58: The economic analysis for the offices, corridors and cafeteria (installation of PCMs).

Zone	Installation area	PCM cost	Payback period	Estimated energy reduction cost
	m^2	RM	Year	RM/kWh
Office GF	1731	225030	4.7	0.0378
Office 1	1731	225030	8.4	0.0677
Office 2	1731	225030	7.0	0.0567
Office 3	1731	225030	9.2	0.0738
Office 4	1731	225030	6.7	0.0542
Office 5	1731	225030	6.2	0.0497
Office 6	1731	225030	7.0	0.0566
Office 7	1731	225030	5.1	0.0412
Corridor GF	115	14950	4.5	0.0360
Corridor 1	115	14950	3.7	0.0297
Corridor 2	115	14950	3.1	0.0251
Corridor 3	115	14950	3.2	0.0262
Corridor 4	115	14950	5.1	0.0408
Corridor 5	115	14950	6.8	0.0550
Corridor 6	115	14950	2.5	0.0203
Corridor 7	115	14950	6.1	0.0488
Corridor South	2505	325650	74.5	0.5996
Café	580	75400	9.1	0.0736
Total cooling load	17853	2,320,890	7.3	0.0584

The calculated cost for the insulation and PCM is RM 2,320,890.0 (the currency exchange used was referred on 15th July 2016) which yields a total simulated energy reduction of 1,019,681.26kWh a year. The potential saving on the energy bill is RM 305,450.07 (RM 185,940.34 potential saving on the electricity bill and RM 119,509.73 potential saving on the chilled water bill). In Malaysia, the electricity price rate for a medium size building under C1 category is RM 0.365/kWh and the chilled water rate is RM 0.271/kWh. The energy price rate for the cooling system is RM 0.322/kWh (based on the energy ratio between electricity and chilled water supply for the cooling system). Hence, the payback period will be 7.3 years. This calculation is based on the ratio of energy used for the cooling system where 53.9% of total energy used by the cooling system is supplied by electricity and 46.4% is supplied by chilled water. The payback period for installing insulation in IT rooms and data centre is lower compared to the installation of ENRG Blanket in the offices, corridors and cafeteria.

Nonetheless, the price to reduce 1 kWh energy using PCM and insulation is more economical than paying for the electricity and chilled water bills for the rest of the building's lifetime. The PCM and insulation material used have an expected lifetime longer than the expected building's lifetime (50 years). ENRG Blanket has a total lifetime of 23,563 cycles (64.55 years for a cycle a day) [190] and the XPS extruded polystyrene (insulation material) has a lifetime more than 100 years [191]. The total energy reduction if based on the estimated building's remaining lifetime (40 years) will be 38,016,838.4 kWh which will make the energy reduction cost as RM0.0583/kWh (assuming that other factors in the building remain the same throughout the years). However, as can be seen in Table 58, installing PCM in the corridor at the South building is not cost-efficient. If the PCM installation does not include the South building's corridor, the payback period for the PCM alone will be 6.3 years and the total energy reduction cost for insulation and PCM is RM0.051/kWh. The benefit of using the passive cooling designed in this study will outstrip the initial cost of the installation and material of PCM and insulation material. Furthermore, the electricity and chilled water price rates have been increasing (refer Table 18 and Table 20) and it is expected to be higher in the future.

4.1.4 Summary

The most optimum configuration for the installation of PCM and insulation material in two types of air-conditioned rooms with high internal heat gain in a tropical climate has been studied in this section. It is learnt that PCM application is more suitable for an office room (and rooms with air conditioning that operates during office hour) while internal insulation is more suitable for a server room with a 24 hour air conditioning requirement. The application of PCM could result in extra energy usage if force ventilation is not provided at night time [182], and it is not effective when paired with a fully insulated room. It is also found that the internal heat gain in the office zone is higher than the external heat gain from the windows. Hence, the envelope's requirement for this building in this particular climate is its ability to absorb the building's heat gain during its operation at daytime and release it at night time when it is vacant, or its ability to release internal heat to the outside. Due to high internal heat gain, passive cooling alone is not sufficient to provide thermal comfort for the occupants. In the next section, further analysis of the building's heat gain was carried out, and a retrofit method based on the thermal analysis was developed.

4.2 Novel retrofit methods based on thermal analysis to reduce cooling load

4.2.1 Introduction

The importance of improving a building's energy performance was emphasized by the government with the enforcement of sustainable building policies. Article 9 of the Directive 2010/31/EU of the European Parliament and the Council (19th May 2010) on the energy performance of buildings states the importance of stimulating refurbishment of existing buildings into near zero-energy buildings. However, the effectiveness of the process depends on the basic building structure and the refurbishment designs. Hence, methods to find the effective strategies for retrofitting and modelling to predict energy reduction is vital. Unlike previous studies, this research presents a method for a deep building retrofit based on the whole building's thermal analysis specifically for cooling demand countries. This work set against recommended best practice office building energy benchmarks in Malaysia, and following a comprehensive building audit, a retrofit strategy was proposed based on the target building's thermal analysis with cooling demand reduction in particular focus.

4.2.2 Reviews on the previous retrofit methods

Due to high numbers of unsustainable existing buildings, great interest was paid on building refurbishment to increase energy efficiency [104]. In many cases this process is more economical and has a less environmental impact compared to a complete demolition and rebuild [99][104][106]. However, the effectiveness of the process depends on the basic building structure and the refurbishment designs [106][107]. Hence, methods to find effective strategies for retrofitting and modelling to predict energy reduction are vital [99][107]. General energy retrofit guides and energy efficient measures (EEMs) were published by various institutions including the US Department of Energy (US DOE) and ASHRAE (in collaboration with other institutes) [98][108][109] as a response to the increasing demand for building refurbishment. Nonetheless, retrofit measures may have different impacts on different buildings due to the variance in design and sub-systems, making the retrofit selection very complex [99]. In previous studies, buildings were audited to determine the area of concerns before applying EEMs [85][92][91][110][111] [112] selected based on the multi-objective optimization methods [99][107][113][114][115] or cost-benefit analysis [93][116]. Mainly, the audit process concerns the end-use energy

consumption to determine the sector that requires retrofitting but not an in-depth holistic approach to defining the building's parameters that contribute towards the large energy share from the sector. Whereas in the early design phase, sensitivity analysis is widely adopted to determine parameters which significantly contributes towards the performance of the design solution [118]. Andarini et al. [119] used a sensitivity analysis to obtain parameters that can significantly reduce cooling demand in a shophouse design for the Indonesian climate. A sensitivity analysis was also performed by Yildiz et al. [120] to define parameters in an apartment's design which greatly contribute towards the heating and cooling load. While Heiselberg et al. [118] studied a wider range of input parameters to determine their impact on the total energy performance of an office building design. Normally, heating and cooling load were assigned as the output variables for the sensitivity analysis as it is a significant energy performance indicator and the major energy consumer globally for buildings [36][40][118][119][120][121]. Whereas, in cooling-dominated countries, air conditioning dominated the building's energy share [27][85][86]. A study by S.Aun et al. [122] concluded that Malaysia's office buildings used 64% of the total building's energy for air conditioning. Meanwhile, other tropical countries such as Indonesia, Thailand, and Singapore, spent 51% to 59% of the building's energy budget on air conditioning [85][119]. Against this background, this study aimed to discover a retrofit method based on a whole building thermal analysis for cooling dominated countries.

4.2.3 Methods

The proposed method consists of four steps as summarized in Figure 59. The process involved the fundamental audit work and building modelling which has been explained in Chapter 3. The building thermal analysis consists of three steps. Step 1 aimed to define the zones with the highest cooling load and cooling load intensity, step 2 aimed to discover the main heat sources in those zones and step 3 aimed to diagnose what causes these components to emit such a high amount of heat which contributes towards the retrofit strategies. The strategies were proposed to the facility manager for implementation. The energy data after a year of implementation was analysed and presented in Chapter 5.

The economic analysis was carried out using equation (4.1.1) to equation (4.1.7) in Section 4.1. The initial implementation cost for light emitting diode (LED) is based on the actual LED price from Lamp Shop Online [192] and the initial cost for PV panels was calculated based on the actual PV panel price distributed by Photonic Universe [193]. While other retrofit costs were derived from the material's price provided in the Design Builder software. The initial cost for LED was calculated based on the equation (4.2.1) which was derived from equation (4.2.2) to equation (4.2.4).

LED price (RM/m²) = (Room's lux × Price per lamp) / Lumen per lamp (4.2.1)

LED price (RM/m²) = (Number of lamps × Price per lamp)/ Area (4.2.2)

Number of lamps $= \frac{\Sigma Lumen\ (req)}{Lamp's\ lumen\ output}$ (4.2.3)

$\Sigma Lumen_{(req)}$ = (Lux × Area) (4.2.4)

Where:

Initial/baseline (i)

After retrofit (n)

Total lumen required to achieved the desired lux in a room ($\Sigma Lumen\ (req)$)

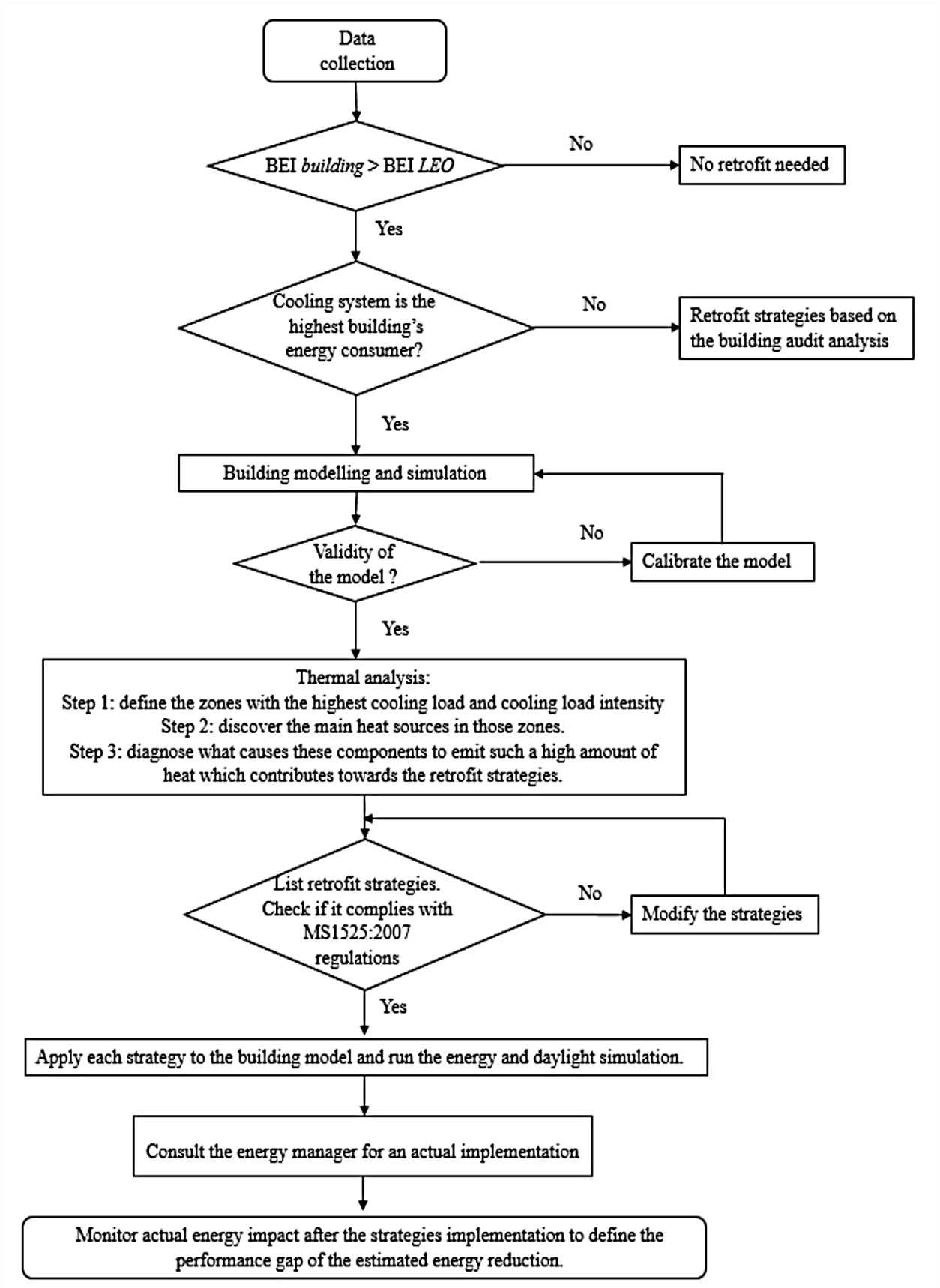

Figure 59: The retrofit method based on the thermal analysis.

4.2.4 Results and Discussion

4.2.4.1 Thermal analysis

Zones with the highest overall cooling load and cooling load intensity were defined (shown in Table 59) for a further heat source analysis. It is found that zones with heavy duty equipment (data centre and IT rooms) were deemed to have the highest cooling load intensity (annual cooling load per zone's area) while total annual cooling loads are largest in bigger areas. Further analysis of the heat sources in the main cooling areas area shown in Table 60. It can be seen that heat distribution in every area varied depending on the zone's internal equipment type, architectural design (fenestration and area), type of activities and operational schedules. In this case study, four important components contributing to the heat gain were highlighted as the lighting system, windows, and equipment and operation settings. An in-depth holistic analysis was carried out and discussed to obtain the causes for the components' high heat emission rate.

Table 59: Annual cooling load in different cooling zones.

Cooling zones	Annual cooling load (kWh)
Offices	3,199,514
Data centre	402,493
Corridors	238,284
Cafeteria	147,128
IT rooms	67,799
Hall and Auditorium	25,963
Total	4,081,181

Table 60: Heat gain distribution in different zones.

	Annual heat gain distribution (%)			
Zones	SG	L	Eq	Occ
Office	18	52	27	4
Data centre	0	5	94	1
Corridors	34	59	0	7

Note: Solar gain from external windows (SG), lighting (L), Equipment (Eq) and Occupancy (Occ).

4.2.4.1.1 Lighting system

Despite the fact that the majority of the office zones received lower than the MS1525:2014 recommended light luminance level, the heat emitted and energy consumed by the lighting system was high. This finding highlighted the actual inefficiency of the lighting system and potential for improvement. An example of the luminance in office areas is shown in Table 28 and Table 29 (in Section 3.1) and a picture of the typical office room taken during a field visit is shown in Figure 60. The actual lighting system efficiency was calculated using equation (4.2.5) which was derived from the equation (4.2.6) [123]. The results are listed in Table 61.

η_{LS} = measured lumen/ total power used (4.2.5)

$\phi = (MF \times U_L \times LOR \times \eta_L \times \eta_g) \times P_{sys}$ (4.2.6)

Where:

Lighting system's efficiency (η_{LS})

Luminous flux at task area (ϕ)

Maintenance factor (MF)

Lamp's utilization factor (U_L)

Light output ratio (LOR)

Lamp's efficiency (η_L)

Lamp's gear efficiency (η_g)

Power consumption by lighting (P_{sys})

Table 61: Measured efficiency of the lighting system.

Office zones	η_{LS} (%)	Power rating (W/m^2)
Level 1	1.94	6
Level 2	4.02	5
Level 3	4.20	5
Level 4	2.82	5
Level 5	3.42	4
Level 6	2.96	5
Level 7	3.74	4

The low average lighting system efficiency in office areas explains the high heat gain as the lamp power losses are emitted into space as heat (radiation and convection) [129]. Previous studies (P.Hanselear et al.) [194] suggested that the light's utilization factor (utilance) is more important than the lighting output ration in reaching energy efficiency and it depends on:

a) the arrangement of the luminaires in the room concerning the position of the task area;
b) the luminous intensity distribution of the luminaires and the spacing to height ratio;
c) the reflectance of the surroundings, which determined the indirect contribution.

Therefore, besides lamp efficiency, their arrangement, maintenance, lamp's control gear efficiency, as well as the construction and space design play a major part in determining the efficiency of the whole lighting system in delivering the minimum required lumen to space. Most of the lamp types used were PL-L (36W) lamps 2008's version that has low lamp efficiency and used a recessed type configuration. Typical fluorescent lamps emit 21% of its input power to visible light, 37% radiant heat and 42% convective heat [129].

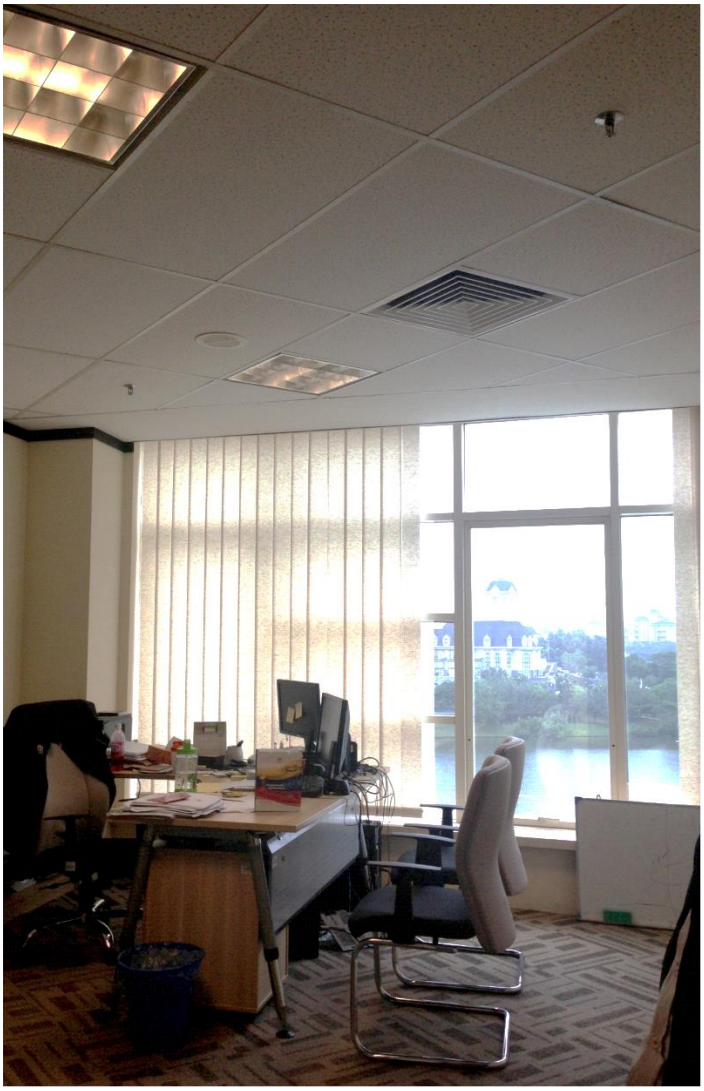

Figure 60: Lighting in a typical office room taken during a field visit in 2014.

The curtain wall windows in corridors and office areas allowed high daylight luminance to light up the spaces without depending on artificial light. The recommended luminance level for a corridor is 50 lux and 100 lux for lift lobbies [143] whereas the daylight luminance measurement in those areas (as listed in Table 62) were in the range of 502 lux to 25,001 lux. In practice, lightings in these areas were switched on 24 hours a day even though it could benefit from the high levels of daylight. A daylight linked installation could have eliminated the unnecessary energy usage and excessive internal heat gains.

Table 62: Daylight luminance measurement.

Zone	Luminance (lux)
Corridor level 2	21,000
Corridor level 3	25,001
Corridor level 4	14,840
Lift lobby level 2	502
Lift lobby level 3	503
Lift lobby level 4	396

4.2.4.1.2 Windows

For countries requiring high cooling demand, windows are an important element in ensuring the occupants' thermal comfort and in providing daylight illumination into the building. Malaysia receives an average of 4.67 kWh/m² average of daily solar radiation [31] where the incident solar radiation on a building's glazing is partially reflected and partially transmitted into the building depending on the glazing properties [195][196]. Despite a degree of overlap, the infrared component of the incoming daylight transmitted into the building materialises itself in the form of internal heat gain whereas the visible light spectrum (which in its lower bands overlaps with the near infra-red) increases daylight luminance. The proportion of infrared component transmitted into the building's space through the windows depends the solar heat gain coefficient value, while the proportion of visible light component that transmits into the building depends on the value of 'visible light transmittance'. In a cooling-dominated country, glazing with high visible light transmittance (VLT) and low solar heat gain coefficient (SHGC) is preferable to maximise daylight luminance and reduce heat gain. The choice of glazing is imperative in determining the amount of sunlight, and heat gain receives from solar energy through windows. The amount of sunlight will reduce the building's dependency on the artificial light when paired up with automatic daylight dimmer and an important factor to control glares. Meanwhile, the heat gain penetrates through windows formatting the building's cooling load. The instantaneous room heat gain is governed by the equation (4.2.7) [195] and SHGC value is defined by equation (4.2.8).

$$Qi = U_g * (T_{out} - T_{room}) + (SHGC * G) \quad (4.2.7)$$

Where:

Instantaneous room's heat gain (Qi)

Glazing's thermal conductivity (U_g)

Outside ambient temperature (T_{out})

Room's temperature (T_{room})

Coefficient of solar heat gain (SHGC)

Solar irradiance (G)

Even though the building has an 85% window to wall ratio (see Figure 61), it benefits from its architectural selection of window pane and shading designs that managed to offset a major fraction of the external solar heat gain. The building windows were made from single panel green float glass: 8 mm thick, SHGC value of 0.447, VLT 0.237 and U-value of 5.7 W/m². However, a further reduction of solar heat gain through windows is achievable by selectively adding a second pane to the existing window to create double panel windows with a lower SHGC and U-value while maintaining the VLT to maintain the daylight received.

Figure 61: The typical windows at the building's corridors (floor 1-7) taken during a field visit in 2015.

4.2.4.1.3 Equipment

The heat gain analysis revealed that zones with heavy duty equipment (data centre and IT rooms) had the highest cooling load intensity (annual cooling load per zone area) that reached up to 5545 kWh/m²/year for the data centre and 938 kWh/m²/year for the IT rooms. The equipment high rating power and 24 hours operation released substantial amounts of heat into the surroundings which in turn requires the building manager to set the cooling set point temperature at 21°C at all times in these zones to avoid equipment overheating and ensure good operating conditions. In the office areas, equipment was responsible for 22% of the total annual heat gain. 529 pieces of office equipment were used in the building with mainly desktop computers (256 units) and small printers (137 units). Office pantries at each level used refrigerators that constantly operate and most of the desktop computers did not have Energy Star rating. Inefficient equipment increased heat gains, which in turn exacerbated the cooling load.

4.2.4.1.4 Operation settings

The air conditioning in office areas was set to 22°C, which is 1°C lower than the suggested value by MS1525:2014 that is 23°C to 26°C. While the cooling system and lighting system were scheduled to turn on at 6.30 am and switched off at 7.30 pm that is an hour earlier than the office opening time and an hour and a half after office hour. These operation settings resulted in energy waste. Furthermore, an analysis of the building's cooling load shows that peak demand occurs every morning at 8.00 am in workdays. This happened due to the highest point of latent cooling load on the day (this can be observed in Figure 62). As the total cooling load is expressed by the equation (4.2.8). The amount of latent load was derived by deducting simulated sensible cooling load from the simulated total cooling load.

Total cooling load = sensible cooling load + latent cooling load (4.2.8)

The demand for a latent cooling load originated from the requirement to maintain a healthy relative humidity in the office and the communal areas. A graph of hourly latent load spanned in a week duration in January against the outside and inside relative humidity (Figure 62) proved this hypothesis. It can be observed that the relative humidity in the office area started to reach its peak at 0700 as the air conditioning was switched on at 0630. The air conditioning system introduced the outside air into the office area. This increase in relative humidity resulted in an increment of latent cooling load at 0800.

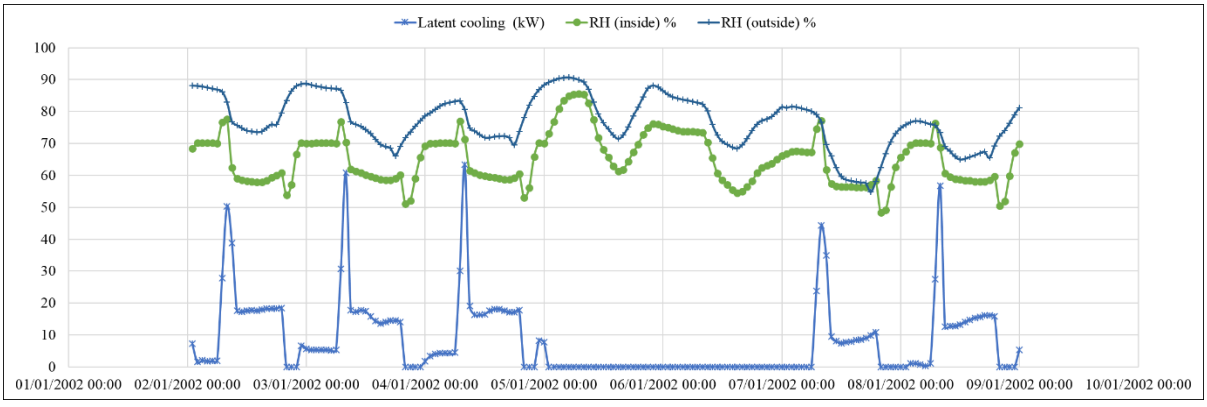

Figure 62: The hourly latent cooling load and relative humidity in the office at the 4th floor and outside the building.

4.2.4.2 Strategies to reduce cooling load

The retrofit plans were designed based on the thermal analysis and primarily aimed at reducing the heat gain that causes an increase in the cooling load. This objective is achieved by following the strategies listed in the subsections below.

4.2.4.2.1 Lighting System

A lighting system that includes automatic daylight dimmer in corridors and office zones as well as replacing existing lamps with high-efficiency LEDs [129]. Luminance in the office zones was adjusted to 300 lux by the recommendations from previous studies [123] and MS1525:2014 [143]. Lighting operating schedule was proposed to accommodate the employees when the area is occupied (i.e. 0730 hours to 1800 hours).

4.2.4.2.2 Glazing

A 6mm thick low emissivity (Low-E) glass panel was added to the existing model as an internal layer of the current green float glass with a 16mm air gap between them. The new glazing has an SHGC value of 0.381, VLT value of 0.6 and U-value of 5.672. The commonly used clear glass window panels were also examined for comparative studies. The impact of different glazing types on building solar heat gain is detailed in Table 63.

Table 63: The impact of different glazing types on the building solar heat gain through external windows.

Glazing type	SHGC	U-value (W/m^2)	SHGW (kWh)
Single panel clear float glass (8mm)	0.815	5.7	2,014,444
Single panel green float glass (8mm)	0.447	5.7	598,054
Double panel (retrofit)	0.381	5.672	175,833

4.2.4.2.3 Equipment

The office equipment in the model was changed so as to represent the latest generation of energy-efficient ICT devices. While the original HP desktop used 300W of power, a 216W Energy Star

rated HP desktop computer was chosen as a replacement. Also, Aficio™ MP C2051 by RICOH multifunction printers (rated power 1680 kWh) were changed to HP Color LaserJet Pro MFP M476dw printers (rated power 640 kWh). Finally, the chest freezers in the kitchens were changed from band F energy rated to band A+.

4.2.4.2.4 Operation settings

24 °C (air temperature) was chosen as the new set point temperature while the new operation schedule for the cooling system is shown in Figure 63 and lighting systems in office zones were set to 0730 to 1730 hours. This new set point temperature was chosen based on a discussion with the building energy manager concerning the occupants' thermal comfort. Previously, a series of trials were conducted by the building energy manager to appraise the sensitivity of the office workers to increases in internal office temperatures. The cooling temperature set points were adjusted within the suggested guideline by MS1525:2014 [143]. Based on the information provided by the building energy manager, 24 ^{O}C was the maximum temperature set point for office areas that was voted acceptable in occupants' feedback trials (the building management increased cooling temperature set point to 24 ^{O}C and 25 ^{O}C to examine space thermal acceptability range). The employees launched complaints when the cooling set point was raised to 25 ^{O}C, but interestingly no negative feedback was received when it was set to 24 ^{O}C. Although this does not conclusively elucidate the neutral thermal point of the occupants, it demonstrates the possibility of raiding zone target temperatures while maintaining occupant satisfaction.

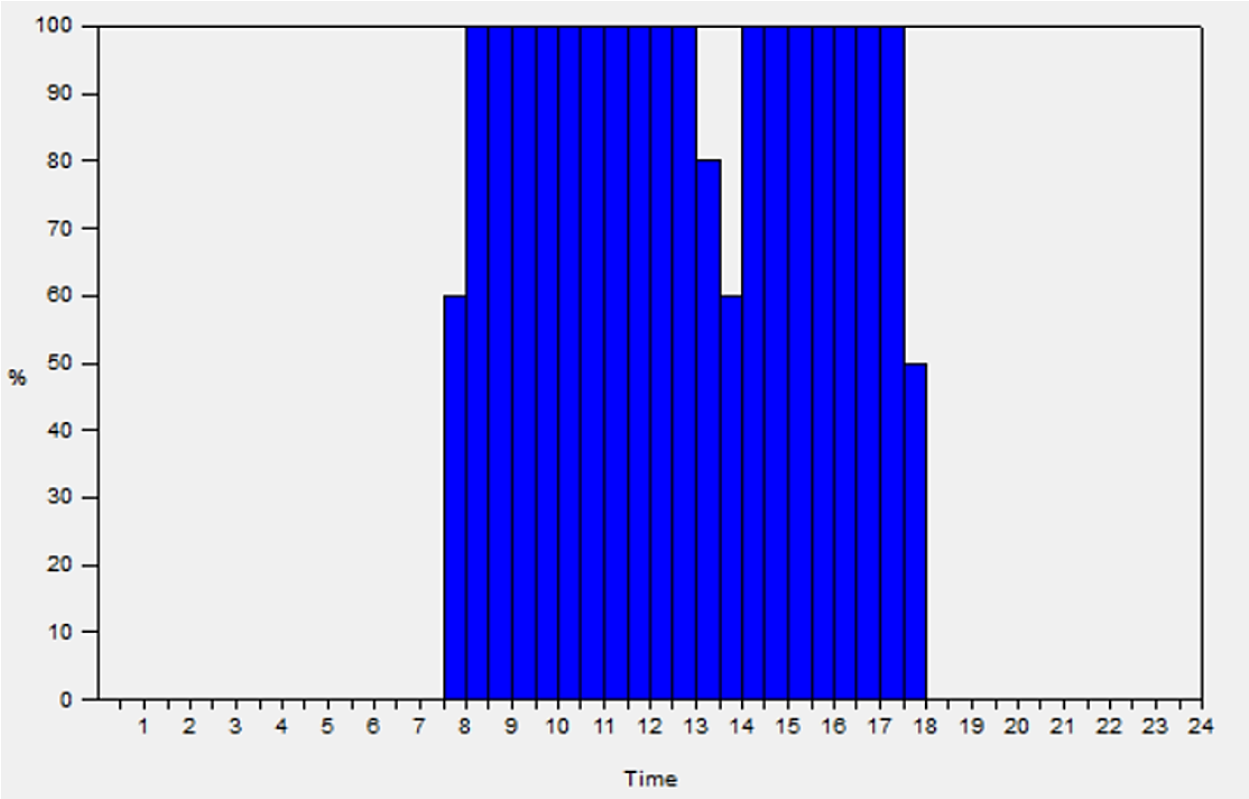

Figure 63: Modified cooling operation schedule (hourly cooling load) for office zones from the Design Builder software.

4.2.4.2.5 Renewable Energy

Solar panels with 15% efficiency were installed on the South building's roof (3,681 m² area) to aid operational de-carbonization and limit the building's envelope heat gain. The generated electricity was directly supplied to the building and was also stored in a battery.

4.2.4.3 Simulated performance

The cumulative effect of all the strategies was estimated to reduce 47% of the total energy consumption, 57% reduction in the annual primary energy demand and 40.2% reduction in the total cooling load. The energy performance and the initial cost for the suggested methods are summarised in Table 64, and the comparison of end-use energy consumption before and after retrofit is shown in Figure 64. The monthly heat gain and cooling load before and after retrofit are shown in Figure 65 and Figure 66. Analysis of the buildings total heat gain, and the building's total cooling load shows that a reduction of 1,724,815.00 kWh in the building's heat

gain resulted in a reduction of 1,915,437.00 kWh in the building's total cooling load. Clearly, managing the heat gain from its sources have a direct impact on the total cooling load. Plus, besides supplying 12% of the total building's annual energy demand the installation of PV panels on the rooftop is estimated to reduce cooling load by 0.3%.

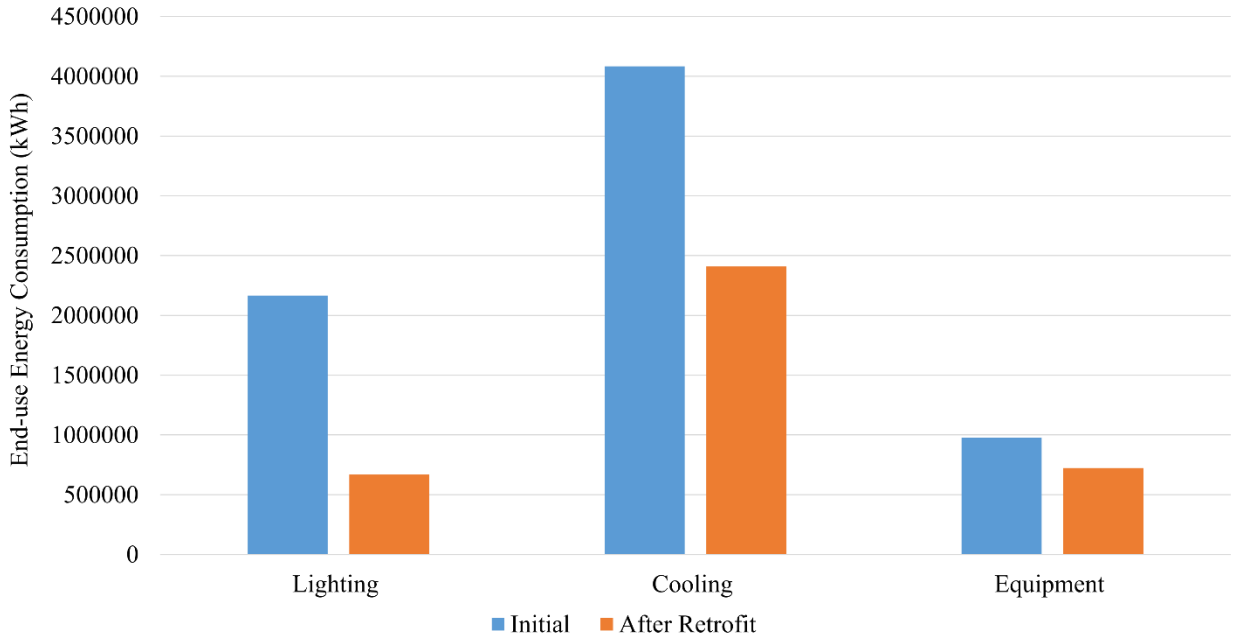

Figure 64: The comparison of end-use energy consumption for the initial and after the retrofit.

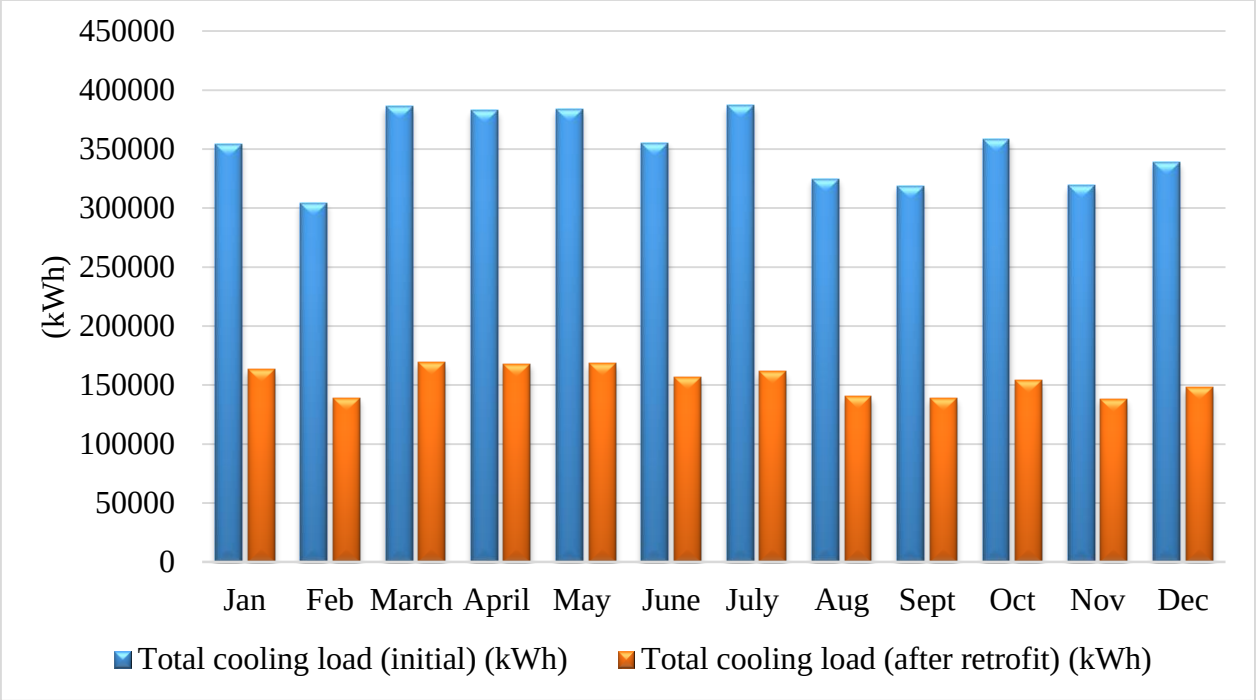

Figure 65: The comparison of the building's monthly cooling load before and after the retrofit.

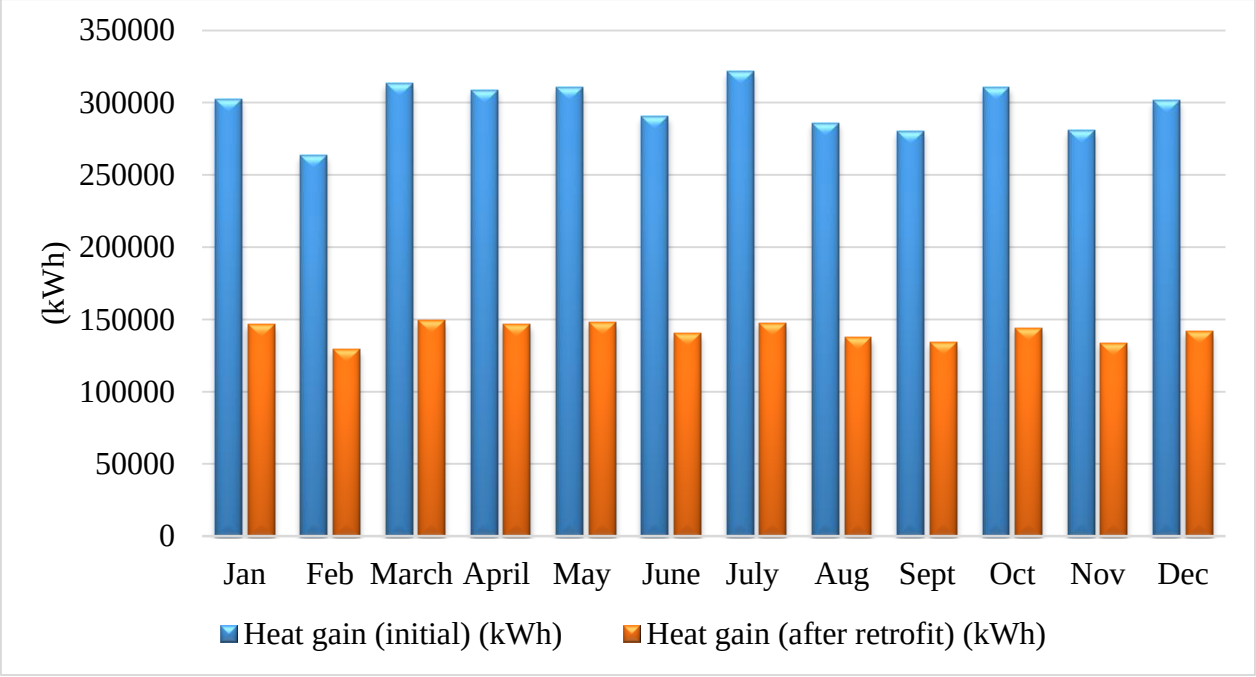

Figure 66: The comparison of the building's heat gain before and after the retrofit.

By switching on only 60% of the cooling system at 0730 hours as pre-cooling, peak latent load that arises due to the high outside humidity at that hour [51] can be significantly reduced. These

changes resulted in a significant reduction in peak cooling load that occurs in the morning. The comparison of hourly building's cooling load before and after retrofit is shown in Figure 67.

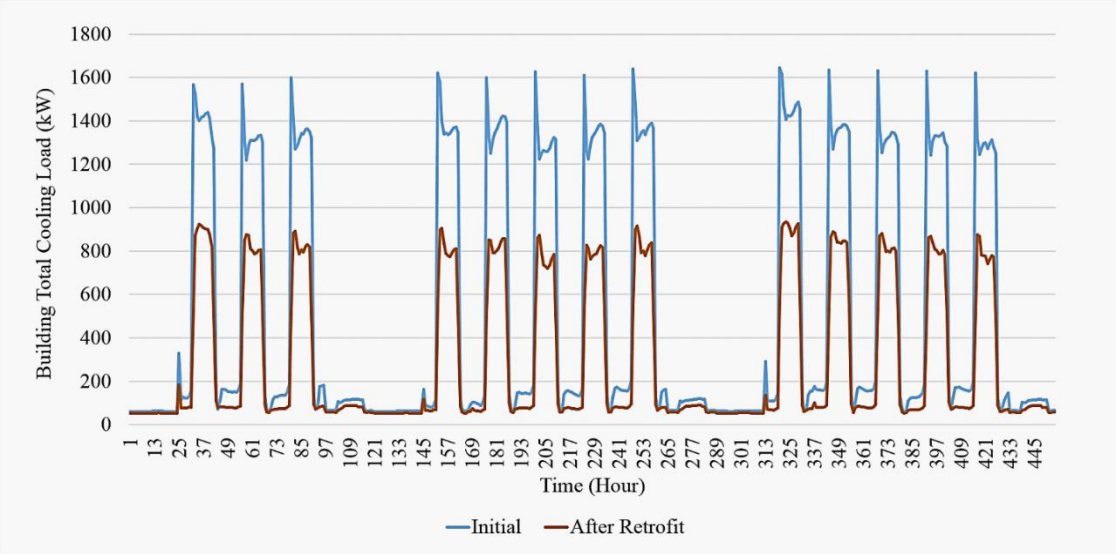

Figure 67: The simulated hourly building's cooling load before and after retrofit - 450 hours data (01/01 to 19/01)

4.2.4.4 Economic analysis

Notably, besides having no cost implication, modification in operational regimes is estimated to be more effective in reducing cooling load compared to the modification in glazing and equipment. While from an economic perspective, modification in operation settings and lighting system deemed to be the most economical compared to other strategies. The shortest payback period is operational changes (0 year/instantaneous), then followed by changes in the lighting system (3.5 years), installation of PV panels (24.1 years) and the longest payback time is changes in glazing (45.7 years). Considering the fact that the average building's lifetime is 50 years and the building's age is 10 years, the installation of glazing is deemed to be uneconomical due to the payback period that was estimated to be 47.1 years. However, the estimated cost for glazing is based on the data given in Design Builder software. Whereas, prices for other products are quoted from manufacturers for bulk purchase. The actual cost will vary depending on the shops or manufacturers, and quantity of purchase made. Bulk buy will be cheaper than small purchase, and direct purchase from the manufacturers will be cheaper than buying from distributors.

On the other hand, the price that is to be paid to reduce the 1kWh energy through retrofitting the lighting system (RM 0.19/kWh) is cheaper than paying the electricity bill (RM 0.365/kWh). This calculation was made based on the LED's lifetime is 30,000 hours and assuming that the lamps were used 12 hours a day for 365 days which make the lamp's lifetime 6.85 years. Meanwhile installing the PV panels is estimated to generate electricity at the price of RM 0.351/kWh. This calculation was made based on the PV panel's lifetime (25 years). The PV panel's lifetime is derived from the distributor's guarantee that the solar cells will produce at least 90% of its nominal power after 10 years of installation and at least 80% of its nominal power after 25 years of its installation [193].

Table 64: The estimated energy performance and initial cost for the suggested methods.

Method	Total energy consumption (kWh)	Renewable energy (kWh)	Total cooling load (kWh)	Primary energy reduction (kWh)	Primary energy reduction (%)	Cooling load reduction (%)	Total retrofit cost (RM)	Energy reduction cost (RM/kWh)	Payback period (Year)
Initial	7,224,042	-	4,082,655	-	n/a	-	-	-	-
Operation	6,594,767	-	3,570,735	629,275	9	12.5	0	0	0
Lighting	4,726,123	-	3,137,779	2,497,919	35	23.1	3,229,262.90	0.190	3.5
Glazing	7,095,982	-	3,954,596	128,059	2	3.1	2,137,560.80	0.417	45.7
Equipment	6,855,625	-	3,941,439	368,417	5	3.5	n/a	n/a	n/a
PV	7,210,797	746,703	4,069,411	759,948	12	0.3	6,675,014.32	0.351	24.1
Combine	3,830,363	746,703	2,439,678	4,140,382	57	40.2	n/a	n/a	n/a

4.2.5 Summary

Reducing building cooling load and increasing the cooling systems efficiency is a major component in the de-carbonisation of buildings in tropical countries. Sensible cooling load arises from the need to remove heat gain in a building as to maintain a comfortable thermal condition. Managing the heat sources and cooling system operation settings proved successful in reducing a significant amount of cooling load. The thermal analysis method proposed in this study enables heat gain components to be mapped, allowing the design of effective strategies to reduce the cooling load. It was found that the heat gain were mainly contributed by the internal factors such as the lighting and equipment. A reduction in 1,724,815.00 kWh in the building's heat gain resulted in a reduction of 1,915,437.00 kWh in the building's total cooling load and a total of 47% total energy reduction. This again shows the importance of HVAC system in prompting the building's total energy consumption. If this HVAC system is powered by solar energy (since Malaysia received high solar radiation all year round) a massive reduction in GHG emission and dependency on primary energy can be reduced. However, will it be sufficient to power up the whole HVAC system with solar energy for a building that used up to 387,152.53 kWh cooling load in a month (March) ? Further investigation of this idea is presented in Section 4.3.

4.3 Hybrid solar powered cooling system

4.3.1 Introduction

Most of the commercial buildings (which include offices, shopping malls, hotels, and museums. [124]) spent most of their energy on HVAC system [86][88][101]. Meanwhile in the cooling dominated countries more than 50% of the building's energy were used for air conditioning and mechanical ventilation (ACMV) [86][88]. HVAC systems are a necessity in the harsh climate countries to ensure a good indoor environment is being delivered to the occupants. Due to the large portion required to power up HVAC system in commercial buildings, this section is aimed to investigate the possibility of powering the cooling system with solar energy. Previous studies proposed various designs on the solar-powered cooling system. However, these studies were mainly focused on domestic and small commercial buildings. This chapter proposes a design for a solar powered cooling system for a typical medium sized office building in a tropical region located in an urban area.

4.3.2 Reviews

A typical Malaysia Office Building consumes about 250 kWh/m²/year which is 400% higher than the recommended Building Energy Index (BEI) for Green Energy Office (GEO) building [57][58][86][122][197]. Research revealed that Heating Ventilation and Air Conditioning (HVAC) system is the highest energy consumer in a commercial building [40]. Meanwhile in cooling demand countries, more than 50% of the building's energy was used for air conditioning [85][86]. The study by Chan and S. Aun discovered that Malaysia's office building used 64% of the total building's energy for air conditioning while other tropical countries such as Indonesia, Thailand, and Singapore, spent 51% to 59% of the building's energy budget on cooling [85]. High heat gain and humidity made it necessary for offices in hot and humid region to adopt ACMV to maintain a good thermal comfort for the occupants. Malaysia receives an average of 4.7 kWh/m² daily solar radiation. Besides being responsible for the external solar heat gain for the building, the energy radiated can be harnessed to cool and power up the building.

Previous research has been exploring the solar assisted cooling system and ways to enhance its efficiency [198][199][200][201][202][203][204][205][206][207][208][209][210][211]. All these

studies were based on computer simulations except for the study conducted by Rosiek and Batles [199] and A. Pongtornkulpanich et al. [210] that were based on the actual data. The reported maximum COP of the solar cooling system ranged between 0.55 to 0.68 [199][200][201][202][204][207][208]. Previous studies mainly combined solar collector with liquid desiccant for the latent cooling while the sensible cooling load was powered by vapour compression chiller using either auxiliary energy or electricity generated by the solar plate [204][207][208], or a combination of solar collector and heat driven chiller [199][201][210]. However, all these studies were conducted for a small scale cooling system (1.5 kWh to 70 kWh) with an exception to the study carried out by G. Mittelman et al. [201] which was modelled for a 1MWh cooling load. The actual results presented by Rosiek and Batles [199] and A. Pongtornkulpanich et al. [210] shows that the cooling systems could not be powered fully by solar energy. Both cases utilized flat plate solar collector with an additional backup system such as an auxiliary heater. It was reported by Rosiek and Batles [184] that for the cooling load more than 70 kWh, the inlet water temperature for the heat driven chiller needed to be more than 80°C. Whereas G. Mittelman developed a concentrating photovoltaic/thermal (CPVT) model to power up 1MWh absorption chiller driven by 85°C and 100°C coolant outlet from the CPVT. The simulated chiller's COP ranged between 0.6 to 0.75 [201].

The photovoltaic/thermal (PV/T) system has been studied three decades ago [212] and it was initially aimed to increase the efficiency of the PV cells [213]. The technology offers a higher PV efficiency compared to the flat plate collector and also produced hot water in the range of 40°C to 60°C [201][212]. This temperature is suitable for a low-grade heat usage such as space heating or a liquid desiccant system for solar cooling and dehumidification. However, for an office building located in a tropical climate with a high cooling demand (~1600 kWh), higher temperature is required to power up the heat-driven chillers such as adsorption chiller and absorption chiller [201]. For this purpose, a concentrating photovoltaic and thermal (CPVT) system deemed to be the most suitable for a building with high cooling demand. A CPVT modelled by G. Mittelman et al. [201] showed 20% electric conversion efficiency at 150°C coolant outlet for a direct insolation flux of 900 W/m² and concentration ratio of 200. Whereas a miniature CPVT (MCPV) system developed by A. Kribus et al. [214] with an aperture area 0.95m² and concentration ratio of 500 showed a combined heat power (CHP) efficiency of 80% when varying the coolant outlet

from 58°C to 200°C. As the coolant outlet increases, the thermal efficiency increases and the PV efficiency was decreased.

4.3.3 Methods

The cooling system was designed based on the cooling load from the simulated base building model in Section 3.3 after being applied operational schedule suggested in Section 4.2.4.2.4. It was intended to substitute the current chilled water supply from the Gas District Cooling (GDC) to the air conditioning unit and also generating solar energy to power up the cooling system. If there is excess electricity generated, it will be used to power up the other electrical equipment in the building. The system is illustrated in Figure 68.

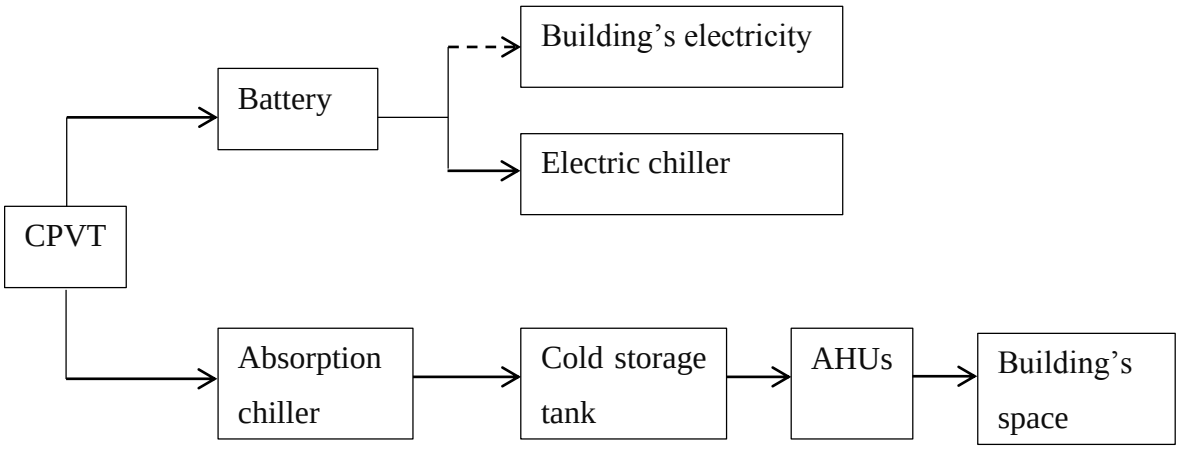

Figure 68: Block diagram of solar assisted air conditioning system.

The system was built to yield a high coolant outlet (85°C – 95°C) to power up the absorption chiller while maintaining a high PV efficiency to generate electricity. The absorption chiller is expected to produce 7°C chilled water which then will be stored in a cold storage tank. The stored electricity will be used to power up the electric chiller during the time when the chilled water stored in the cold storage is not sufficient. Any excess electricity will then be used to power up the absorption chiller's pumps, AHUs, and the building electricity (priority usage is in the mentioned order). Detailed design for every component is described in the sub-sections below.

4.3.3.1 Miniature concentrating photovoltaic/thermal (MCPV) systems

The MCPV model (see Figure 69) established by A. Kribus et al. [214] was used in the system for its efficiency for large scale cooling and its ability to operate at higher temperatures than PVT or flat plate collector, which is deemed to be more suitable to support absorption chiller's operation [201][214]. The size of the MCPV is also suitable for rooftop installation and in fact it is made to cater to urban environments [214]. It comes in a 0.95m² parabolic size with tracking mechanism, and the project was collaboration between Tel Aviv University and Distributed Solar Power Ltd. It used a triple-junction PV cells that have 32% nominal conversion efficiency [214].

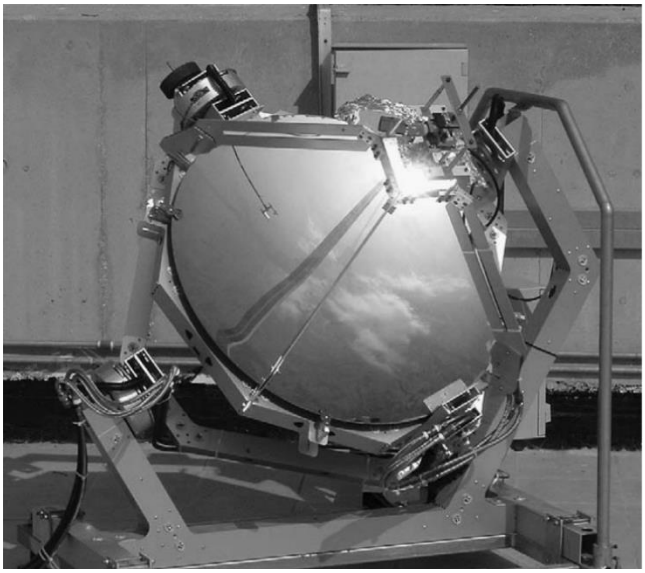

Figure 69: The MCPV unit as published by A. Kribus et al. [214].

The system was modelled using the simplified equations derived from A. Kribus et al. [214]. The mathematical equations (equation (4.3.1) to (4.3.10) were solved using Excel spreadsheet and compared to the PV efficiency and thermal efficiency values at different coolant outlet published by A. Kribus et al. [214] for model validation.

$$Q_{thermal} = Q_{incident} \times \eta_{optical} \times (1- \eta_{PV}) \text{ [214]} \quad (4.3.1)$$

$$Q_{electric} = (Q_{incident} \times \eta_{optical} \times \eta_{PV} - Q_{loss}) \times \eta_{inverter} \text{ [201]} \quad (4.3.2)$$

$$Q_{incident} = \text{Global solar radiation} \times \text{collection area [215]} \quad (4.3.3)$$

$$\eta_{pv} = \eta_{collector} \times \eta_{module} \quad (4.3.4)$$

$$\eta_{collector} = 0.288 - 0.000558 \times (T_{cell} - 25) \quad (4.3.5)$$

$\dot{m} = Q_{thermal} / C_p \times (T_{out} - T_{ambient})$ (4.3.6)

$\eta_{electric} = \eta_{optical} \times \eta_{PV} \times (1 - (Q_{loss}/Q_{gross})) \times \eta_{inverter}$ (4.3.7)

$Q_{gross} = Q_{incident} \times \eta_{optical} \times \eta_{PV}$ (4.3.8)

$Q_{loss} = 0.02 \times Q_{incident} + Q_{pump}$ (4.3.9)

$Q_{pump} = \dot{m} (\Delta P) / \rho \times \eta_{pump}$ (4.3.10)

It is assumed that;

$\eta_{optical} = 0.85$

$\eta_{inverter} = 0.9$

$T_{cell} = T_{outlet} + 10°C$

Concentration factor = 500

$Q_{thermal} = Q_{coolant,}$ it is assumed that the sides losses are neglected.

Where:

Thermal energy ($Q_{thermal}$)

Incident solar energy ($Q_{incident}$)

Electricity generated ($Q_{electric}$)

Coolant's thermal energy ($Q_{coolant}$)

Thermal losses (Q_{loss})

Energy used for pumps (Q_{pump})

Gross DC power produced by the modul (Q_{gross})

Optical efficiency ($\eta_{optical}$)

Efficiency of the PV cells (η_{PV})

Efficiency of the inverter ($\eta_{inverter}$)

Efficiency of the coolant's collector ($\eta_{collector}$)

Efficiency of the module ($\eta_{modules}$)

Efficiency of the pump (η_{pump})

Mass flow rate of the coolant outlet ($\dot{m}$)

Pressure drop (ΔP)

Fluid density (ρ)

Temperature of the PV cell (T_{cell})

Temperature of the outlet (T_{outlet})

For the model validation, the input used in A. Kribus et al. [214] were employed in the simplified equations and the results were compared with the results published in A. Kribus et al. [214] to measure its accuracy. The global solar radiation used was 900W/m² and the collection area 0.95m². The results are shown in Table 65.

Table 65: The calculated overall system efficiency by varying the coolant exit temperature.

T_{cell}	Global Solar	$Q_{incident}$	η_{PV}	$Q_{electric}$	$Q_{thermal}$	$\eta_{electric}$	$\eta_{thermal}$	η_{CHP}
°C	W/m²	W		W	W			
68	900	855	0.26	172	535	0.18	0.61	0.80
110	900	855	0.24	155	552	0.17	0.63	0.80
160	900	855	0.21	135	572	0.14	0.66	0.80
210	900	855	0.18	115	592	0.12	0.68	0.80

The graph plotted from the calculation achieved in this work (Figure 70) seems to agree with the output graph published by the original author shown in Figure 71. At T_{cell} 68°C the electric power achieved by A. Kribus et al. [214] was 172W and the thermal output was 530W.

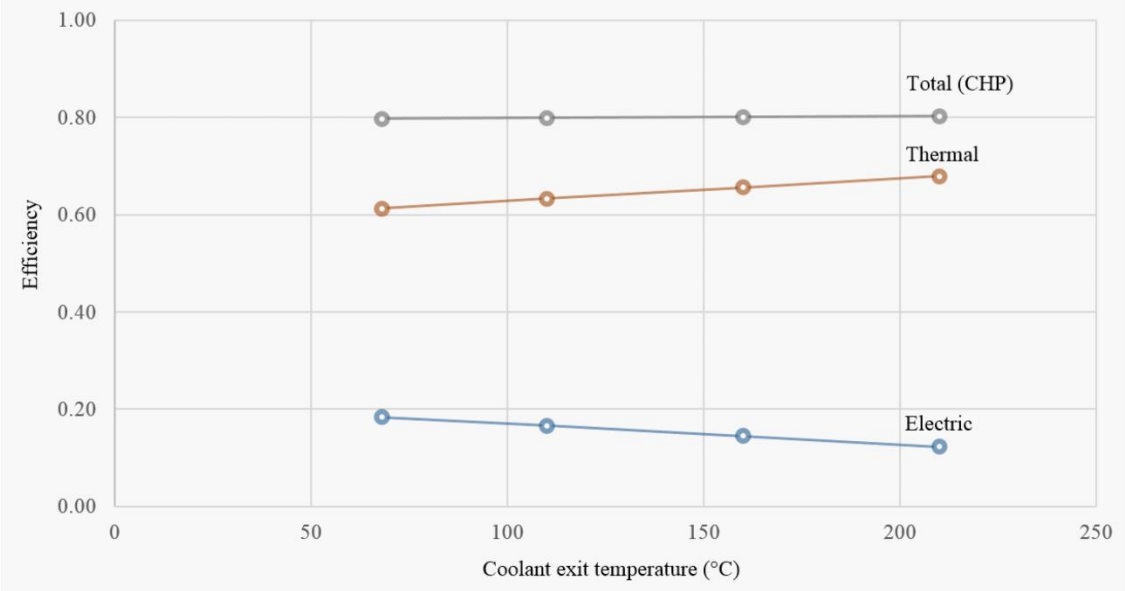

Figure 70: The overall system efficiency calculated in this work.

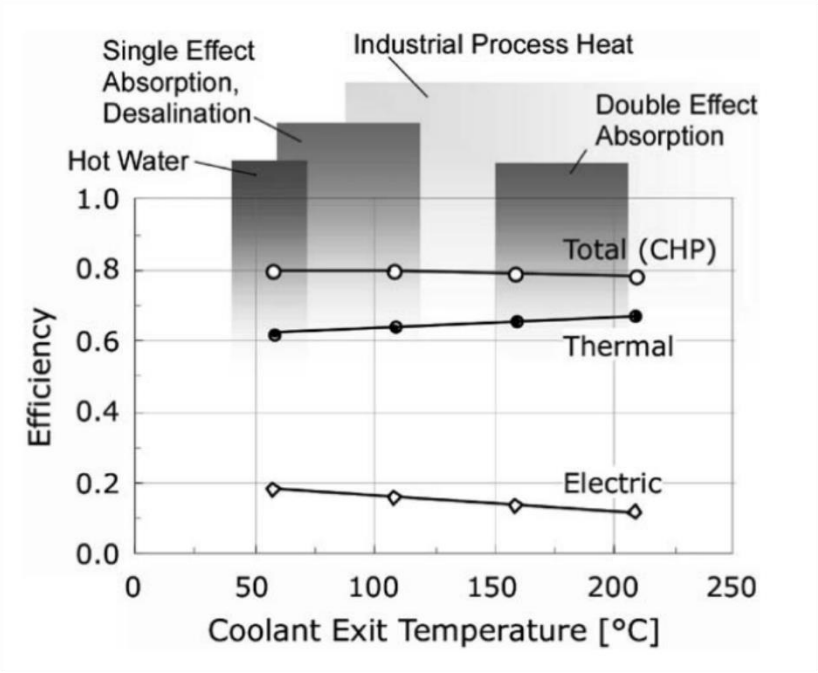

Figure 71: The diagram of overall system efficiency from A. Kribus et al. [214]

The equations for MCPV model were validated with a standard deviation of 0.94% in thermal power and 100% accuracy in electrical power. However, the 5W difference in thermal power originated from the power loss from pumps which was not yet included in the calculation. Hence, it is assumed here that the pumps' power used by A. Kribus et al. [214] was 5W. The cost analysis conducted by A. Kribus et al. [214] shows that when both electricity and thermal power were used, the system is more economical than PV/T whereas when the system only used electricity, it is still cheaper than flat plate photovoltaic panels and PV/T systems.

4.3.3.2 Absorption chiller

A heat driven refrigeration can be divided into two categories that are adsorption chiller and absorption chiller. The thermal input requirement for absorption chiller is higher than adsorption chiller. However, the coefficient of performance for an absorption chiller is greater compared to adsorption chiller. A lithium bromide/water (LiBr/water) absorption system is chosen for this work due to its high COP, less environmental impact, non-volatile, less pump work and simpler components compared to other heat driven refrigeration systems [216]. A simplified analytical expression of the cycles in the LiBr/water absorption chiller established by F.L. Lansing [101] was used. The mathematical expressions (equation (4.3.11) to (4.3.33)) were processed in Excel

as a simple modelling. The mathematical expression and assumptions made in the modelling equations are divided into two categories that are the input data and the steps of analysis.

4.3.3.2.1 Input data

T_g, °C generator temperature

T_e, °C evaporator temperature

T_c, °C condenser temperature

T_a, °C absorber temperature

E_L, exchanger effectiveness

Q_E, kcal/hr, load

4.3.3.2.2 Steps of analysis

$$X_1 = \frac{(49.04 + 1.125Ta - Te)}{(134.65 + 0.47Ta)} \quad \text{kg LiBr/kg solution} \qquad (4.3.11)$$

$$X_2 = \frac{(49.04 + 1.125Tg - Tc)}{(134.65 + 0.47Tg)} \quad \text{kg LiBr/kg solution} \qquad (4.3.12)$$

If $0.5 < (X_1 \text{ and } X_4) < 0.65$ proceed, else stop. (4.3.13)

$H_8 = (T_c - 25)$ kcal/kg (4.3.14)

$H_{10} = 572.8 + 0.417T_e$ (4.3.15)

$m_R = Q_E/(H_{10} - H_8)$ kg/hr (4.3.16)

$m_s = m_R \times X_4/(X_4 - X_1)$ kg/hr (4.3.17)

$m_w = m_R \times X_1/(X_4 - X_1)$ kg/hr (4.3.18)

$T_s = T_g - E_L(T_g - T_a)$ °C (4.3.19)

$C_{X1} = 1.01 - 1.23X_1 + 0.48X_1^2$ kcal/kg°C (4.3.20)

$C_{X4} = 1.01 - 1.23X_4 + 0.48X_4^2$ kcal/kg°C (4.3.21)

$T_3 = T_a + [E_L \times (X_1/X_4) \times (Cx_4/Cx_1) \times (T_g - T_a)]$ °C (4.3.22)

$H_1 = (42.81 - 425.92X_1 + 404.67X_1^2) + (1.01 - 1.23X_1 + 0.48X_1^2) \times (T_a)$, kcal/kg (4.3.23)

$H_5 = (42.81 - 425.92X_4 + 404.67X_4^2) + (1.01 - 1.23X_4 + 0.48X_4^2) \times (T_5)$, kcal/kg (4.3.24)

$H_7 = (572.8 - 0.46T_g + 0.43T_{c)}$ kcal/kg (4.3.25)

$Q_C = m_R/(H_7 - H_8)$ kcal/hr (4.3.26)

$Q_G = m_{10}H_5 - m_RH_7 - m_8H_1$ kcal/hr (4.3.27)

$Q_A = m_{10}H_5 - m_RH_{10} - m_8H_1$ kcal/hr (4.3.28)

$COP = Q_E/Q_G$ (4.3.29)

$(COP)_{max} = ((T_e + 273.15)(T_g - T_a))/((T_g + 273.15)(T_c - T_e))$ (4.3.30)

Relative performance $= COP/(COP)_{max}$ (4.3.31)

$P_e = \text{antilog}\,[7.8553 - (1555/(T_e + 273.15)) - ((11.2414 \times 10^4)/(T_e + 273.15)^2$, mmHg (4.3.32)

$P_c = \text{antilog}\,[7.8553 - (1555/(T_c + 273.15)) - ((11.2414 \times 10^4)/(T_c + 273.15)^2)$, mmHg (4.3.33)

Where:

Strong solution (X_1, X_2, X_3)

Weak solution (X_4, X_5, X_6)

Enthalpy of saturated liquid water (H_8)

Enthalpy of saturated water vapor (H_{10})

Heat exchanger effectiveness (E_L)

Refrigerant flow rate (m_R)

Water flow rate (m_w)

Solution flow rate (m_s)

Specific heat of the strong solution (C_{X1})

Specific heat of the weak solution (C_{X4})

Enthalpy (H)

Heat balance of the condenser (Q_c)

Heat balance of the generator (Q_G)

Heat balance of the absorber (Q_A)

Pressure in the evaporator (P_e)

Pressure in the condenser (P_c)

Input data published in F.L. Lansing [101] were used in the calculation and the results were compared with the published results to validate the mathematical model. The input data given were listed below, and the results were compared in Table 66.

T_g = 90°C generator temperature

T_e = 7°C evaporator temperature

T_c = 40°C condenser temperature

T_a = 40°C absorber temperature

E_L = 0.8

Q_E = 3014 kcal/h

Table 66: A comparison of the values published by F.L. Lansing [101] with values that were calculated in this study, and the standard deviation.

Types	Unit	Published	Calculated	Standard deviation
X_1	kg LiBr/kg	0.5672	0.5672	0.00%
X_4	kg LiBr/kg	0.6233	0.6233	0.00%
H_8	Kcal/kg	15	15	0.00%
H_{10}	Kcal/kg	575.72	575.72	0.00%
m_R	Kg/hr	5.3931	5.3931	0.00%
m_s	Kg/hr	59.199	59.958	1.27%
m_w	Kg/hr	54.5268	54.5649	0.07%
T_5	°C	50	50	0.00%
Cx_1	Kcal/kg°C	0.4677	0.4675	-0.04%
Cx_4	Kcal/kg°C	0.42982	0.42983	0.00%
T_3	°C	73.52	73.52	0.00%
H_1	Kcal/kg	-49.9124	-49.9123	0.00%
H_5	Kcal/kg	-43.9594	-43.9601	0.00%
H_7	Kcal/kg	612.48	612.48	0.00%
Q_c	Kcal/hr	3222.3	3222.3	0.00%
Q_G	Kcal/hr	3896.9	3897.1	0.01%
Q_A	Kcal/hr	3698.6	3698.9	0.01%
COP		0.776	0.776	0.00%
$(COP)_{max}$		1.1689	1.1689	0.00%
Relative performance ratio		0.664	0.664	0.00%
P_e	mmHg	7.45	7.45	0.00%
P_c	mmHg	55.37	55.37	0.00%

The highest standard deviation was the mass flow rate of the strong solution (1.27%) followed by the mass flow rate of the weak solution (0.07%), the specific heat of the strong solution (-0.04%), the rate of heat transfer of the generator and absorber (both 0.01%). Mass flow rate of the strong and weak solution are both dependent on the X_1, X_4, H_8 and H_{10} values which are all 100% accurate. Similarly, the specific heat of the strong solution reliant on the X_1 value which is 100% accurate too. It is possible that the deviations were rooted from X_1 value since m_w, m_s and Cx_1 are all dependent on X_1. The difference in the rate of heat transfer of the generator and absorber were

originated by the deviance in the m_s and m_w values. However, all of the values calculated are within 1.27% standard deviation with seventeen out of 22 values are 100% accurate. Hence, the model is validated with a standard deviation of ±1.27%. However, the main characteristic that is going to be used in the further calculation is the COP value that is 100% accurate.

The input component was modified based on the requirement for this study. The COP values are then used in the whole system's calculation. Below is the input parameters used in the new absorption chiller model that will be utilized in the solar cooling system.

T_g = 85°C generator temperature
T_e = 5°C evaporator temperature
T_c = 40°C condenser temperature
T_a = 40°C absorber temperature
E_L = 0.8
Q_E = 1,612,209.8 kcal/h

The absorption chiller's capacity was designed based on the peak cooling load recorded in 2012 that is 1,631.65 kWh at 10.00 am on March 4th. The building's hourly cooling load on the 8th (Friday) and 9th (Saturday) of July are shown in Figure 72 and the hourly cooling load for the whole year is shown in Figure 73. As can be seen in Figure 72, the cooling load varied depending on the air conditioning operation. Out of office hour, the cooling load remains below 246.7 kWh. Meanwhile during office hour, cooling load varied from as low as 569.9 kWh to 1631.6 kWh depending on the air conditioning's load schedule which varied from 50% to 100% (see Figure 63).

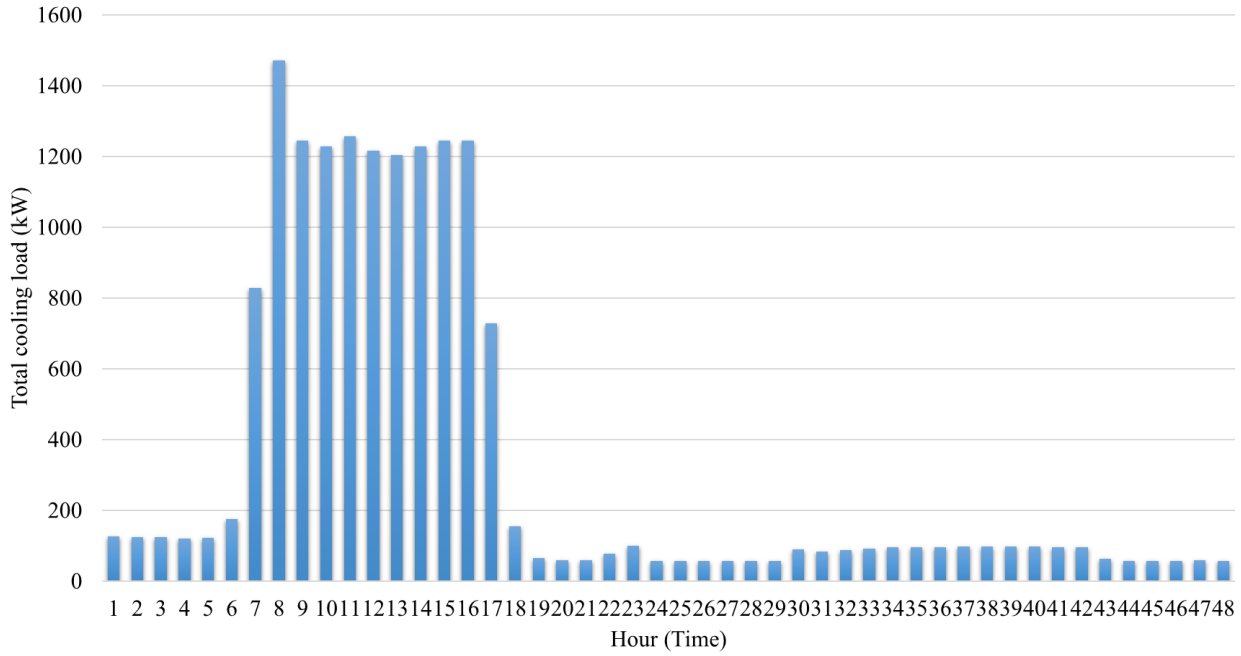

Figure 72: The building's hourly total cooling load on the 8th (weekday) and 9th (weekend) of March.

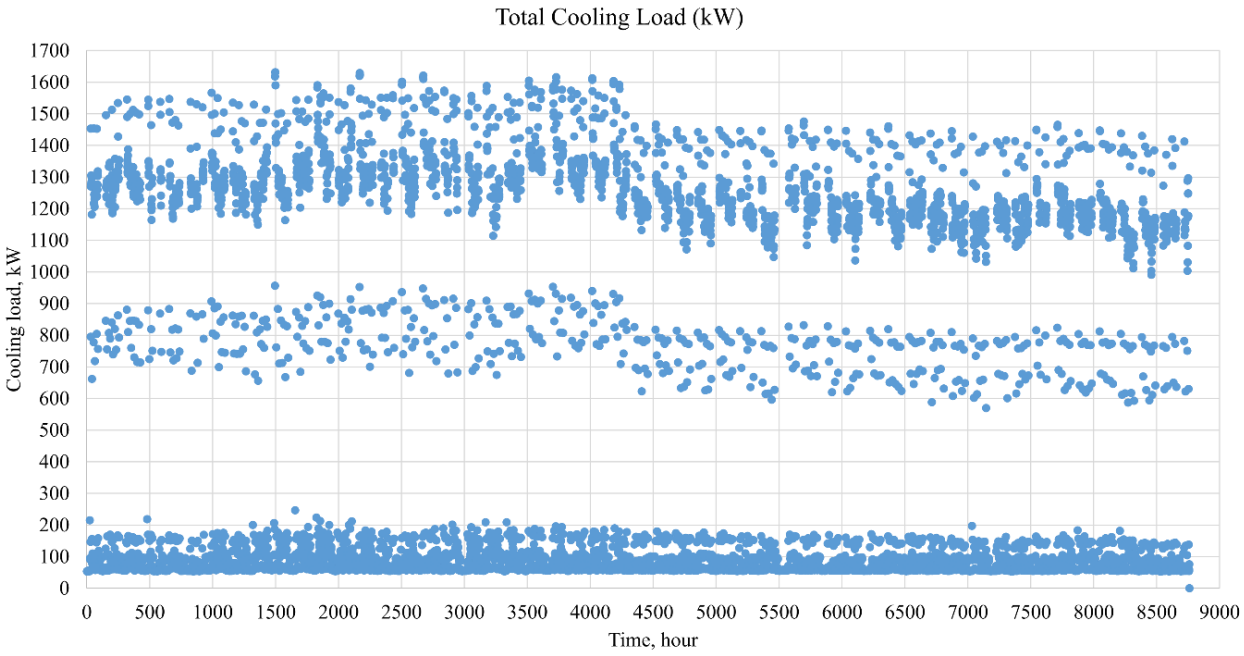

Figure 73: The building's hourly total cooling load for the whole year.

The Q_E value used in the model considered additional 15% load, making it 1,612,209.8 kcal/hour or 1875.65 kWh. The maximum COP value for the system is 0.9985, and the COP value is 0.704. The maximum coolant temperature is fixed at 85°C. The values for every parameter are listed in Table 67, and the model is illustrated in Figure 74.

Table 67: The values of the model's parameters.

Model's parameter	Value	Unit
X_1	0.5803	kg LiBr/kg
X_4	0.5995	kg LiBr/kg
H_8	15	Kcal/kg
H_{10}	574.89	Kcal/kg
m_R	8.6958	Kg/hr
ms	271.4722	Kg/hr
mw	262.7764	Kg/hr
T_5	49	°C
Cx_1	0.4579	Kcal/kg°C
Cx_4	0.4452	Kcal/kg°C
T_3	73.88	°C
H_1	-49.7655	Kcal/kg
H_5	-45.2805	Kcal/kg
H_7	610.18	Kcal/kg
Q_c	5175.6	Kcal/hr
Q_G	6917.3	Kcal/hr
Q_A	6610.4	Kcal/hr
COP	0.704	
$(COP)_{max}$	0.9985	
Relative performance ratio	0.705	
P_e	6.48	mmHg
P_c	55.37	mmHg

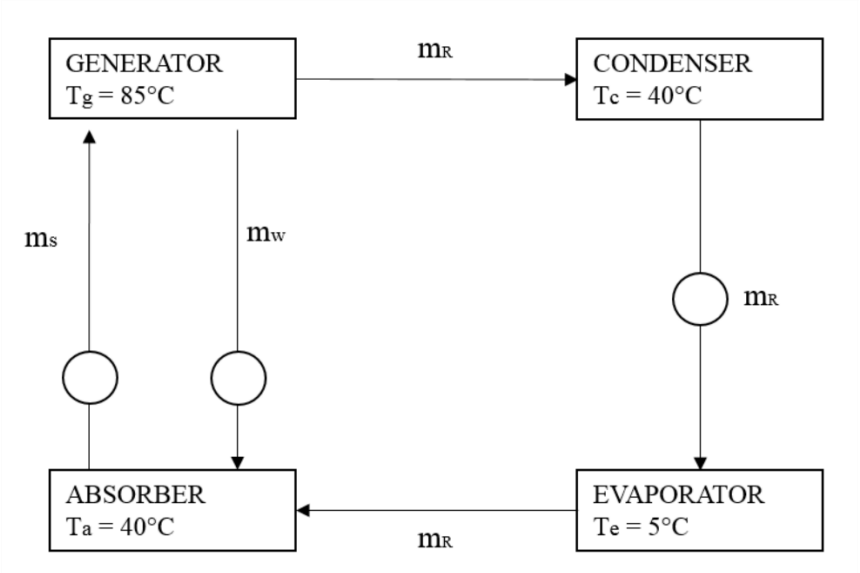

Figure 74: Flow diagram for the lithium bromide/water absorption system.

4.3.3.3 Backup system

An electric chiller powered up by the electricity harnessed by solar energy, and cold energy storage was chosen as the backup to the lithium bromide/water absorption chiller. The high building's cooling load demand and the limited area for solar energy collection might require a backup system that can fully utilise the energy harnessed when the solar energy is available. Hence, a battery to store the electricity generated by the MCPV and a thermal energy storage to store the chilled water produced by the absorption chiller are included in the design as a backup system.

Cold energy storage is chosen due to the fact that the thermal losses rate is higher for hot energy storage compared to the cold energy storage. Heat loss rate is governed by the equation (4.3.34) and (4.3.35) where it is proportionate to the temperature difference between the stored energy and the ambient temperature.

$$Q = k \times \Delta T \qquad (4.3.34)$$

$$k = m \times C / t \qquad (4.3.35)$$

Where:

Amount of heat transfer (Q)

Heat transfer coefficient (k)

Temperature gradient (ΔT)

Mass flow rate (m)

Specific heat capacity (C)

Time (t)

A hot water with an initial temperature of 100°C stored in a normal conditioned room will experience a temperature difference of 65°C during peak daytime. Meanwhile, the temperature difference for chilled water stored at 5°C in a normal conditioned room is 30°C. Hence, the hot energy storage has 2.2 times higher heat loss rate compared to the cold energy storage. Moreover, it is more energy efficient to use the stored electricity to drive the environmental friendly chiller with a high COP at night time rather than to use the stored hot water to power up a big capacity absorption chiller for an average of 100 kWh cooling loads at night time.

4.3.3.3.1 Thermal energy storage

Phase change material was opted to store cold energy due to its capability of storing high latent heat capacity in a smaller volume compared to sensible heat storage. PlusICE Eutectic PCM [217] was selected due to the substance attributes that are non-toxic, non-combustible and inorganic. The PlusICE product range was manufactured by Phase Change Material Products Limited aimed for a heating and cooling purposes. The range comes in a wide range of operating temperature (between -40°C to 117°C) with three different kinds of capsules that are a cylindrical tube, sphere, and rectangular shape containers. The cylindrical tube containers were selected due to its tank capacity and feasibility to store it in a storage tank. The number of tubes and storage tank volume requirement are calculated using equation (4.3.36) and (4.3.37) [217]. The capacity for each cylindrical tube is 0.099 kWh or 43 kWh/m³ for the TES tank. The tubeICE phase change temperature is 7°C.

$$\text{Tank volume } (m^3) = \frac{\text{load (kWh)}}{\text{tube ice capacity } (\frac{\text{kWh}}{m^3})} \quad (4.3.36)$$

$$\text{Number of tubes} = 440 \times \text{tank volume} \quad (4.3.37)$$

The ice melting rate (K) is given by the equation (4.3.38)

$K = (A \times U) / L$, kg/h°C (4.3.38)

Where:

A = Area of the tank, m^2

L = latent heat fusion of the ice, kcal/kg

U = coefficient of heat transfer for the element, kcal/m^2h°C

Meanwhile, the heat loss rate can be calculated using the equation (4.3.39)

$Q = A \times U \times (t_o - t_i)$ (4.3.39)

Where:

Q = total heat loss rate, kcal/h

A = area of the element, m^2

U = coefficient of heat transfer for the element, kcal/m^2h°C

t_o = outside temperature of the element, °C

t_i = inside temperature of the element, °C

4.3.3.3.2 Environmental friendly electric chiller

The electric chiller was included in the design as a backup during inadequate chilled water in the cold storage. It is intended to be powered by the solar electricity harnessed by the MCPV, however in the case of a shortage, the primary electricity will be used. The chiller's capacity will be chosen based on the peak load requirement. The chiller has been selected based on the COP and refrigerant types. An environmental friendly refrigerant with a satisfactory COP value was prioritised. In this study, a two-stage centrifugal chiller AART-I model, manufactured by Mitsubishi Heavy Industries Ltd was chosen. The COP for the chiller when the auxiliary power was included is 5.73, and the temperature of the chilled water outlet is 6.7°C. An environmental friendly refrigerant R134-a was used in the chiller. The chiller's specification is shown in Table 68 [218].

Table 68: The specification data of the electric chiller [218].

Parameters		Unit	Value
Chilled water	Entering temperature	°C	12.2
	Leaving temperature	°C	6.7
	Flow rate	m³/h	272
	Pressure drop	kPa	117
	Piping connection/ nozzle size	inch	8
	No. of pass	-	3
Cooling water	Entering temperature	°C	
	Leaving temperature	°C	34.5
	Flow rate	m³/h	342
	Pressure drop	kPa	107
	Piping connection/ nozzle size	inch	8
	No. of pass	-	3
Inverter input	50Hz	kW	270
	60 Hz	kW	273
Inverter output	50Hz	kW	231
	60 Hz	kW	231
COP	50Hz		6.51
	60 Hz		6.44
Cooling capacity		RT	500
		kW	1758

4.3.3.4 Whole system mathematical modelling

The mathematical modelling of the whole system was solved using Excel, and the equations are listed below:

4.3.3.4.1 Mathematical modelling of the cooling system

The flow chart of the cooling system (Figure 75) is described using the simplified mathematical modelling derived from the equations (4.3.40) to (4.3.48). Excel was used to solve the mathematical modelling.

$Q_{incident}$ = Global solar radiation × collection area [215] (4.3.40)

$Q_{thermal} = Q_{incident} \times \eta_{optical} \times (1- \eta_{PV})$ [214] (4.3.41)

$Q_{electric} = (Q_{incident} \times \eta_{optical} \times \eta_{PV} - Q_{loss}) \times \eta_{inverter}$ [201] (4.3.42)

$$E_{battery(n)} = Q_{electric\ (n)} - E_{electric\ chiller(n)} - E_{abs\ pumps(n)} - E_{building's\ load(n)} + E_{battery\ (n-1)} \quad (4.3.43)$$

$$Q_{cool\ abs} = Q_{thermal} / COP_{abs} \quad (4.3.44)$$

$$Q_{TES\ (n)} = Q_{cool\ abs\ (n)} - Q_{load\ (n)} + Q_{TES\ (n-1)} \quad (4.3.45)$$

$$\Sigma Q_{cool\ supplied} = Q_{cool\ abs} + Q_{TES} + Q_{cool\ aux} \quad (4.3.46)$$

$$\Sigma Q_{cool\ supplied} = \Sigma Q_{cool\ load} \quad (4.3.47)$$

$$E_{electric\ chiller} = Q_{cool\ aux} / COP_{\ electric\ chiller} \quad (4.3.48)$$

Where:

COP of the absorption chiller (COP_{abs})

Thermal energy generated by the MCPV ($Q_{thermal}$)

Incident solar energy ($Q_{incident}$)

Electricity generated ($Q_{electric}$)

Coolant's thermal energy ($Q_{coolant}$)

Thermal losses (Q_{loss})

Energy used for pumps (Q_{pump})

Gross DC power produced by the modul (Q_{gross})

Optical efficiency ($\eta_{optical}$)

Efficiency of the PV cells (η_{PV})

Efficiency of the inverter ($\eta_{inverter}$)

Efficiency of the coolant's collector ($\eta_{collector}$)

Electricity stored in the battery ($E_{battery}$)

Electricity generated at that hour ($Q_{electric\ (n)}$)

Electricity required to power up chiller at that hour ($E_{chiller}$)

Electricity required to power up absorption chiller's pumps at that hour ($E_{abs\ pumps}$)

Electricity required by the building's electricity load at that hour ($E_{building's\ load}$)

Total electricity stored in the battery an hour earlier ($E_{battery\ (n-1)}$)

Cold energy/chilled water generated by the absorption chiller ($Q_{cool\ abs}$)

Thermal energy stored in the thermal energy storage system at that hour (n) ($Q_{TES\ (n)}$)

Thermal energy stored in the thermal energy storage system at (n-1) hour ($Q_{TES\ (n-1)}$)

Thermal energy demand at that hour (n) ($Q_{load\ (n)}$)

Cold energy/chilled water generated by the absorption chiller at that hour (n) ($Q_{cool\ abs\ (n)}$)

Total cold energy supplied ($\Sigma Q_{cool\ supplied}$)

Cold energy/chilled water generated by electric chiller ($Q_{cool\ aux}$)

Total cooling load ($\Sigma Q_{cool\ load}$)

Energy demand/Auxiliary energy by electric chiller ($Q_{aux\ chiller}$)

Coefficienct of performance of the electric chiller ($COP_{\ electric\ chiller}$)

At that hour (n)

An hour before (n-1)

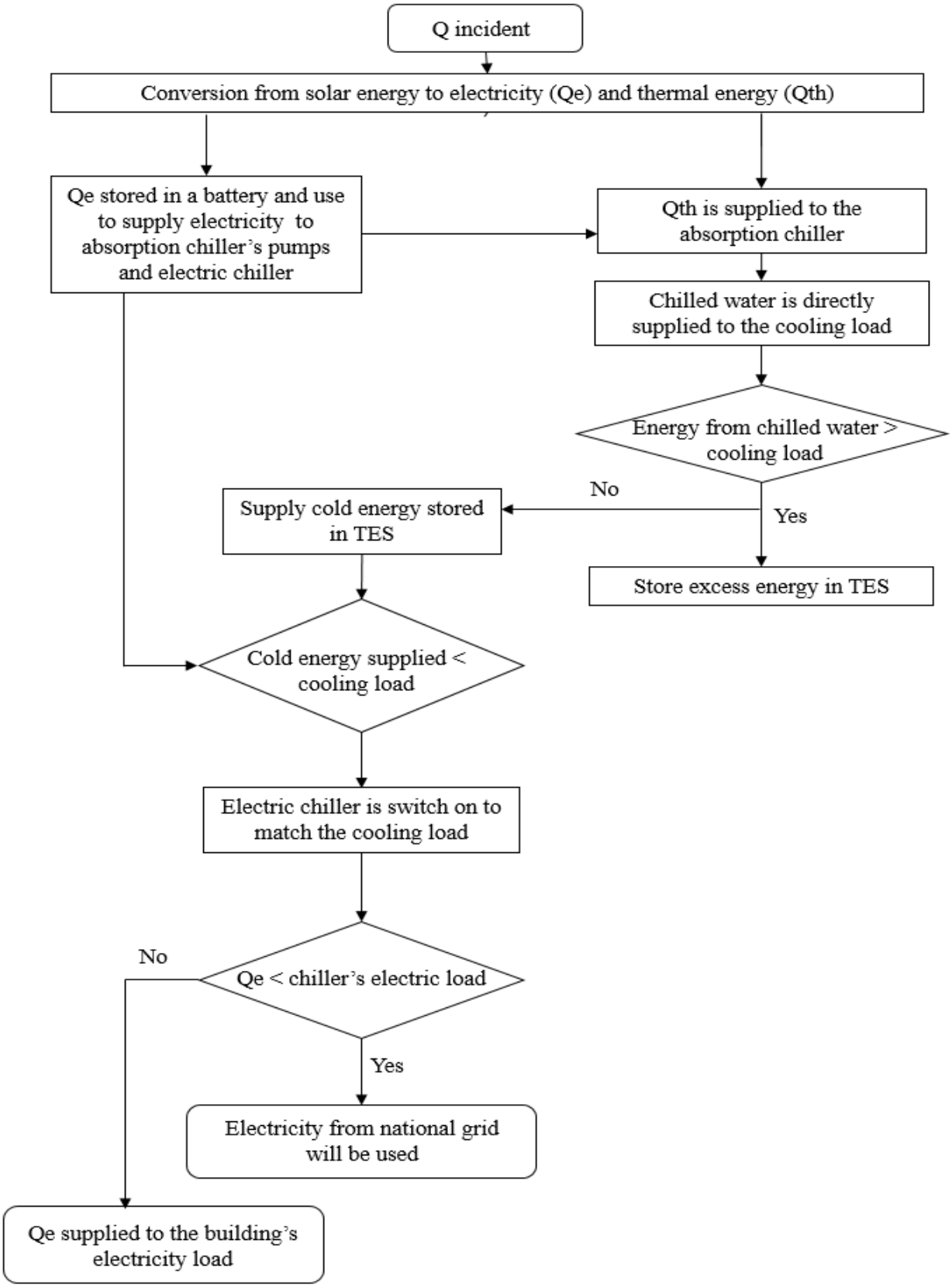

Figure 75: The cooling system's flow chart.

4.3.3.5 Performance and economic analysis

The energy and economic performance were evaluated based on the equation (4.1) to (4.7) in Section 4.1.2.2. The maximum cost for retrofitting to achieve the desired payback period is calculated based on the equation (4.3.49) [219] and (4.3.50). The maintenance is assumed to be 10% of the total retrofit cost throughout the system's lifetime. The maintenance includes cleaning the MCPV, repairs and replacement of the system's components such as pumps, etc.

$$\text{Payback period} = \frac{Retrofit\ Cost}{[(Income\ tariff + \Sigma Saving\ (energy\ bill)) - Cost\ maintenance]} \quad (4.3.49)$$

$$\text{Retrofit cost} = \text{Cost of products} + \text{Installation cost} \quad (4.3.50)$$

Where:

Retrofit cost (Retrofit cost)

The desired payback period (Payback period)

Total saving in energy bills (ΣSaving $_{(\text{energy bill})}$)

Income gain from excess electricity fed into the main grid (Income tariff)

Cost to maintain the whole system (cost maintenance)

4.3.4 Results and Discussion

This section will be presented in two sections. The first section (Section 4.3.4.1) will present the overall performance of the cooling system. Section 4.3.4.2 will discuss the technical detail of the cooling system such as the energy storage, peak demand, and the demand in the cooling load and the supply. While section 4.3.4.3 discussed the economic analysis.

4.3.4.1 The system's overall performance

The hybrid solar cooling system is projected to supply a total cooling load of 3,655,150.67 kWh a year, powered by 99.99% (6,595,232 kWh) solar energy and 0.01% (956.8 kWh) electricity from the main grid. The whole cooling system's coefficient of performance (COP) is calculated to be 0.678. It is projected that 5,474,042.56 kWh collected solar energy will generate 4,349,957.15 kWh thermal energy and 1,124,085.41 kWh electricity in a year. The electricity generated by the

MCPV is expected to be used by the cooling system with a remaining of 124,935.20 kWh stored in the battery which can be utilised by the building for other means or fed it into the main grid.

The calculated COP of the MCPV for combined heat and power usage is 0.83. The estimated chilled water generated by the absorption chiller is 3,349,467.01 kWh and the estimated chilled water produced by the electric chiller is 314,902.88 kWh. The electricity requirement for the cooling system (including the electricity to power up the system fans, pumps, AHUs and the backup chiller) is 999,710.36 kWh. 99.904% of this requirement will be supplied by the electricity generated from the solar energy, and the remaining 0.096% will be provided by the electricity from the grid.

By using the hybrid solar cooling system and changes in the operational management, the building is predicted to cut down 4,730,510 kWh (65.7%) from the 7,195,646 kWh of its dependency on the primary energy. The installation of the hybrid solar cooling system will make the building's total primary energy consumption as 2,465,135.90 kWh and the building's energy index (BEI) as 67.08 kWh/m²/year. The energy data before and after retrofit were simplified in Table 69. The reduction in the primary energy consumption enables the building to be categorised as a LEO building.

Table 69: The building's energy data before and after the retrofit.

Type	Value (kWh)
Initial primary energy consumption	7,195,646.00
Total energy reduction	4,730,510.10
Primary energy consumption	2,465,135.90
BEI	67.08

4.3.4.2 Technical discussion

A solar collection area of 4,000 m² was used in the calculation to meet the cooling demand. In this study, the potential space for installation is the South buildings' rooftops that come with a total rooftop area of 4,330 m². The total incident solar in a year was 1648 kW/m² and the total solar energy collected 935,708.8 kWh. Figure 76 shows the hourly incident solar energy and the hourly collected solar energy for the whole year (8763 hourly data presented in 24hours time

range). It can be observed that the solar energy was available from 0900 to 1900. Meanwhile, the server rooms in the building require a 24 hours cooling and the cooling system started at 0700. Hence, backup energy sources are needed to supply the cooling load demand from 2000 to 0800 the next day.

The cooling load was supplied by the absorption chiller, cold energy storage, and the backup electric chiller. Figure 77 shows the hourly collected solar energy, hourly electricity generated by the MCPV, the hourly total cooling demand and the hourly cooling provided by the absorption chiller. The graph summarises 8763 hourly data into 24hours time range. As shown in the graph (Figure 77), the building requires 24 hours cooling where the cooling load stays in the range of 50.00 kWh to 208.00 kWh during the night time to the early morning (2000 to 0600 the next morning). Meanwhile, at 0700, the cooling load reached 1,000.00 kWh (maximum load for that hour) and increased to 1,612.00 kWh (maximum load for that hour) at 0800. During these hours, solar energy was not available. Hence, a backup system to supply the energy required is indispensable.

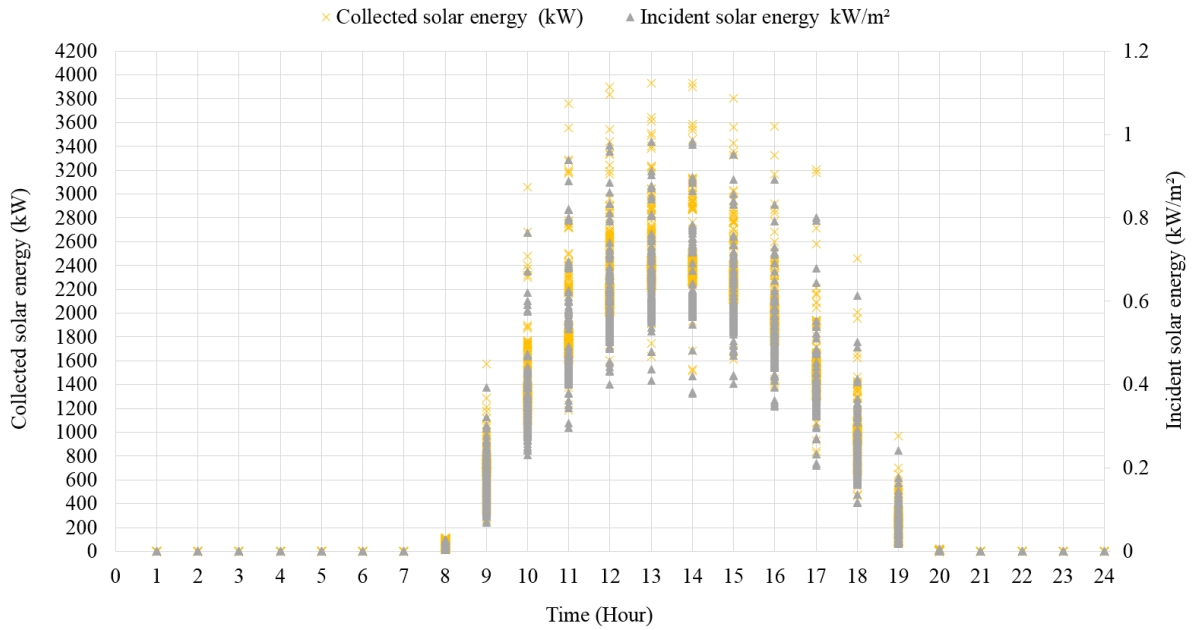

Figure 76: The hourly incident and collected solar energy for a year presented in 24 hours range.

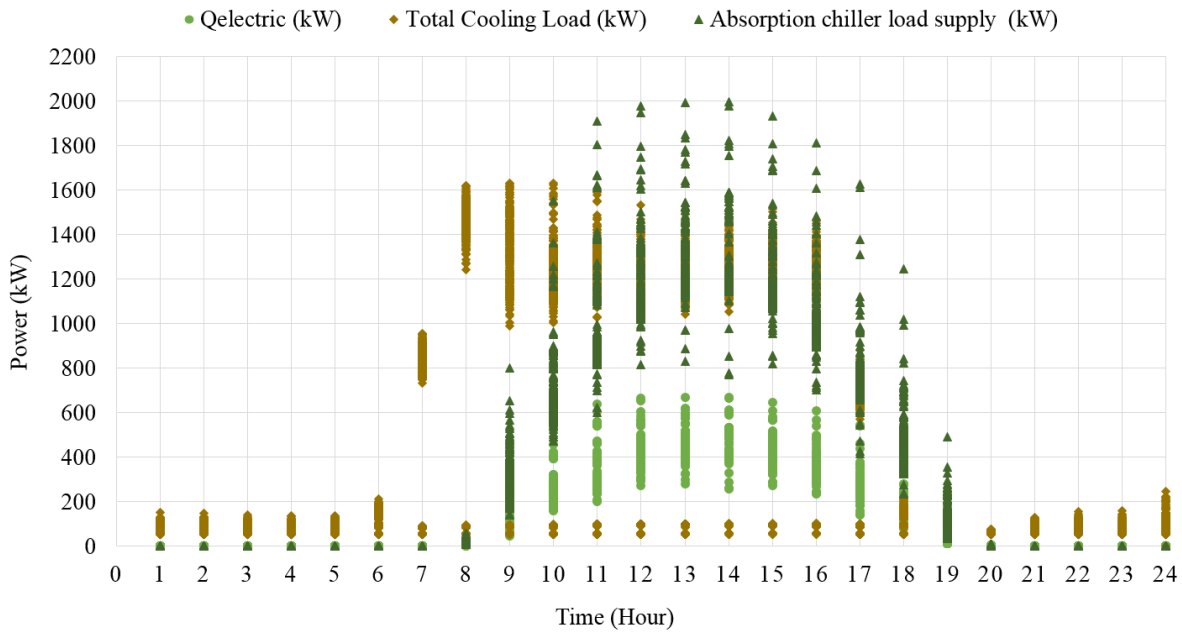

Figure 77: The hourly collected solar energy, electricity and cooling generated.

At 1100 to 1900, the cold energy generated by the absorption chiller was higher than the cooling demand. This excess chilled water enables us to store the cold energy and uses it during the time when the solar energy was not available. Four cylindrical tanks of PCM cold energy storage with a total capacity of 51,600 kWh was designed to maximise the storing of the generated cold energy. The cylindrical storage tank manufactured by Lacaze Energies Groupe Cahors [220] were chosen to store the PCM ice tubes at 7°C. The specification of each cold storage tank is listed in Table 70.

Table 70: The specification of each cold storage tank.

Specification	Unit	Value
k	W/m²/°C	0.02
Volume	m³	300
Radius	m	1.5
Length	m	42.44
Total surface area	m²	414.12
Thermal loss per hour	kW	0.025
Ice melting rate	kg/h°C	0.0352
Storage capacity	kWh	12,900

Each storage tank has a volume of 300 m³ with 528,000 PCM ice tubes. The cold energy storage will be placed in an air-conditioned room with air temperature setpoint 10°C. A graph of the calculated hourly energy storage in a year is shown in Figure 78.

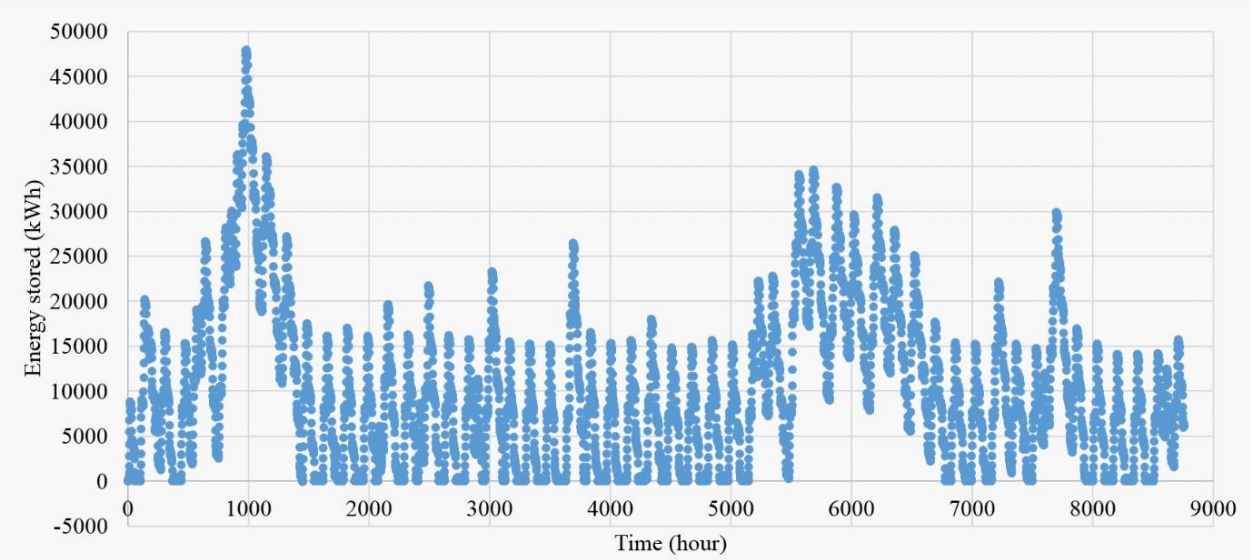

Figure 78: The calculated hourly cold energy storage in a year.

The cold energy is mainly stored during the holidays and weekends and lasts for a few days during the weekday. The backup chiller is mostly required to meet the morning peak load and when the energy storage was not sufficient to supply the cooling demand. A graph of the cooling load provided by the backup chiller, the hourly energy storage and total cooling load supply in every month from January to December are shown in Figure 79 to Figure 90.

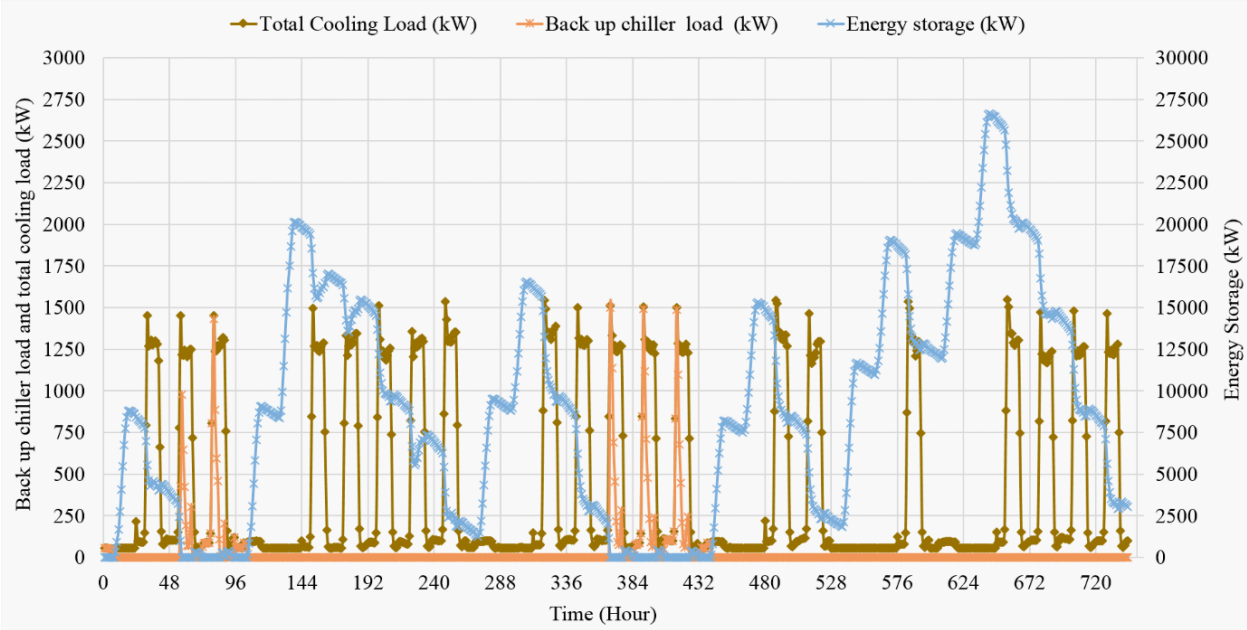

Figure 79: The hourly cooling demand, energy storage and the energy supplied by the backup chiller in January.

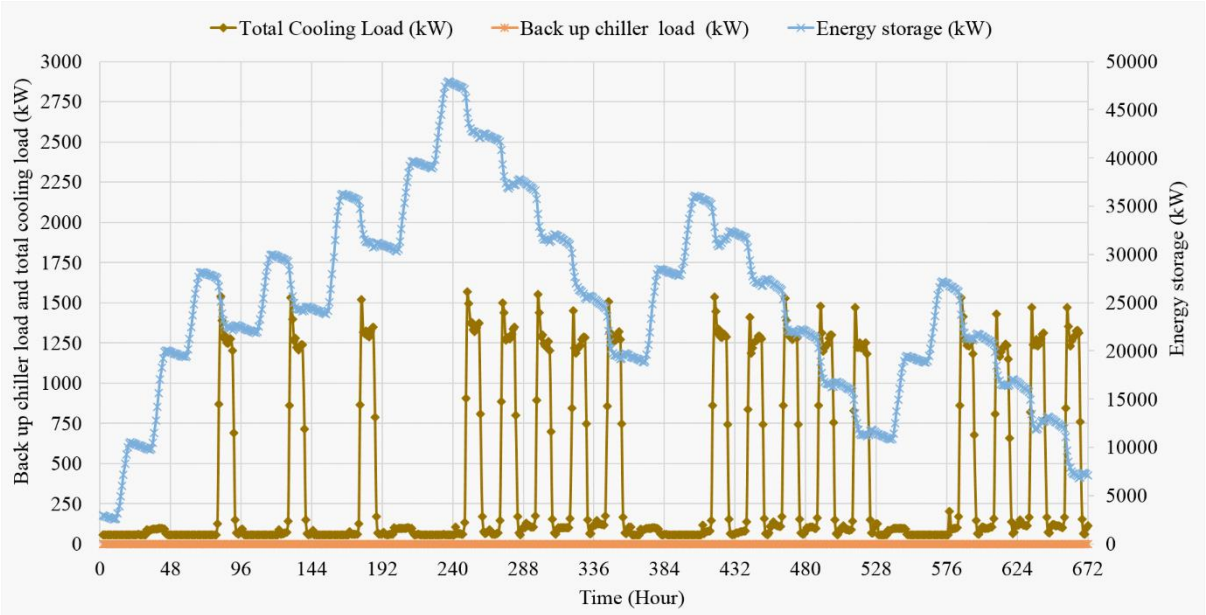

Figure 80: The hourly cooling demand, energy storage and the energy provided by the backup chiller in February.

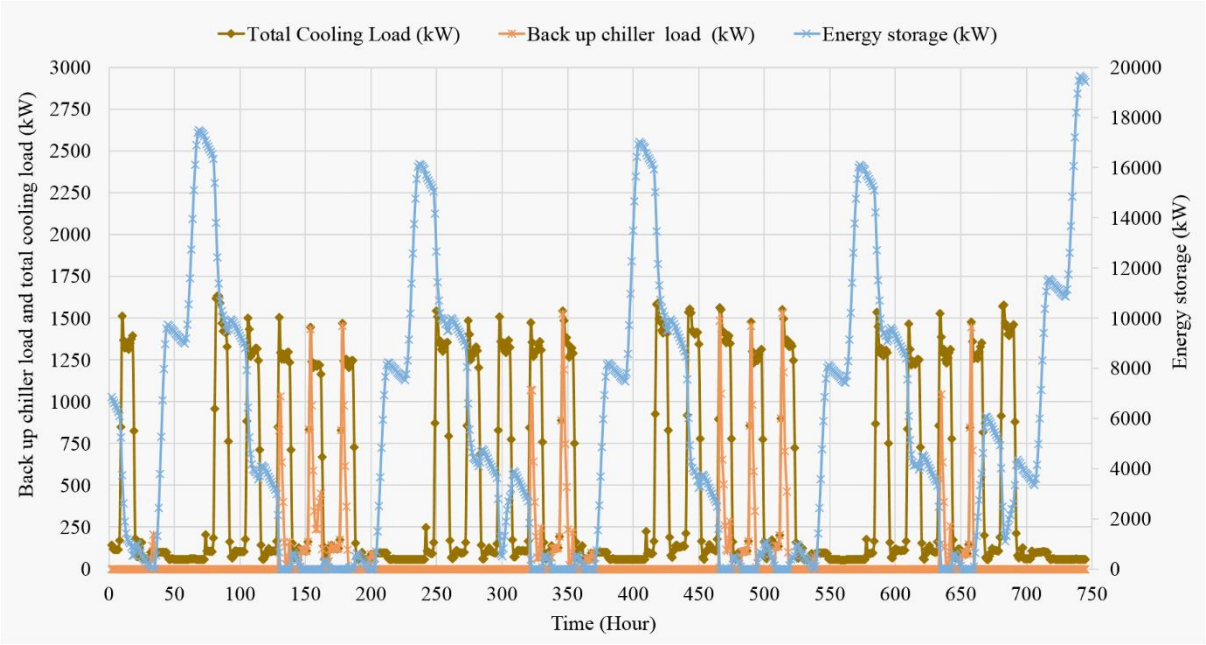

Figure 81: The hourly cooling demand, energy storage and the energy supplied by the backup chiller in March.

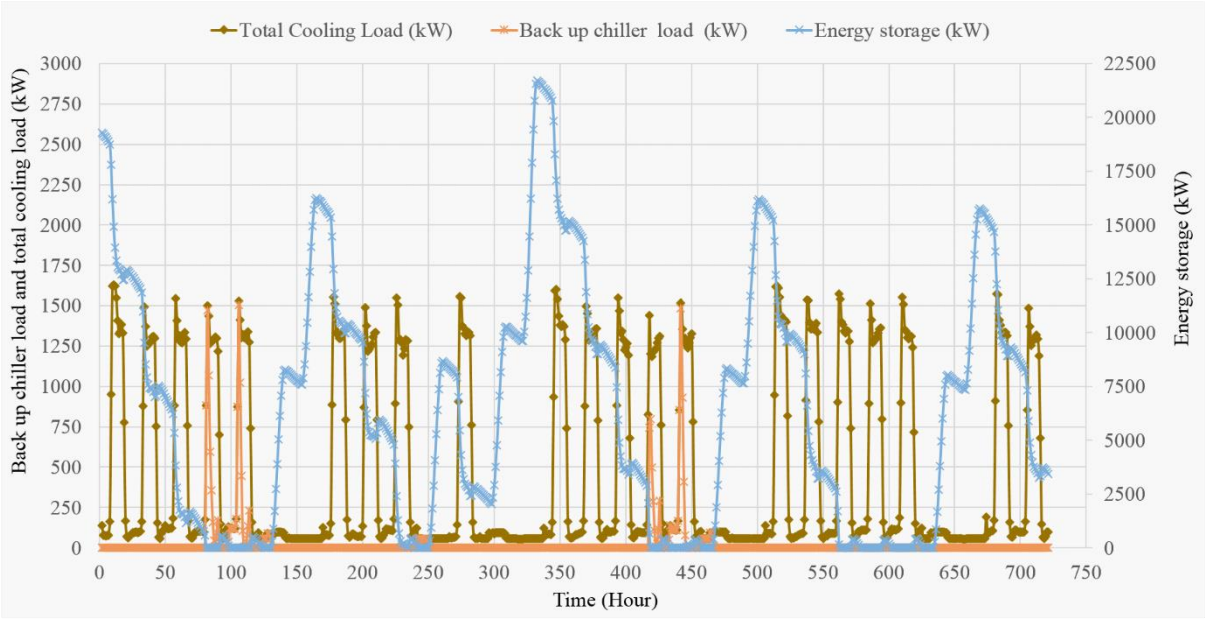

Figure 82: The hourly cooling demand, energy storage and the energy supplied by the backup chiller in April.

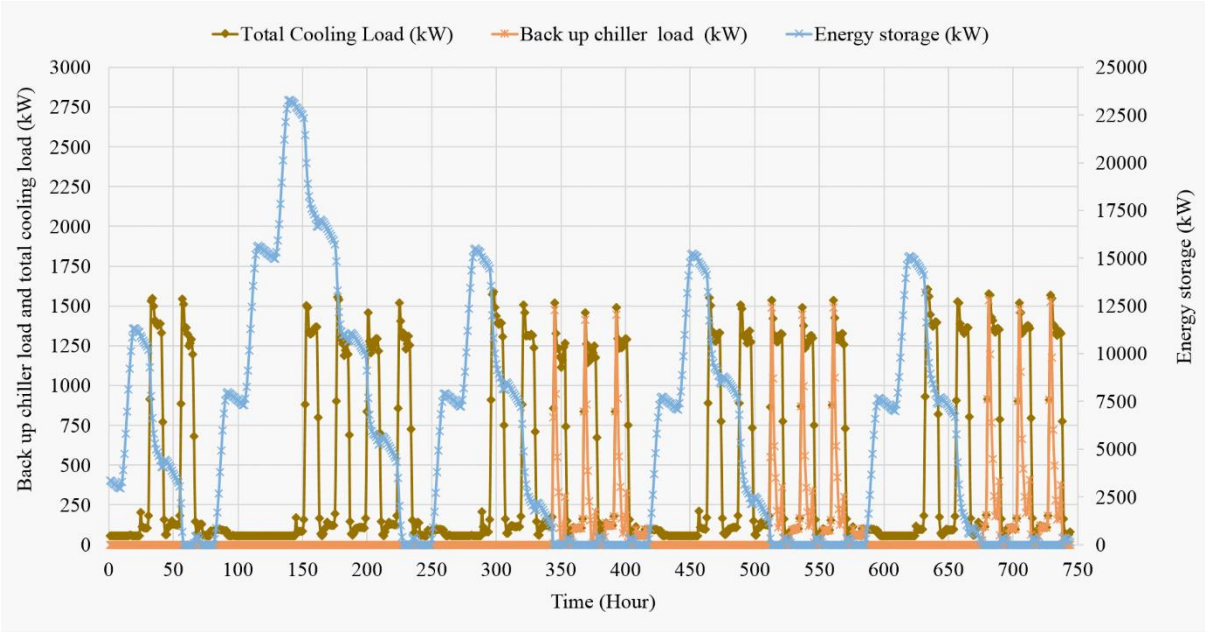

Figure 83: The hourly cooling demand, energy storage and the energy supplied by the backup chiller in May.

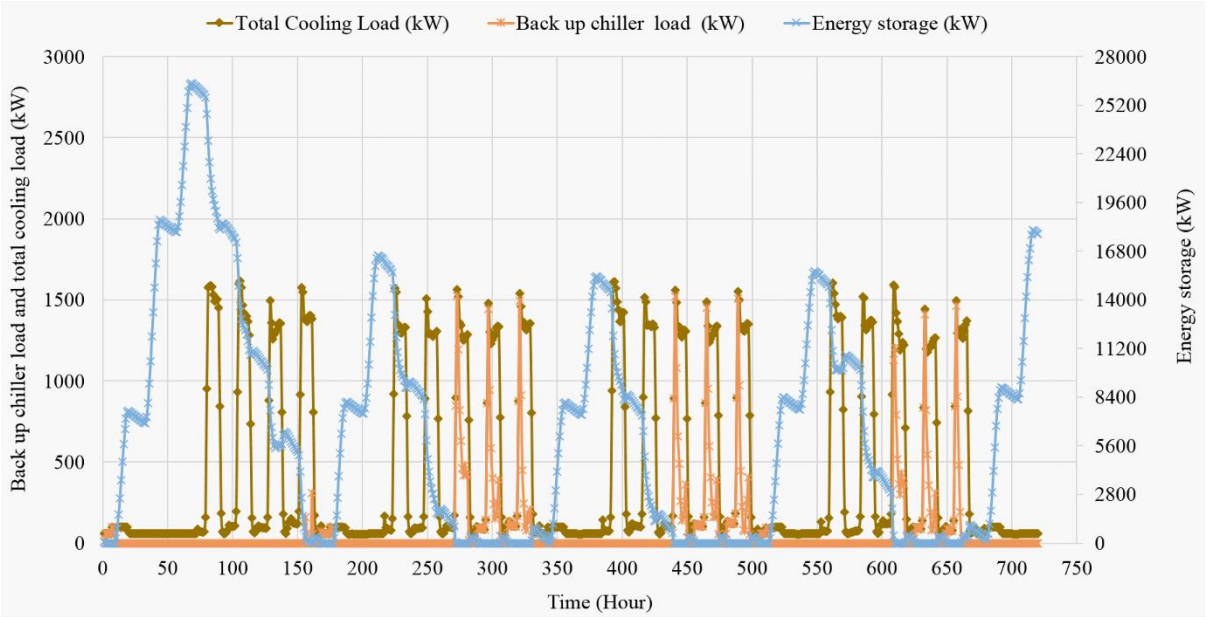

Figure 84: The hourly cooling demand, energy storage and the energy supplied by the backup chiller in June.

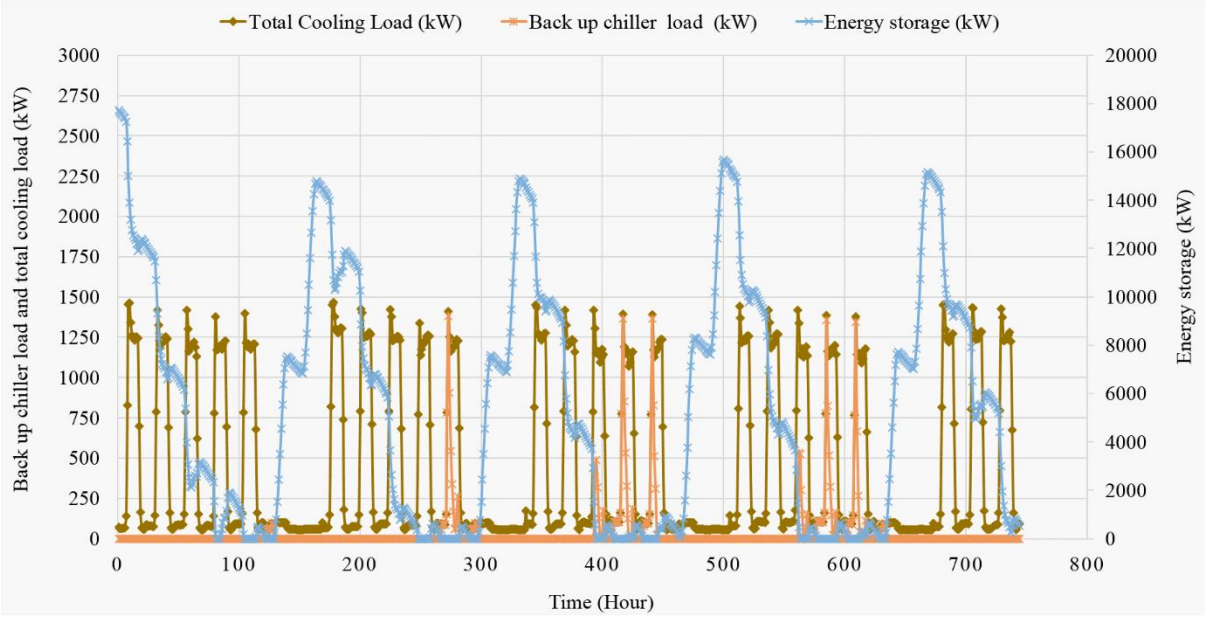

Figure 85: The hourly cooling demand, energy storage and the energy supplied by the backup chiller in July.

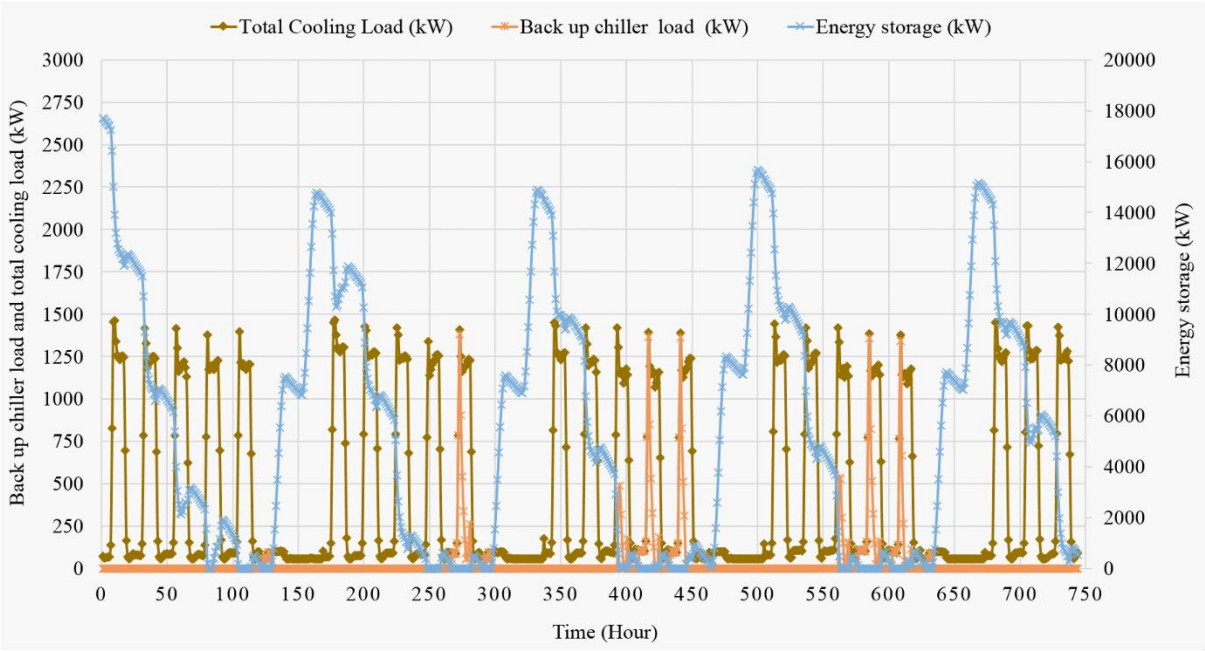

Figure 86: The hourly cooling demand, energy storage and the energy supplied by the backup chiller in August.

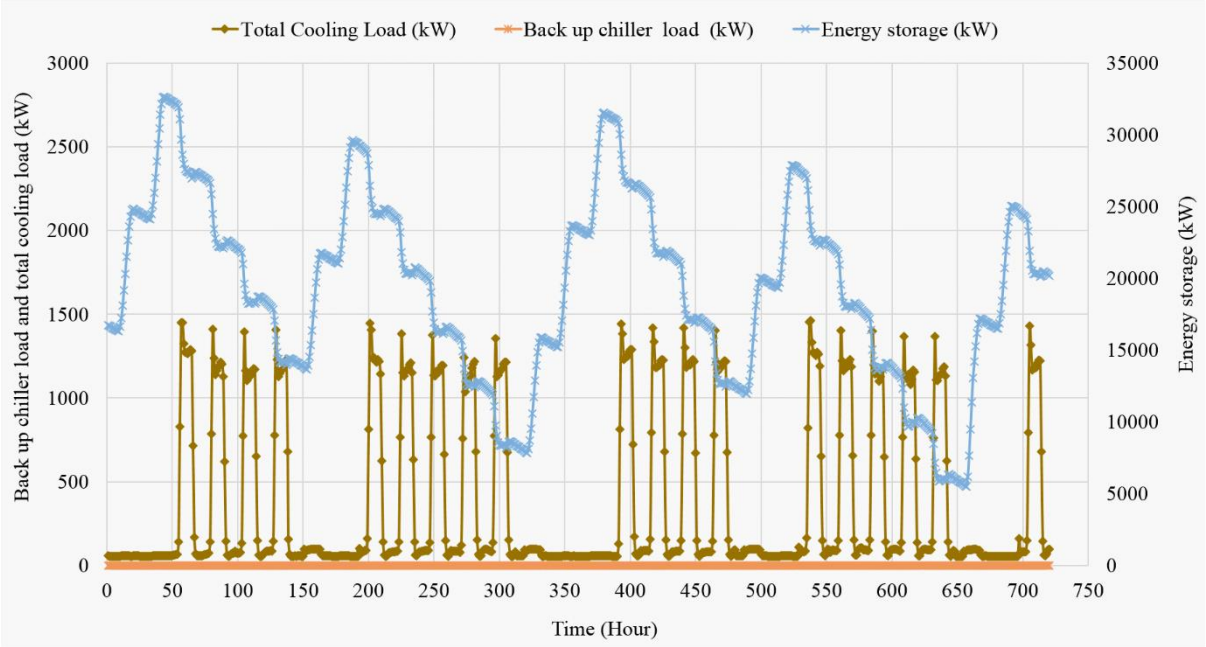

Figure 87: The hourly cooling demand, energy storage and the energy supplied by the backup chiller in September.

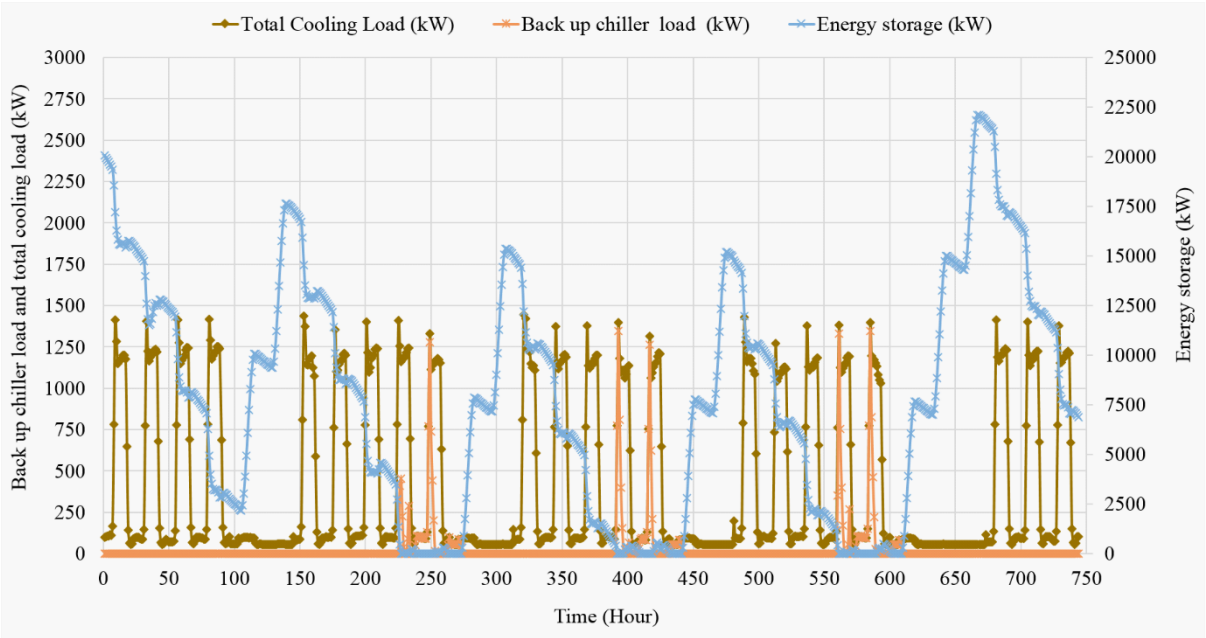

Figure 88: The hourly cooling demand, energy storage and the energy supplied by the backup chiller in October.

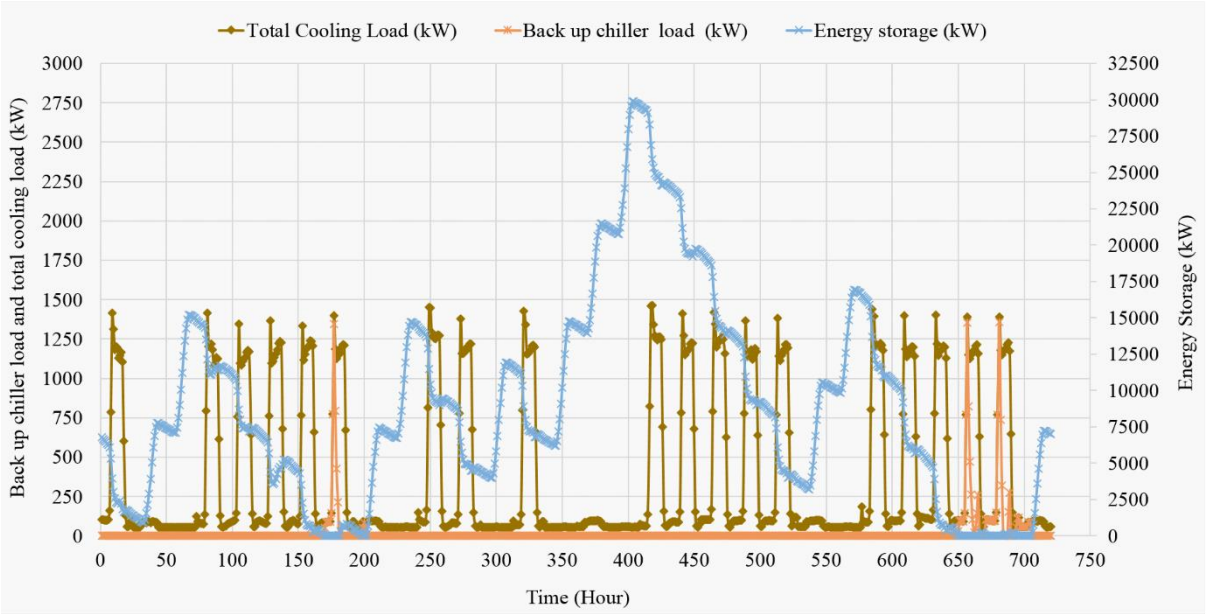

Figure 89: The hourly cooling demand, energy storage and the energy supplied by the backup chiller in November.

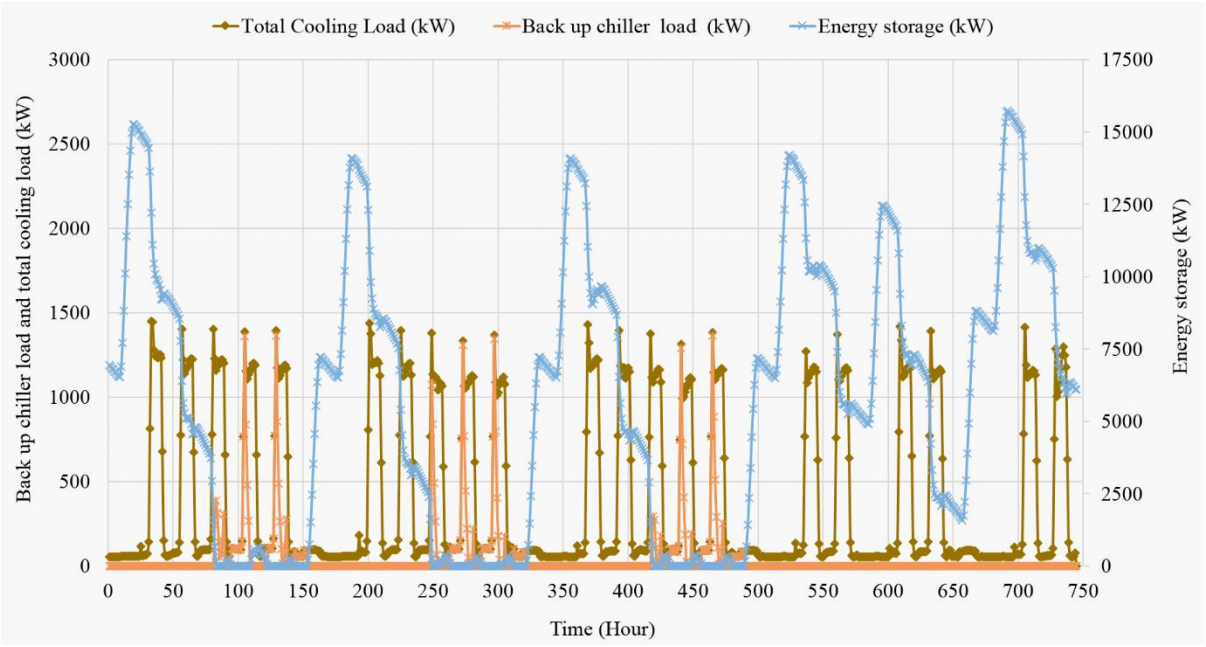

Figure 90: The hourly cooling demand, energy storage and the energy supplied by the backup chiller in December.

The highest amount of energy stored was 47,916.88 kWh on the 11th of February during a weekend. It is possible for the energy storage to reach this peak due to the three days of holidays that occur early in that week. Figure 91 demonstrates the incident solar energy and the total cooling load every month in a year. The incident solar energy was highest in March and lowest in December. However, the highest cooling load was in March, but the lowest cooling load was in February. This observation shows that the cooling load was not proportionate with the incident solar energy, but instead, it is mainly influenced by the operational schedule and the building's usage. In February, the employee has more holidays compared to any other month which means that the hours of operation for the air conditioning was lowest. This cooling operation schedule resulted in lowest cooling load demand in February.

Meanwhile, the backup chiller was required to meet the cooling load demand in the morning when the total cooling load was at its peak, and the solar energy was not available. The backup chiller is estimated to be mainly used to meet the peak cooling load in March and June followed by May, December, July, August, October, January, April, November, February and September. The backup chiller is also required at the night time of the first day the cooling system was in operation since the cooling started from 0000 of the 1st of January. The target building's total cooling load and incident solar energy every month is shown in Figure 91 and the target building's monthly total cooling load, collected solar energy, incident solar energy and the number of days that requires backup chiller during the morning peak load is shown in Table 71.

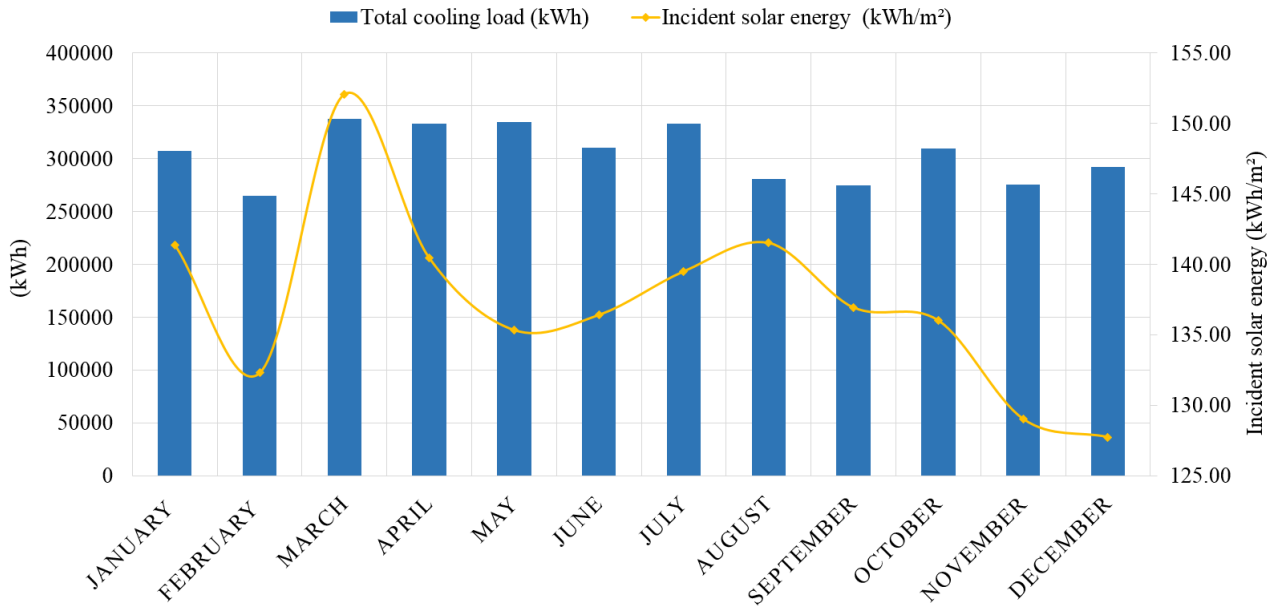

Figure 91: The incident solar energy and the total cooling load every month in a year.

Table 71: The incident and collected solar energy, the total cooling load and number of days that requires the use of backup chiller for the morning peak load every month in a year

Month	Incident solar energy (kWh/m²)	Collected solar energy (kWh)	Total cooling load (kWh)	Number of days that requires backup chiller for the morning peak load (day)
January	141.35	565416.00	307444.29	5
February	132.32	529296.00	264765.02	0
March	152.08	608316.00	338072.58	10
April	140.50	561980.00	333276.59	4
May	135.36	541424.00	334928.08	9
June	136.43	545712.00	310342.60	10
July	139.49	557952.00	333189.00	7
August	141.54	566172.00	280838.05	7
September	136.95	547788.00	274777.78	0
October	136.01	544036.00	309450.27	6
November	129.03	516132.00	275864.01	3
December	127.75	511008.00	292202.34	9

4.3.4.3 Economic analysis

The total building's energy reduction is estimated to be 4,855,445.20 kWh where 4,730,510 kWh is the reduction in cooling system, and the other 124,935.20 kWh is the reduction in the building's electricity. The projected cost saving for a year is RM 4,776,111.67. If the same amount of energy is to be reduced every year for the period of the building's lifetime and the CHP system's lifetime is 25 years, the accumulated reduction in energy cost will be RM 119,402,791.80. This calculation does not consider degradation rate of PV cells which is estimated to be 0.7% a year [NREL] and possibility of an increase in energy prices or a reduction in feed-in tariff to the main grid. To achieve a payback period less than 25 years, the total cost for the CHP system should be equal to or lower than RM 108,547,992.50.

The price for the whole system could not be predicted due to insufficient data on the CHP's components prices. The CHP solar system mainly consists of MCPV, electric chiller, PCM tubeICE, absorption chillers, chilled water storage tank, and pumps. The MCPV is not yet being commercialized, and the prices for the chillers were not attainable from the manufacturers. However, the comparative cost for the MCPV was made by the author of the original paper, A. Kribus [214]. Based on the quotes given by the manufacturers for the major components of the MCPV, A. Kribus et al. [214] compared the cost of peak electric generated by flat plate PV (FPPV), MCPV and PVT. It was found that the MCPV will cost $2.50 per peak electric Watt which is lower than the FPPV and PVT peak electric cost which is $6 per peak electric Watt for FPPV and $4 per peak electric Watt for the PVT system. This comparison does not include the thermal energy harnessed by the MCPV and also the PVT. Hence, there is a high potential that the MCPV will be more attractive for the developers and building owners in the future compared to the FPPV and PVT. The article was published in 2006, so the prices published by the author might have changed since the paper was published.

Meanwhile, based on the actual cost of FFPV with 15% efficiency, the electricity cost is estimated to be RM0.351/kWh (refer Table 64 in Section 4.2.4.3). The quoted FFPV price was GBP3.20/m² or RM 16.64/m² [193]. If it is assumed that the MCPV's price is three times higher than FFPV, the estimated cost for the installation of MCPV is RM 199,680.00. Meanwhile the price for thermal energy storage as quoted from Phase Change Products Ltd [221] is expected to be RM 13 Million/GBP 2.5 Million. The combined cost for both MCPV and TES is

RM13,199,680.00 (12.16 % of the required cost to achieve payback period 25 years). The figure is just for a basic indication.

4.3.5 Summary

The designed hybrid cooling system has shown a positive possibility in powering the whole cooling system for a medium sized office building with an average hourly cooling load of 1600kW during office hours. 99.99% of total energy required to power up the whole system is estimated to be coming from solar energy and the remaining 0.01% of the total energy requirement is from the main grid. A combination of a high efficient technology in harnessing the solar energy, energy storage, and a high efficient electric chiller could avoid unnecessary energy surplus throughout the whole process which in return managed to increase the whole system's COP to 0.678. Powering the cooling system with solar energy enables the building to cut down a massive amount of primary energy consumption since cooling system typically consumes more than 50% of the building's energy for a hot and humid country. A combination of this hybrid solar cooling system with a passive cooling and a reduction in the cooling demand may yield to a larger energy saving in the building's energy consumption. The combined methods from Section 4.1, 4.2 and 4.3 will be investigated and presented in Section 4.4.

4.4 Holistic approach to achieve ZECB

4.4.1 Introduction

This chapter investigates the impact of combining all the three methods suggested in Section 4.1, Section 4.2 and Section 4.3 on the target building. When combined, this method caters energy reduction based on a holistic approach (combine passive and active). Previous studies (on academic buildings [90][92][96], offices [37][38][91][93][100] and residential buildings [94]) that used the holistic approach to improve a building's efficiency for an existing and a new building estimated a reduction of between 36% to 55% on total energy consumption [90][91][92] [93][94][96][100] and between 64% and 69% reduction in total cooling and heating load [92]. These studies included lighting, appliances, operational management, facades, orientation, thermal mass, night ventilation, insulation, PV panels, HVAC systems, cool roof technologies, air filtration and indoor environmental adjustment in their studies but did not combined solar cooling system, thermal based retrofit designs, PCM and insulation material application in their solution. This study aims to retrofit the target building to reduce building's energy requirement to deliver a good indoor comfort for the occupant and optimise renewable energy utilisation.

4.4.2 Methods

The methods from Section 4.1, Section 4.2 and Section 4.3 were applied on the baseline building model as a retrofit mean. The baseline building model was applied with the methods established in Section 4.1 and 4.2 before being simulated to acquire its cooling load, energy consumption, cost, and indoor environmental performance. The simulated cooling load is then used to design a CHP solar system from Section 4.3. The process that has been used for the retrofit is simplified in the flow chart in Figure 92.

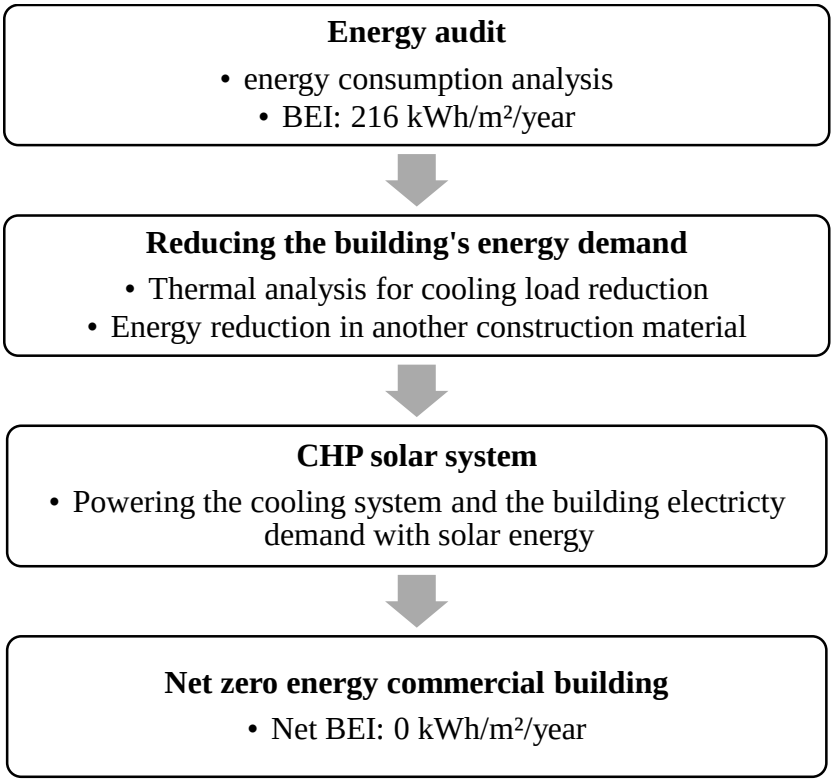

Figure 92: The diagram illustrates the whole retrofit process used in this section (section 4.4).

The building's baseline model was calibrated based on the findings in Section 4.1 and 4.2. The calibration made to the equipment, air conditioning, operation and construction are listed in Table 72 to Table 76.

Table 72: Equipment consumption in every zones.

Floor	Zones	Equipment consumption (W/m^2)
Lower Ground	Parking space	0
Underground	Parking space	0
	Cafeteria	3
	Kitchen	30
Ground floor (South)	Auditorium	1.78
	Multi-purpose hall	1.78
	Corridors	0
	Kitchen	20
	Data center	500
	AHU room	*
Ground floor (Atrium)	Lobby	0
	Reception area	6.19
North building (ground floor to floor 7)	AHU rooms	*
	Custodian's room	50
	Lifts	60
	Office ground floor	9
	Office floor 1	5
	Office floor 2	4
	Office floor 3	6
	Office floor 4	3
	Office floor 5	5
	Office floor 6	5
	Office floor 7	4
	Pantry	30
	Stairs	0
	Toilets	0
	Corridors	0
	IT rooms	50
Floor 8	Light plant room	30

*equipment power consumption are included in the cooling system's energy consumption.

Table 73: Data input for air conditioning and mechanical ventilation system in every zones.

Floor	Zones	Type	Settings
Lower Ground	Parking space	Mechanical ventilation	2 (ac/h)
Underground	Parking space	Mechanical ventilation	3 (ac/h)
	Cafeteria	KWP Cooling system	26.5 C
	Kitchen	Mechanical ventilation	Minimum fresh air (sum per person and area)
Ground floor (South)	Auditorium	KWP Cooling system	24
	Multi-purpose hall	KWP Cooling system	24
	Corridors	KWP Cooling system	27
	Kitchen	Mechanical ventilation	Minimum fresh air (sum per person and area)
	Cold room	-	-
	Toilets (OKU)	KWP Cooling system	-
	Data center	KWP Cooling system	21.5
	AHU room	-	-
Ground floor (Atrium)	Lobby	Natural ventilation	-
	Reception area	KWP Cooling system	24
North building (ground floor to floor 7)	AHU rooms and custodian's room	-	-
	lifts	-	-
	office ground the floor	KWP Cooling system	24
	office floor 1	KWP Cooling system	24
	office floor 2	KWP Cooling system	24
	office floor 3	KWP Cooling system	24
	office floor 4	KWP Cooling system	24
	office floor 5	KWP Cooling system	24
	office floor 6	KWP Cooling system	24
	office floor 7	KWP Cooling system	24
	Pantry	-	-
	Stairs	-	-
	Toilets	-	-
	Corridors	KWP Cooling system and FCU (for ground floor and 1st floor)	27
	IT rooms	KWP Cooling system	21.5
Floor 8	Light plant room	-	-

Table 74: Construction design for the offices, corridors, auditorium, hall, and cafeteria.

Construction	U-value (W/m^2K)	Layers from outer to inner skins and its thickness
Wall	1.838	[1] Granite 30mm [2] Plaster Cement 30mm [3] Brick outer leaf 100mm [4] Brick inner leaf 100mm [5] Plaster Cement 30mm
Ceilings	0.742	[1] Concrete slab 100mm [2] Air gap 100mm [3] BioPCM ENRG Blanket 74mm [4] Ceiling tiles 25mm
Partition	1.69	[1] Plaster lightweight 13mm [2] Brickwork inner leaf 105mm [3] Plaster lightweight 13mm
Internal floor	1.702	Concrete slab 100mm
Glazing	5.67	[1] Green float glass 8mm [2] Air gap 16mm [3] Low-emissivity glass 6mm

Table 75: Construction design for the IT rooms and data centre.

Construction	U-value (W/m^2K)	Layers from outer to inner skins and its thickness
Wall	0.188	[1] Granite 30mm [2] Plaster Cement 30mm [3] brick outer leaf 100mm [4] brick inner leaf 100mm [5] XPS extruded polystyrene 160mm [5] Plaster Cement 30mm
Ceilings	0.175	[1] Concrete slab 100mm [2] Air gap 100mm [3] XPS extruded polystyrene 160mm [4] Ceiling tiles 25mm
Internal floor	0.185	[1] Concrete slab 100mm [2] Cement plaster 30mm [3] XPS extruded polystyrene 160mm [4] Floor/roof screed 50mm
Partition	0.187	[1] Plaster lightweight 13mm [2] Brickwork inner leaf 105mm [3] Plaster lightweight 13mm

Table 76: Schedules for the building's main areas.

Zones	Cooling system	Lighting system
Offices	Monday to Friday:0700 to 1700 Weekend: Off	Monday to Friday:0730 to 1800 Weekend: Off
Corridors	Monday to Friday: 0600hours to 1900hours Weekend: Off	24hours
Data centre	24hours	24hours
Cafeteria	Monday to Saturday: 0600 to 1900 Sunday: Off	

The performance analysis was measured based on the energy performance, indoor environment quality and the cost analysis. The energy performance was evaluated based on the comparison between the simulated energy of the baseline building model and the results after the retrofit. Equation (4.4.1) to (4.4.4) were used for the evaluations. Meanwhile for the cost analysis, equation (4.1.1) to (4.1.7) were used.

$$\Sigma E_{CHP} = \Sigma Q_e + \Sigma Q_{th} \quad (4.4.1)$$

$$\Sigma E_{FiT} = \Sigma Q_e - \Sigma E_{bldg} - \Sigma E_{battery} \quad (4.4.2)$$

$$\Sigma Q_{cold\text{-}exs} = \Sigma Q_{cold} - \Sigma Q_{cool\ load} - \Sigma Q_{th\ stored} \quad (4.4.3)$$

$$\text{Net BEI} = \frac{\text{Total energy consumption from the grid}}{\text{Conditioned building area}} \quad (4.4.4)$$

Where:

Total energy delivered by the solar CHP (ΣE_{CHP})

Electricity (Q_e)

Thermal energy (Q_{th})

Electricity feed into the grid (ΣE_{FiT})

Excess cold energy ($Q_{cold\text{-}exs}$)

Total cold energy (Q_{cold})

Total cooling load ($Q_{cool\ load}$)

Total thermal energy stored ($Q_{th\ stored}$)

Building's energy consumption (ΣE_{bldg})

Electricity stored in the battery ($\Sigma E_{battery}$)

4.4.3 Results and Discussion

The results will be discussed in three main parts that are Section 4.5.3.1 for energy performance, Section 4.5.3.2 for indoor environmental performance and Section 4.5.3.3 for the economic analysis.

4.4.3.1 Energy performance

Combining all the three methods, passive cooling (Section 4.1), retrofit methods based on thermal analysis to reduce cooling load (Section 4.2) and CHP solar system (Section 4.3) is projected to result in a net-zero energy commercial building (ZECB) with an excess of 8,652.40 kWh electricity that can be fed into the grid. The building is projected to consume 52.2% less energy consumption, 49.68% reduction in cooling load and 55.53% reduction in the building's electricity consumption compared to the baseline building. 62% of 3,439,316.75 kWh total energy consumption is allocated to the cooling system, and another 38% allocated to the building's electricity consumption. This energy requirement will be provided by the CHP solar system explained in Section 4.3 where the chilled water requirement will be provided by the CHP's thermal energy, and the whole building's electricity requirement will be supplied by the electricity generated by the CHP solar system. The building's energy consumption after retrofit is presented in Table 77.

Table 77: The building's energy consumption after the retrofit.

Type	Value (kWh)
Total energy consumption	3,439,316.75
Total energy provided by solar CHP	9,237,446.82
Clean energy feeds into the grid	573,674.77
Excess cold energy	3,531,703.26
Cooling load after retrofit	2,120,523.32
Electricity load after retrofit	1,318,794.43
Net BEI	0

A similar design of CHP solar system in Section 4.3 was utilised with a total solar collection area of 6,750.00 m². The system is expected to collect a total of 11,129,454.00 kWh solar energy to produce 1,896,894.12 kWh electricity and 7,340,552.70 kWh thermal energy. The MCPV's COP is predicted to be 0.83. The whole generated thermal energy is assumed to drive two absorption

chiller with a capacity of 1875 kWh each that will generate a total of 5,652,225.57 kWh chilled water (cold energy) a year. The overall CHP solar system's COP (including the cooling and electricity supply) is predicted to be 0.678.

After the retrofit, the building only requires 2,639,643.20 kWh of energy to deliver a good indoor environment (IEQ) to the occupants, instead of 6,005,582.11 kWh. The building is predicted to use 56% less energy to maintain a good IEQ for the occupants. Additionally, the simulated IEQ after retrofit shows an improvement regarding the indoor luminance level and daylight factor. The reduction in energy requirement to maintain a good IEQ for the occupants shows that with a proper design, energy management, and efficient equipment, a building can maximise its renewable energy utilisation which in return will reduce the building's dependency on non-renewable energy. The energy consumption by sectors before and after retrofit is shown in Figure 93.

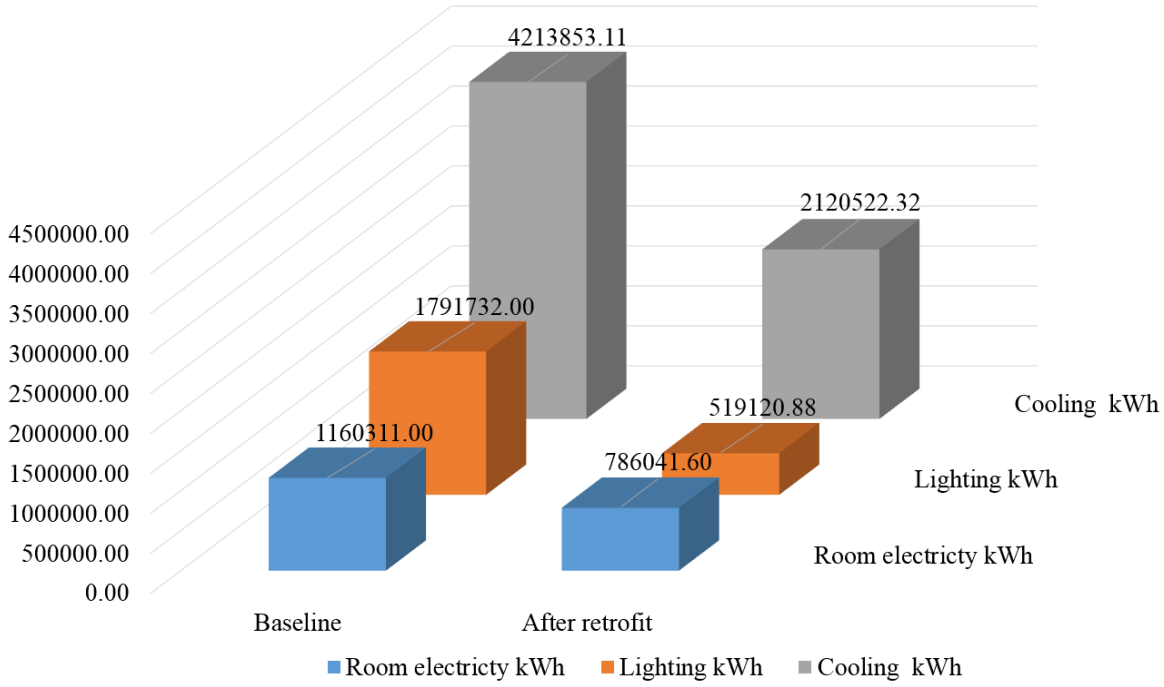

Figure 93: The building's energy consumption by sectors before and after the retrofit.

Nonetheless, the cooling system still consumes the highest amount of energy compared to other sectors even after the retrofit. Air conditioning is required when the air temperature and humidity level exceeds a human's comfort level. The fluctuation in the air temperature results from the

fluctuation of the air sensible heat capacity. Meanwhile, the fluctuation in the air humidity is influenced by the moisture content. The sensible and latent heat gain is contributed by the internal and external factors. As can be seen in Figure 94 and Figure 95, the building's heat gain (before and after retrofit) is mainly contributed by the internal factors compared to external factors. Hence, this observation of heat gain pattern highlighted the importance of utilising efficient equipment (such as the lighting, computer and office equipment) and managing the equipment's operation to reduce the heat gain, hence reducing the cooling load.

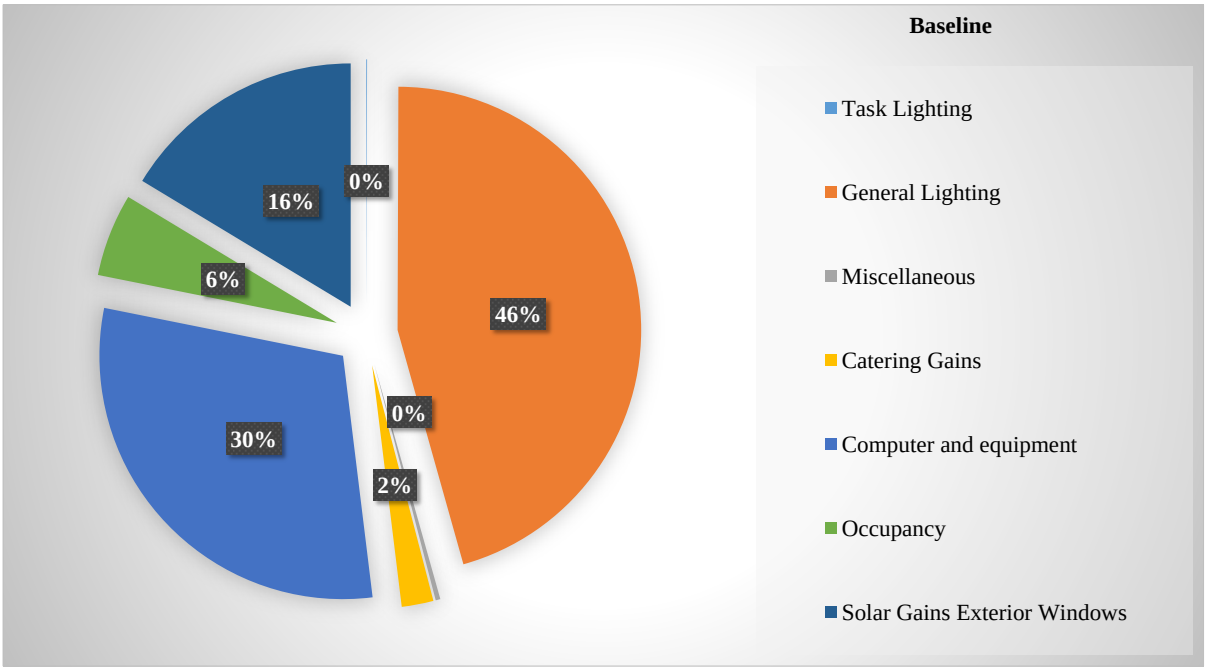

Figure 94: The simulated building's heat gain sources before retrofit (baseline model).

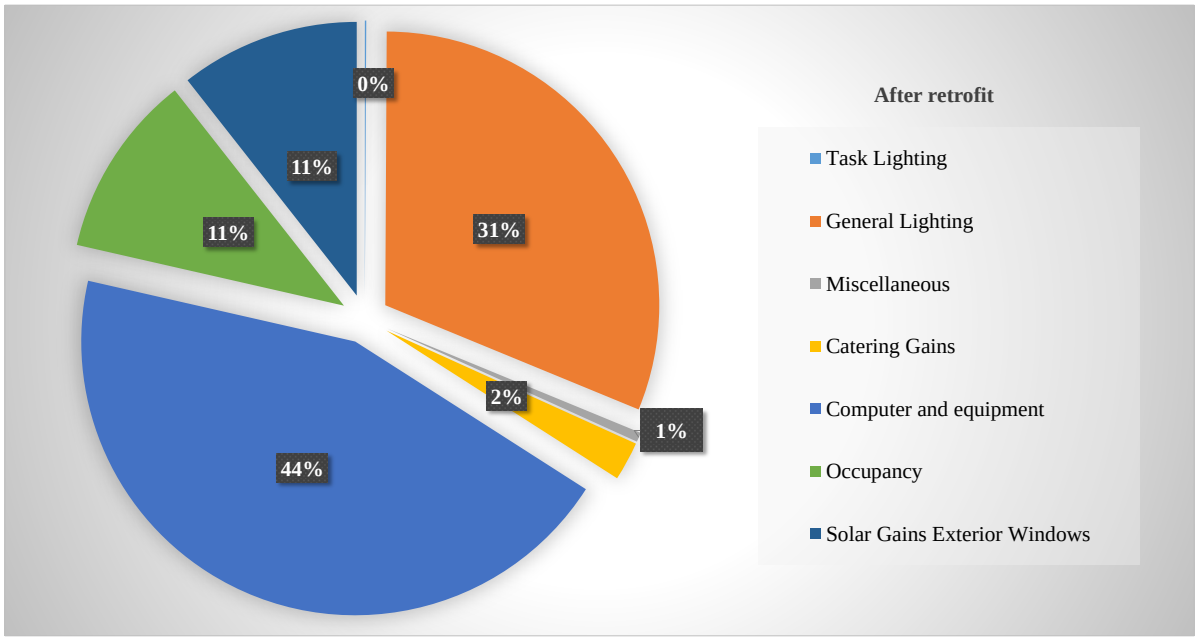

Figure 95: The building's simulated heat gain sources after the retrofit.

A total of 1,908,729.48 kWh heat gain was reduced after the retrofit. The highest heat gain reduction was projected to be originated from changing the lighting system followed by the changes of the glazing and the changes in the computer and office equipment to more energy efficient computers and equipment. The changes in the three sectors mentioned earlier contributed to 97% of the total annual heat gain reduction after the retrofit. Whereas the rest of overall heat gain reduction is resulted from the changes made in other sectors. The heat gain from every sector is listed in Table 78.

Table 78: The amount of heat gain from different sources before and after the retrofit.

Sector	Baseline (kWh)	After retrofit (kWh)	Heat gain reduction (kWh)	Heat gain reduction (%)
Task Lighting	1879.67	1387.63	492.04	26
General Lighting	1627100.00	516912.80	1110187.20	68
Miscellaneous	11093.52	9237.36	1856.16	17
Catering Gains	75117.10	38083.42	37033.68	49
Computer and equipment	1074100.00	738720.80	335379.20	31
Solar Gains Exterior Windows	583380.90	175833.00	407547.90	70
Occupants	196216.4	196216.4	0	0

Meanwhile, the simulated total hourly cooling load for the whole year before and after the retrofit spanned into 24hours is shown in Figure 96. It can be observed that the peak cooling load is kept below 1,000.00 kWh at all time and the cooling load after office hours was reduced below 161.13 kWh as opposed to the peak cooling load demand during the non-office hours before retrofit that reached 266.34 kWh.

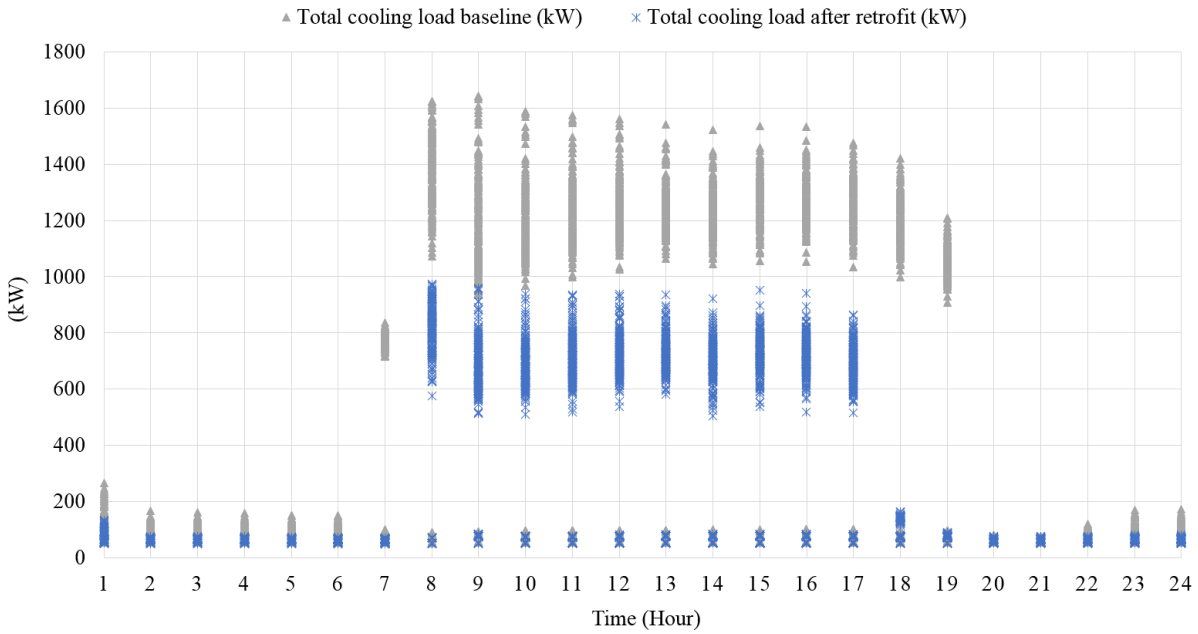

Figure 96: The hourly total cooling load in a year spanned into 24 hours view before and after the retrofit.

4.4.3.2 Technical discussion

A similar design of CHP solar system in Section 4.3 was utilised with a total solar collection area of 6,750.00 m². The system is expected to collect a total of 11,129,454.00 kWh solar energy to produce 1,896,894.12 kWh electricity and 7,340,552.70 kWh thermal energy in a year. The MCPV's COP is predicted to be 0.83. The outlet temperature of the coolant outlet is kept at 90°C, and the PV efficiency is estimated to be 0.224. The whole generated thermal energy is assumed to drive two absorption chillers with a capacity of 1,875 kWh each that will generate a total of 5,652,225.57 kWh chilled water (cold energy) a year. The overall CHP solar system's performance is predicted to be 0.678.

The building requires electricity and cooling supply 24 hours in a day for every day. However, the solar energy is only available from 0800 to 2000 every day, and the amount of solar energy radiated from the sun fluctuates from low during sunrise to its peak at the noon and decreasing again until it approaches night. Figure 97 and Figure 98 show the hourly demand and supply and the differences in the demand and supply of electricity and cold energy for the first 10 days of the year. The positive values in the differences between demand and supply mean excess in energy while the negative values indicate that the building is short in supply.

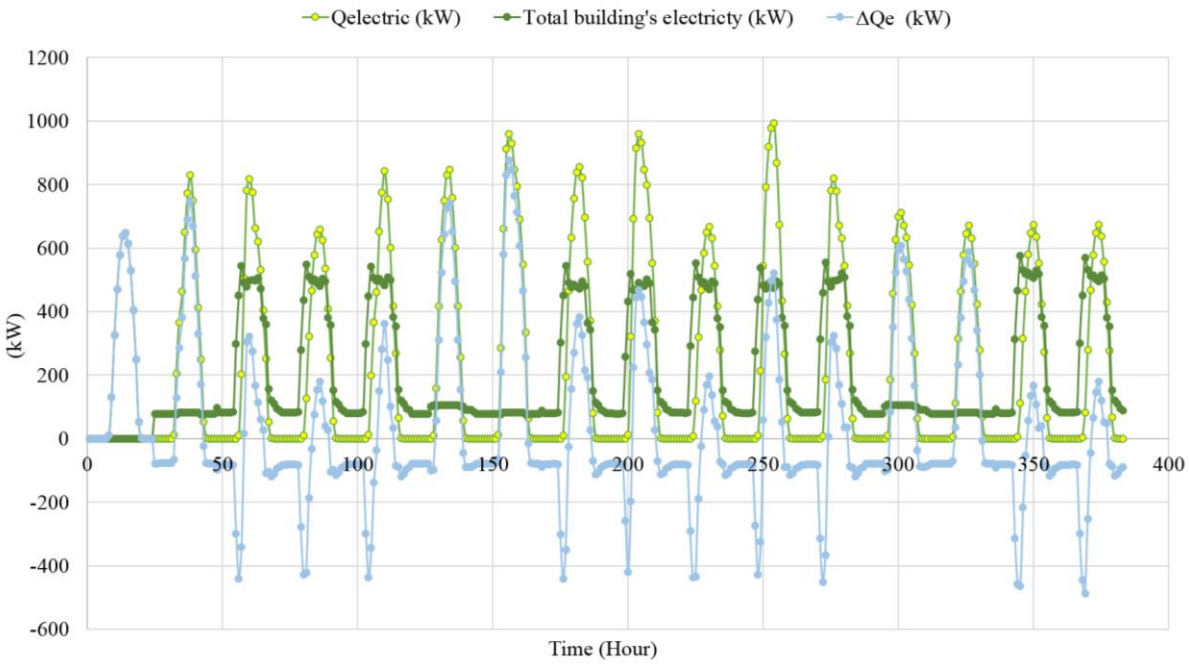

Figure 97: The comparison of the hourly electricity generated, total building's electricity demand and the differences between the demand and the supply on the 1st to the 10th of January.

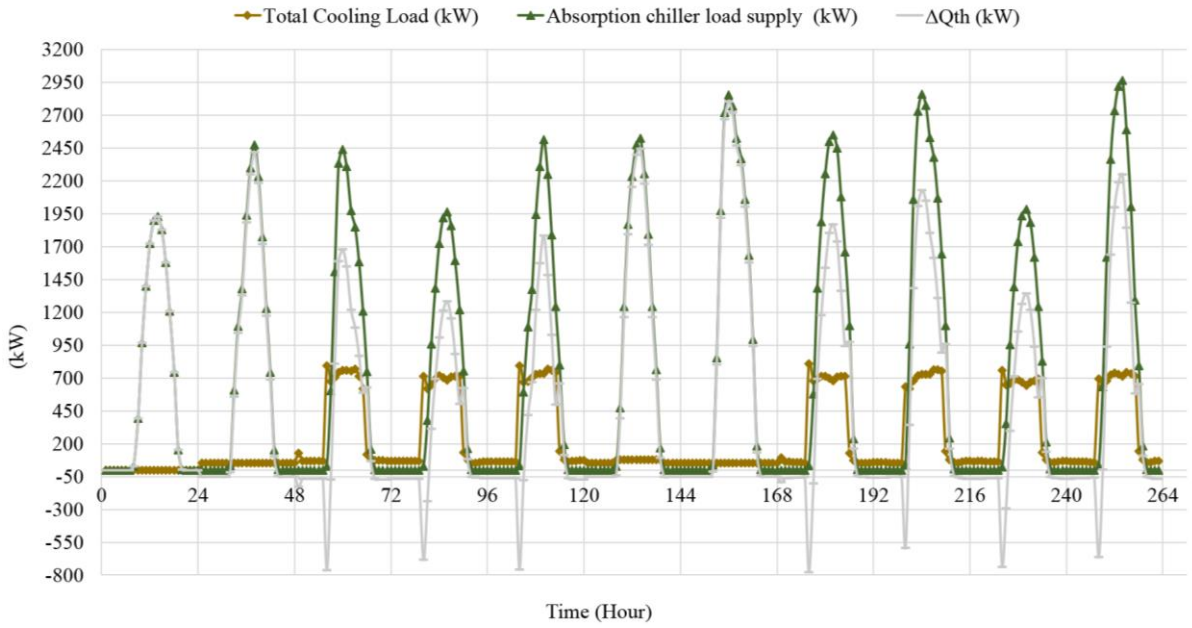

Figure 98: The comparison of the hourly chilled water generated, total building's cooling demand and the differences between the demand and the supply on the 1st to the 10th of January.

As can be seen in the graphs, the building requires additional supply for electricity and cooling from 2000 to 2400 and from 0000 to 0900 during work days. The highest insufficient supply for both cooling and electricity occur at 0800 during work days (which can be seen as a spike every morning in the graph). However during the afternoon, an increase in the solar radiation results in excess energy. The graph of the differences in the supply energy and the demand for the whole year can be seen in Figure 99 and Figure 100. The excess energy reaches its peak at 1400 with the highest excess electricity 1,048 kWh and the highest excess cold energy 3,317 kWh. The deficient in electricity are always below 515 kWh and the deficient in cold energy for cooling load are always below 949 kWh. This variation in excess energy and insufficient supply is solved by utilizing energy storage.

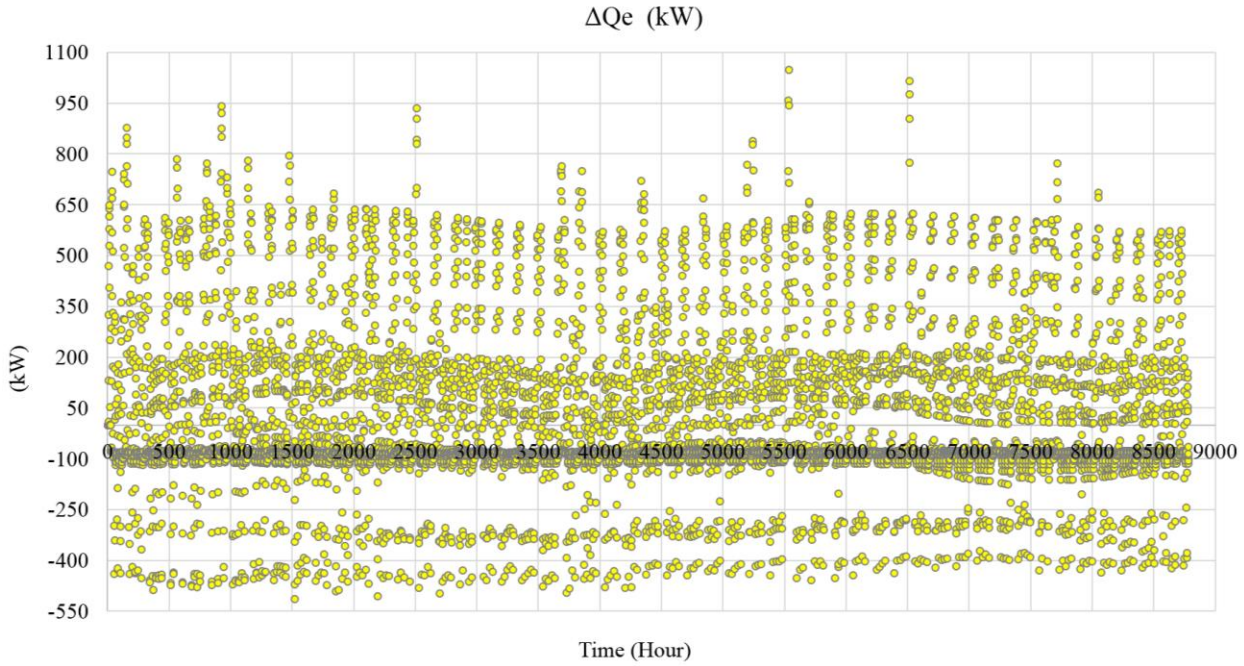

Figure 99: The hourly differences between generated electricity and the electricity demand in a year.

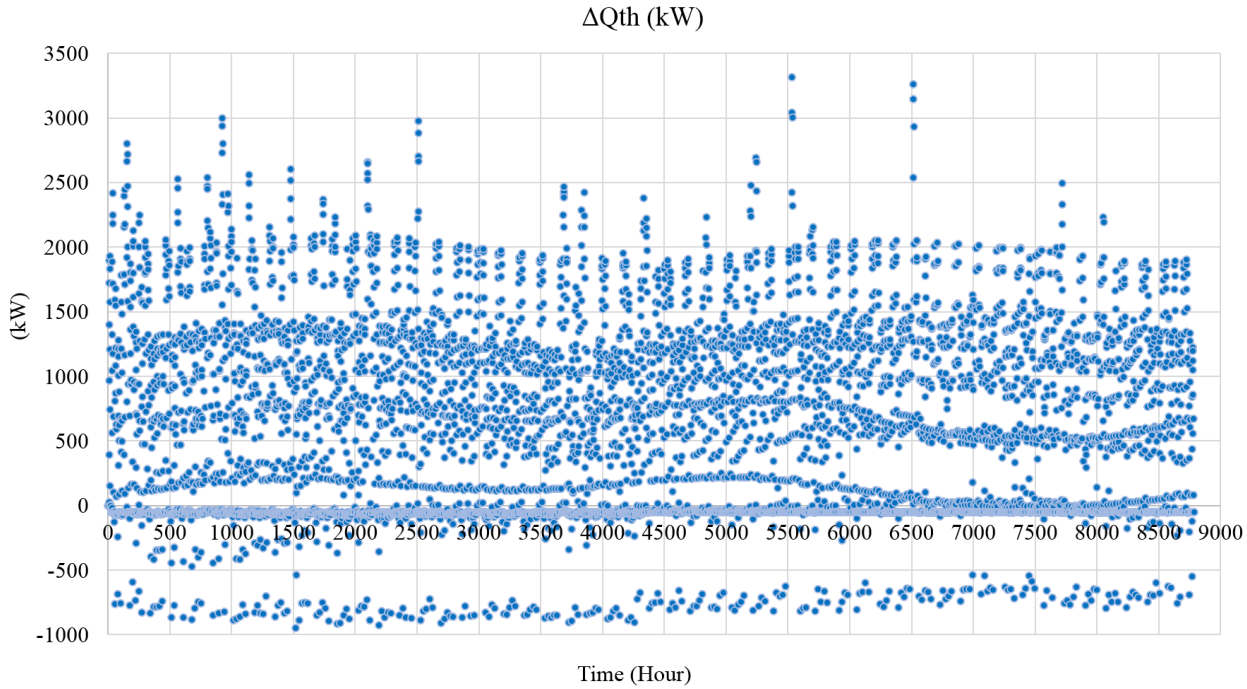

Figure 100: The hourly differences between generated cold energy and the cooling demand in a year.

The CHP solar system is set to start on the 31st of December, a day before the building started to operate. This operation schedule managed to eliminate the electricity requirement from the grid

since the stored cold energy and electricity on the first day of the CHP solar system's operation can be used to power up the building's system during the hours without solar energy. A cylindrical storage tank that contains PCM ice tubes with a total storage capacity of 6,000.00 kWh will be used to store the cold energy. Meanwhile, the generated electricity is stored in a DC battery with a total capacity of 5,000 kWh. The excess electricity and cold energy not including stored energy are estimated to be 573,674.77 kWh and 3,525,955.51 kWh. The excess cold energy can be supplied or sold to the neighbouring offices in the South building which are rented by non-government agencies while the excess electricity can be sold to the primary energy provider by feeding it into the grid. The technical data of the designed cold energy storage and the battery is shown in Table 79, and Figure 101, and Figure 102 show the hourly electricity and cold energy storage for the building in a year.

Table 79: The PCM thermal energy storage for the building.

Specification	Unit	Value
k	W/m²/°C	0.02
Volume	m³	116.28
Radius	m	1.5
Length	m	16.45
Total surface area	m²	169.17
Thermal loss per hour	kW	0.01
Ice melting rate	kg/h°C	0.0143
Storage capacity	kWh	6000.00
Heat loss rate	kWh	0.01
Cold room temperature	°C	10

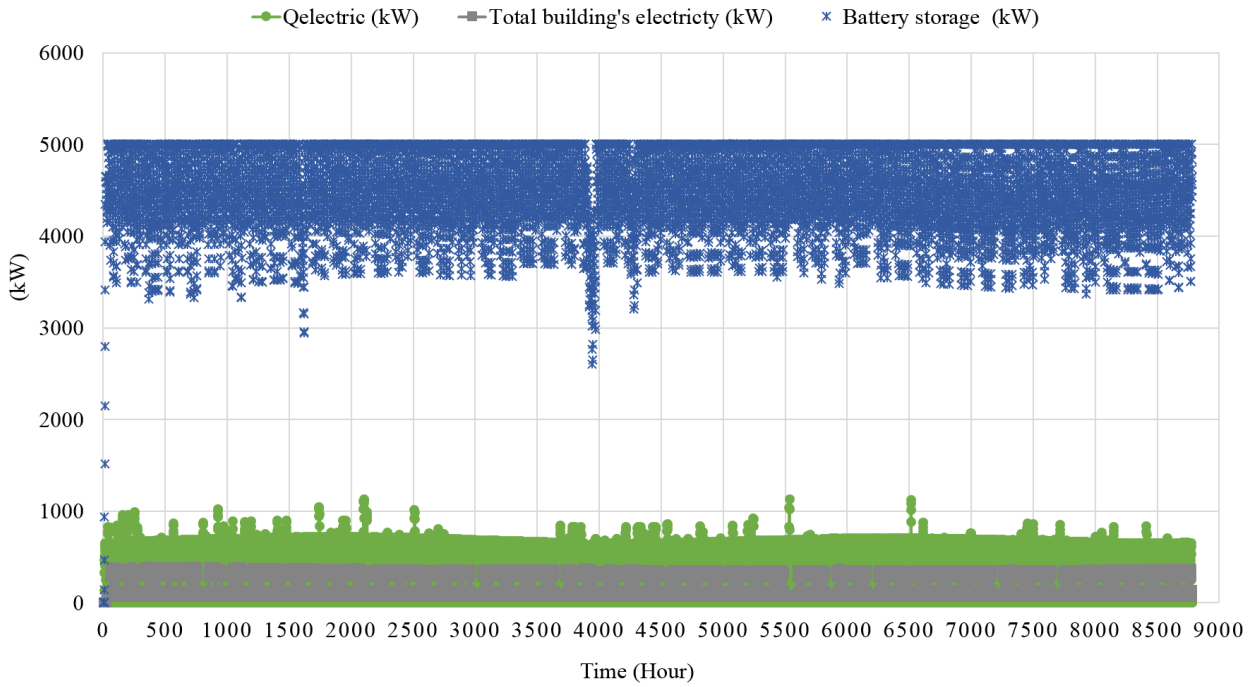

Figure 101: The building's hourly electricity demand, hourly generated electricity and battery storage in a year.

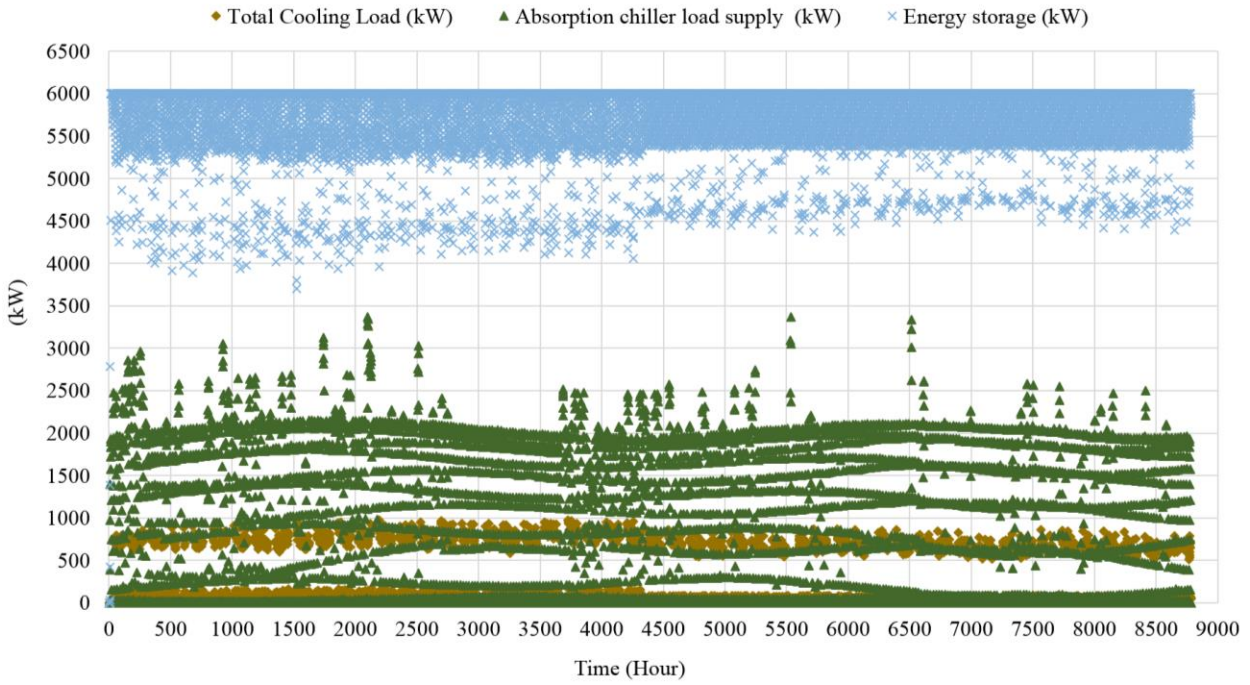

Figure 102: The building's hourly cooling demand, hourly generated chilled water, and cold energy stored in a year.

4.4.3.3 Indoor environmental performance

Part of the definition of a high efficient building is its ability to provide a good indoor comfort for the occupant while being resource efficient. In this study, only three aspects of IEQ were included which are indoor air quality (IAQ), indoor thermal comfort (ITC) and indoor visual quality (IVQ). The simulated building's indoor condition after retrofit was adjusted until it reaches the suggested indoor conditions by the local regulation which is MS1525:2014 and DOSH. A mean predictive vote (PMV) established by P.O Fanger [138][150][151] was used as a mean of comparison for the offices' thermal comfort. The indoor air temperature in the office building was set at 24°C during office hours based on the occupants' feedback on thermal preference. An actual air temperature adjustment was made to the building by raising the set point air temperature from 22.5°C to 23°C, 24°C and 25°C. No negative feedback was issued when the temperature was raised to 24°C. However, concerns of discomfort were made by the occupants when the temperature was raised to 25°C. Hence, 24°C was chosen as the air set point temperature throughout this study. The simulated hourly indoor air temperature in all the offices in workdays spanned in a 24 hours' time frame is shown in Figure 103.

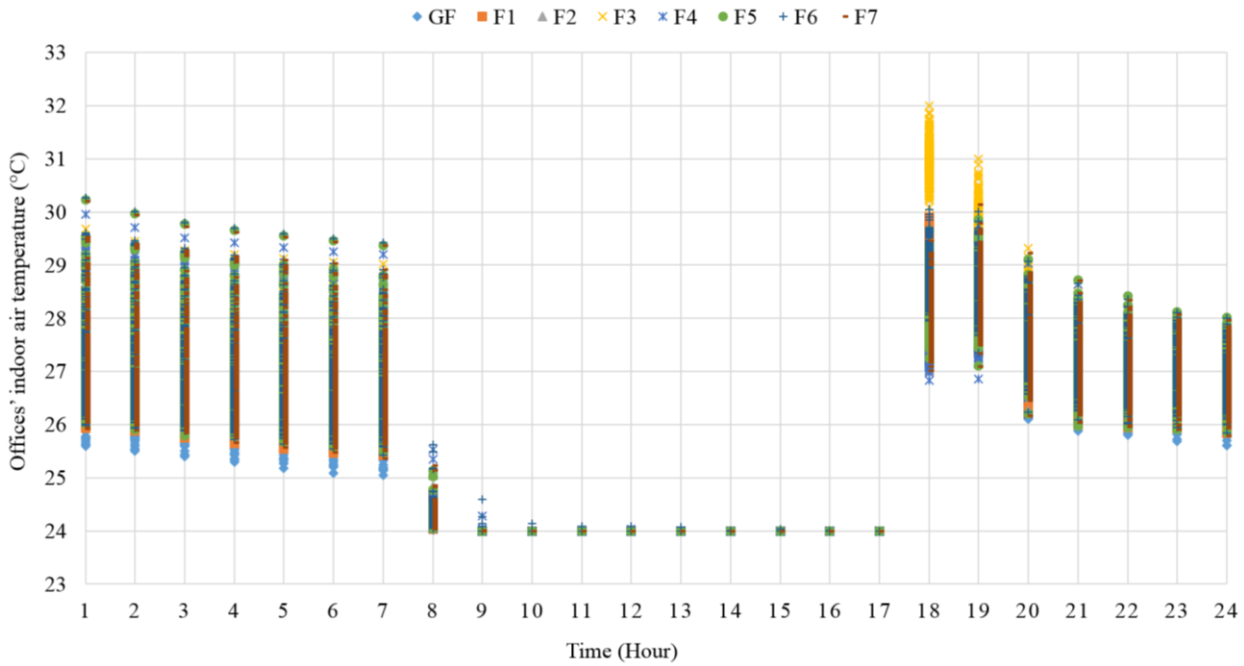

Figure 103: The hourly indoor air temperature in the offices (a year data during workdays) captured in 24 hours time slot.

As can be observed in Figure 103, the air temperature during the office hours is within the guidelines given by the local authorities in MS1525:2014 and DOSH. At 0900 to 1700, the simulated air temperature is projected to be at 24.0±0.5 °C at all times for the whole year during workdays. However, it took up to two hours after the air conditioning was switched on to achieve indoor air temperature 24.0±0.5 °C and maintain the same air temperature until 1700. Figure 104 analysed the simulated air temperature in the offices at 0800 during work days. The highest simulated air temperature recorded at 0800 was 25.62°C in the office on the 6th floor on day 152 (4th June). It can be observed that the air temperature in the offices at the 1st to the 7th floor was higher than normal on day 60, 88, 109 and 152. On these dates, the air temperature at 0800 exceeds 25.0°C for the offices at the 4th, 6th and 7th floor. Whereas, for the ground floor office, the air temperatures were most of the time, the lowest. The same observation can be clearly seen in Figure 105.

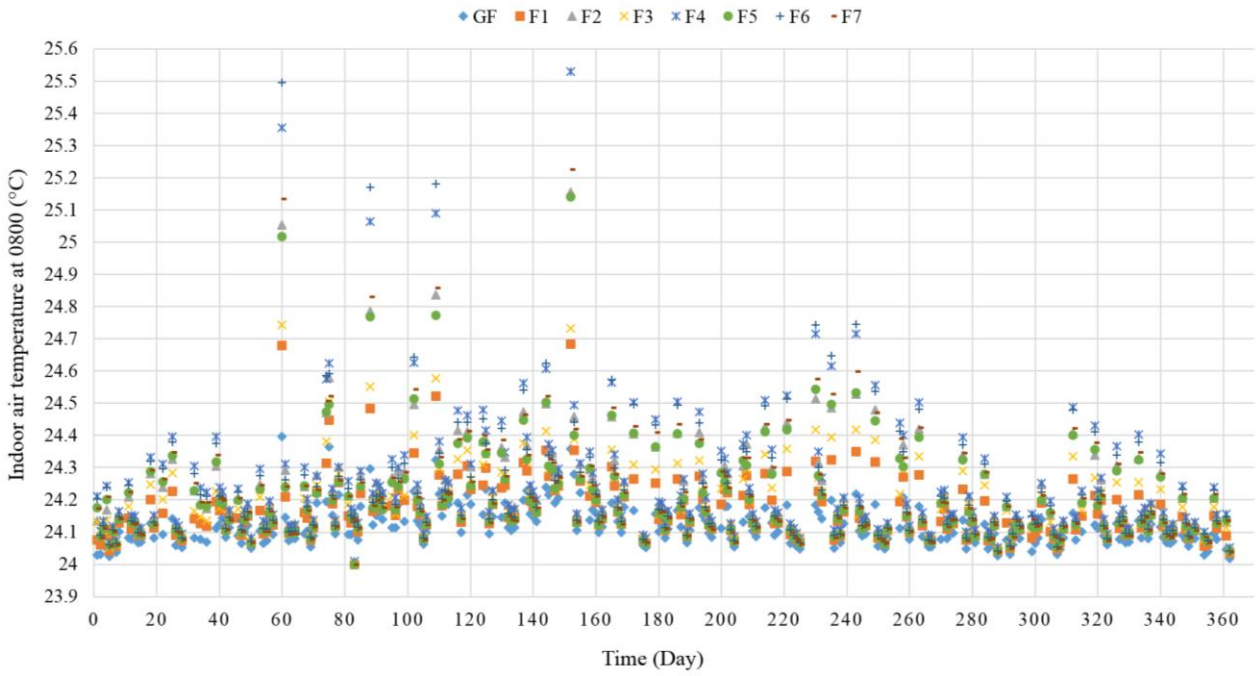

Figure 104: The simulated hourly offices' air temperature at 0800 during workdays.

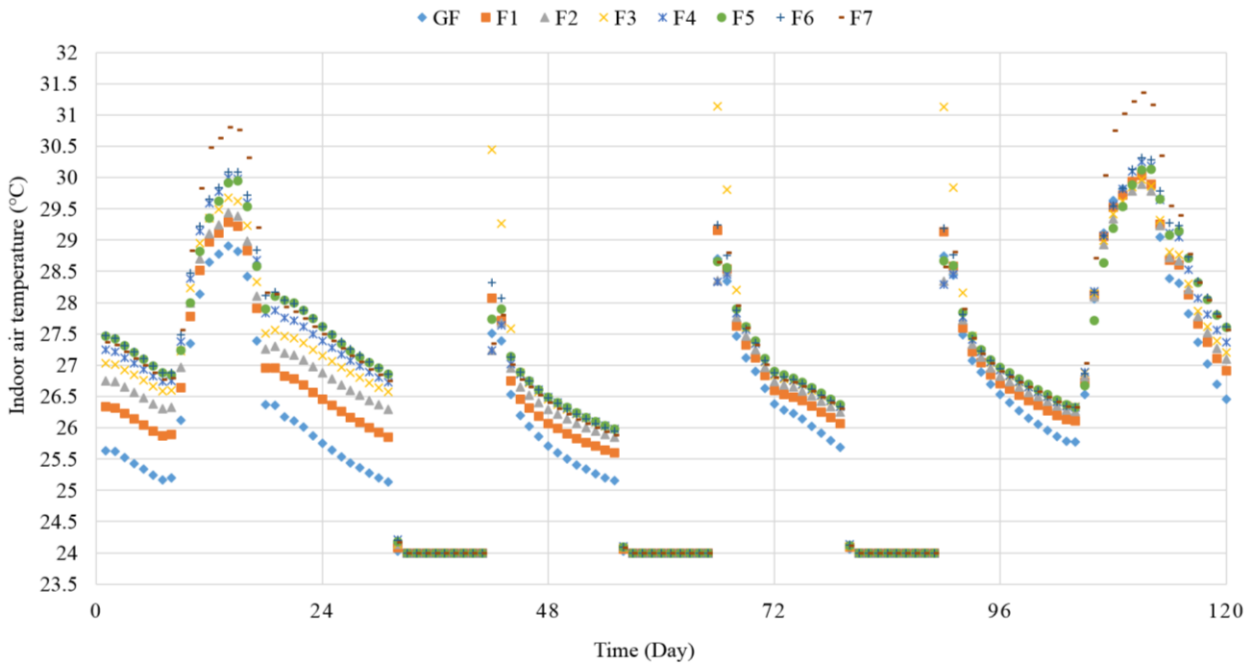

Figure 105: The hourly indoor air temperature from 1st to 5th day of the year.

Air temperature is a measure of how hot or cold the air is which is influenced by the kinetic energy of the air molecules which is influenced by the sensible heat gain in the atmosphere. However, the analysis of the total annual heat gain in every office (Figure 106) shows that the differences in the air temperature between every floor was not influenced by the room's heat gain since the total heat gain at the ground floor's office was not the lowest. Instead, the lowest total annual heat gain was the office at the 4th floor then followed by the office on the 7th floor. However, the total heat gain does influence the total annual cooling load. This statement is supported by the graph in Figure 107.

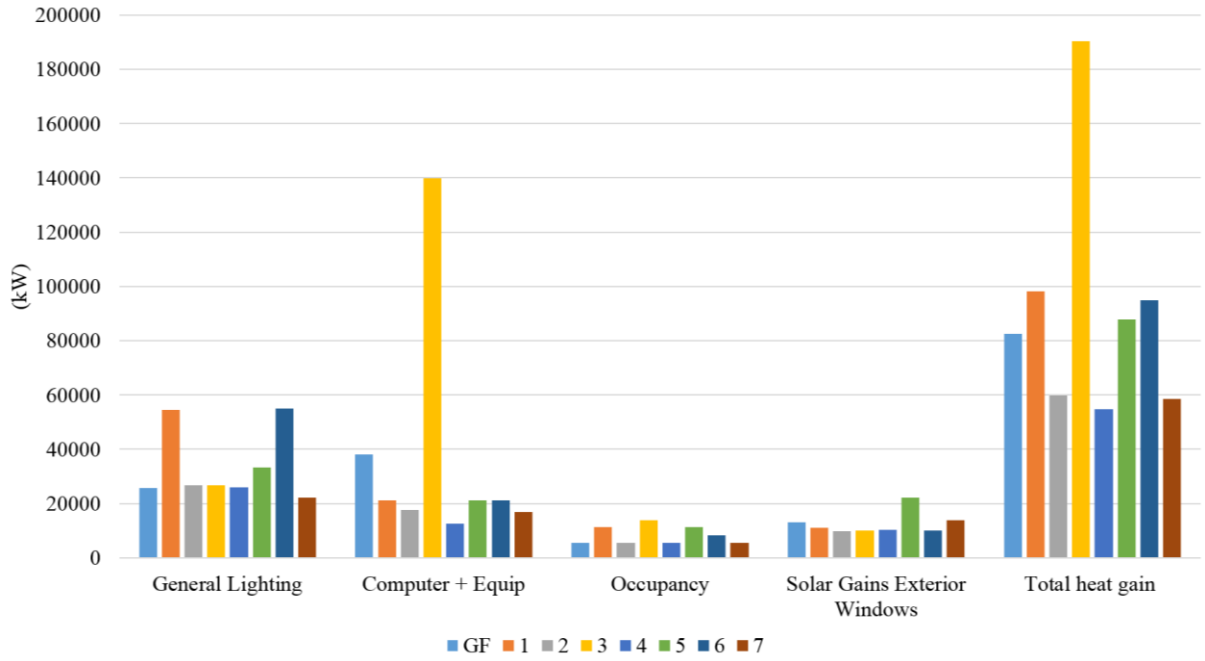

Figure 106: The comparison of the total heat gain sources in a year for every office.

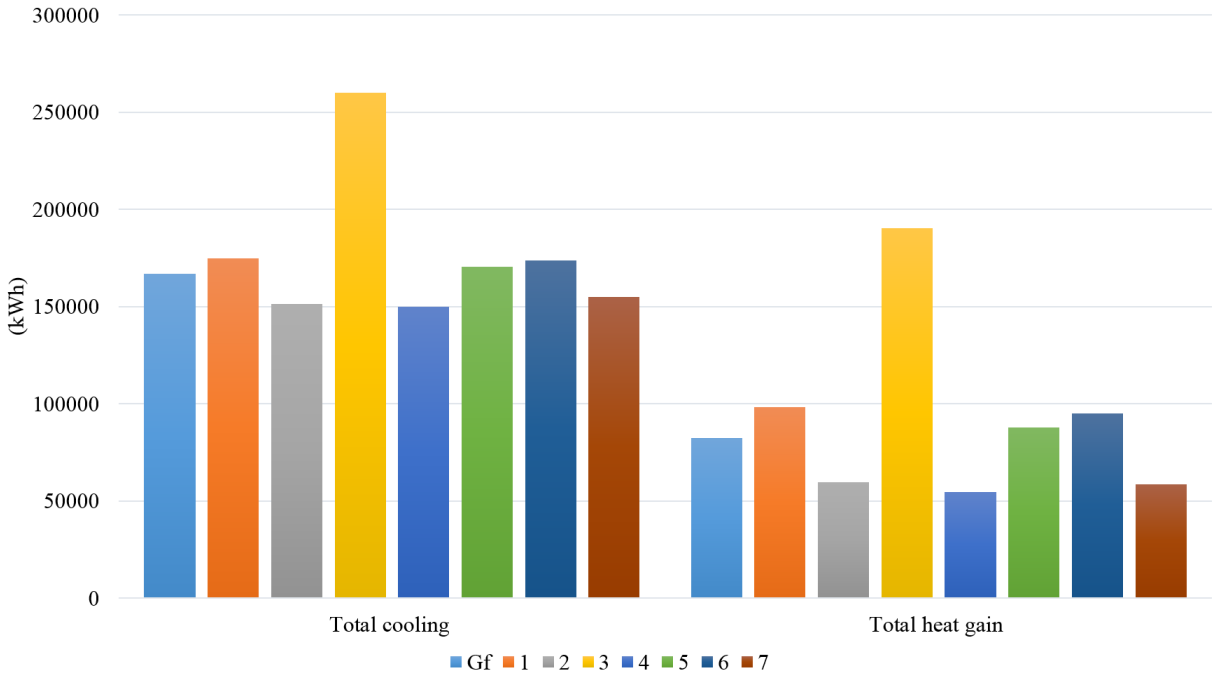

Figure 107: The comparison between the total heat gain and the total cooling load in a year for every office.

It is found that the moisture content in the air did influence the air temperature. Figure 108 analysed the relative air humidity (R.H) in the offices on the 1st to the 3rd of January. The R.H's pattern was inverse of the simulated air temperature in the offices. It can be observed that during the non-office hours, the humidity decreases and the air temperature increases as the altitude increases. Meanwhile, the simulated R.H during office hours were in the range of 50% to 70% (see Figure 109). The simulated hourly operative and radiant temperature during workdays for a year spanned into 24 hours view are illustrated in Figure 110 and Figure 111.

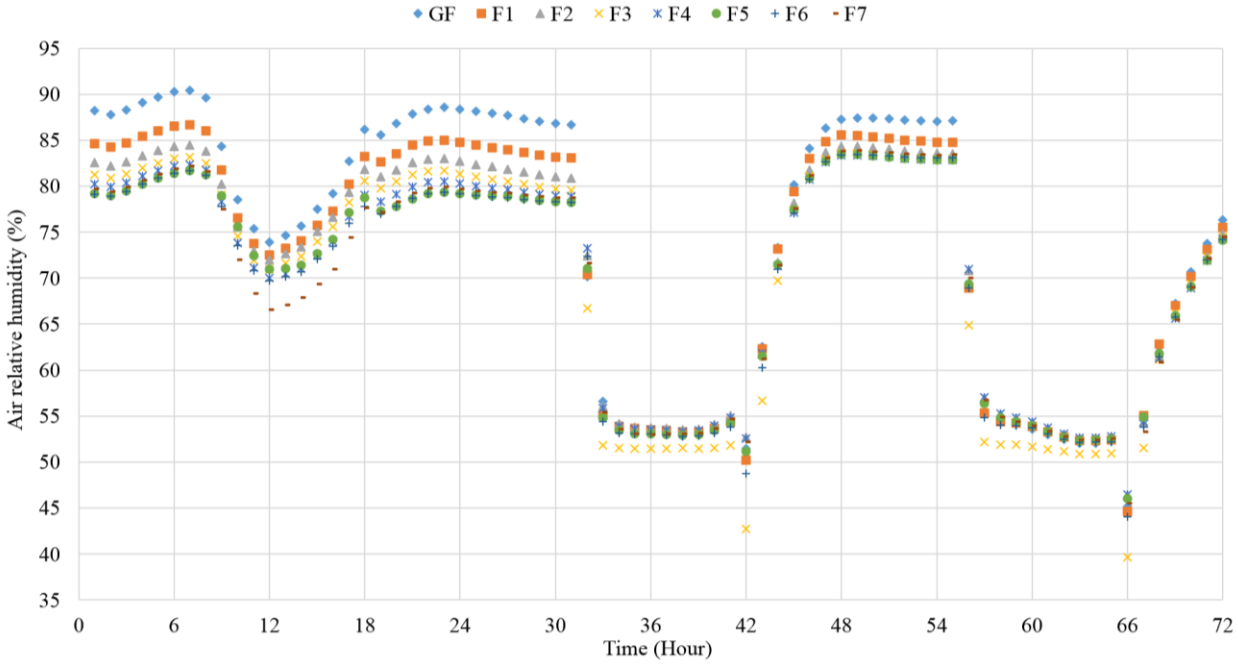

Figure 108: The simulated air relative humidity in the offices for the first three days of the year.

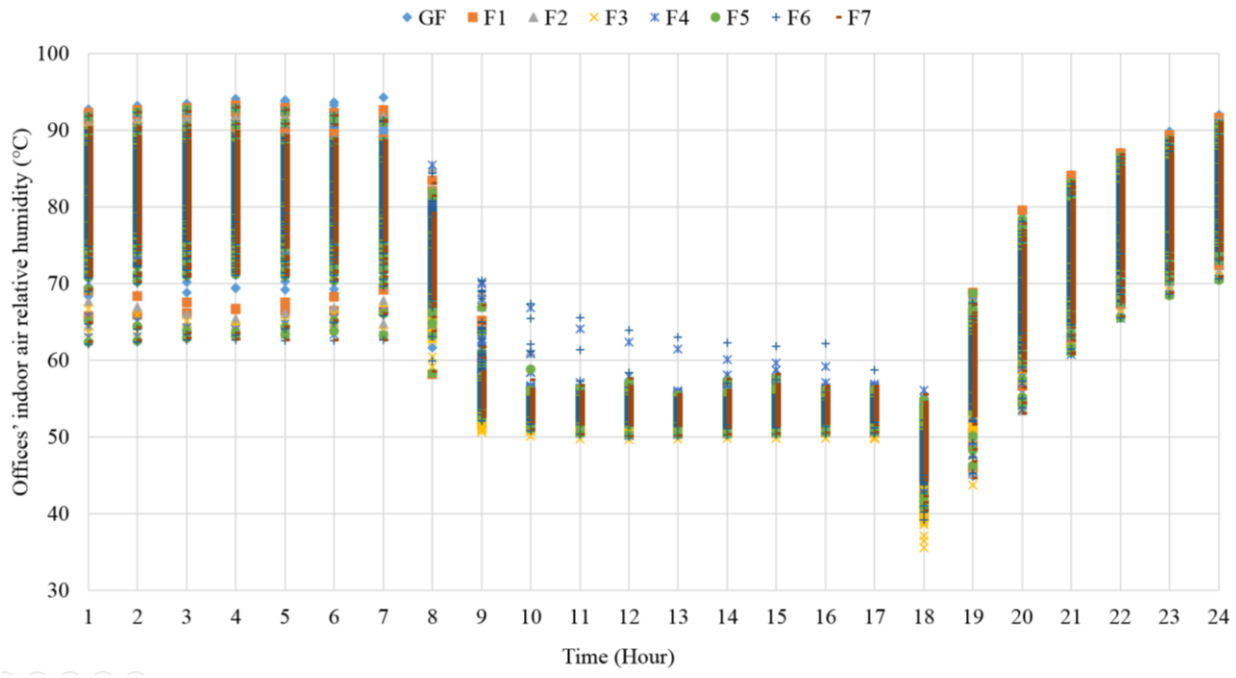

Figure 109: The simulated air relative humidity at the offices during workdays in a year (spanned into 24 hours).

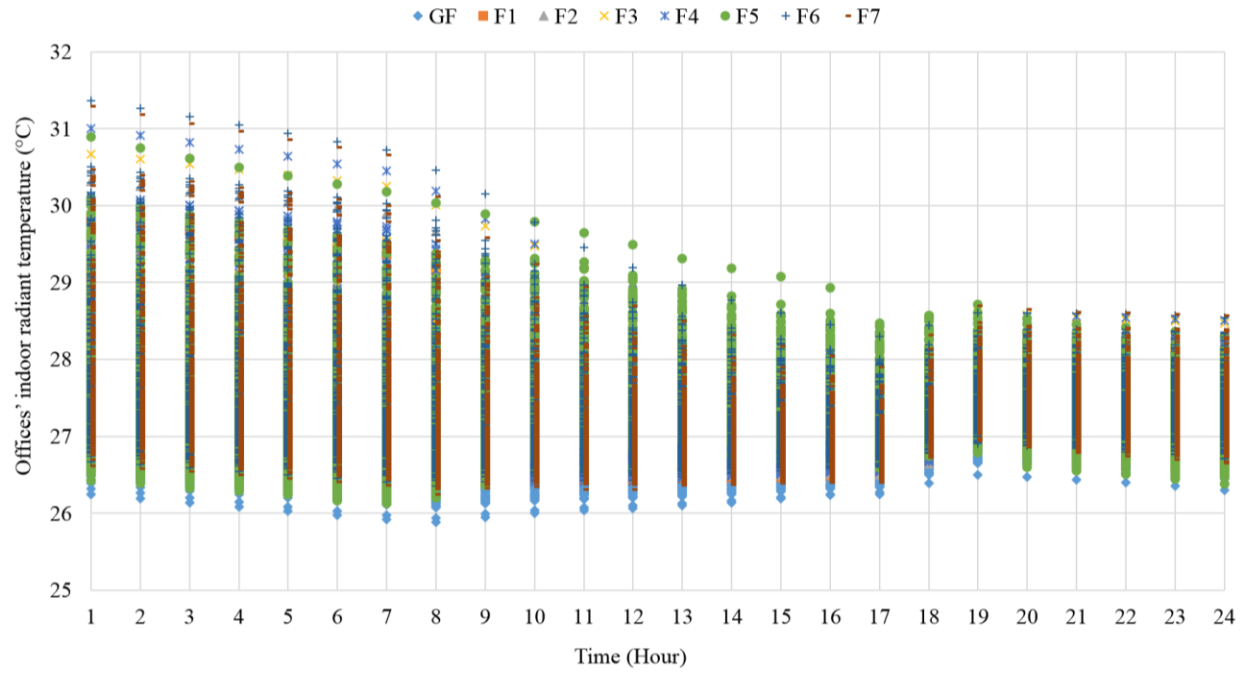

Figure 110: The simulated offices' indoor hourly mean radiant temperature during workdays spanned into 24 hours.

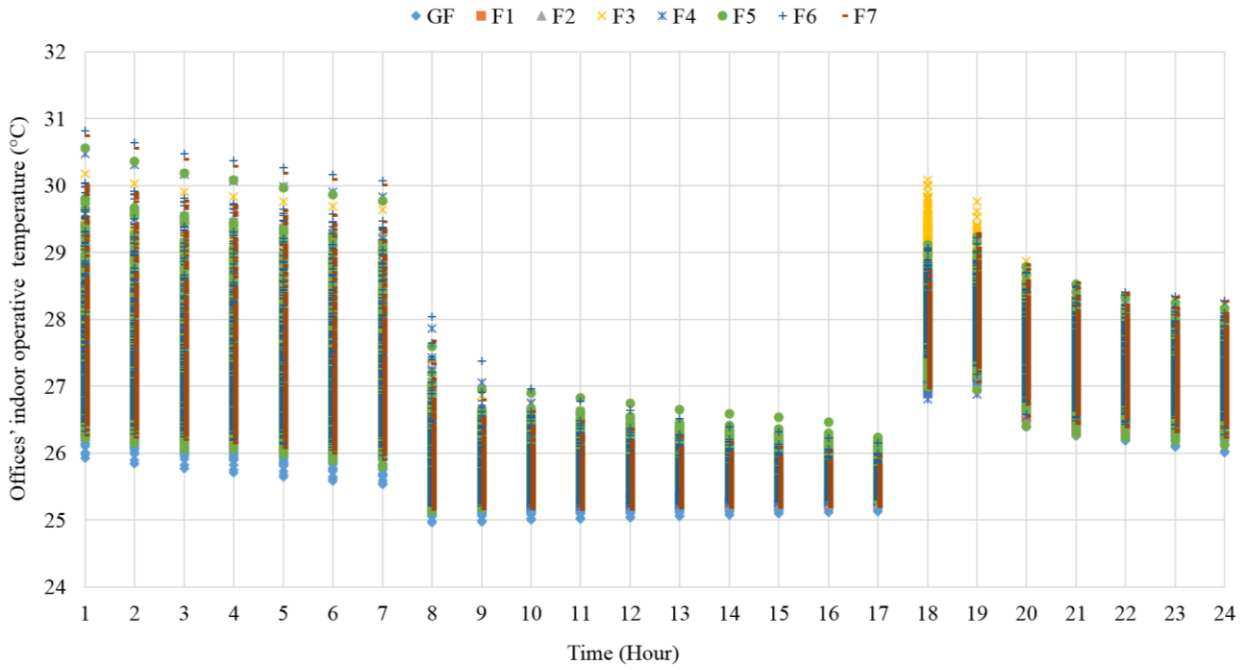

Figure 111: The simulated hourly operative temperature in the offices during workdays.

The luminance level in every area was set based on the guidelines given by the local authority. Hence, the indoor light quality does satisfy the requirement. Regarding the daylight at the offices and the communal areas that were exposed to the daylight such as the cafeteria and corridors, the simulated daylight factor (D.F) ranged in between 1.47 to 4.08. The main problem for a tropical country is the glare issue. With the suggested new glazing, it is predicted that glare does not occur since the D.F are below 6. The simulated D.F values at the offices and communal areas during a clear sunny day are shown in Table 80 and the simulated daylight distribution in the areas are attached at the Appendices A. The daylight distribution were simulated using BREEAM Credit HEA1 Report.

Table 80: The average simulated D.F values at the offices and communal areas.

Area	D.F	Illuminance (lux)
Office ground floor	2.08	208
Office Level 1	1.94	194
Office Level 2	1.75	175
Office Level 3	1.62	162
Office Level 4	1.82	182
Office Level 5	4.08	408
Office Level 6	1.78	178
Office Level 7	1.96	196
Corridor Level 2	2.38	239
Corridor Level 3	2.39	240
Corridor Level 4	2.39	239
Corridor Level 5	2.39	239
Corridor Level 6	2.39	240
Corridor Level 7	2.41	242
Cafeteria	1.47	147

4.4.3.4 Economic analysis

If the same building was to be constructed again but this time including the recommended changes, the estimated building's material and sub-systems cost is £34,009,027.25. This figure is 5.25% lower than the simulated cost for the baseline building (£35,893,865.00). The building's cost reduction is mainly due to the changes made to the lighting system. This value does not consider the budget for equipment and the CHP solar system. The advancement in technologies and the increase in demand for high efficient equipment have enabled a high efficient gadget to be sold at a competitive price as the non-energy star rated equipment. Plus, the suggested building is estimated to use 52% less energy which enables the building's owner to reduce more than half of the expenditure for energy bills for the building's lifetime (average building's lifetime is 50 years). The cost for retrofitting is listed in Table 81. The payback period for double glazing exceeds 40 years (remaining building's lifetime) which is deemed to be uneconomical. However, the retrofit cost for glazing is based on the estimated cost given by the Design Builder while the estimated costs other EEMs suggested were quoted from the manufacturers. The actual cost varied depending on the type of seller either it is a distributor or a manufacturer. The price

quote also highly depends on the purchase quantity. The prices given in this study are based on bulk price.

The economic analysis for each retrofitting was discussed in Section 4.1, 4.2 and 4.3. The cost for the PCM thermal energy storage (PCM TES) with a capacity of 6,000 kWh as quoted by the manufacturer, is RM 1.3 Million/ GBP250,000.00 [221]). The figure is 90% less than the cost for PCM TES in Section 4.3 due to its smaller size and capacity. Meanwhile, for this holistic approach, 6,750.00 m² roof area will be used. Hence the total cost for MCPV is expected to be more than the estimated cost in Section 4.3. If the same assumption is used (that the cost for MCPV is three times higher than the cost for FFPV) the total cost for MCPV will be RM112,320.00. Therefore, the estimated total cost for MCPV and PCM TES is RM1,412,320.00.

Besides the reduction in energy bills, when CHP solar system is used to power up the whole building, the building is predicted to feed 573,674.77 kWh of electricity into the grid and produce 3,525,955.51 kWh of excess cold energy in a year. The feed-in tariff (FiT) was introduced by the government of Malaysia to encourage the utilisation of renewable energy by enabling any individuals or non-individual that hold Feed-in Approval Holders (FIAHs) to employ renewable energy generation systems. The amount of electricity from the renewable energy being fed into the grid will be paid by the Distribution Licenses (DLs) based on the FiT assigned by the government [222]. As of 22nd May 2016, FiT for solar PV is listed in Table 82. It is estimated that the building will generate RM 429,108.73 a year by selling the produced electricity to the grid at RM0.748 per 1kWh rate. Since the CHP solar system is installed on the building's rooftop which enables the FIAH to get additional bonus price of RM 0.155 per 1 kWh besides a fixed energy price of RM 0.593.

A system that enables a private institution to sell cold energy does not yet exist. However, if buildings widely employ the CHP solar system, a possibility to create the same system which allows an approved vendor to sell cold energy (as a form of chilled water) might surface in the future. Currently, the chilled water is provided by a Gas District Cooling (GDC) company that charges RM 0.248 per 1 kWh and the maximum demand charge of RM114.33 per 1 kWh. If the same tariff is used, the building could sell the chilled water to the neighbouring buildings for the

total price of RM 874,436.97 a year. This calculation does not include maximum demand charges.

Table 81: The summary of the suggested retrofitting.

Method	Clean on-site energy (kWh)	Electricity fed into the grid (kWh)	Cold energy fed into the grid (kWh)	Cooling load reduction (kWh)	Cooling load reduction (%)	Total retrofit cost (RM)	Energy reduction cost (RM/kWh)	Payback period (Year)
Initial	-	-	-	-	-	-	-	-
Operation	-	-	-	511920	12.5	0	0	0
Lighting	-	-	-	944876	23.1	3,229,262.90	0.190	3.5
Glazing	-	-	-	128059	3.1	2,137,560.80	0.417	45.7
Equipment	-	-	-	141216	3.5	n/a	n/a	n/a
PCM	-	-	-	993900	26.9	2320890	0.058	7.3
Insulation	-	-	-	25781	38.0	7687713.7	0.054	6.7
CHP	9,237,446.82	573,674.77	3,531,703.26	-	-	n/a	n/a	n/a

Table 82: The feed into the grid tariff established by Malaysia's government [222].

FiT Rates for Solar PV (Non-individual) (21 years from FiT Commencement Date)	
Description of Qualifying Renewable Energy Installation	**FiT Rates (RM per kWh)**
(i) up to and including 4kW	0.8249
(ii) above 4kW and up to and including 24kW	0.8048
(iii) above 24kW and up to and including 72kW	0.6139
(iv) above 72kW and up to and including 1MW	0.593
(v) above 1MW and up to and including 10MW	0.4651
(vi) above 10MW and up to and including 30MW	0.4162
(b) Bonus FiT rates having the following criteria (one or more):	
(i) use as an installation in buildings or building structures	0.155
(ii) use as building materials	0.1325
(iii) use of locally manufactured or assembled solar PV modules	0.05
(iv) use of locally manufactured or assembled solar inverters	0.05

4.5.4 Summary

Tackling the energy issue based on the core problems proved to be the most effective. This study developed a retrofit method based on the building's energy consumption by focusing on the sectors which used the highest amount of energy that is cooling. The developed method enables a retrofit designers to diagnose parts of the building that contributed the most to the building's heat gain that causes the rise in cooling demand. Passive cooling and solar driven cooling systems are also adopted to reduce the building's dependence on primary energy. From the results, it can be seen that a high-efficiency technology to harness the renewable energy combined with efficient energy management that includes the cooling system and energy storage can highly influence the change in building's landscape to achieve ZECB in the future. The simulated and calculated results after retrofit show that the target building could achieve a net zero energy consumption and also act as a renewable energy provider. Besides the high-energy performance, the simulated results show that the building also satisfies the local indoor environmental quality requirement.

Chapter 5. Actual Retrofit Application on the Target Building

5.1 Introduction

The retrofit methods based on the thermal analysis as suggested in Section 4.2 was proposed to the target building's facility management company for their reference and implementation. The actual implementation took place at different phases within 3 years (from 2013 to 2016) that involves operational schedule, replacement of lamps to LED lamps at certain areas in the building and installation of 94 PV panels on the rooftop. The actual implementation resulted in 299,344.88 kWh energy reduction in two months and an average of 24.15% energy reduction every month. The customer's feedback, detail implementation and energy consumption results are discussed in this chapter.

5.2 Methods

The retrofit procedures based on a thermal analysis published in Section 4.2 were implemented in the target building in 2013. The results were presented to the building's owner and the building's energy manager for their evaluation and future reference. The retrofit process taken place is simplified in Figure 112. The strategies were implemented by the building's facility management company and the building's owner in different phases depending on the time required implementing the strategies, the practicality of replacing the old equipment and lamps and the budget allocation. The strategies were modified based on the feedback given by the occupants and also their budget allocation. The list of the retrofit strategies suggested in Section 4.2 and the retrofit strategies applied by the building's owner are summarised in Table 83.

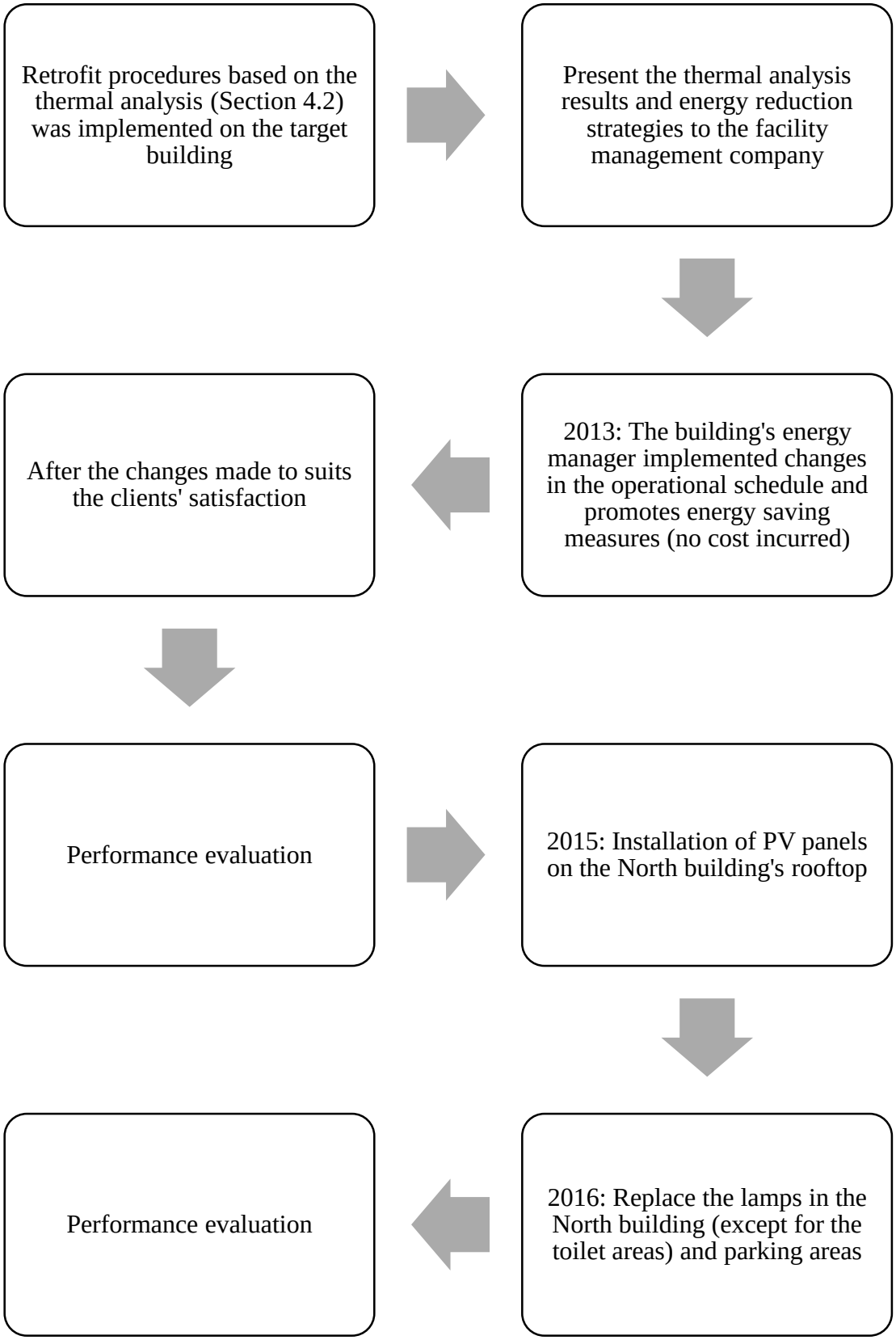

Figure 112: The actual retrofit process implemented on the target building.

Table 83: The list of the retrofit strategies suggested in Section 4.2 and the retrofit strategies applied by the building's owner.

	Suggested	Implemented
Operation	• Air condition air temperature is set to 24 °C and scheduled to operate from 0730 to 1730 (see Figure 113). • Lighting systems in office zones were set to 0730 to 1800.	• Air condition air temperature was set to 24 °C. The system was switched on at 0700 to 1300 and 1400 to 1800 every workday. When a special occasion took place, the air condition will be switched on from 0700 to 1800. • The lighting system in the office zones was switched on from 0700 to 1800 and switched off during the recess hour. However, the occupants can manually control the lighting. • The implementation took place in 2013.
Lighting	• A lighting system that includes automatic daylight dimmer in corridors and office zones as well as replacing existing lamps with high-efficiency LEDs [52]. • Luminance in the office zones was adjusted to 300 lux by the recommendations from previous studies [47] and MS1525:2007 [62]. • Lighting operating schedule was proposed to accommodate the employees when the area is occupied (i.e. 0730 hours to 1800 hours).	• Some of the lamps in the corridors were removed leaving 4 lamps in each corridor to match the suggested luminance for the corridors (100 lux). • All lamps in the north building were replaced with LEDs except for the toilet areas. • The lighting system in the office zones was switched on from 0700 to 1900. However, the occupants can manually control the lighting. • The implementation took place at the end of January 2016.
Renewable energy	• Solar panels with 15% efficiency proposed to be installed on the South building's roof utilising 3,681 m² area. The generated electricity was proposed to directly supply to the building and stored in a battery.	• 94 PV panels (24.44 kWp) were installed in the north building. • The implementation took place in 2015.

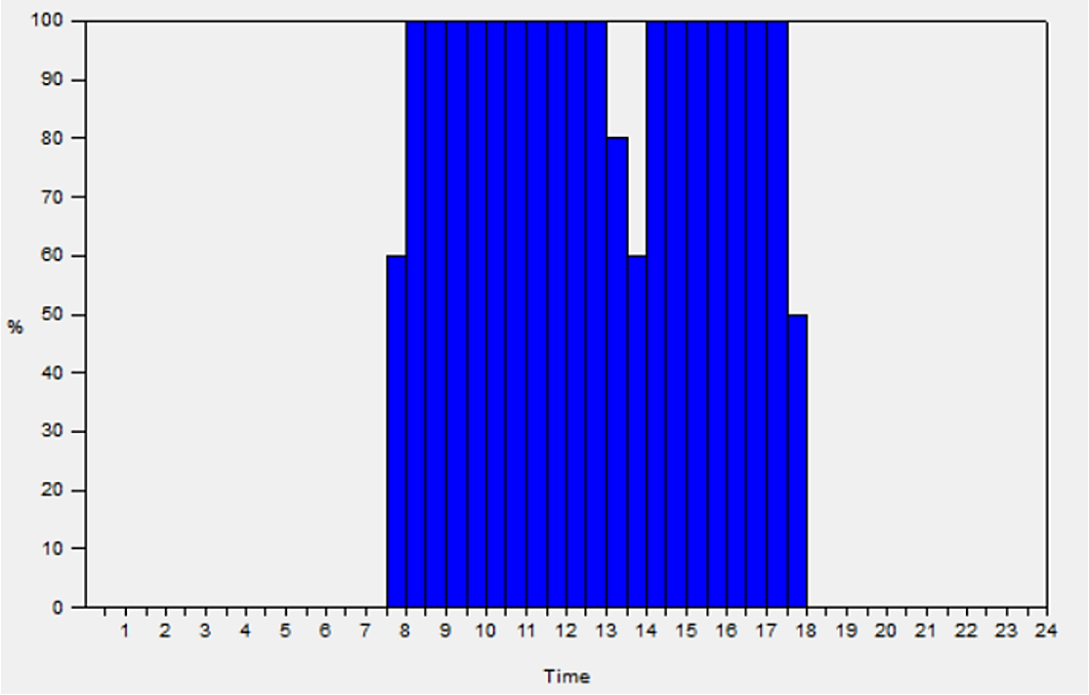

Figure 113: Modified cooling operation schedule for office zones from the Design Builder software (hourly cooling load percentage).

The selected retrofit strategies were fully installed at the end of January 2016. The changes were made at different phases. The actual retrofit started with the shifts in the operational schedule in 2013, then followed by the installation of PV panels on the North building's rooftop in May 2015 and the replacement of the lamps in the North building (except for toilets) and parking areas to LEDs at the end of January 2016. Figure 114 shows the image of the PV panels installed on the target building's rooftop and Figure 115 shows the inverters used for the solar energy generation system. These pictures were taken during a field visit in May 2015.

Figure 114: The PV panels installed on the target building's rooftop.

Figure 115: The inverters for the solar energy generation system.

All the strategies implemented by the building's owner were applied to the base building model. The simulated building's energy in February and March 2016 is then compared to the building's actual energy data that were gathered from the building's energy manager. Equations (5.1) to (5.4) were used for the calculation.

$$Er_{(actual)} = Ec_{(2012)} - Ec_{(2016)} \quad (5.1)$$

$$Er_{(estimated)} = Ec_{(simulated\ 2012)} - Ec_{(simulated\ 2016)} \quad (5.2)$$

$$Percentage\ Er = Er / Ec_{(2012)} \quad (5.3)$$

$$Percentage\ Er_{(estimated)} = Er_{(estimated)} / Ec_{(simulated\ 2012)} \quad (5.4)$$

Where:

Energy reduced (Er)

Energy consumption (Ec)

5.3 Results and Discussion

This section is presented in three different sections that are Section 5.3.1 (total energy reduction), Section 5.3.2 (generated solar energy), Section 5.3.3 (lighting system), Section 5.3.4 (changes in the operation schedule) and Section 5.3.5 (other discussion).

5.3.1 Total energy reduction

The estimated energy reduction based on the simulation results for February and March are 102,691.42 kWh (19.73% estimated energy reduction) and 129,085.83 kWh (19.99% estimated energy reduction). The actual energy reduction achieved by the building after retrofit was 132,506.15 kWh in February and 166,828.73 kWh in March. The average differences in the estimated energy reduction and the actual energy reduction every month is 33,778.82 kWh and the average difference in the percentage energy reduction is 4.29%. This result is in agreement with the results published earlier which compared the energy reduction after operational changes implemented by the building's owner [38]. The comparison of the actual and estimated energy reduction is shown in Table 84.

Table 84: The comparison of the actual and estimated energy reduction.

Month	Energy reduction (kWh)		Energy reduction (%)	
	Simulated	Actual	Simulated	Actual
Feb	102,691.42	132,506.15	19.73%	23.49%
March	129,085.83	166,828.73	19.99%	24.81%

Meanwhile, the simulated total energy consumption in February is 1.9% lower than the actual energy consumption, and the simulated total energy consumption in March is 3.4% higher than the actual energy consumption. The difference in the estimated energy reduction and the actual energy reduction achieved is mainly originated from the deviation in the base model's energy consumption where the model has 1.89% (138,985 kWh) lower energy consumption compared to the actual energy consumption in 2012 and the actual amount of electricity generated by the PV system. The mean bias error (MBE) between the simulated and actual energy consumption is shown in Table 85.

Table 85: The mean bias error (MBE) between the simulated and actual energy consumption.

Month	Energy consumption (kWh)		MBE
	Simulated	Actual	
Feb-12	520383.39	563991.82	7.73%
Feb-16	417691.97	431485.67	3.20%
Mar-12	645808.84	672395.03	3.95%
Mar-16	516723.01	505566.29	-2.21%

5.3.2 Renewable energy generation

The solar panels were installed by the Malaysia's Sustainable Energy Authority (SEDA), a statutory body under the Ministry of Energy, Green Energy and Water as part of their 'PV Installation on the Government Buildings in Putrajaya' project. It was not part of the project that was handled by the facility management company. Hence, the specification of the PV panels and the generated energy data for the whole duration since it was first installed could not be accessed. However, the solar panels performance was directly connected to an equipment (see Figure 116) that displays the daily generated solar energy in a different month. The equipment was located in the building's lounge nearby the entrance to educate and alert the occupants about sustainable

energy. The data taken from the display screen during a field visit in the afternoon on the 6th of May 2015 is compared to the simulated data. The comparison graph of the generated electricity for 1st to the 5th May is shown in Figure 117. As told by the energy manager and SEDA's officer (Mr. Al-Fadzriq) the generated electricity from these solar panels were fully utilized by the building without being fed into the grid.

Figure 116: Direct display of the building's daily electricity generated by the PV panels.

The actual specifications of the PV panels were not provided by the building's owner, hence, the efficiency of the PV panels were set to a range of typical solar panel's efficiency. To predict the PV panels' efficiency, a number of simulations were carried out by varying the PV panels' efficiency from 9% to 15%. The results suggested that PV panels' with 9.5% efficiency matches the actual electricity generated by the PV panels installed on the building's rooftop (see Figure 117). It can be observed that the efficiency of the PV panels might have varied throughout the

day. It is worth noting that in May, West-Coast Malaysia received heavy rainfall due to the South-West monsoon [155]. This weather condition (heavy rainfall and could cover) might have caused reduction in solar radiation. Other possible reason is the fluctuation in PV cell's temperature that has influenced the PV panels' efficiency. As the outside air temperature increases, the PV cells also increases which leads to the declination of the PV cells' efficiency [201]. Hence, installing a MCPV will be more efficient for a hot and humid country such as Malaysia since the temperature of the PV cells can be cooled down by the coolant outlet which in return will retain the efficiency of the PV cells. Plus, the MCPV has higher efficiency for thermal and electric generation.

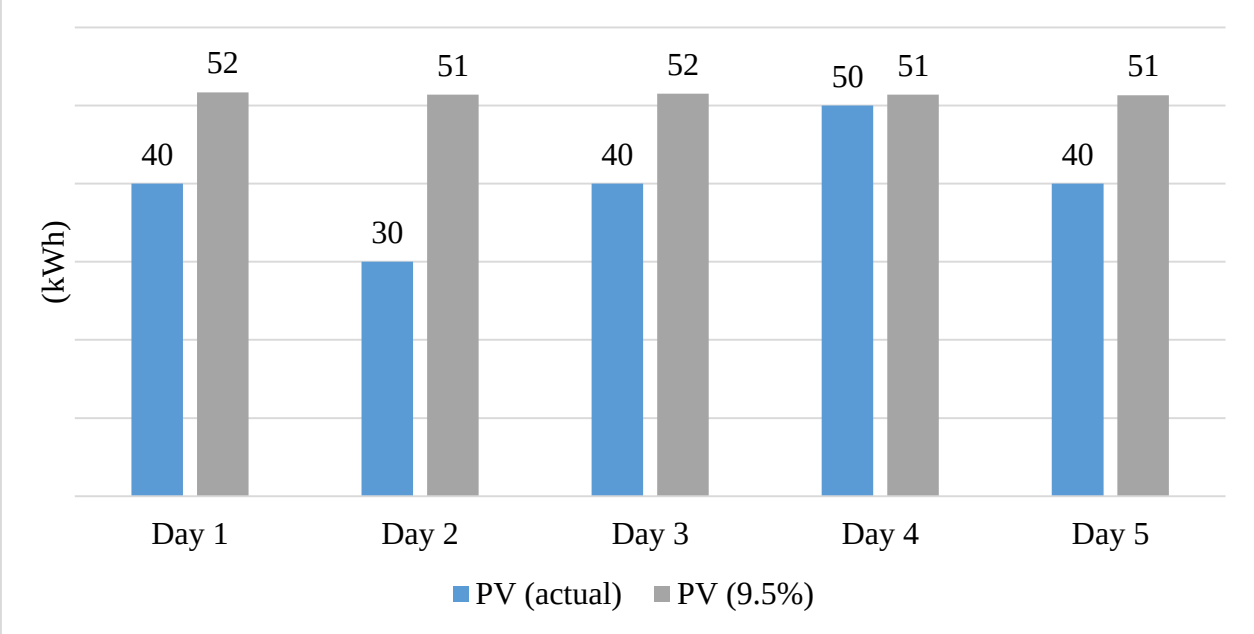

Figure 117: The actual and simulated electricity generated by PV panels in early May.

5.3.3 Lighting system

Pictures of the lift lounge that has been installed with new LED lamps at the north building and one with fluorescent lamps at the South building were taken during a visit in May 2015 (see Figure 118) to compare the differences in the illumination level. Whereas another picture of the cafeteria in the north building taken in 2012 (before retrofit) and 2015 (after retrofit) is shown in Figure 119.

It can be seen that the installed LED lamps gave a better luminance compared to the previous lamp types. This is because the LEDs have a higher luminous efficacy. Hence, it generates more light at the same power input compared to the fluorescent lamps. Another point to note is the number of halogen lamps used in the cafeteria after retrofit were reduced since the illumination provided by the ceiling's indirect lighting from the LED lamp are sufficient to provide the required illumination level (200 lux). Therefore, besides reducing the energy consumption, LED lamps also gives a better indoor lighting quality to the occupants. However, the efficiency of the lighting system can be further enhanced with the application of the daylight dimmer that enables the lighting system to adjust its luminous output automatically according to the daylight received by the room.

Figure 118: Pictures of the lift lounge that has been installed with new LED lamps at the north building (left) and one with fluorescent lamps at the South building (right), taken during a visit in May 2015.

Cafeteria before retrofit

Cafeteria after retrofit

Figure 119: The cafeteria in the north building taken in 2012 (before retrofit) and 2015 (after retrofit).

5.3.4 Changes in the air condition settings

Changes in the operational schedule were implemented in two phases, the first one was in 2013 and then in 2014. In 2013, the energy manager changed the air conditioning operation schedule from 0630 - 1900 to 0700 - 1900, and raised the air temperature set point in the offices from 23°C to 24° and finally 25°C. No negative feedback was received when the temperature was raised from an average of 22.5°C to 24°C. However, when the air temperature was raised to 25°C, negative feedback was received from the occupants. Hence, the air conditioning set point temperature was set to 24°C to satisfy clients' thermal comfort.

In 2014, the building's owner made another change in the air conditioning operation schedule, where the air conditioning was switched off during the recess time (1300 to 1400) since the offices are mostly vacant during this time. It is worth mentioning here that it is a culture for the Malaysian government employees to spend their time outside during the recess time spent mainly visiting the cafeteria or nearby restaurants. During the first few days of the changes being implemented, some complaints were made, but after a week, the occupants had adjusted to the changes and no negative feedback was received afterwards. The changes in the air conditioning schedule have been used since 2014 up to now.

An analysis of the simulated offices' temperature and relative humidity ranged in between 35% to 70% during the recess hour which shows that the air temperature varied between 28°C to 34.5°C during the recess hour. This simulation result does not consider the possibility of having natural ventilation (if the occupants opened the windows). The simulated temperature and relative humidity in the ground floor office during recess hour (1300 to 1400) are shown in Figure 120. While the simulated temperature and relative humidity in other offices can be found in Appendices B. Plus, it is possible to open the windows if the occupants feel uncomfortable. So this could explain why there is no complaint received from the occupants even though the air conditioning was switched off during the recess hour.

A comparative analysis of the preferred air temperature and the PMV sensation was carried out (see Figure 121). Even though the air temperature was fixed at 24°C, PMV values varied depending on four other factors (metabolism, clothing, humidity, mean radiant temperature and air velocity). The PMV values (when the air conditioned was in operation) varied in between 0.65

to 1.8. High PMV values are spotted after recess hour (1400 to 1500). Meanwhile, the PMV values from 0900 to 1300, and 1500 to 1800 were in the range of 0.65 to 1.35. Based on the P.O Fanger sensation scale, the values lingers around slightly warm and slightly exceeds the comfort range ($-1 \leq PMV \leq +1$). This is aligned with the findings from the previous studies on thermal comfort in offices and classrooms in tropical regions. Authors reported that the thermal neutrality was 24.7°C to 26.2°C. While the preferred temperature in summer varied in between 22.9°C to 28°C [159]. Findings from Chen and Chang (Singapore) and S.Yatim et al. (Malaysia) also reported that the occupants thermal sensation vote were different from the PMV sensation scale. The occupants in both case studies perceived neutral sensation in the PMV scale (-0.5 to +0.5) as slightly cool [156] and too cold [157]. The finding from this study also confirmed to the previous discoveries that the sensation scale for the occupants from tropical regions is more lenient towards warmer temperature [156][157][159]. The occupants might have adapted to warm climate which resulted in the differences.

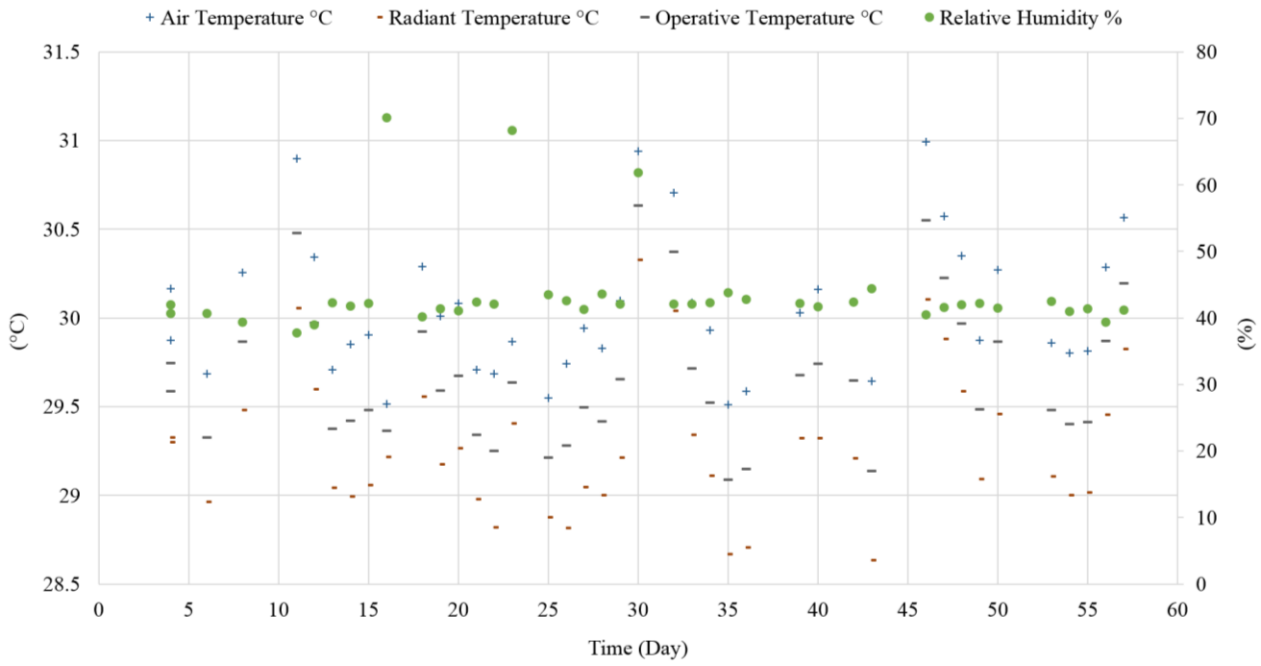

Figure 120: The simulated temperature and relative humidity in the office at the ground floor during recess hour (1300 to 1400).

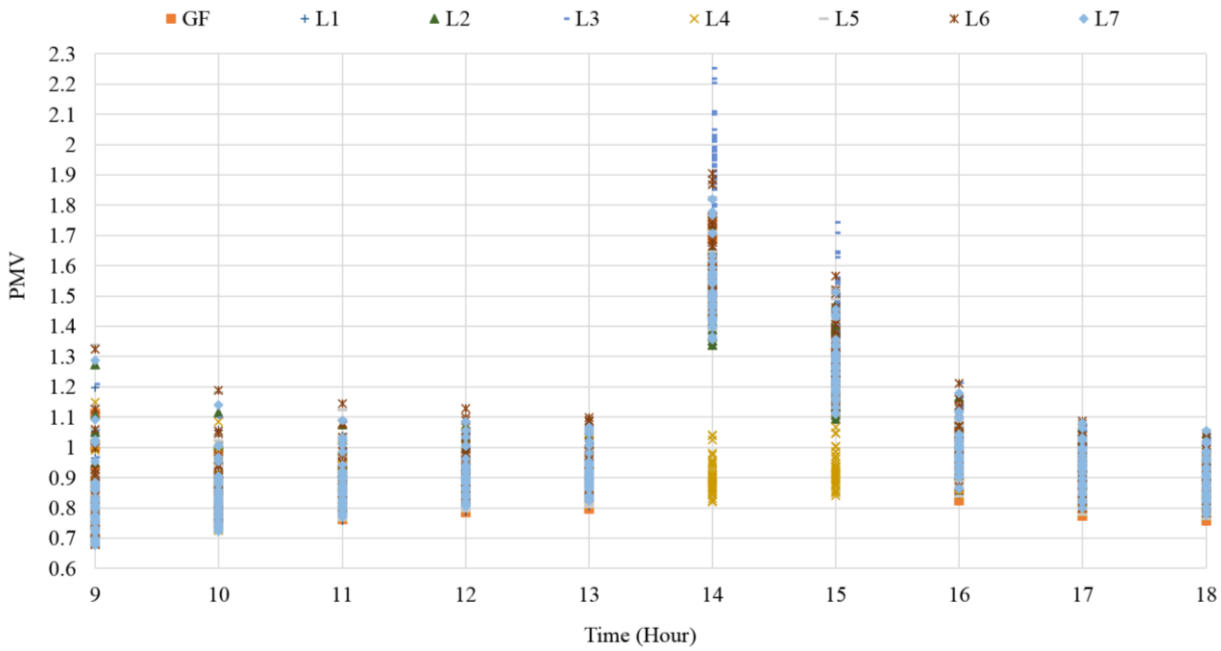

Figure 121: The hourly PMV values in the offices during office hours in workdays (February to March).

5.3.5 Other discussion

Based on the retrofit approach taken by the target building's owner (Ministry of Federal Territory, Malaysia), it can be presumed that budget and feasibility play a significant role in their decision making. The building's owner has been progressively making effort and changes in reducing the building's energy consumption. The retrofit process took place at different phases since 2013 to now (2016). Instead of making a full renovation at a time which will distract their daily operation, the installation process for the lamps' replacement to LEDs took place at difference phases. The building owner opted to install the retrofit strategies that does not involve any cost first then followed by the one with least cost. This is in agreement with the estimated cost analysis per energy reduction (in Section 4.2) where the operational changes are the most cost optimum (no additional cost) then followed by changes in the lighting system (GBP 0.96 per 1 kWh energy reduction).

Moreover, the lamps were only replaced once they have reached their lifetime. It can be observed that instead of changing PL-C and PL-L to LEDs with the same lamp type, the energy manager opted to remove the older PL-C and PL-L lamp types to T8 LED tubes installed as indirect

lighting on the ceilings. This is because the T8 LED tubes are more economical compared to LED PL-C lamp even though the T8 LED range offers a higher lumen output. A comparison of different lamp types is listed in Table 86.

Table 86: A comparison of different lamp types [192].

Lamp type	Power rating W	Lumen output lumen	Current market price GBP	Lifetime hours
PL-C	18	n/a	1.55	10,000
PL-L	36	n/a	2.28	10,000
PL-C LED (replacement for PL-C 18W)	6.5	650	14.96	30,000
T8 LED	9	1470	6.62	30,000
T8 LED	18	1850	10.8	30,000

The building owner does have the interest to reduce their energy consumption. However, it is mainly for the benefit of reducing their running cost (energy bills) and the enforcement made by Parliament. In a commercial world, profit is perceived as more important than the social responsibility unless there is enforcement by the government or the society. Hence, the payback period and the cost of the retrofitting must align with their budget, and the feasibility to carry out the retrofit work is their top priority so it will not distract their daily operation.

5.4 Summary

The retrofit method based on the thermal analysis to reduce cooling load as suggested in Section 4.2 has been applied on the target building and the post-retrofit feedback gathered shows a clients' satisfaction and a reduction of 299,344.88 kWh in the energy consumption in two months after the installation. The actual percentage of energy reduction is 5.3% more than the estimated percentage energy reduction attained from the simulation results. The differences are originated from the deviation in the base model constructed in the software. It is hoped that the target building will implement the methods suggested in Section 4.1 and 4.3 in the future once those methods are proposed to them later.

Chapter 6. Conclusion and Future Work

This thesis has presented a detailed investigation into the retrofit methods for a typical medium-sized commercial office building located in tropical climate. This work considered the impact on the building's energy consumption, indoor environment (IAQ, IVQ, and ITQ) and basic cost analysis. The results from the simulation work were compared to the actual retrofit application.

This study started with three main questions that are:

- What is the thermal pattern of typical medium-sized commercial office buildings in a tropical climate?
- What are the suitable criteria for buildings in hot regions to reduce the building's HVAC demand?
- What is the best retrofit approach to achieve ZEB for this type of building?

The answers to these questions were discovered throughout the study. The findings will be recapped and evaluated to summarise them in one piece, and in a broad-spectrum (presented in Section 6.1). The recommendation for future work will be presented in Section 6.2.

6.1 Conclusion

Retrofit methods for an existing commercial office building in a tropical country have been studied. A comprehensive energy audit was carried out to map out building's energy consumption (detail in Chapter 3). Outcomes from this study confirm the findings from foregoing studies related to the building's energy consumption, where most of the buildings, despite the climatic condition, spent most of the energy to deliver a good indoor comfort for the occupants (IAQ, IVQ, and ITQ). The case-study building spent an average of 238.53 kWh/m²/year (from 2009 to 2012) with 87.5% of the total energy consumption in 2012 was spent on providing indoor comfort to the occupants. HVAC system's energy intensity alone was 128 kWh/m²/year in 2012. This finding is in agreement with the outcomes from former studies that more than 50% of total building's energy were spent on HVAC system.

Based on this discovery, retrofit methods to achieve zero energy building was developed through a combination of building's energy audit (Chapter 3), computer-based analysis (Chapter 4) and actual implementation of the proposed methods (Chapter 5). A well-known method called Passivhaus concept has been widely used in cold climate regions and has managed to achieve nZEB. The main principal used by Passivhaus method was to reducing HVAC load by decreasing heat loss through building's envelope. Taking the same principal, this study investigates the most effective building's envelope for buildings in cooling dominated country (Section 4.1) to reduce its dependency on HVAC system and lighting system. A retrofit approach was also developed to reduce building's heat gain from the main sources (Section 4.2). Combining the findings from Section 4.1 and Section 4.2, it can be concluded that for buildings in tropical climate regions, different construction criteria deemed to be more suitable to reduce the building's dependency on HVAC system and artificial lighting. As opposed to buildings in cold regions, the building's heat gain in a hot region needed to be removed from a building as to attain a good thermal comfort. Meanwhile, in cold regions, the building's construction was aimed to retain heat and reduce heat loss. The requirement for HVAC system such as cooling in tropical regions arose due to the accumulation of heat gain which increases the air temperature and the changes in the moisture content in the air. Studying the heat gain sources in a building (detail in Section 4.2) enables us to discover that these heat gains are highly dependent on the building's structure and sub-systems. In this study, the heat gain in the office rooms in the case-study building mainly emitted by the lighting system (52%) then followed by office equipment (27%), solar heat gain through windows (18%) and occupancy (4%). Hence, the use of high efficient lighting and equipment do not only benefit the energy sector, but indeed, it plays a significant role in reducing a building's heat gain and providing indoor comfort for the occupants.

Besides the internal heat gain, external heat gain also has a major impact on the overall building's cooling load. The external heat gain emanated from solar radiation. However, this solar radiation is also useful to reduce the building's dependency on artificial lighting. For this reason, most of the buildings in the 1990s to the early 2000s mainly opted for a large window to wall design. In this case-study building, it has curtain wall designed where windows to wall ratio in the offices and corridors are 85%. However, the main objective of this design may not result in a fruitful outcome if it is not paired with the automatic dimmer to regulate the lamps' luminance output based on the daylight received in the particular room. Plus, a high amount of solar heat gain

radiated and conducted through the windows will contribute to the buildings' heat gain, which in return, will increase the building's cooling load. It is suggested to use window glass that has a low SHGC value and high VLT value to limit the infrared penetration and allow high visible light penetration into the room to encounter this issue. Meanwhile for the wall construction, high U-value, high thermal mass and airtight is more preferable. Moreover, with the use of PCM material and night time ventilation, the building is capable of naturally removing a significant amount of the heat gain. The building's criteria mentioned above will reduce the building's energy requirement for indoor comfort, particularly for the tropical climate.

Applying the principals mentioned above (detail in Section 4.1 and 4.2), the building is estimated to reduce 52.2% of its primary energy demand and 49.68% reduction in cooling load. This enables the building to be classified as an nZEB. If the same building was to be constructed again but this time including the recommended changes, the estimated building's material, and sub-systems cost is £34,009,027.25. This figure is 5.25% lower than the simulated cost for the baseline building (£35,893,865.00). The building's cost reduction is mainly due to the changes made to the lighting system. This value does not consider the budget for equipment and the CHP solar system.

While, the remaining energy demand from the building can be powered up by solar energy. For this case-study building (a medium to a large sized commercial building), the energy consumption even after the retrofit is still high compared to other building types. Hence, to be fully powered by renewable energy, a mini concentration PV/T (MCPV) system is deemed to be the most suitable for the buildings located in the dense urban areas but are not being shadowed by nearby buildings. The reason is, the MCPV is capable of maintaining optimum efficiency even at a high temperature, and the waste heat can be recycled to power up heat driven chiller. The combined heat power (CHP) MCPV system designed in Section 4.3 was estimated to supply 9,237,446.82 kWh energy a year (thermal energy and electricity). The thermal energy will be used to drive absorption chillers, and the generated electricity will be used to drive electric chillers, pumps for absorption chillers, and building's electricity load. Energy storage is crucial in the design to ensure the energy is adequate at all time (especially during at early morning and night time). Besides supplying energy demand from the building, the CHP MCPV is estimated to generate 573,674.77 kWh excess electricity and 3,531,703 kWh excess cold energy which can be

fed into the grid or supply to neighbouring buildings. Combining all the three methods developed in this study (detail in Chapter 4), the building is estimated to achieve ZEB standard.

Nevertheless, most of the modern commercial office buildings are high rise. This structure limits the solar collection area which can be a drawback for the solar flat plate collector, PV panels, and MCPV if the building's energy consumption is too high. Hence, pairing up the MCPV with concentrating building integrated photovoltaic (CBIPV) can be a good option to this limited roof area. BIPV was not covered in this study. However, it is recommended for future work. The visual summary of the suggested criteria for buildings in tropical climates is illustrated in Figure 122.

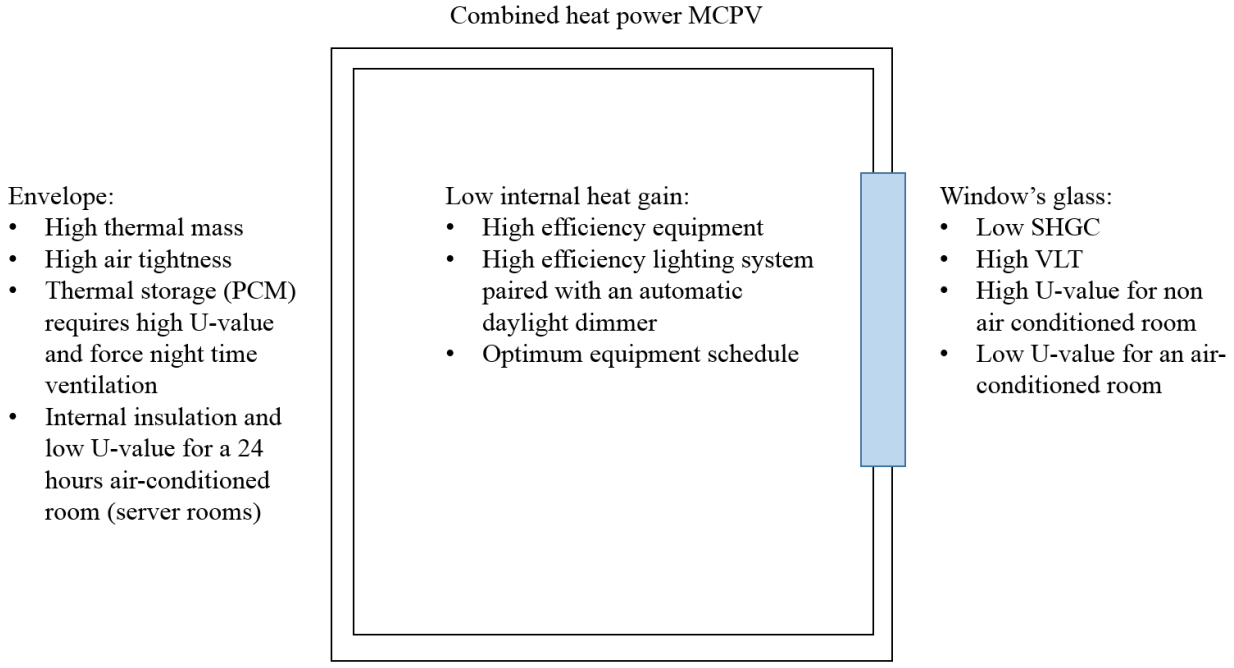

Figure 122: The visual summary of the suggested building's criteria in tropical climates.

Based on the comparison of the actual retrofit application and the simulated results (detail in Chapter 5), it can be concluded that if the base model can be validated, the building simulation software is a reliable tool to predict a building's energy consumption for a retrofit design. One of the reasons that slow down the adoption of green buildings is unstructured decision making in the retrofit process. This study developed a retrofit method based on computer simulations. If the simulation work is included in the retrofit decision-making process before the actual

implementation, it could reduce the take-back effect. This tool could increase stakeholder's confidence to retrofit their buildings if they are exposed to knowing the accuracy of the software tool in predicting a building's energy and indoor environment. Based on the feedback from the stakeholders (the facility management company and energy manager) on the retrofit approach based on thermal analysis developed in Section 4.2, the methods helps them to identify the key areas which require improvement before implementing EEMs for retrofit. This highly helped them in making a high impact retrofit to the building within their budget allocation. It also aids them to understand the main sources of heat gain and be informed about the fact that building's sub-systems such as lighting system and equipment highly contributed towards the enormous cooling load. Though, before the implementation of the proposed EEMs, they do convey their concern about take-back effect and performance gap. However, the actual energy reduction achieved after the implementation has gained their trust in the method used and proved that the building's energy simulation software is a reliable tool to predict building's energy performance and helped to reduce performance gap for retrofit design.

6.2 Recommendations for future work

This thesis has contributed to some fundamental findings in the typical medium-sized commercial buildings in tropical regions. The methods developed in this study are predicted to assist similar type of buildings in achieving ZEB.

(a) This study has contributed to some essential criteria for buildings in tropical regions to reduce its energy dependency. An experimental study on this area is highly recommended especially for a low-rise residential area since these type of buildings use less energy and have lower heat gain, and the impact of passive construction can be very significant. A simpler building type such as a residential building will allow a better analysis of the building's thermal impact which enables the researcher to come out with more concrete evidence. Tropical countries are mainly developing countries while most of the building's regulations were adopted from developed countries that have an entirely different climate. Previous studies have shown that climate contributed to significant differences in the building's behaviour. Therefore, it is hoped that the building's regulations are revised and

developed based on experiment or actual analysis from the local buildings instead of recaptured from other regions.

(b) The simulations made in this study were limited to certain technologies that are available in the software's library. For that reason, it is desirable to include other types of a smart control system in the building (such as the occupancy sensor) and BIPV system.

(c) One of the factors that slow down the adoption of high efficient buildings either as a retrofit or new construction is the lack of exposure to the benefits of employing the green measures. Accordingly, it is suggested to conduct a study to build a database of the building's performance before and after retrofit, and the simulated/expected energy reduction predicted by the simulation work. Public access to this database can increase the public exposure to the benefit of green measures, enhance their confidence on the pre-retrofit simulation designs and the green measures, and educate the retrofit designers on what works and what does not work.

References

[1] S. Prasad, V. Schulte, and P. Bijay, *Global Energy Policy and Security*, vol. 16. 2013.

[2] International Energy Agency, "Resources to Reserve 2013," *New Dir. Youth Dev.*, vol. 2013, no. 140, pp. 5–8, 2013.

[3] Office of The Historian, "Oil Embargo, 1973–1974," *United State of America*, 2016. [Online]. Available: https://history.state.gov/milestones/1969-1976/oil-embargo.

[4] U.S Department of Energy, "TIMELINE OF EVENTS: 1971 TO 1980," *United State of America*, 2016. [Online]. Available: http://energy.gov/management/office-management/operational-management/history/doe-history-timeline/timeline-events-1.

[5] Thomson Reuters, "China's Guangdong faces severe power shortage," *United Kingdom*, 2008. [Online]. Available: http://uk.reuters.com/article/guangdong-power-shortage-idUKL0640101120080306?sp=true.

[6] BBC News, "South Asia's energy crisis demands collective action." [Online]. Available: http://www.bbc.co.uk/news/business-19107372.

[7] H. H. Landsberg, "Energy: the next fifty years.," *Technol. Forecast. Soc. Change*, vol. 18, no. 4, pp. 293–300, 1981.

[8] S. Arrhenius, "On the Influence of Carbonic Acid Air upon the Temperature of the Ground," *Philos. Mag. J. Sci.*, vol. 41, no. page 270, pp. 237–279, 1896.

[9] United Nations Framework Convention on Climate Change (institution), "United Nations Framework Convention on Climate Change," *Germany*, 2016. [Online]. Available: http://unfccc.int/2860.php.

[10] World Meteorological Organisation, "World Climate Conferences," *Geneva, Switzerland*, 2016. [Online]. Available: https://www.wmo.int/pages/themes/climate/international_wcc.php.

[11] European Comission, "European Comission," *Brussels*, 2016. [Online]. Available: http://ec.europa.eu/clima/policies/strategies/index_en.htm.

[12] Macrotrends, "Macrotrends," 2016. [Online]. Available: http://www.macrotrends.net/.

[13] NASA, "Global Temperature," *United State of America*, 2016. [Online]. Available: http://climate.nasa.gov/system/internal_resources/details/original/647_Global_Temperature_Data_File.txt.

[14] United States Environmental Protection, "Global Green House Gas Emission Data," *United State of America*, 2016. [Online]. Available:

https://www3.epa.gov/climatechange/ghgemissions/global.html#three.

[15] British Geological Survey, “What causes the man-made greenhouse effect,” *United Kingdom*, 2016. [Online]. Available: http://www.bgs.ac.uk/discoveringGeology/climateChange/CCS/man-madeEffect.html.

[16] World Energy Council, “World Energy Resources: 2013 survey,” 2013.

[17] The World Bank, “Towards a Sustainable Energy Future for all.” 2013.

[18] International Energy Agency, “International Energy Agency,” 2016. [Online]. Available: http://www.iea.org.

[19] IEA, “WORLD ENERGY OUTLOOK 2014 FACTSHEET How will global energy markets evolve to 2040 ?,” p. 1, 2014.

[20] IEA, “World Energy Outlook 2014 Factsheet - Power and renewables,” p. 1, 2014.

[21] B. C. Publication, “BP Statistical Review of World Energy June 2014 About this review,” no. June, 2014.

[22] The World Bank, “Total Population,” *United State of AmericaUni*, 2016. [Online]. Available: http://data.worldbank.org/indicator/SP.POP.TOTL/countries?page=6&display=default.

[23] Worldometers.info, “Worldometers,” *Dover, Delaware, U.S.A.* [Online]. Available: http://www.worldometers.info/faq/.

[24] United Nation, “United Nation Framework Convention on Climate Change,” *Germany*. [Online]. Available: http://unfccc.int/kyoto_protocol/items/2830.php.

[25] Ren21, “The First Decade: 2004-2014, 10 Years of Renewable Energy Progress,” pp. 2004–2014, 2014.

[26] S. Zaid and P. Graham, “The Need for Energy Efficiency Legislation in Malaysian Building Sector . A Comparative Study of South East Asian Policies,” pp. 1–16, 2009.

[27] IEA, *Transition to sustainable buildings*. .

[28] U.S Department of Energy, “Buildings Data Energy Book,” *United State of America*, 2016. [Online]. Available: http://buildingsdatabook.eren.doe.gov/ChapterIntro1.aspx.

[29] COM(2013) 483, “Report from the Commission to the European Parliament and the Council: Progress by Member States towards Nearly Zero-Energy Buildings,” *Eur. Comm.*, p. Brussels, 2013.

[30] F. P. Birol, “Southeast Asia Energy Outlook,” *World Energy Outlook*, 2013.

[31] U.S. EIA, “The International Energy Outlook 2016,” 2016.

[32] UNEP, “Buildings and climate change: a summary for decision-makers,” *United Nations Environ. Program. Sustain. Build. Clim. Initiat.*, pp. 1–62, 2009.

[33] C. Händel, “Nearly Zero Energy Buildings in Europe,” *Energy*, no. February, pp. 18–22, 2010.

[34] T. Gartner and P. Haves, “High-performance commercial buildings,” *Environ. Energy Technol. Div. News (EETD News)*, vol. 1, no. 3, pp. 1–2, 1999.

[35] F. Zhang, P. Cooke, and A. Studies, “Green Buildings and Energy Efficiency,” no. Figure 2, pp. 1–28, 2013.

[36] L. Pérez-Lombard, J. Ortiz, and C. Pout, “A review on buildings energy consumption information,” *Energy Build.*, vol. 40, no. 3, pp. 394–398, 2008.

[37] W. I. W. Nazi, Y. D. Wang, and T. Roskilly, “Methodologies to Reduce Cooling Load using Heat Balance Analysis: A Case Study in an Office Building in a Tropical Country,” *Energy Procedia*, vol. 75, no. 0, pp. 1269–1274, 2015.

[38] W. I. Wan Mohd Nazi, M. Royapoor, Y. Wang, and A. P. Roskilly, “Office building cooling load reduction using thermal analysis method – A case study,” *Appl. Energy*, 2015.

[39] P. A. Fokaides, E. A. Christoforou, and S. A. Kalogirou, “Legislation driven scenarios based on recent construction advancements towards the achievement of nearly zero energy dwellings in the southern European country of Cyprus,” *Energy*, vol. 66, pp. 588–597, 2014.

[40] W. C. Turner and S. Doty, *Energy Management Handbook*. 2013.

[41] R. Cassidy, “White Paper on Sustainability,” *Build. Des. Constr.*, vol. 11.03, no. November, pp. 1–47, 2003.

[42] B. G. Bilau, “Challenges Green Building,” *Plumb. Mech.*, no. 7, pp. 31–33, 2008.

[43] R. Ruparathna, K. Hewage, and R. Sadiq, “Improving the energy efficiency of the existing building stock: A critical review of commercial and institutional buildings,” *Renew. Sustain. Energy Rev.*, vol. 53, pp. 1032–1045, 2016.

[44] D. Kolokotsa, D. Rovas, E. Kosmatopoulos, and K. Kalaitzakis, “A roadmap towards intelligent net zero- and positive-energy buildings,” *Sol. Energy*, vol. 85, no. 12, pp. 3067–3084, 2011.

[45] United States Environmental Protection, “Green Building,” *United State of America*, 2016. .

[46] M. Barcik, “Defining a Sustainable Building,” pp. 1–22, 1978.

[47] Passive House Institute 2015, “Passive House Definition,” *Germany*, 2015. [Online]. Available: http://passipedia.passiv.de/ppediaen/basics/the_passive_house_-_definition.

[48] Zero Carbon Hub, “Zero Carbon Policy,” *United Kingdom*, 2016. [Online]. Available:

http://www.zerocarbonhub.org/zero-carbon-policy/zero-carbon-policy.

[49] Rolf Disch SolarArchitektur, “Rolf Disch Solar Architecture,” *Germany*, 2016. [Online]. Available: http://www.rolfdisch.de/.

[50] T. V. Esbensen and V. Korsgaard, “Dimensioning of the solar heating system in the zero energy house in Denmark,” *Sol. Energy*, vol. 19, no. 2, pp. 195–199, 1977.

[51] M. Panagiotidou and R. J. Fuller, “Progress in ZEBs-A review of definitions, policies and construction activity,” *Energy Policy*, vol. 62, pp. 196–206, 2013.

[52] (DOE) US Department of Energy, “A Common Definition for Zero Energy Buildings,” no. September, p. 22, 2015.

[53] Z. Szalay and A. Zold, “Definition of nearly zero-energy building requirements based on a large building sample,” *Energy Policy*, vol. 74, no. C, pp. 510–521, 2014.

[54] D. Crawley, S. Pless, and S. Torcellini, “Getting to Net Zero Energy Buildings,” *AHSRAE J.*, no. September, 2009.

[55] P. Torcellini, S. Pless, M. Deru, and D. Crawley, “Zero Energy Buildings: A Critical Look at the Definition,” *ACEEE Summer Study Pacific Grove*, p. 15, 2006.

[56] A. J. Marszal, P. Heiselberg, J. S. Bourrelle, E. Musall, K. Voss, I. Sartori, and A. Napolitano, “Zero Energy Building - A review of definitions and calculation methodologies,” *Energy Build.*, vol. 43, no. 4, pp. 971–979, 2011.

[57] KeTTHA, “Laman Web Rasmi Kementerian Tenaga, Teknologi Hijau dan Air.” 2014.

[58] H. . Xin and S. . Rao, “Active Energy Conserving Strategies of the Malaysia Energy Commission Diamond Building,” *Procedia Environ. Sci.*, vol. 17, pp. 775–784, 2013.

[59] O. Suzer, “A comparative review of environmental concern prioritization: LEED vs other major certification systems,” *J. Environ. Manage.*, vol. 154, pp. 266–283, 2015.

[60] M. J. Berning, “LEED for Existing Buildings,” *Sustain. Facil.*, vol. 33, no. 6, p. 44, 2008.

[61] G. S. D. N. Bhd, J. Tangsi, and K. Lumpur, “Gbi Assessment Criteria Contents,” no. March, pp. 0–57, 2011.

[62] G. R. Tools, “Summary Benchmark,” no. January, 2011.

[63] Green Mark Singapore, “BCA Green Mark for New Residential Buildings,” *BCA Green Mark*, pp. 0–18, 2010.

[64] M. A. Aktacir, O. Büyükalaca, and T. Yılmaz, “A case study for influence of building thermal insulation on cooling load and air-conditioning system in the hot and humid regions,” *Appl.*

Energy, vol. 87, no. 2, pp. 599–607, 2010.

[65] A. Pasupathy, R. Velraj, and R. V. Seeniraj, "Phase change material-based building architecture for thermal management in residential and commercial establishments," *Renew. Sustain. Energy Rev.*, vol. 12, no. 1, pp. 39–64, 2008.

[66] B. Güçyeter and H. M. Günaydın, "Optimization of an envelope retrofit strategy for an existing office building," *Energy Build.*, vol. 55, no. 2012, pp. 647–659, 2012.

[67] C. Y. Jim, "Air-conditioning energy consumption due to green roofs with different building thermal insulation," *Appl. Energy*, vol. 128, pp. 49–59, 2014.

[68] L. Yang and Y. Li, "Cooling load reduction by using thermal mass and night ventilation," *Energy Build.*, vol. 40, no. 11, pp. 2052–2058, 2008.

[69] H. Campaniço, P. Hollmuller, and P. M. M. Soares, "Assessing energy savings in cooling demand of buildings using passive cooling systems based on ventilation," *Appl. Energy*, vol. 134, pp. 426–438, 2014.

[70] D. M. S. Al-Homoud, "Performance characteristics and practical applications of common building thermal insulation materials," *Build. Environ.*, vol. 40, no. 3, pp. 353–366, 2005.

[71] Z. Fang, N. Li, B. Li, G. Luo, and Y. Huang, "The effect of building envelope insulation on cooling energy consumption in summer," *Energy Build.*, vol. 77, pp. 197–205, 2014.

[72] M. . Huang, P. . Eames, and N. . Hewitt, "The application of a validated numerical model to predict the energy conservation potential of using phase change materials in the fabric of a building," *Sol. Energy Mater. Sol. Cells*, vol. 90, no. 13, pp. 1951–1960, 2006.

[73] F. Kuznik, D. David, K. Johannes, and J.-J. Roux, "A review on phase change materials integrated in building walls," *Renew. Sustain. Energy Rev.*, vol. 15, no. 1, pp. 379–391, 2011.

[74] M. K. Nematchoua, C. R. R. Raminosoa, R. Mamiharijaona, T. René, J. A. Orosa, W. Elvis, and P. Meukam, "Study of the economical and optimum thermal insulation thickness for buildings in a wet and hot tropical climate: Case of Cameroon," *Renew. Sustain. Energy Rev.*, vol. 50, pp. 1192–1202, 2015.

[75] D. B. Özkan and C. Onan, "Optimization of insulation thickness for different glazing areas in buildings for various climatic regions in Turkey," *Appl. Energy*, vol. 88, no. 4, pp. 1331–1342, 2011.

[76] S. B. Sadineni, S. Madala, and R. F. Boehm, "Passive building energy savings: A review of building envelope components," *Renew. Sustain. Energy Rev.*, vol. 15, no. 8, pp. 3617–3631,

2011.

[77] S. S. Shrestha, K. Biswas, and A. O. Desjarlais, “A protocol for lifetime energy and environmental impact assessment of building insulation materials,” *Environ. Impact Assess. Rev.*, vol. 46, pp. 25–31, 2014.

[78] F. Ascione, N. Bianco, R. F. De Masi, F. de’ Rossi, and G. P. Vanoli, “Energy refurbishment of existing buildings through the use of phase change materials: Energy savings and indoor comfort in the cooling season,” *Appl. Energy*, vol. 113, pp. 990–1007, 2014.

[79] A. Ucar and F. Balo, “Determination of the energy savings and the optimum insulation thickness in the four different insulated exterior walls,” *Renew. Energy*, vol. 35, no. 1, pp. 88–94, 2010.

[80] H. Sozer, “Improving energy efficiency through the design of the building envelope,” *Build. Environ.*, vol. 45, no. 12, pp. 2581–2593, 2010.

[81] Y. Huang, J. L. Niu, and T. M. Chung, “Study on performance of energy-efficient retrofitting measures on commercial building external walls in cooling-dominant cities,” *Appl. Energy*, vol. 103, pp. 97–108, 2013.

[82] J. Yu, L. Tian, C. Yang, X. Xu, and J. Wang, “Optimum insulation thickness of residential roof with respect to solar-air degree-hours in hot summer and cold winter zone of china,” *Energy Build.*, vol. 43, no. 9, pp. 2304–2313, 2011.

[83] C. a. Balaras, “The role of thermal mass on the cooling load of buildings. An overview of computational methods,” *Energy Build.*, vol. 24, pp. 1–10, 1996.

[84] M. Ozel, “Thermal performance and optimum insulation thickness of building walls with different structure materials,” *Appl. Therm. Eng.*, vol. 31, no. 17–18, pp. 3854–3863, 2011.

[85] R. Saidur, M. Hasanuzzaman, S. Yogeswaran, H. A. Mohammed, and M. S. Hossain, “An end-use energy analysis in a Malaysian public hospital,” *Energy*, vol. 35. pp. 4780–4785, 2010.

[86] R. Saidur, “Energy consumption, energy savings, and emission analysis in Malaysian office buildings,” *Energy Policy*, vol. 37, pp. 4104–4113, 2009.

[87] J. C. Lam, C. L. Tsang, and L. Yang, “Impacts of lighting density on heating and cooling loads in different climates in China,” *Energy Convers. Manag.*, vol. 47, pp. 1942–1953, 2006.

[88] M. Fasiuddin and I. Budaiwi, “HVAC system strategies for energy conservation in commercial buildings in Saudi Arabia,” *Energy Build.*, vol. 43, no. 12, pp. 3457–3466, 2011.

[89] W.-P. Sung, T.-T. Tsai, H.-J. Wang, and M.-J. Wu, “Analysis of energy and carbon dioxide emission caused by power consumption,” *Int. J. ENERGY Res.*, vol. 35, no. 11, pp. 1014–1022,

2011.

[90] T. Hong, H. Kim, and T. Kwak, “Energy-Saving Techniques for Reducing CO 2 Emissions in Elementary Schools,” *J. Manag. Eng. ASCE*, no. January, pp. 39–50, 2011.

[91] I. Iqbal and M. S. Al-Homoud, “Parametric analysis of alternative energy conservation measures in an office building in hot and humid climate,” *Build. Environ.*, vol. 42, no. 5, pp. 2166–2177, 2007.

[92] A. L. Pisello, A. Petrozzi, V. L. Castaldo, and F. Cotana, “On an innovative integrated technique for energy refurbishment of historical buildings: Thermal-energy, economic and environmental analysis of a case study,” *Appl. Energy*, vol. 162, pp. 1313–1322, 2015.

[93] D. Griego, M. Krarti, and A. Hernandez-Guerrero, “Energy efficiency optimization of new and existing office buildings in Guanajuato, Mexico,” *Sustain. Cities Soc.*, vol. 17, pp. 132–140, 2015.

[94] É. Mata, A. S. Kalagasidis, and F. Johnsson, “A modelling strategy for energy, carbon, and cost assessments of building stocks,” *Energy Build.*, vol. 56, pp. 100–108, 2013.

[95] Y. V. Perez and I. G. Capeluto, “Climatic considerations in school building design in the hot–humid climate for reducing energy consumption,” *Appl. Energy*, vol. 86, no. 3, pp. 340–348, 2009.

[96] H. H. Sait, “Auditing and analysis of energy consumption of an educational building in hot and humid area,” *Energy Convers. Manag.*, vol. 66, pp. 143–152, 2013.

[97] Y. Zhang, K. Lin, Q. Zhang, and H. Di, “Ideal thermophysical properties for free-cooling (or heating) buildings with constant thermal physical property material,” *Energy Build.*, vol. 38, no. 10, pp. 1164–1170, 2006.

[98] Pacific Northwest National Laboratory and PECI, “Office Buildings,” no. September, 2011.

[99] Z. Ma, P. Cooper, D. Daly, and L. Ledo, “Existing building retrofits: Methodology and state-of-the-art,” *Energy Build.*, vol. 55, pp. 889–902, 2012.

[100] D. Jenkins and M. Newborough, “An approach for estimating the carbon emissions associated with office lighting with a daylight contribution,” *Appl. Energy*, vol. 84, no. 6, pp. 608–622, 2007.

[101] E. Dascalaki and M. Santamouris, “On the potential of retrofitting scenarios for offices,” *Build. Environ.*, vol. 37, no. 6, pp. 557–567, 2002.

[102] D. Griego, M. Krarti, and A. Hernández-Guerrero, “Energy efficiency optimization of new and

existing office buildings in Guanajuato, Mexico," *Sustain. Cities Soc.*, vol. 17, pp. 132–140, 2015.

[103] S. Chirarattananon and J. Taweekun, "A technical review of energy conservation programs for commercial and government buildings in Thailand," *Energy Convers. Manag.*, vol. 44, pp. 743–762, 2003.

[104] GVA Grimley Ltd, "UK Offices : Refurbishment vs. redevelopment," 2010.

[105] EU, "Directive 2010/31/EU of the European Parliament and of the Council of 19 May 2010 on the energy performance of buildings (recast)," *Off. J. Eur. Union*, pp. 13–35, 2010.

[106] S. Burton, *energy efficient office refurbishment*. James & James, 2001.

[107] Y. Shao, P. Geyer, and W. Lang, "Integrating requirement analysis and multi-objective optimization for office building energy retrofit strategies," *Energy Build.*, vol. 82, pp. 356–368, 2014.

[108] C. Rocky, "Guide to Building the Case for Deep Energy Retrofits," 2012.

[109] ASHRAE, *Advanced Energy Design Guide for Small to Medium Office Buildings*. 2014.

[110] J. Park and T. Hong, "Maintenance management process for reducing CO2 emission in shopping mall complexes," *Energy Build.*, vol. 43, no. 4, pp. 894–904, 2011.

[111] J. Zhao, N. Zhu, and Y. Wu, "The analysis of energy consumption of a commercial building in Tianjin, China," *Energy Policy*, vol. 37, no. 6, pp. 2092–2097, 2009.

[112] S. M. Silva, P. P. Silva, M. Almeida, and L. Bragança, "Operative Conditions Evaluation for Efficient Building Retrofit—A Case Study," *Indoor Built Environ.*, vol. 22, no. 5, pp. 724–742, 2013.

[113] D. Gossard, B. Lartigue, and F. Thellier, "Multi-objective optimization of a building envelope for thermal performance using genetic algorithms and artificial neural network," *Energy Build.*, vol. 67, pp. 253–260, 2013.

[114] E. Asadi, M. G. da Silva, C. H. Antunes, and L. Dias, "A multi-objective optimization model for building retrofit strategies using TRNSYS simulations, GenOpt and MATLAB," *Build. Environ.*, vol. 56, pp. 370–378, 2012.

[115] K. Parrish and C. Regnier, "Proposed Design Process for Deep Energy Savings in Commercial Building Retro fit Projects," vol. 19, no. June, pp. 71–80, 2013.

[116] M. Ferreira, M. Almeida, A. Rodrigues, and S. M. Silva, "Comparing cost-optimal and net-zero energy targets in building retrofit," *Build. Res. Inf.*, vol. 3218, no. December, pp. 1–14, 2014.

[117] J. Park and T. Hong, “Maintenance management process for reducing CO2 emission in shopping mall complexes,” *Energy Build.*, vol. 43, no. 4, pp. 894–904, 2011.

[118] P. Heiselberg, H. Brohus, A. Hesselholt, H. Rasmussen, E. Seinre, and S. Thomas, “Application of sensitivity analysis in design of sustainable buildings,” *Renew. Energy*, vol. 34, no. 9, pp. 2030–2036, 2009.

[119] R. Andarini, H. Schranzhofer, W. Streicher, and a. K. Pratiwi, “Thermal simulation and cooling energy sensitivity analysis of a typical shophouse in Jakarta, Indonesia,” *Build. Simul.*, pp. 1887–1893, 2009.

[120] Y. Yıldız and Z. D. Arsan, “Identification of the building parameters that influence heating and cooling energy loads for apartment buildings in hot-humid climates,” *Energy*, vol. 36, no. 7, pp. 4287–4296, 2011.

[121] T. Hong, M. A. Piette, Y. Chen, S. H. Lee, S. C. Taylor-Lange, R. Zhang, K. Sun, and P. Price, “Commercial Building Energy Saver: An energy retrofit analysis toolkit,” *Appl. Energy*, vol. 159, pp. 298–309, 2015.

[122] A. C. S. Aun., “Green Building Index – MS1525 Applying MS1525:2007 Code of Practice on Energy Efficiency and Use of Renewable Energy for Non-Residential Buildings,” pp. 1–22, 2009.

[123] M. C. Dubois and Å. Blomsterberg, “Energy saving potential and strategies for electric lighting in future north european, low energy office buildings: A literature review,” *Energy Build.*, vol. 43, pp. 2572–2582, 2011.

[124] P. Xu, J. Huang, P. Shen, X. Ma, X. Gao, Q. Xu, H. Jiang, and Y. Xiang, “Commercial building energy use in six cities in Southern China,” *Energy Policy*, vol. 53, pp. 76–89, 2013.

[125] AccuWeather Inc., “AccuWeather.com,” *United State of America*, 2016. [Online]. Available: http://www.accuweather.com/.

[126] USA Environmental Protection Agency, “Heating, Ventilation and Air-Conditioning Systems, Part of Indoor Air Quality Design Tools for Schools,” *United State of America*, 2016. [Online]. Available: https://www.epa.gov/iaq-schools/heating-ventilation-and-air-conditioning-systems-part-indoor-air-quality-design-tools.

[127] B. W. Olesen, “International standards for the indoor environment,” *Indoor Air*, vol. 14, no. 7, pp. 18–26, 2004.

[128] The Chartered Institute of Architectural Technologists: CIAT, “Air conditioning systems.,” vol.

1.0, pp. 1–68, 2006.

[129] B. L. Ahn, C. Y. Jang, S. B. Leigh, S. Yoo, and H. Jeong, “Effect of LED lighting on the cooling and heating loads in office buildings,” *Appl. Energy*, vol. 113, pp. 1484–1489, 2014.

[130] Whole Building Design Guide, “Provide Comfortable Environments,” *United State of America*, 2016. [Online]. Available: https://www.wbdg.org/design/provide_comfort.php.

[131] Department of Occupational Safety and Health, “Guidelines on Occupational Safety and Health in the Office,” 1996.

[132] Green Building Index Sdn Bhd, “Green Building Index,” *Malaysia*, 2016. [Online]. Available: http://new.greenbuildingindex.org/.

[133] US Green Building Council, “US Green Building Council,” *United State of America*, 2016. [Online]. Available: http://www.usgbc.org/leed.

[134] Green Building Council Indonesia, “Rating Tools,” *Indonesia*, 2016. [Online]. Available: http://www.gbcindonesia.org/greenship/rating-tools.

[135] Building and Construction Authority, “BCA GREEN MARK ASSESSMENT CRITERIA AND ONLINE APPLICATION,” *Singapore*, 2016. [Online]. Available: https://www.bca.gov.sg/GreenMark/green_mark_criteria.html.

[136] U.S. Department of Health & Human Services, “The National Institute for Occupational Safety and Health (NIOSH),” *United State of America*, 2016. [Online]. Available: http://www.cdc.gov/niosh/topics/indoorenv/.

[137] US Green Building Council, “Green Building 101: What is indoor environmental quality?,” *United State of America*, 2016. [Online]. Available: http://www.usgbc.org/articles/green-building-101-what-indoor-environmental-quality.

[138] P. O. Fanger, “Assessment of thermal comfort practice,” *Occup. Environ. Med.*, vol. 30, pp. 313–324, 1973.

[139] ASHRAE, “The Standards For Ventilation And Indoor Air Quality,” *United State of America*, 2016. [Online]. Available: https://www.ashrae.org/resources--publications/bookstore/standards-62-1--62-2.

[140] B. W. Olesen, “Indoor environmental input parameters for the design and assessment of energy performance of buildings . Contents,” *REHVA J.*, pp. 1–8, 2015.

[141] DOSH, “Industry Code of Practice on Indoor Air Quality,” *Minist. Hum. Resour. Dep. Occup. Saf. Heal.*, pp. 1–50, 2010.

[142] I. A. Izdihar, “MS 1525,” 2014.

[143] Department of Standard Malaysia, *Malaysia Standard: Code of Practice on Energy Efficiency and Use of Renewable Energy for Non-Residential Buildings*. Department of Standards Malaysia, 2007.

[144] Canadian Centre for Occupational Health and Safety, “Indoor Air Quality - General,” *Canada*, 2016. [Online]. Available: http://www.ccohs.ca/oshanswers/chemicals/iaq_intro.html.

[145] American Industrial Hygiene Foundation, “Improving Indoor Air Quality at Work,” *United State of America*, 2016. [Online]. Available: https://www.aiha.org/about-aiha//AIHFoundation/Pages/default.aspx.

[146] Health and Safety Executive of United Kingdom, “Lighting at Work,” 1997.

[147] G. On, “office ergonomics.”

[148] Autodesk® Sustainability Workshop, “Measuring Light Levels,” 2016. [Online]. Available: http://sustainabilityworkshop.autodesk.com/about-us.

[149] ASHRAE, “Standard 55,” *United State of America*, 2013. [Online]. Available: by American Society of Heating, Refrigerating and Air-conditioning Engineers.

[150] Y. Yau and B. Chew, “A review on predicted mean vote and adaptive thermal comfort models,” *Build. Serv. Eng. Res. Technol.*, vol. 35, no. 1, pp. 23–35, 2012.

[151] P. O. Fanger, *Thermal comfort : analysis and applications in environmental engineering*. .

[152] B. . Olesen, *Thermal Comfort*, vol. 2. 1982.

[153] P. . Fanger, *Thermal Comfort*, 2nd ed. Robert E. Krieger Publishing Company Malabar, Florida, 1982.

[154] A. A. Chowdhury, M. G. Rasul, and M. M. K. Khan, “Thermal-comfort analysis and simulation for various low-energy cooling-technologies applied to an office building in a subtropical climate,” *Appl. Energy*, vol. 85, no. 6, pp. 449–462, 2008.

[155] L. Yang, H. Yan, and J. C. Lam, “Thermal comfort and building energy consumption implications - A review,” *Appl. Energy*, vol. 115, pp. 164–173, 2014.

[156] S. R. M. Yatim, M. A. M. M. M. Zain, F. M. Darus, and Z. S. Ismail, “Thermal comfort in air-conditioned learning environment,” *3rd ISESEE 2011 - Int. Symp. Exhib. Sustain. Energy Environ.*, no. June, pp. 194–197, 2011.

[157] A. Chen and V. W. C. Chang, “Human health and thermal comfort of office workers in Singapore,” *Build. Environ.*, vol. 58, pp. 172–178, 2012.

[158] N. D. Dahlan and Y. Y. Gital, “Thermal sensations and comfort investigations in transient conditions in tropical office,” *Appl. Ergon.*, vol. 54, pp. 169–176, 2016.

[159] S. C. Sekhar, “Thermal comfort in air-conditioned buildings in hot and humid climates - why are we not getting it right?,” *Indoor Air*, pp. 138–152, 2015.

[160] Design Builder Software, “Design Builder Software,” 2016. [Online]. Available: http://www.designbuilder.co.uk/.

[161] M. Taleghani, M. Tenpierik, S. Kurvers, and A. Van Den Dobbelsteen, “A review into thermal comfort in buildings,” *Renew. Sustain. Energy Rev.*, vol. 26, pp. 201–215, 2013.

[162] Google, “Google map,” *United State of America*, 2016. [Online]. Available: https://www.google.co.uk/maps/place/Kementerian+Wilayah+Persekutuan/@2.3807129,101.5165909,78211a,20y,37.16t/data=!3m1!1e3!4m5!3m4!1s0x31cdb63995555555:0x797ed94067461053!8m2!3d2.9305817!4d101.688257.

[163] Pulau Reka Sdn Bhd, “Building Audit Report 2012,” 2013.

[164] IEN Sdn Bhd, “Building Energy Audit Report 2012,” Putrajaya, Malaysia, 2013.

[165] Mosti, “Malaysian Meteorological Department,” *MET Malaysia*. 2013.

[166] Enhance Track Sdn Bhd, “Energy Management and Conservation: An Energy Audit of Facilities and Energy System at Menara Seri Wilayah, Kementerian Wilayah Persekutuan, Blok 1 & 2, Putrajaya.”

[167] Energy Commission, “Malaysia Energy Statistics 2014,” p. 84, 2014.

[168] “Gas District Cooling (M) Sdn Bhd.” [Online]. Available: http://www.gdc.com.my/.

[169] J. P. M. M. Jawatankuasa Kecil Piawaian dan Kos Bagi JPPN, “Garis Panduan dan Peraturan Bagi Perancangan Bangunan,” 2005.

[170] Malaysian Green Technology Corporation, “Building Consumption Input System.” [Online]. Available: http://www.greentownship.my/v2/.

[171] “International Energy Agencies,” 2015. [Online]. Available: https://www.iea.org/aboutus/faqs/energyefficiency/.

[172] M. Royapoor and T. Roskilly, “Building model calibration using energy and environmental data,” *Energy Build.*, vol. 94, pp. 109–120, 2015.

[173] G. Mustafaraj, D. Marini, A. Costa, and M. Keane, “Model calibration for building energy efficiency simulation,” *Appl. Energy*, vol. 130, pp. 72–85, 2014.

[174] F. Sehar, M. Pipattanasomporn, and S. Rahman, “A peak-load reduction computing tool

sensitive to commercial building environmental preferences," *Appl. Energy*, vol. 161, pp. 279–289, 2016.

[175] K. L. Gillespie, J. D. Cowan, C. W. Frazell, J. S. Haberl, K. H. Heinemeier, J. P. Kummer, C. H. Culp, T. E. Watson, C. G. Arnold, V. D. Baxter, R. a Evans, J. F. Hogan, F. H. Kohloss, and R. D. Montgomery, "Measurement of Energy and Demand Savings," vol. 8400, p. 170, 2002.

[176] D. B. Crawley, J. W. Hand, M. Kummert, and B. T. Griffith, "Contrasting the capabilities of building energy performance simulation programs," *Build. Environ.*, vol. 43, no. 4, pp. 661–673, 2008.

[177] D. B. Crawley, L. K. Lawrie, C. O. Pedersen, and F. C. Winkelmann, "EnergyPlus : Energy Simulation Program," *ASHRAE J.*, vol. 42, no. 4, pp. 49–56, 2000.

[178] R. Zeng, X. Wang, H. Di, F. Jiang, and Y. Zhang, "New concepts and approach for developing energy efficient buildings: Ideal specific heat for building internal thermal mass," *Energy Build.*, vol. 43, no. 5, pp. 1081–1090, 2011.

[179] X. Kong, S. Lu, J. Huang, Z. Cai, and S. Wei, "Experimental research on the use of phase change materials in perforated brick rooms for cooling storage," *Energy Build.*, vol. 62, pp. 597–604, 2013.

[180] X. Kong, S. Lu, Y. Li, J. Huang, and S. Liu, "Numerical study on the thermal performance of building wall and roof incorporating phase change material panel for passive cooling application," *Energy Build.*, vol. 81, pp. 404–415, 2014.

[181] D. Heim, "Isothermal storage of solar energy in building construction," *Renew. Energy*, vol. 35, no. 4, pp. 788–796, 2010.

[182] M. H. M. Isa, X. Zhao, and H. Yoshino, "Preliminary study of passive cooling strategy using a combination of PCM and copper foam to increase thermal heat storage in building facade," *Sustainability*, vol. 2, no. 8, pp. 2365–2381, 2010.

[183] U. Stritih and V. Butala, "Energy saving in building with PCM cold storage," *Int. J. Energy Res.*, vol. 31, no. 15, pp. 1532–1544, 2007.

[184] J. Niu, J. v d Kooi, and H. v d Rhee, "Energy saving possibilities with cooled-ceiling systems," *Energy Build.*, vol. 23, no. 2, pp. 147–158, 1995.

[185] W. Technologies, "ENERCIEL PCM." [Online]. Available: http://www.enerciel-pcm.fr/index.php. [Accessed: 05-Apr-2016].

[186] Phase Change Energy Solution, "Phase Change Energy Solutions." [Online]. Available:

http://www.phasechange.com/. [Accessed: 05-Apr-2016].

[187] M. Hall, *Materials for Energy Efficiency and Thermal Comfort in Buildings (Woodhead Publishing Series in Energy)*. Woodhead Publishing Ltd, 2010.

[188] M. G. Davies, *Building heat transfer*. John Wiley & Sons, 2004.

[189] Cellecta, "Cellecta," *United Kingdom*, 2016. [Online]. Available: http://www.cellecta.co.uk/contact-cellecta/.

[190] Phase Change Energy Solutions, "Phase Change Energy Solution," *United State of America*. [Online]. Available: http://www.phasechange.com/biopcmat/. [Accessed: 09-Feb-2016].

[191] Improvemebt Center, "Insulation: Can it last as long as your home?," *United State of America*, 2016. [Online]. Available: http://www.improvementcenter.com/insulation/insulation-can-it-last-as-long-as-your-home.html.

[192] LampShopOnline Ltd, "Lamp Shop Online," *United Kingdom*, 2016. [Online]. Available: http://www.lampshoponline.com/.

[193] Photonic Universe Ltd., "Photonic Universe," *United Kingdom*, 2016. [Online]. Available: http://www.photonicuniverse.com/en/catalog/full/229-Large-Off-Grid-Household-Solar-Power-System.html.

[194] P. Hanselaer, C. Lootens, W. R. Ryckaert, G. Deconinck, and P. Rombauts, "Power density targets for efficient lighting of interior task areas," *Lighting Research and Technology*, vol. 39, no. 2. pp. 171–184, 2007.

[195] T. T. Chow, C. Li, and Z. Lin, "Innovative solar windows for cooling-demand climate," *Sol. Energy Mater. Sol. Cells*, vol. 94, no. 2, pp. 212–220, 2010.

[196] S. B. Sadineni, S. Madala, and R. F. Boehm, "Passive building energy savings: A review of building envelope components," *Renew. Sustain. Energy Rev.*, vol. 15, pp. 3617–3631, 2011.

[197] K. W. Chan and K. S. Chan, "Experimental Study of the Performance of Porous Materials to Enhance the Soil Cooling in Hot and Humid Regions," *Int. J. Environ. Sci. Dev.*, vol. 3, no. 6, pp. 522–527, 2012.

[198] H. M. Henning, "Solar assisted air conditioning of buildings - an overview," *Appl. Therm. Eng.*, vol. 27, no. 10, pp. 1734–1749, 2007.

[199] S. Rosiek and F. J. Batlles, "Integration of the solar thermal energy in the construction: Analysis of the solar-assisted air-conditioning system installed in CIESOL building," *Renew. Energy*, vol. 34, no. 6, pp. 1423–1431, 2009.

[200] K. F. Fong, C. K. Lee, T. T. Chow, Z. Lin, and L. S. Chan, “Solar hybrid air-conditioning system for high temperature cooling in subtropical city,” *Renew. Energy*, vol. 35, no. 11, pp. 2439–2451, 2010.

[201] G. Mittelman, a Kribus, and a Dayan, “Solar cooling with concentrating photovoltaic/thermal (CPVT) systems,” *Energy Convers. Manag.*, vol. 48, no. 9, pp. 2481–2490, 2007.

[202] G. Lychnos and P. A. Davies, “Modelling and experimental verification of a solar-powered liquid desiccant cooling system for greenhouse food production in hot climates,” *Energy*, vol. 40, no. 1, pp. 116–130, 2012.

[203] K. Gommed and G. Grossman, “Experimental investigation of a liquid desiccant system for solar cooling and dehumidification,” *Sol. Energy*, vol. 81, no. 1, pp. 131–138, 2007.

[204] K. Gommed and G. Grossman, “A Liquid Desiccant System for Solar Cooling and Dehumidification,” *J. Sol. Energy Eng.*, vol. 126, no. August 2004, p. 879, 2004.

[205] A. Preisler and M. Brychta, “Results of system configurations to optimize solar-driven desiccant evaporative cooling systems in full year operation,” in *Energy Procedia*, 2014, vol. 48, pp. 956–965.

[206] R. Z. Wang, T. S. Ge, C. J. Chen, Q. Ma, and Z. Q. Xiong, “Solar sorption cooling systems for residential applications: Options and guidelines,” *International Journal of Refrigeration*, vol. 32, no. 4. pp. 638–660, 2009.

[207] A. K. Mohaisen and Z. Ma, “Development and modelling of a solar assisted liquid desiccant dehumidification air-conditioning system,” *Build. Simul.*, vol. 8, no. 2, pp. 123–135, 2015.

[208] A. Al-Alili, Y. Hwang, R. Radermacher, and I. Kubo, “A high efficiency solar air conditioner using concentrating photovoltaic/thermal collectors,” *Appl. Energy*, vol. 93, pp. 138–147, 2012.

[209] M. D. Moldovan, I. Visa, M. Neagoe, and B. G. Burduhos, “Solar Heating & Cooling Energy Mixes to Transform Low Energy Buildings in Nearly Zero Energy Buildings,” *Energy Procedia*, vol. 48, pp. 924–937, 2014.

[210] A. Pongtornkulpanich, S. Thepa, M. Amornkitbamrung, and C. Butcher, “Experience with fully operational solar-driven 10-ton LiBr/H2O single-effect absorption cooling system in Thailand,” *Renew. Energy*, vol. 33, no. 5, pp. 943–949, 2008.

[211] U. Desideri, S. Proietti, and P. Sdringola, “Solar-powered cooling systems: Technical and economic analysis on industrial refrigeration and air-conditioning applications,” *Appl. Energy*, vol. 86, no. 9, pp. 1376–1386, 2009.

[212] V. V. Tyagi, S. C. Kaushik, and S. K. Tyagi, “Advancement in solar photovoltaic/thermal (PV/T) hybrid collector technology,” *Renew. Sustain. Energy Rev.*, vol. 16, no. 3, pp. 1383–1398, 2012.

[213] A. Fudholi, K. Sopian, M. H. Yazdi, M. H. Ruslan, A. Ibrahim, and H. A. Kazem, “Performance analysis of photovoltaic thermal (PVT) water collectors,” *Energy Convers. Manag.*, vol. 78, pp. 641–651, 2014.

[214] A. Kribus, D. Kaftori, G. Mittelman, A. Hirshfeld, Y. Flitsanov, and A. Dayan, “A miniature concentrating photovoltaic and thermal system,” *Energy Convers. Manag.*, vol. 47, no. 20, pp. 3582–3590, 2006.

[215] A. Akair, “Combined Solar Power anc Cooling Syste Using an Organic Rankine Cycle,” 2012.

[216] F. Lansing, “Computer modeling of a single-stage lithium bromide/water absorption refrigeration unit,” *Deep Space Network Progress Report*. 1976.

[217] Phase Change Material Products Ltd, “Plus-ICE Phase Change materials (PCM) THERMAL ENERGY STORAGE DESIGN GUIDE,” *Strategy*, no. 0, pp. 1–43, 2011.

[218] Mitsubishi Heavy Industries Ltd, “AART-I AART-I,” *Japan*, 2016. [Online]. Available: http://www.mhiae.com/products/chillers/aart.

[219] N. Kalkan, K. Bercin, O. Cangul, M. G. Morales, M. M. K. M. Saleem, I. Marji, A. Metaxa, and E. Tsigkogianni, “A renewable energy solution for Highfield Campus of University of Southampton,” *Renew. Sustain. Energy Rev.*, vol. 15, no. 6, pp. 2940–2959, 2011.

[220] Lacaze Energies, “GLACEO® CHILLED WATER CYLINDER,” *France*, 2016. [Online]. Available: http://www.lacaze-energies.fr/IMG/pdf/GLACEO.pdf.

[221] M. View and I. Estate, “12 th International Conference on Sustainable Energy technologies (SET-2013) Paper ID : SET2013-023 PHASE CHANGE MATERIAL BASED PASSIVE COOLING SYSTEMS DESIGN AUTHORS (1) Phase Change Material Products Limited KEYWORDS : Phase Change Material , PCM , ,” pp. 26–29, 2013.

[222] “Sustainable Energy Development Authority Malaysia (SEDA).” [Online]. Available: http://seda.gov.my/.

[223] E. Pikas, M. Thalfeldt, and J. Kurnitski, “Cost optimal and nearly zero energy building solutions for office buildings,” *Energy Build.*, vol. 74, pp. 30–42, 2014.

Appendix A

The simulated daylight factor and daylight luminance level (lux) in areas that are exposed to sunshine. A continuation from Section 4.4.

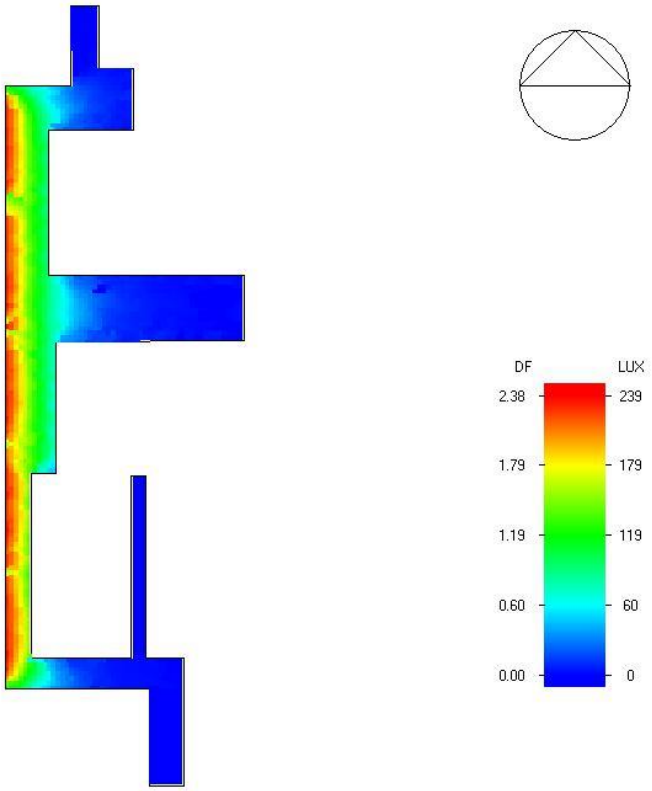

Figure 123: The simulated daylight factor and daylight luminance at the level 2's corridor.

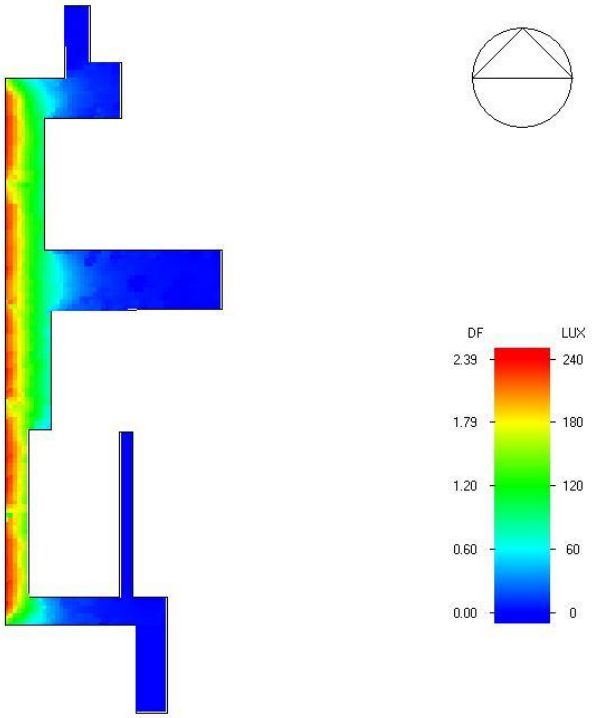

Figure 124: The simulated daylight factor and daylight luminance at the level 3's corridor.

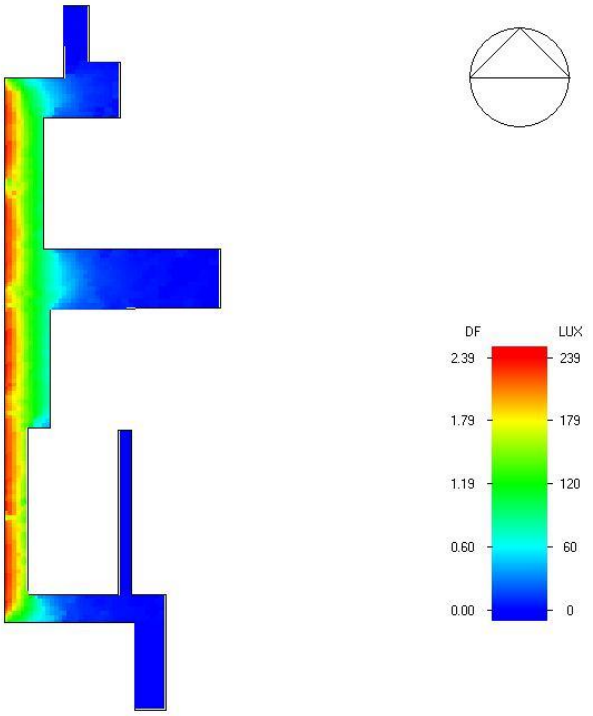

Figure 125: The simulated daylight factor and daylight luminance at the level 4's corridor.

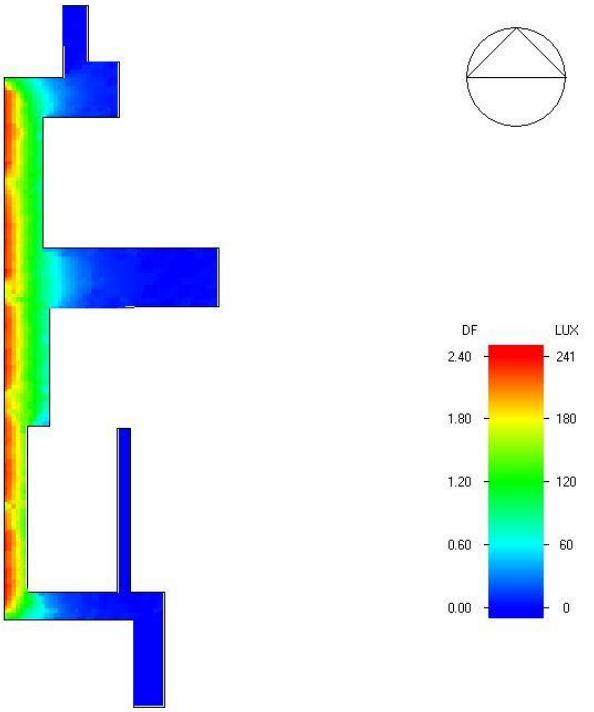

Figure 126: The simulated daylight factor and daylight luminance at the level 5's corridor.

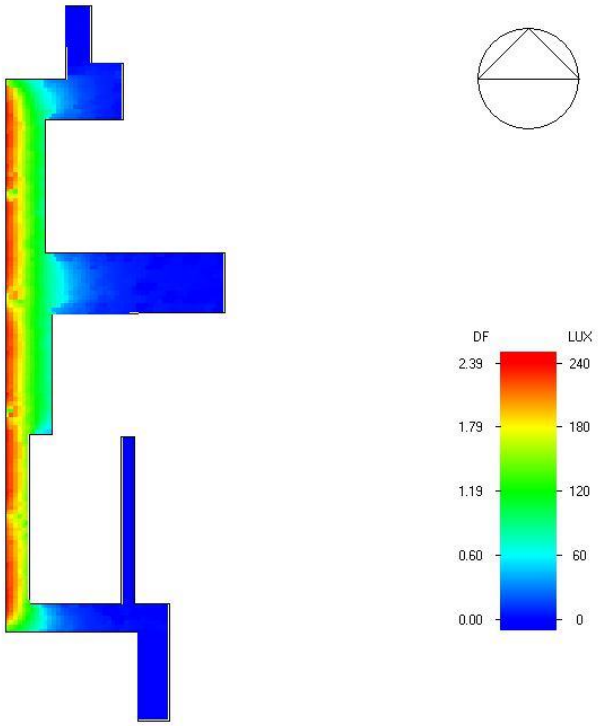

Figure 127: The simulated daylight factor and daylight luminance at the level 6's corridor.

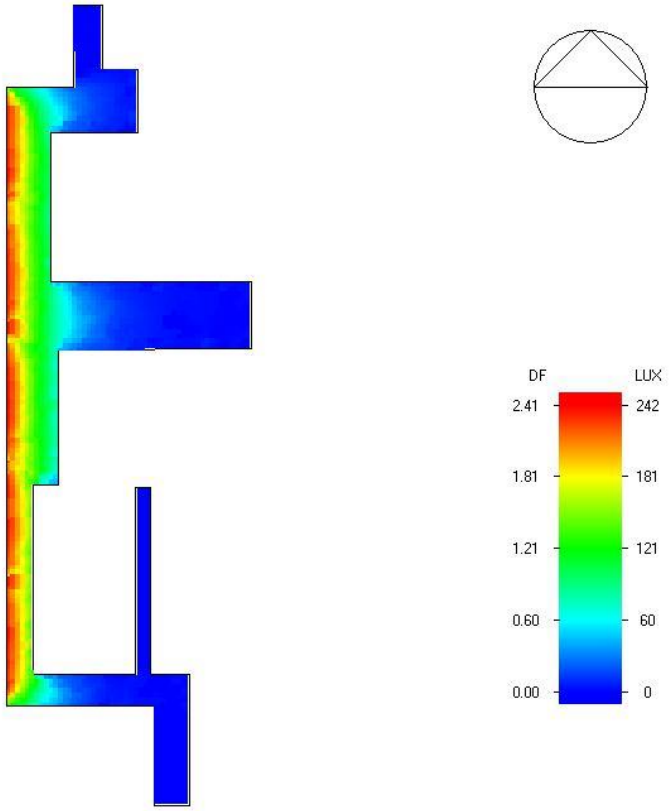

Figure 128: The simulated daylight factor and daylight luminance at the level 7's corridor.

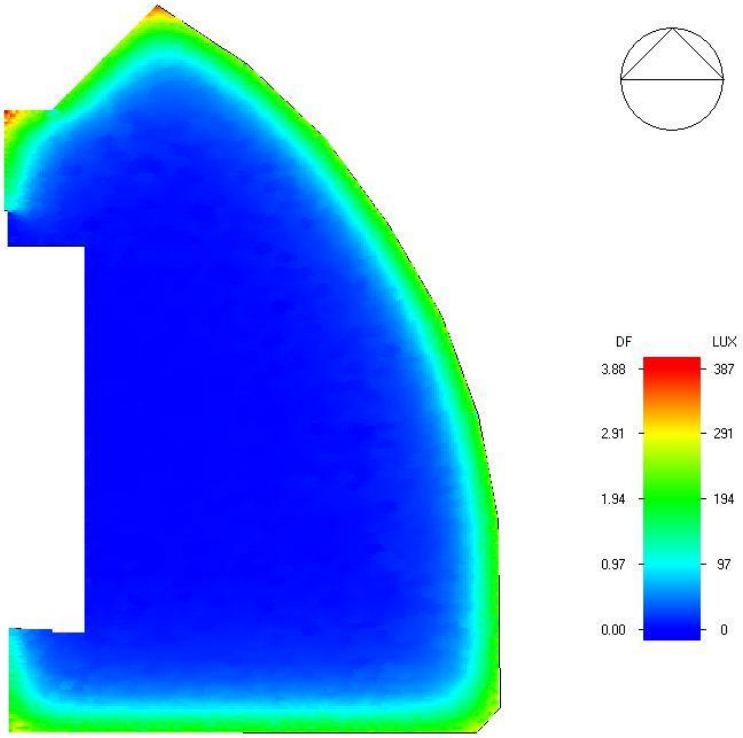

Figure 129: The simulated daylight factor and daylight luminance at first floor's office.

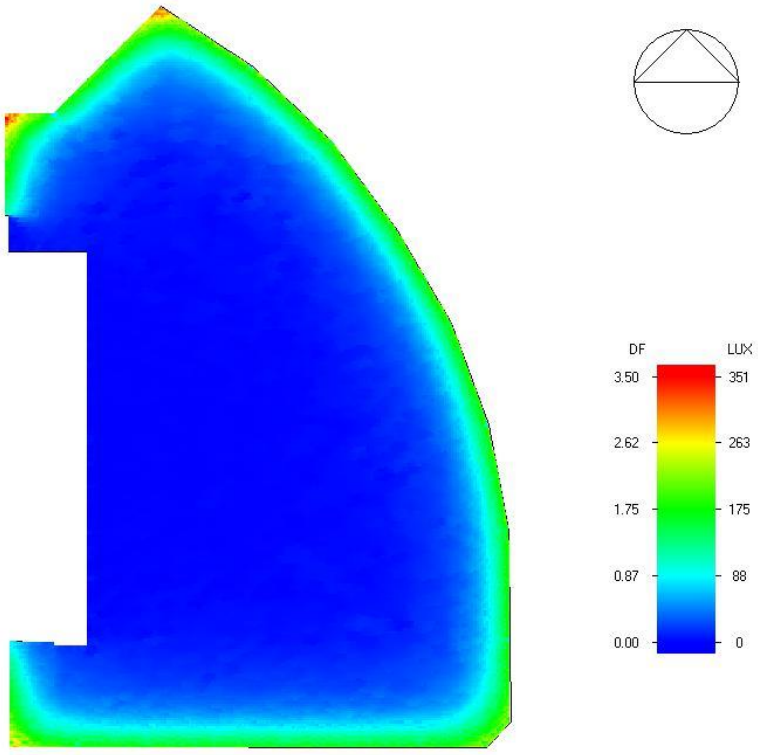

Figure 130: The simulated daylight factor and daylight luminance at second floor's office.

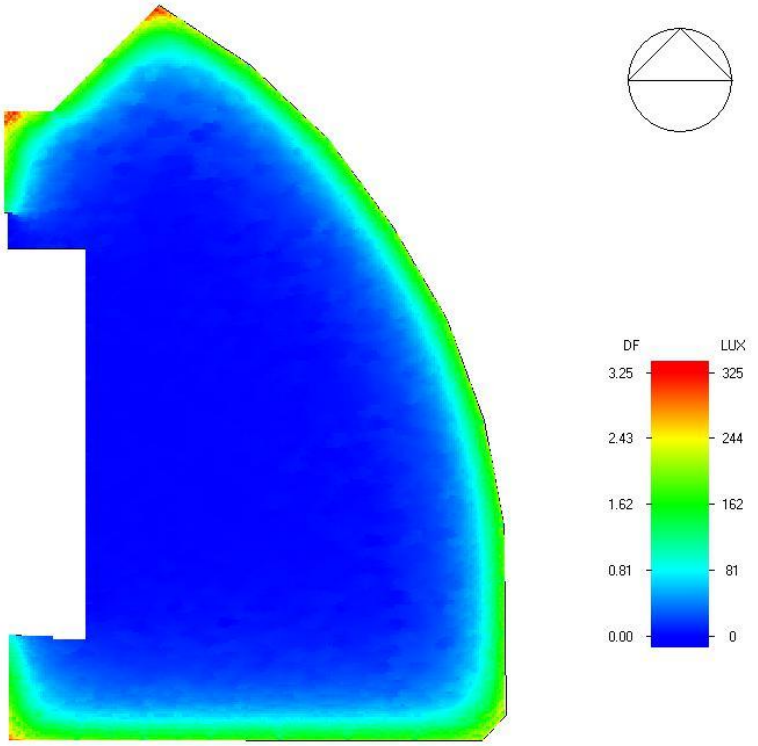

Figure 131: The simulated daylight factor and daylight luminance at third floor's office.

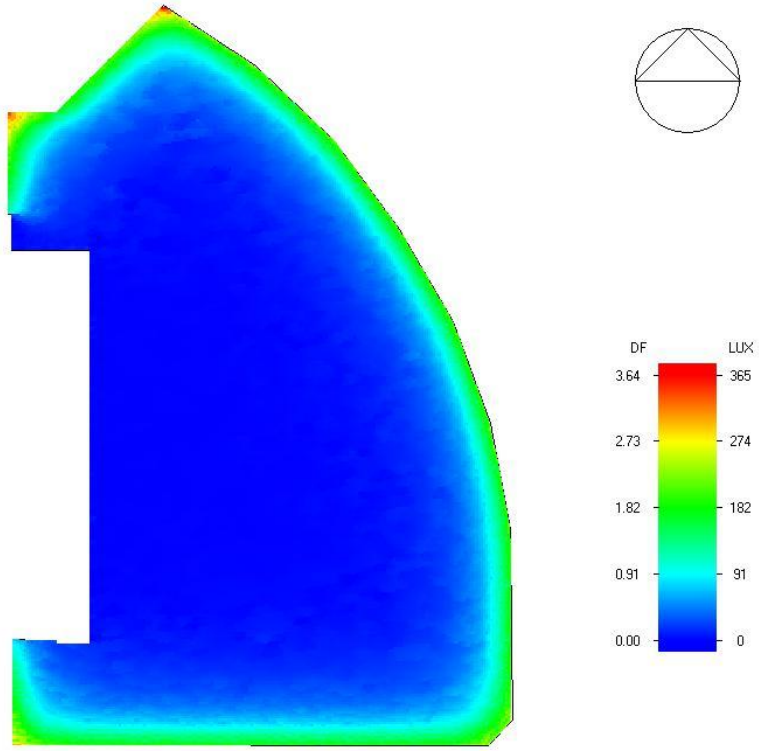

Figure 132: The simulated daylight factor and daylight luminance at fourth floor's office.

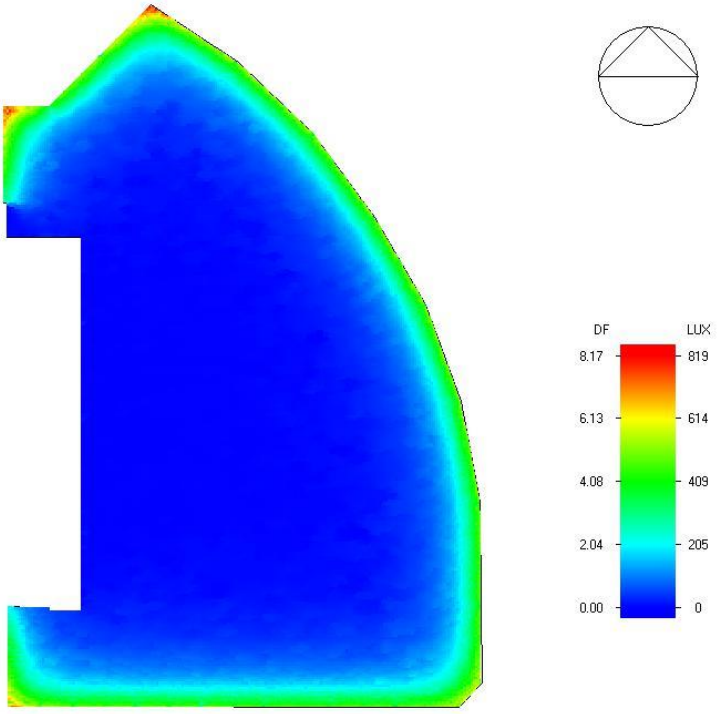

Figure 133: The simulated daylight factor and daylight luminance at fifth floor's office.

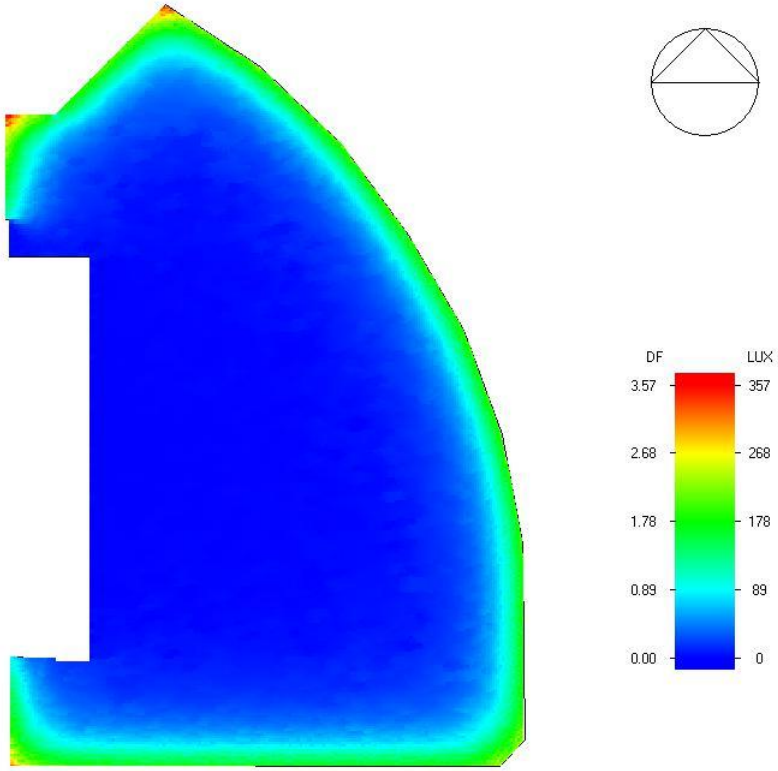

Figure 134: The simulated daylight factor and daylight luminance at sixth floor's office.

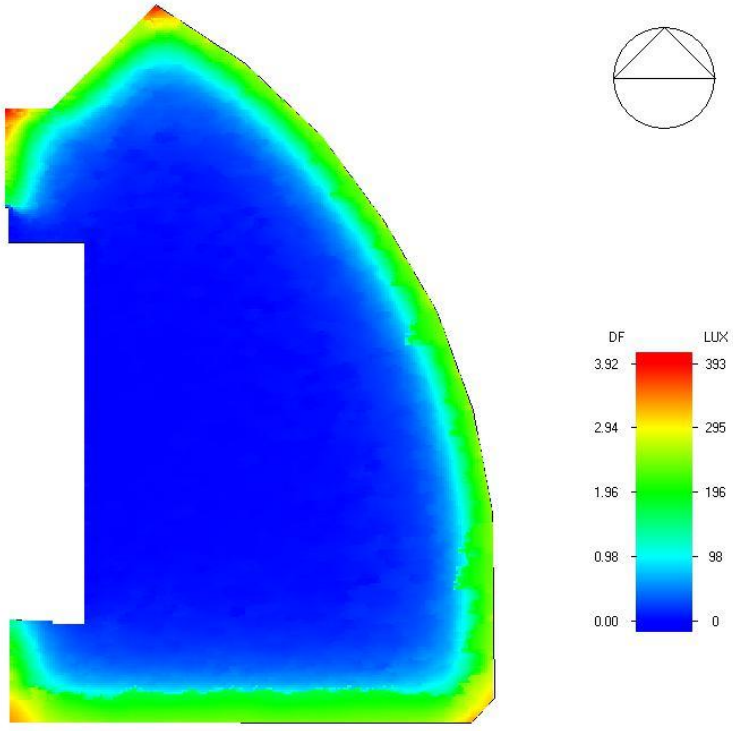

Figure 135: The simulated daylight factor and daylight luminance at seventh floor's office.

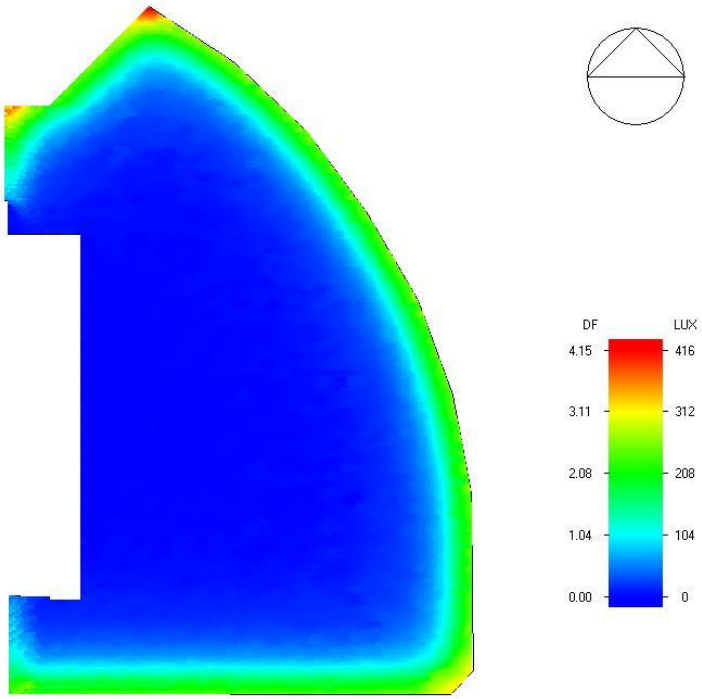

Figure 136: The simulated daylight factor and daylight luminance at ground floor's office.

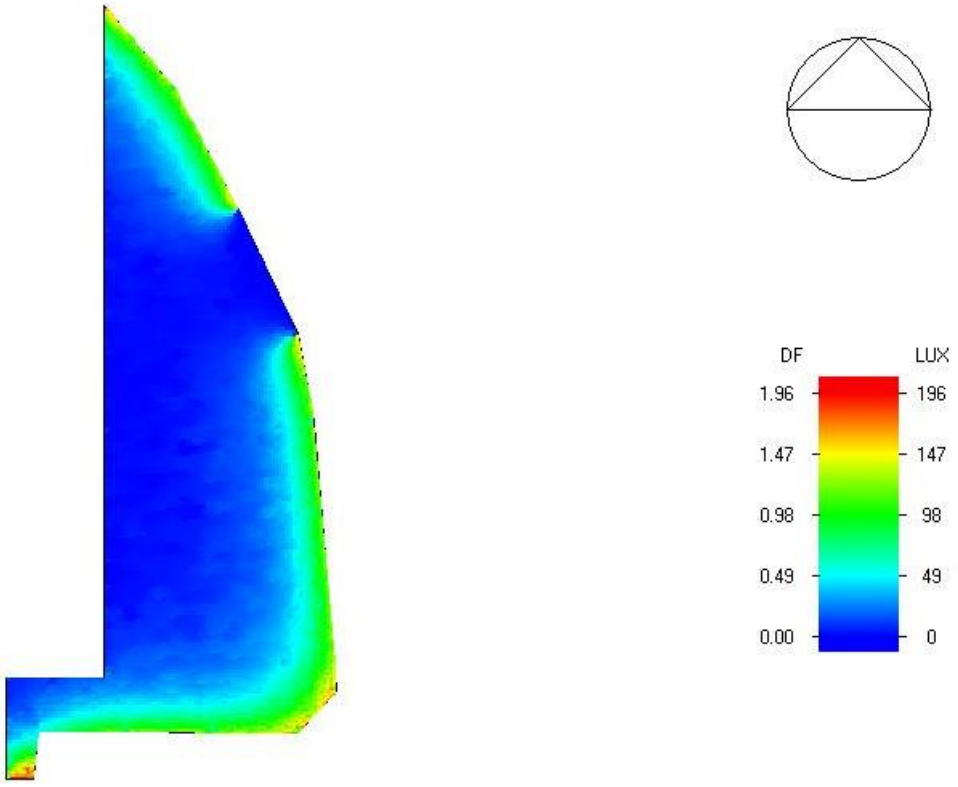

Figure 137: The simulated daylight factor and daylight luminance at the cafeteria.

Appendix B

The simulated temperature and relative humidity in the office at the first to the seventh floor during recess hour (1300 to 1400). A continuation from Chapter 5.

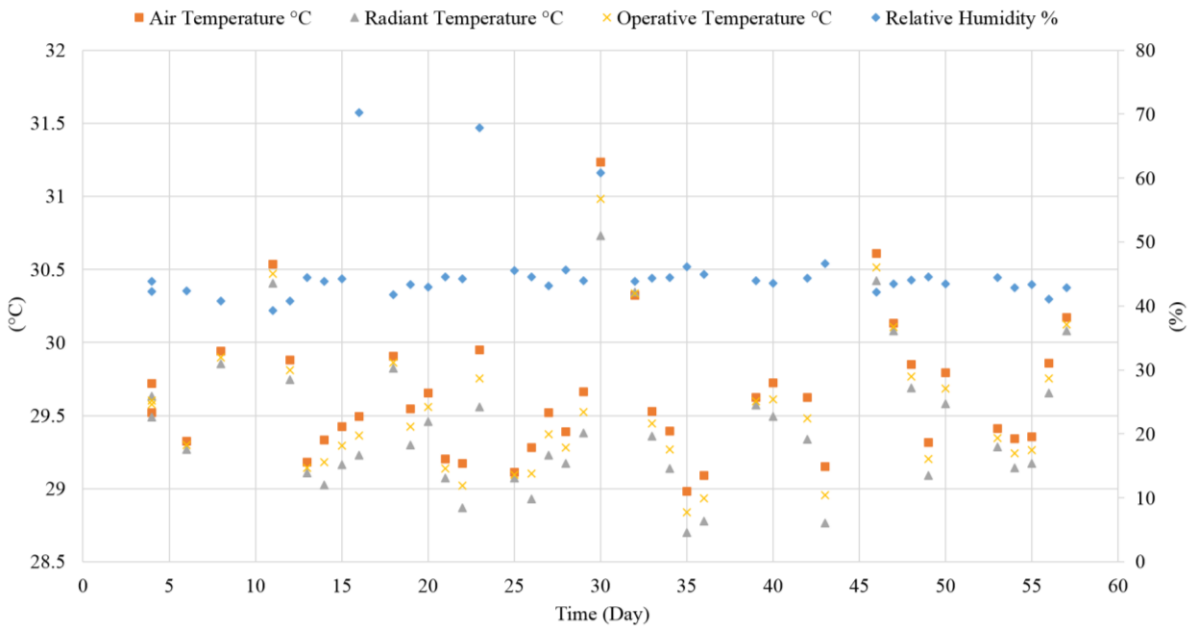

Figure 138: The simulated temperature and relative humidity in the office at the first floor during recess hour (1300 to 1400).

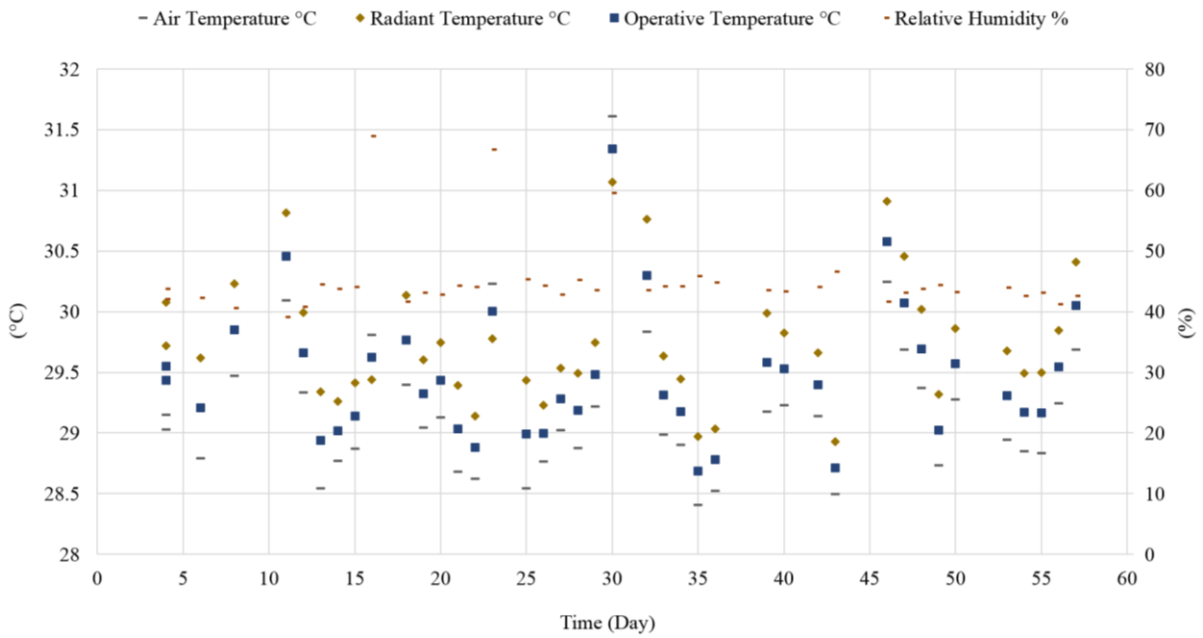

Figure 139: The simulated temperature and relative humidity in the office at the second floor during recess hour (1300 to 1400).

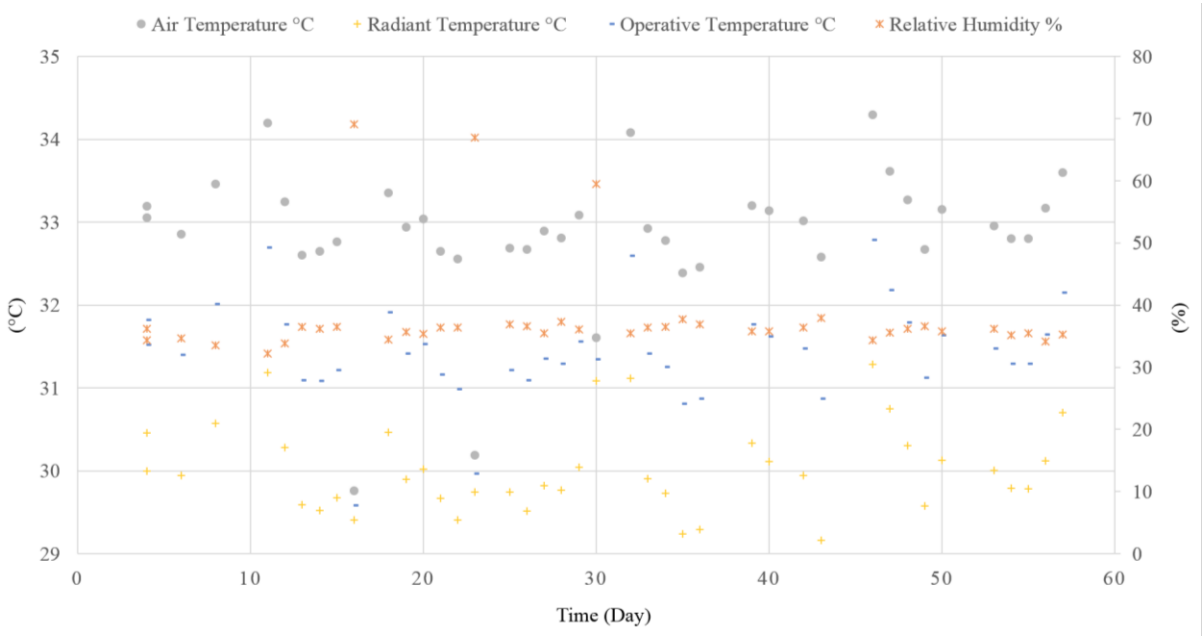

Figure 140: The simulated temperature and relative humidity in the office at the third floor during recess hour (1300 to 1400).

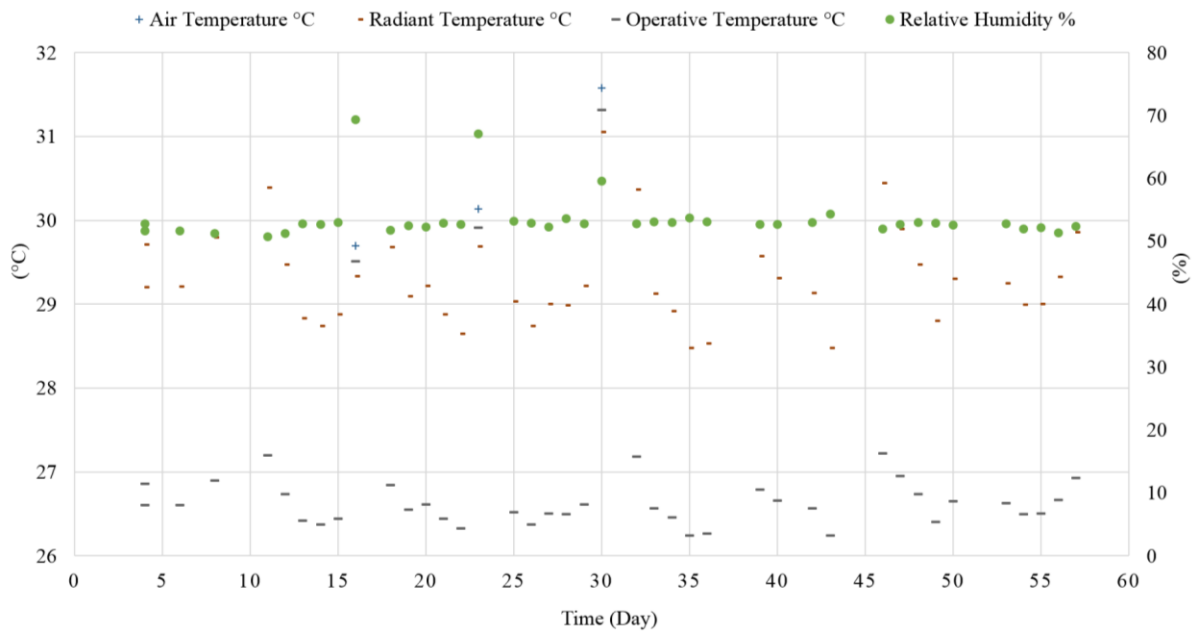

Figure 141: The simulated temperature and relative humidity in the office at the fourth floor during recess hour (1300 to 1400).

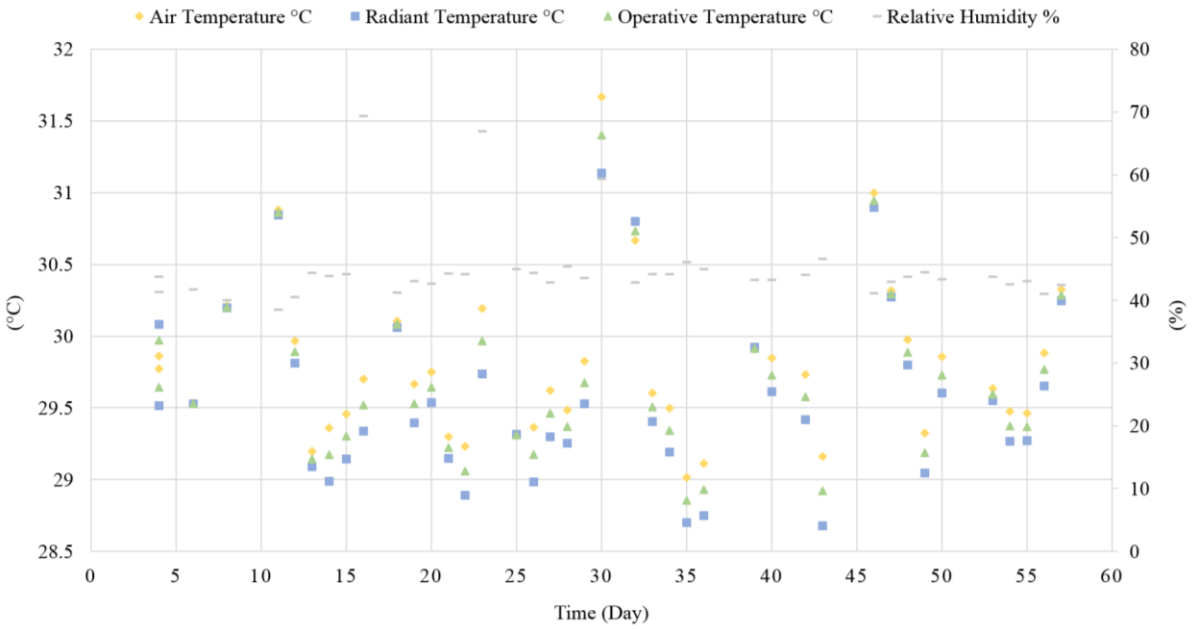

Figure 142: The simulated temperature and relative humidity in the office at the fifth floor during recess hour (1300 to 1400).

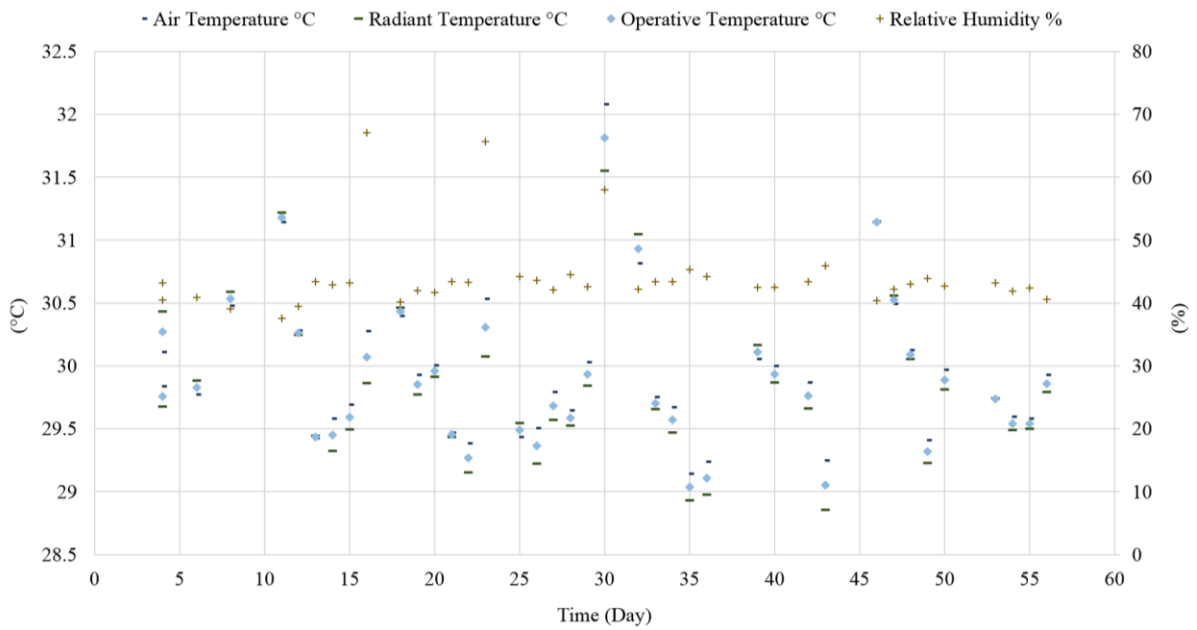

Figure 143: The simulated temperature and relative humidity in the office at the sixth floor during recess hour (1300 to 1400).

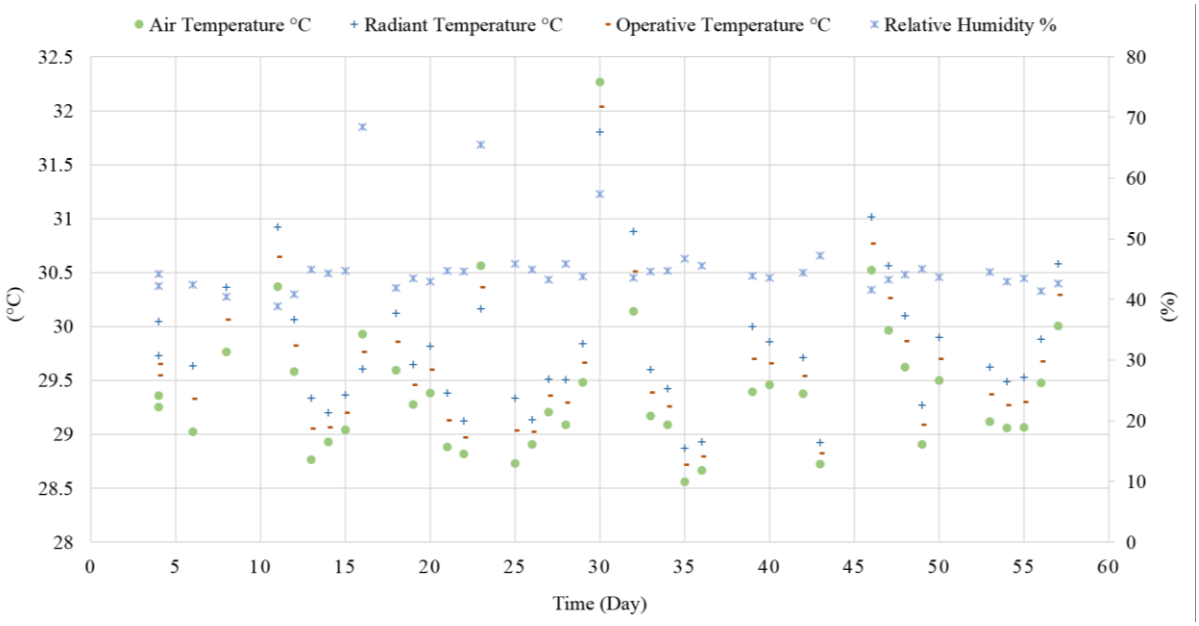

Figure 144: The simulated temperature and relative humidity in the office at the seventh floor during recess hour (1300 to 1400).